Spatial and temporal trends of anthropogenic pollutants in a tropical, urban environment in East Africa

Dissertation for the degree of Philosophiae Doctor

By

Maja Nipen

Department of Chemistry

Faculty of Mathematics and Natural Sciences

University of Oslo

2022

Series of dissertations submitted to the
Faculty of Mathematics and Natural Sciences, University of Oslo
No. 2520

ISSN 1501-7710

Cover: Hanne Baadsgaard Utigard.
Print production: Graphics Center, University of Oslo.

Acknowledgements

This work, which has been carried out under the AnthroTox project, has been made possible by funding from the University of Oslo (UiO) Life:Science initiative, and from the Department of Social Anthropology and Department of Biosciences at UiO. My thanks go to the AnthroTox project seniors who secured this funding; Paul Wenzel Geissler (project leader) from the Department of Social Anthropology, UiO, Katrine Borgå (leader of the natural science part of the project) from the Department of Biosciences, UiO, Knut Breivik from the Department of Chemistry, UiO, and NILU – Norwegian Institute for Air Research, Aviti John Mmochi from the Institute for Marine Sciences, University of Dar es Salaam, Tanzania, Peter Mangesho from the National Institute for Medical Research (NIMR), Tanzania, Susanne Bauer from Centre for Technology, Innovation and Culture, UiO, and Ruth Jane Prince from the Department of Community Medicine and Global Health, UiO. I would also like to thank the project collaborators; Vendelin Simon from the University of Dar es Salaam, Tanzania, Anders Ruus from the Norwegian Institute for Water Research, Martin Schlabach from NILU, and Jan Ludwig Lyche and Anoushka Polder from the Norwegian University of Life Sciences. Special thanks to Eliezer Brown Mwakalapa from Mbeya University of Natural Sciences, Tanzania, for essential contributions during both the planning and conduction of the research. I am extremely grateful for having been allowed to work on this exiting project, and it has been a privilege to work with all of you.

Acknowledgements also go to the Tanzania Commission for Science and Technology (COSTECH) for providing research permit to the AnthroTox project, and to the local authorities, residents, and businesses of Dar es Salaam and the Coastal Region for allowing us to collect environmental samples on their properties.

Further, I would like to thank my fellow PhD students on the AnthroTox project; Ane Haarr, Samwel Moses Ntapanta, Signe Mikkelsen, Franziska Klaas, and Christian Medaas. We have shared some great experiences during fieldwork in Dar es Salaam and Zanzibar (and some not-so-great ones, like unpleasant boat trips). I am also grateful for all our interesting and useful discussions, where our different backgrounds have provided new perspectives.

A big thank you goes to my main supervisor, Knut Breivik, for believing in my potential, for good feedback and advice, and for reminding me of the bigger picture when I was burying myself in detail. You have been a great guide for this "*dannelsesreise*". Thank you also to my supervisor Rolf David Vogt (formerly Department of Chemistry, UiO, currently Norwegian

Institute for Water Research) for many good discussions (on and off topic) and for all your critical questions. Thank you to my supervisors Pernilla Bohlin-Nizzetto (NILU), Katrine Borgå, and Martin Schlabach for useful feedback and many good discussions. Special thanks to Frank Wania (University of Toronto Scarborough, Canada), Guttorm Christensen (Akvaplan-niva, Norway), and Anders Røsrud Borgen (NILU) for contributions crucial for the successful completion of this work.

Many others deserve thanks, including article co-authors, the laboratory staff, and scientists at the Environmental Chemistry department at NILU, and the Environmental Chemistry group at UiO. Special thanks to Helene, Kine, Alexander, and Susanne for good conversations and for sharing joys and frustrations.

This journey, from starting my bachelor's degree in chemistry ten years ago, to now handing in my PhD thesis has been long, but at the same time it feels like it started only yesterday. I would not have gotten this far without the support of family; Nick, Muttern and Fattern, Helge and Katrine. Nick, you have been my rock throughout, and your support means the world to me.

Finally, I would like to dedicate this thesis to my dad, Jan Ottar Nipen (Fattern), who I know would have been proud, and would have loved to be part of this final stage of my PhD, but who sadly passed away late last year. Your love for nature, science, systems and statistics, and your endless curiosity about how the world works has been hugely inspirational to me. Thank you.

Nannestad, 24.02.2022

Table of content

List of abbreviations

aBFRs	alternative brominated flame retardants
ASE	accelerated solvent extraction
ASGM	artisanal and small-scale gold mining
B	bioaccumulative
BAF	bioaccumulation factor
BCF	bioconcentration factor
BTBPE	1,2-bis(2,4,6-tribromophenoxy)ethane
CPs	chlorinated paraffins
DBDPE	decabromodiphenyl ethane
Dec 602	Dechlorane 602
Dec 603	Dechlorane 603
DP	Dechlorane Plus
GAPS	Global Atmospheric Passive Sampling
GC/Q-TOF	gas chromatography quadrupole time-of-flight high-resolution mass spectrometry
GC-HRMS	gas chromatography high-resolution mass spectrometry
GDP	gross domestic product
GEM	gaseous elemental mercury
GMOS	Global Mercury Observation System
Hg	mercury
K_{AW}	air water equilibrium partitioning coefficient
K_{OA}	octanol air equilibrium partitioning coefficient
K_{OW}	octanol water equilibrium partitioning coefficient
K_{SG}	sorbent gas-phase equilibrium partitioning coefficient
LCCPs	long chain chlorinated paraffins
LOD	limit of detection
LOQ	limit of quantification
LRT	long-range transport
MCCPs	medium chain chlorinated paraffins
MONET	MOnitoring NETwork
P	persistent
PAS	passive air sampler

PBDEs	polybrominated diphenyl ethers
PCBs	polychlorinated biphenyls
POPs	persistent organic pollutants
PUF	polyurethane foam
REACH	Registration, Evaluation, Authorization, and Registration of Chemicals
SCCPs	short chain chlorinated paraffins
SR	sampling rate
SRM	standard reference material
SVOCs	semi-volatile organic contaminants
T	toxic
TBPH	bis(2-ethylhexyl)-3,4,5,6-tetrabromo-phthalate
vB	very bioaccumulative
vP	very persistent
vSCCPs	very short chain chlorinated paraffins

List of papers

Paper I:

Maja Nipen, Rolf David Vogt, Pernilla Bohlin-Nizzetto, Katrine Borgå, Eliezer Brown Mwakalapa, Anders Røsrud Borgen, Susanne Jøntvedt Jørgensen, Samwel Moses Ntapanta, Aviti John Mmochi, Martin Schlabach, and Knut Breivik (2021).

Spatial trends of chlorinated paraffins and dechloranes in air and soil in a tropical urban, suburban, and rural environment.

Environmental Pollution 292: 118298.

Paper II:

Maja Nipen, Rolf David Vogt, Pernilla Bohlin-Nizzetto, Katrine Borgå, Eliezer Brown Mwakalapa, Anders Røsrud Borgen, Martin Schlabach, Guttorm Christensen, Aviti John Mmochi, and Knut Breivik (2022).

Increasing trends of legacy and emerging organic pollutants in a dated sediment core from East-Africa.

Frontiers in Environmental Science 9: 805544.

Paper III:

Maja Nipen, Susanne Jøntvedt Jørgensen, Pernilla Bohlin-Nizzetto, Katrine Borgå, Knut Breivik, Aviti John Mmochi, Eliezer Brown Mwakalapa, M. Isabel Quant, Martin Schlabach, Rolf David Vogt, and Frank Wania.

Mercury in air and soil on an urban-rural transect in East-Africa.

Manuscript accepted for publication in Environmental Science: Processes & Impacts.

Summary

A range of chemicals which are potentially harmful to human health and the environment are used in industrial and consumer products including electronics. Some of these chemicals have physicochemical properties which may make them environmentally persistent, bioaccumulative, toxic, and/or have the potential for long-range environmental transport. This includes mercury (Hg), persistent organic pollutants (POPs) e.g., polychlorinated biphenyls (PCBs) and polybrominated diphenyl ethers (PBDEs), and chemicals of emerging concern, e.g., alternative brominated flame retardants (aBFRs), chlorinated paraffins (CPs), and dechloranes. Many of these chemicals were produced and more extensively used in the Global North, though it has been hypothesized there may be an ongoing shift in global source regions for POPs to the Global South. This may also be the case for some chemicals of emerging concern and Hg. Reasons include global trade in products, used products, and waste including electronic waste (e-waste) which contain these chemicals, as well as shortcomings in environmentally sound waste handling and in the ability to enforce environmental regulation. However, there are still large knowledge and data gaps concerning environmental occurrence, emissions, and fate of these chemicals in the Global South.

The original contribution of this thesis is to increase the understanding of occurrence, spatial and temporal distribution, sources, and environmental fate of the above-mentioned chemicals in the Global South. To achieve this, a sediment core was collected in a river system in urban Dar es Salaam, Tanzania. Layers were dated, and analysed for PCBs, PBDEs, aBFRs, CPs and dechloranes. Except for PCBs, this is the first report of long-term temporal trends of these chemicals derived from sediment cores from the African continent. Samples were also collected from the atmosphere, using passive sampling techniques, and from soil along two transects in and around Dar es Salaam. These samples were analysed for CPs, dechloranes, and Hg. This is the first reported data on CPs in air and dechloranes in soil from the African continent. In addition, it is the first spatially resolved data of gaseous elementary mercury (GEM) across an urban area in the Southern Hemisphere.

The results show that concentrations of PCBs and PBDEs increased in sediment layers corresponding to the late 2010s. Also, the chemicals of emerging concern aBFRs, some dechloranes, and especially the CPs showed increasing concentrations. These increases can partly be explained by regional increases in population, consumption, and waste generation. CPs were ubiquitous in the Dar es Salaam region, with higher concentrations in air and soil in

more urbanized areas and near municipal waste and e-waste handling facilities. Dechlorane concentrations in air and soil were lower compared to CPs, with the highest concentrations close to e-waste handling sites, although spatial trends differed for the analysed dechlorane compounds. Some high levels of GEM in air were observed in the urban environment, while concentrations of total Hg in soil were generally low.

The increasing trends of PCBs and PBDEs in sediments may suggest that regulatory efforts have been less effective in lowering environmental burdens of these POPs in Dar es Salaam compared to the Global North. Strongly increasing trends of the studied chemicals of emerging concern, and significant sources for GEM in the region also merits further attention. Establishing new- and/or strengthening existing environmental monitoring programs for these chemicals locally and elsewhere in the Global South is therefore recommended to assess the effectiveness of existing regulation and to document needs for further regional and international regulatory efforts.

1. Introduction

A considerable research effort has been committed during the past decades to understand sources, emissions, and the processes controlling the global cycling of persistent organic pollutants (POPs). When released to the environment, POPs potentially have harmful effects on ecosystems and human health. POPs can travel globally with air and ocean currents, as well as in the anthroposphere, by international trade in products and waste where these chemicals are embedded (Breivik et al., 2015). These processes bring POPs to regions far from where they were originally produced and initially used, making POPs truly global contaminants.

This thesis has been produced as part of the AnthroTox convergence environment. *The vision of AnthroTox is to understand how environmental and societal processes and their relationships dictate flows and impacts of anthropogenic toxicants within and across societies and ecosystems.* AnthroTox brings together social anthropologists, historians, science and technology scholars, toxicologists, and chemists to study a sub-set of anthropogenic toxicants, POPs and POPs-like chemicals which are extensively used in industrial and consumer products, e.g., electrical products and electronics. Although the AnthroTox convergence environment is interdisciplinary, this thesis is focused on the environmental chemistry aspects of these challenges. The thesis ventures to increase the understanding of the environmental occurrence, spatial and temporal distribution, emissions, and fate of a range of POPs and POPs-like compounds in the abiotic environment in an urban area in the Global South. Dar es Salaam, Tanzania, was chosen as study region to represent a tropical region with growing economy and increasing population and consumption, yet limited capacity to handle waste and e-waste (Mahenge et al., 2018; Yhdego, 2017). To facilitate a thorough discussion of this topic, the following sections provide some background regarding the targeted chemicals and their production, use, and regulation. In addition, some background is provided regarding the research gap between the Global North and the Global South in terms of the chemical's environmental emissions, occurrence, and fate.

1.1 POPs and POPs-like chemicals

1.1.1 POPs

In the late 1950s, the development of James Lovelock's electron capture detector enabled the analysis of trace amounts of halogenated chemicals in the environment. Followed by the publication of Rachel Carson's "Silent spring" in the early 1960s, this brought awareness about POPs environmental effects to the public and the scientific community. POPs have physicochemical properties which makes them persistent (P), bioaccumulative (B), toxic to humans and/or wildlife (T) and gives them the potential to undergo long-range environmental transport (LRT). The presence of POPs in remote regions like the Arctic was documented in the 1970s and 1980s, followed by programs to monitor atmospheric concentrations (Hung et al., 2010; Hung et al., 2016; Ottar, 1981). International regulations in the form of the 1998 Aarhus Protocol of the Convention on Long-range Transboundary Air Pollution (CLRTAP), and the 2001 Stockholm Convention on POPs, were introduced to protect the environment and human health from these chemicals (UNECE, 2010; UNEP, 2017). The chemicals included in these regulations include chlorinated pesticides, some unintentionally formed by-products, and chemicals used in industrial and consumer products, the latter group being the fucus of this thesis. Originally 12 and 16 chemicals and groups of chemicals were regulated under the Stockholm Convention and Aarhus Protocol, respectively (Table A1), aiming to eliminate or restrict their production, use, and emissions. More chemicals have been included as information has emerged regarding their fulfilment of the POPs hazard criteria P, B, T, and LRT, and after evaluations of potential for emissions and exposure. In the European Economic Area, regional regulations exist in addition to the Aarhus Protocol and the Stockholm Convention. The European Chemicals Agency oversee the REACH (Registration, Evaluation, Authorisation, and Restriction of Chemicals) regulation (EU, 2006). Under REACH, industry and importers of products are held responsible for registering all chemicals imported (as pure substance or in products) or produced in amounts exceeding one tonne. Registered chemicals are evaluated and classified as substances of very high concern if they fulfil the POPs hazard criteria (PBT), or if they are considered very persistent (vP) and very bioaccumulative (vB).

1.1.1.1 Hazard criteria

Persistence is determined by resistance to degradation via chemical, biological, or physical processes, and is typically characterized by the half-life of a chemical in a given media due to such processes. The three regulatory bodies classify a chemical as persistent if its half-life in water, soil, or sediment is above the threshold values listed in Table 1. REACH operate with different half-life thresholds for freshwater and marine water and sediment, and also separate between persistent and very persistent. POPs and POPs-like chemicals may however also be lost from an environmental medium via processes involving diffusion and advection. The approach of classifying a chemical as persistent if its half-life in a single media exceeds a threshold thus fails to consider the potential for multimedia partitioning of these chemicals (further discussed in section 3.1) (Gouin et al., 2000; Mackay et al., 2001; Webster et al., 1998).

It is also important to note that the half-life for a given chemical in a given media will be dependent on the environmental conditions, e.g., temperature, in addition to the physicochemical properties of the chemical (Mackay et al., 2001; Webster et al., 1998). Therefore, the half-life of a given chemical in e.g., soil may vary greatly between the Arctic and the Tropics.

Table 1: Hazard criteria in the Aarhus Protocol, the Stockholm Convention, and REACH. For REACH, half-life thresholds for water and sediment are given for freshwater with thresholds for marine conditions in parenthesis.

		Aarhus Protocol	**Stockholm Convention**	**REACH PBT/ vPvB**
Persistency	Half-life water	> 2 months	> 2 months	> 40 (60) days/ > 60 days
	Half-life soil	> 6 months	> 6 months	> 120 days/ > 180 days
	Half-life sediment	> 6 months	> 6 months	> 120 (180) days/ > 180 days
Bioaccumulation	BCF	> 5000	> 5000	> 2000/ > 5000
	BAF	> 5000	> 5000	
	Log K_{OW}	> 5	> 5	
Toxicity		Potential to adversely affect human health or the environment	Evidence of adverse effects to human health or the environment	NOEC or EC10 < 0.01 mg/L, carcinogenic (cat. 1A or 1B), mutagenic (cat. 1A or 1B), reproduction toxicity (cat. 1A, 1B, or 2), or evidence for chronic toxicity
Long-range transport	Detection remote location	Yes	Yes	
	Potential for LRT shown by modelling		Yes	
	Half-life air	> 2 days	> 2 days	
	Vapour pressure	< 1000 Pa		

vP: very persistent, vB: very bioaccumulative, BCF: bioconcentration factor, BAF: bioaccumulation factor, NOEC: no effect concentration, EC10: effect concentration at 10%

Bioaccumulation is the uptake and accumulation of a chemical in an organism, by e.g., ingestion, dermal contact, or respiration. The term is related to bioconcentration, which is strictly the retention of a chemical in an organism via respiration in water (in aquatic ecosystems) or air (in terrestrial ecosystems), and biomagnification, which refer to increasing concentrations of a chemical in organisms with increasing trophic levels. In the regulatory frameworks, chemicals are classified as bioaccumulative (or very bioaccumulative) if the bioconcentration factor (BCF) or bioaccumulation factor (BAF) exceeds the thresholds given in Table 1. The Aarhus Protocol and the Stockholm Convention classify a chemical as bioaccumulative also if its octanol water equilibrium partition coefficient (log K_{OW}) exceeds 5.

Classification of toxicity is more problematic compared to the other hazard criteria, as it depends mainly on dose, an extensive property of the chemical in question, rather than intensive properties (Mackay et al., 2001). Quasi-intensive metrics, such as LC50 (lethal dose for 50% of the population), may be used as a measure for toxicity. REACH includes such categorization (Table 1). However, the Aarhus Protocol and Stockholm Convention includes statements referring to “adverse effects to human health and the environment” rather than thresholds.

The potential for Long-range environmental transport (LRT) describes a chemicals ability to travel via air and water currents, to regions far from where it was emitted to the environment (Wania and Mackay, 1996). LRT potential is a function of a chemicals tendency to partition into (and out of) mobile media such as air or water, the velocity of these media, and the chemicals degradation rates (Mackay et al., 2001). Processes involving repeated volatilization and deposition in combination with prevailing air and ocean currents, in addition to increased persistence, have been shown to enhance the potential for bringing semi-volatile POPs to remote regions (Wania and Mackay, 1996). While REACH does not include LRT as a hazard criterion, the Aarhus Protocol and Stockholm Convention classify a chemical as having LRT potential based on its detection in remote regions, modelling data indicating LRT, its half-life in air, or its vapour pressure (Table 1).

1.1.1.2 Targeted POPs: PCBs and PBDEs

Polychlorinated biphenyls (PCBs) is one of the original 12 groups of chemicals regulated under the Stockholm convention (UNEP, 2009). Production of PCBs was phased out from the production peak in the 1970s, and ended in the 1990s (Breivik et al., 2002a). Prior to phase out, PCBs were used for different purposes in closed systems in electrical equipment, e.g., as cooling liquid in transformers and as dielectric fluid in large and small capacitors, and as an additive in hydraulic fluids in mining equipment and vacuum pumps (Voogt and Brinkman, 1989). Many of the products that contain PCBs in closed systems have long use-phase lifetimes. PCBs were also used in open systems, as laminating agents, impregnating agents, as plasticizers in lubricants, inks, paints, adhesives, waxes, and carbonless copy paper, as casting agents, dedusting agents in cement and plaster, as well as sealing liquids, fire retardants, immersion oils and pesticides (Voogt and Brinkman, 1989). These uses generally have shorter use-phase lifetimes than the closed system applications. Inventories of production, uses, current stocks, and emissions have been assembled for PCBs (Breivik et al., 2007). PCBs were mainly produced in Europe, USA, Russia, and Japan. No known production of PCBs occurred on the African continent, and only a very small proportion of the total historical use of PCBs.

Production of polybrominated biphenyl ethers (PBDEs) started around the 1970s and peaked around year 2000 (Abbasi et al., 2019). PBDEs were used as flame-retardants in electronics, furniture foam and textiles, as well as in construction materials and vehicles. PBDEs were mainly produced in three commercial mixtures with different bromination degree. The lower brominated penta- and octaBDEs were listed under the Stockholm Convention in 2009, while decaBDE was listed in 2017 (UNEP, 2017). An inventory of global stocks and emissions of PBDEs has recently been assembled (Abbasi et al., 2019). PBDEs were mainly produced in China, Japan, Asia, Europe, USA, and Israel, with no production of PBDEs reported on the African continent (Abbasi et al., 2019).

Although PCBs and PBDEs are no longer produced and used, they remain in the anthroposphere in the stock of in-use and/or waste products which contain them.

1.1.2 Chemicals of emerging concern

The term POP is often reserved for the chemicals regulated under the Stockholm Convention, though a number of other chemicals used in commerce potentially meet one or more of the POPs hazard criteria (Muir and Howard, 2006). The term chemical of emerging concern is often applied to chemicals that are not yet subject to regulation, but which are suspected to exhibit some or all the POPs hazard criteria. A range of chemicals fit this category, e.g., some pharmaceuticals and personal care products, nanomaterials, and currently used pesticides, as well as some industrial-use chemicals which are added to consumer products. The industrial-use chemicals of emerging concern are in focus in this thesis, as these chemicals, like the targeted POPs, may be transported globally via trade in products and waste. These chemicals are often replacements for chemicals which have become subject to regulation. An example of this is the current use of alternative brominated flame retardants (aBFRs) in electronics to meet fire safety guidelines, a function previously filled by the now regulated flame retardant PBDEs. aBFRs are used due to their functional similarity to PBDEs in products, but similar function often also implies similar physicochemical properties and thus potentially similar hazard potential in the environment (de Wit et al., 2010). Inclusion of new chemicals into the Stockholm Convention and the Aarhus Protocol is a time-consuming process, given strict requirements for documentation in addition to evaluation of consequences for stakeholders. This leaves many chemicals of emerging concern in production and use, even after fulfilment of the hazard criteria and potential for exposure has been documented. As for POPs, chemicals of emerging concern which are included in products may also remain in the anthroposphere in products and waste long after production is decommissioned.

1.1.2.1 Targeted chemicals of emerging concern: aBFRs, CPs, and dechloranes

The aBFRs discussed more extensively in this thesis are decabromodiphenyl ethane (DBDPE), 1,2-bis(2,4,6-tribromophenoxy)ethane (BTBPE), and bis(2-ethylhexyl)-3,4,5,6-tetrabromophthalate (TBPH). BTBPE and DBDPE have been produced since the 1970s and mid-1980s, respectively. Their production increased after they were recommended as replacements for octa- and decaBDE (Covaci et al., 2011; Kierkegaard et al., 2004; Renner, 2004). TBPH is recommended as a replacement for pentaBDE and has been produced at least since 1990 (Covaci et al., 2011). These aBFRs remain unregulated at an international level. Production of aBFRs is expected to largely take place in countries with a bromine industry, given challenges associated with bromine export (Alaee et al., 2003). These countries to a large extent coincide with the countries producing PBDEs.

Chlorinated paraffins (CPs) are a complex mixture of chlorinated n-alkanes with varying chain length (very short chain CPs (vSCCPs); $C_{<10}$, short chain CPs (SCCPs); $C_{10} - C_{13}$, medium chain CPs (MCCPs); $C_{14} - C_{17}$, long chain CPs (LCCPs); $C_{>17}$) and varying chlorination degree (typically between 40 and 70%) (Fiedler, 2010). LCCPs are not assessed in this thesis. CPs are used as metalworking fluids, and as plasticisers and flame retardants in a wide range of consumer products (Fiedler, 2010). CPs have been produced since the 1930s, but in recent years production (mainly in China) has increased rapidly to more than a million tonnes/year (Glüge et al., 2016). SCCPs have recently been added to the Stockholm Convention, while vSCCPs and MCCPs remain unregulated at an international level. For simplicity, all CPs (including SCCPs) are collectively referred to as chemicals of emerging concern herein. Because of the complexity of CPs, there are significant challenges relating to their instrumental analysis and quantification (Mézière et al., 2020; van Mourik et al., 2020a; van Mourik et al., 2015).

Of the dechloranes, Dechlorane Plus (DP) is used as a flame retardant in electronics and some building materials (Qiu et al., 2007), and is currently under review for inclusion in the Stockholm Convention (UNEP, 2019b). DP has been in production from the 1960s, but it first came to the attention of environmental scientists in the mid-2000s (Hoh et al., 2006). Knowledge is limited regarding the production history and use of the other dechloranes discussed in this thesis, i.e., Dechlorane 602 (Dec 602) and Dechlorane 603 (Dec 603).

The different histories in terms of production, use, regulation, and waste disposal for the targeted POPs and chemicals of emerging concern are reflected in their emissions, and thus their loadings in the physical environment.

1.1.3 Mercury

Although not an organic chemical, mercury (Hg) also fulfils the hazard criteria associated with POPs. Hg is inherently persistent, a neurotoxic that can accumulate in organisms, and can be transported globally because of its high volatility and long atmospheric half-life (a few months to a year) (Driscoll et al., 2013; Pirrone et al., 2010; Selin, 2009). Monitoring of atmospheric Hg began in the 1990s, though until 2010 atmospheric Hg monitoring was mainly limited to the Northern Hemisphere (Martin et al., 2017; Sprovieri et al., 2010; Temme et al., 2007). In 2010, the Global Mercury Observation System (GMOS, www.gmos.eu) was launched, which included six (of a total of 40) monitoring sites on the Southern Hemisphere (Sprovieri et al., 2016). In 2013, the Minamata Convention on Hg was implemented internationally to protect human health and the environment. The Minamata convention aims to control supply and trade and to reduce use and emissions of Hg (UNEP, 2013).

In contrast to most POPs and chemicals of emerging concern, Hg has both natural and anthropogenic sources, although the latter are of greater magnitude (Streets et al., 2011). Natural sources include rock weathering and volcanism, while the main anthropogenic Hg sources include artisanal and small-scale gold mining (ASGM), fossil fuel combustion, cement production, metal smelting, waste incineration, processing of e-waste, and burning of biomass (Huang et al., 2011; Pacyna et al., 2010; Pirrone et al., 2010; Selin, 2009; Snow et al., 2021).

1.2 The North-South research gap

Most monitoring efforts and case studies reporting POPs in the environment have been conducted in the Northern Hemisphere. One of the reasons for this is that a particular motivation has been to understand how POPs end up in remote regions like the Arctic (de Wit et al., 2010; Wania and Mackay, 1996). Another reason is that POPs were generally produced in temperate regions of the Northern Hemisphere, so emissions associated with production and primary use largely occurred in this Hemisphere. For instance, between 80 and 90% of intentional production and use of PCBs occurred between 30 and 60° N (Breivik et al., 2002b). Additionally, the high cost associated with POPs analysis has limited the possibility to carry out such work in developing regions in the Global South (Leslie et al., 2013; UNEP, 2021). The environmental and health risks associated with POPs are however not equally distributed between Global North and Global South. Reasons for this include differences in capacities for environmentally sound handling of waste and enforcement of regulation, in addition to differences in environmental monitoring and awareness of the risk associated with POPs in the community (Hoornweg and Bhada-Tata, 2012; Robinson, 2009; UNEP, 2021).

POPs intended for use in products are not only emitted to the environment during their production and primary use. Overall, emissions can occur to varying degree depending on the life cycle of the chemical and the products in question; (i) production and formulation of the chemical and inclusion of the chemical in products, (ii) the use-phase of the products, and (iii) the end-of-life (waste) phase of the products (Li and Wania, 2018). Recently, there has been focus on how POPs embedded in products and waste can be transported globally in the anthroposphere, via international trade (Abbasi et al., 2019; Breivik et al., 2015; Li and Wania, 2016). Like the Arctic, sub-Saharan Africa is a region where production and primary use of POPs have not occurred to any great extent. Unlike the Arctic however, sub-Saharan Africa is home to a large human population, and consequently products containing POPs are imported, and waste containing POPs is generated and handled by generally substandard methods (Hoornweg and Bhada-Tata, 2012). Some countries in sub-Saharan Africa are also known to be recipients of e-waste from developed economies (further discussed in section 1.2.1) (Baldé et al., 2017).

Differences in climate between the Global North and the Global South may further play a role for both emissions and environmental fate of POPs, as higher temperature promotes emissions from products and waste, and enhances their transport potential, though reduces their persistence (further discussed in section 3.1) (Breivik et al., 2011; Wania and Mackay, 1996; Webster et al., 1998).

The POPs targeted in this thesis are currently no longer under production and many products containing them are passed, at, or near the end of their life cycle in the Global North. At the same time, the Global North is exporting used products, waste, and e-waste containing POPs to the Global South. Overall, this could imply a shift in global source regions for POPs (Breivik et al., 2011). Many of the factors described above are also applicable to the targeted chemicals of emerging concern. Although generally not yet subject to international regulation, stricter regional regulations, like REACH in Europe, limits the production of some chemicals of emerging concern in many industrialized countries in the Global North. This implies that chemicals of emerging concern also merit particular concern in the Global South.

This indication of a shift in source regions for POPs is described in the literature. Long-term time trend studies from the Northern Hemisphere, using sediment cores, have shown highest POPs concentrations around the time of peak production (Arp et al., 2011; Iozza et al., 2008; Vauclin et al., 2021). Monitoring of atmospheric concentrations of POPs on the Northern Hemisphere documents declining concentrations and primary emissions (Halvorsen et al., 2021; Hung et al., 2016; Wong et al., 2021). On the contrary, in the Global South, some sediment core studies show increasing concentrations of POPs (Ontiveros-Cuadras et al., 2019), and some studies of atmospheric concentrations show signs of ongoing emissions (Bogdal et al., 2013; Gioia et al., 2011; Klánová et al., 2009). In a recent study reporting data from the MOnitoring NETwork (MONET) in Africa, concentrations of some POPs, e.g., PCBs, were reported to be declining, while other POPs, e.g., PBDEs, had unchanged or increasing concentrations (White et al., 2020). Monitoring in the Global North or South has generally not been in place for long enough to determine temporal trends of chemicals of emerging concern (Wong et al., 2021). Recent Global studies on atmospheric concentrations document high levels for some chemicals of emerging concern in the Global South (Rauert et al., 2018; Saini et al., 2020).

A shift in source regions for Hg has been documented. Recent global emissions estimates from Streets et al. (2019) show declining trends in emissions in North America and Europe and increasing trends in South Asia and Africa. The increases outweigh the decreases leading to increases on the global scale (Streets et al., 2019). Corresponding to the trends in emissions, monitoring of air concentrations have shown declining regional concentrations in North America and Europe (Streets et al., 2019; Zhang et al., 2016b) and increasing concentrations in Africa (Martin et al., 2017; Slemr et al., 2020).

1.2.1 E-waste

The terms e-waste is used to describe discarded electrical and electronic equipment, such as mobile phones, televisions, and computers (Robinson, 2009). E-waste is of particular concern regarding the transboundary translocation of POPs, chemicals of emerging concern, and Hg.

This is caused by the relatively high content of these chemicals in e-waste (Robinson, 2009), the high volume and often illicit nature of this waste stream (Breivik et al., 2014), in combination with the fact that environmentally sound dismantling and recycling of e-waste is a highly complex and expensive process in the Global North. Previously, large un-authorized e-waste processing sites were located in some regions of China, leading to significant local pollution (Chen et al., 2011; Fu et al., 2008; Wong et al., 2007; Xu et al., 2019). After China implemented import restrictions on e-waste, other countries in Asia and West Africa have become major recipients of e-waste (Asante et al., 2019; Chakraborty et al., 2018; Iqbal et al., 2017; Möckel et al., 2020).

Management of e-waste is addressed in several regional and international regulations (Forti et al., 2020). In Europe, the use of some hazardous substances in electronics is regulated through the RoHS directive (EU, 2011), and the WEEE directive promotes collection and recycling of electronics (EU, 2012). At a global level, transboundary export of hazardous waste (including e-waste) is regulated through the Basel Convention (UNEP, 2019a). However, the largest producer of e-waste in the world, the US, has not yet ratified the Basel Convention, and e-waste regulation in general suffers from loopholes and lack of enforcement (Forti et al., 2020).

1.2.2 Urban environments

Urban environments have been shown to represent important diffuse source regions for many anthropogenic pollutants which are associated with consumer products, including the targeted POPs, chemicals of emerging concern, and Hg (Barber et al., 2005; Harner et al., 2004; McGrath et al., 2017; McLagan et al., 2018; Saini et al., 2020). It is hypothesized that the urban environments in the Global South may be particularly important source regions for these contaminants, given a rapidly growing population and consumption in combination with inadequate waste and e-waste handling as outlined above.

2. Objectives

The overall objective of the thesis is to contribute to the understanding of the emissions, occurrence, and environmental fate of some POPs, chemicals of emerging concern, and Hg in the abiotic environment in the Global South. This is done by investigating their spatial and temporal trends in an urban environment in sub-Saharan Africa, and through the objectives of the individual papers:

Paper I: The main objective of the first paper is to determine occurrence and spatial distribution of two groups of chemicals of emerging concern, the CPs and dechloranes, in air and soil in and around Dar es Salaam in order to i) provide insights into contemporary emissions, and ii) study the historical accumulation of the studied contaminants in soil, and iii) assess municipal waste and e-waste as potential emission sources, as well as iv) identify other factors governing the spatial distribution and environmental fate of CPs and dechloranes in a tropical environment.

Paper II: The main objective of the second paper is to describe the long-term temporal trends of a range of POPs and chemicals of emerging concern, and the likely socioeconomic and biogeochemical drivers behind these trends, in an urban environment in sub-Saharan Africa by analysing a dated sediment core. To gain insights into potential effects of differences in production, use, and regulation we compare the long-time time trends with sediment core data from other developing or newly industrialized regions and industrialized regions.

Paper III: The main objective of the third paper is to assess spatial distribution and emissions of gaseous elemental mercury (GEM) in and around an urban environment in sub-Saharan Africa, using Dar es Salaam as study region. To provide a fuller picture of Hg contamination in the urban environment, we also report data on total Hg in soil. Additionally, we wanted to assess municipal waste and e-waste as potential sources for GEM and total Hg.

3. Theory

3.1 Environmental fate

3.1.1 Physicochemical properties

One of the key features of most POPs is their tendency to partition between multiple environmental media. The distribution between phases is determined both by the physicochemical properties of the chemical in question, and the properties of the environment, especially its temperature (Mackay, 2001). POPs are generally hydrophobic, indicating a preference for partitioning to lipids (biota) and also to soils and sediments rich in organic matter (Jones and De Voogt, 1999). Most POPs are also semi-volatile, making partitioning to the gas phase possible, and enabling LRT via advection on air currents. Less volatile POPs may also be subject to LRT as they can partition to particles which may be subject to advection, in particular during dry conditions.

Equilibrium partition coefficients between octanol and water (K_{OW}), air and water (K_{AW}), and octanol and air (K_{OA}) are key parameters that describe and are used to predict how chemicals distribute between and within environmental compartments. Octanol serves as a surrogate for lipids, as octanol has a similar carbon/oxygen ratio (Mackay, 2001). Gouin et al. (2000) developed a two-dimensional graphical technique for visualizing the phase-distribution at equilibrium of chemicals based on their partition coefficients. Two of the three partition coefficients are sufficient to describe partitioning behaviour, due to thermodynamic consistency ($\log K_{OA} = \log K_{OW} - \log K_{AW}$). Figure 1 shows a generic chemical space plot with some POPs and chemicals of emerging concern assessed in this thesis. More volatile chemicals are found towards the upper left corner, more water soluble towards the bottom left, while less volatile, more hydrophobic chemicals are found in the upper right corner. The position of a chemical in a chemical space plot provides information about the degree to which the chemical will partition to air, water, and/or organic material (in soil, sediment, or biota).

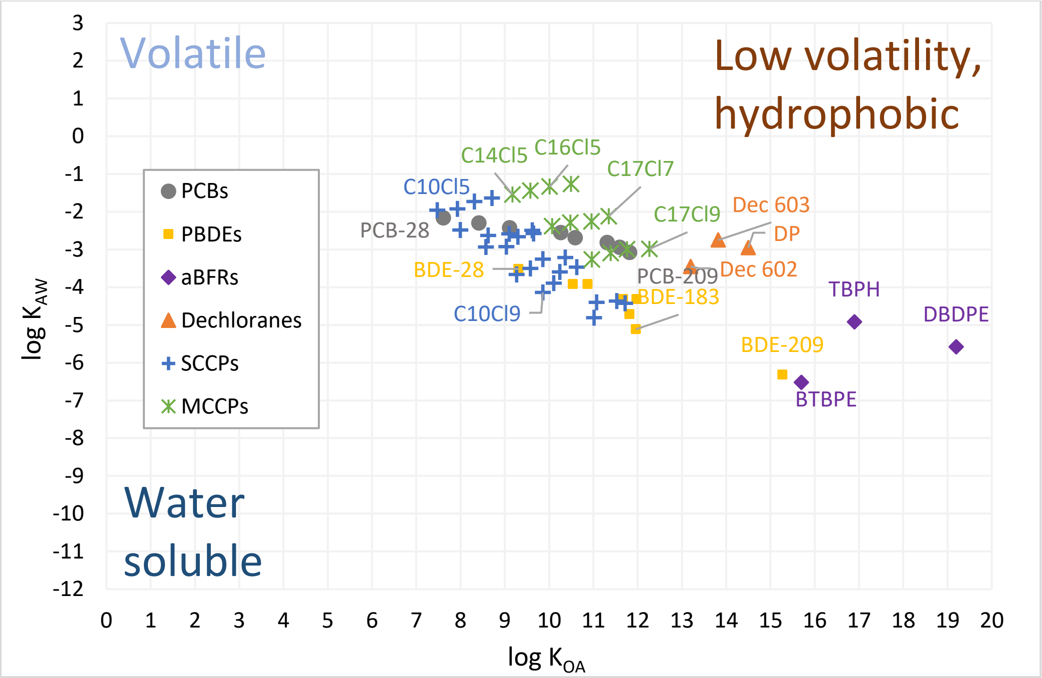

*Figure 1: Chemical space plot illustrating partitioning properties for PCBs and PBDEs (Harner, 2016; Wania and Dugani, 2003), aBFRs (Zhang et al., 2016a), CPs (Glüge et al., 2013), and dechloranes (Sverko et al., 2011) (**Paper II**).*

The concept of chemical space plots has been further developed by Wong and Wania (2011). They applied it to assess the distribution of chemicals within soil compartments (pore air, pore water, and organic matter), given varying properties of the soil and environment in question (organic matter content, water content, temperature). They also expanded the concept to include mobility of chemicals in soil through leaching, evaporation, and erosion. These concepts are useful for predicting the environmental fate of new chemicals, but also for evaluating the environmental fate of well-studied chemicals under different environmental conditions. The latter is of relevance in the context of the Global North Global South research gap, as chemical space plots and mobility plots can give an indication on how the climate in the Global South affects environmental fate of chemicals. Partition coefficients for a given chemical are temperature dependent, and this is particularly the case for the coefficients involving air (K_{AW} and K_{OA}). In the chemical space plot, increased temperature will shift chemicals up and left, indicating increased volatility. This implies a higher potential for volatilization of the targeted POPs and chemicals of emerging concern from surfaces (and from products and waste) in warmer climates. There is also often lower content of organic matter in soil in warmer climates, implying a lower capacity for retention of hydrophobic POPs and chemicals of emerging concern (Dalla Valle et al., 2005; Meijer et al., 2003; Sweetman et al., 2005).

The concept of fugacity is also useful for determining environmental fate of the studied POPs and chemicals of emerging concern (Mackay, 1979). Fugacity is an equilibrium criterion, similarly to chemical activity and potential, and describes a chemicals tendency to “flee” or escape a system (Mackay, 2001). The unit of fugacity is Pa. A chemical will have a tendency to migrate from a phase where it has high fugacity to a phase where it has low fugacity, and when fugacities in the two phases are equal, the chemical is in equilibrium between the two phases. The advantage of using the fugacity concept is that each phase is treated separately in calculations, unlike when using partitioning coefficients where phases are treated in pairs. This makes it possible to derive from which phase variability in chemicals partitioning behaviour originates (Mackay, 2001).

3.1.2 Mercury

Because of its unique properties in terms of high vapour pressure and volatility, Hg can also partition between multiple environmental compartments, although through different mechanisms than for the targeted POPs and chemicals of emerging concern. In this thesis, the focus is on air and soil. In general, Hg occurs as GEM (Hg(0)) in the atmosphere (Driscoll et al., 2013), and in the Hg(II) form in soil (O'Connor et al., 2019). Transfer from atmosphere to soil can occur through oxidation of GEM to Hg(II), the latter form being more subject to both wet and dry deposition. It can also be transferred by uptake of GEM in vegetation. This process occurs through uptake via the stomata in leaves and subsequent oxidation to Hg(II) in the leaf interior, followed by deposition via litterfall (Obrist et al., 2018; Rutter et al., 2011). Transfer from soil to atmosphere can occur through photoreduction of Hg(II) to GEM (Carpi and Lindberg, 1997; Xin and Gustin, 2007) or reduction via other biotic or abiotic processes (Eckley et al., 2016).

Like for the targeted POPs and chemicals of emerging concern, climate impacts the environmental fate of Hg via e.g., increased volatility with increased temperature (O'Connor et al., 2019).

3.2 Targeted environmental media

In this thesis, concentrations of CPs, dechloranes, and GEM/Hg are reported from air and soil (**Paper I** and **Paper III**), and concentrations of PCBs, PBDEs, aBFRs, CPs, and dechloranes are reported from a dated sediment core (**Paper II**). In this sub-section, these environmental compartments are introduced, along with the rationale for their selection. The atmosphere and passive sampling techniques are given particular focus.

3.2.1 Atmosphere

Air is a key environmental media to study, as it responds rapidly to changes in emissions, and therefore gives a good image of current emissions. For this reason, air is one of the core media in the Global Monitoring Plan, used to evaluate the effectiveness of the Stockholm Convention (Hung et al., 2013; UNEP, 2021). Semi-volatile organic contaminants (SVOCs), such as CPs and dechloranes, and GEM in air are commonly sampled using active sampling techniques. However, active sampling is associated with high costs and requirement for trained personnel, electricity, and compressed carrier gasses. These factors make it difficult to collect active samples in remote and/or developing regions as well as simultaneously on a broad spatial scale. Passive air samplers (PAS) offer a good alternative, as they are low-cost, easy to use, do not need electricity, and can be deployed simultaneously at multiple locations. For these reasons, PAS were used in the work for this thesis, both for the SVOCs and GEM. There are however limitations with passive air sampling methods (Bohlin et al., 2014; McLagan et al., 2016; Melymuk et al., 2014), some of which are discussed below.

Several types of PAS for SVOCs have been developed, in the form of semipermeable membrane devices or a range of other sorbents and designs (Harner et al., 2003; Petty et al., 1993; Shoeib et al., 2008; Wania et al., 2003). The PAS used for this thesis for sampling of SVOCs is a polyurethane foam-based PAS (PUF-PAS) developed by Shoeib and Harner (2002). The PUF-PAS has been extensively used for various SVOCs around the world in both case studies and long-term regional and international monitoring networks, such as the Global Atmospheric Passive Sampling (GAPS) network (Pozo et al., 2008; Pozo et al., 2006) and MONET (Klánová et al., 2009). The performance of PUF-PAS under various environmental conditions is also well studied (Bohlin-Nizzetto et al., 2020; Bohlin et al., 2014; Holt et al., 2017; Klánová et al., 2007). The PUF-PAS has been previously calibrated and used for CPs (Chaemfa et al., 2014; Li et al., 2012; Niu et al., 2021; Nøst et al., 2015; Wang et al., 2013) and dechloranes (Drage et al., 2016; Ren et al., 2008; Saini et al., 2020; Schuster et al., 2020).

PAS of various designs have also been developed, studied, and used for GEM (Gustin et al., 2011; Huang et al., 2012; Skov et al., 2007; Zhang et al., 2012). In this work, we apply a PAS developed by McLagan et al. (2015), which recently was shown to be the most precise and accurate PAS in a study comparing the performance of three different PAS for GEM (Naccarato et al., 2020).

3.2.1.1 Passive sampling theory

The theory of PAS for SVOCs is described in detail in e.g., Bartkow et al. (2005) and Wania and Shunthirasingham (2020) and is briefly outlined here. The basic principles of PAS for SVOCs are also applicable to PAS for GEM (McLagan et al., 2016). In active air samplers, a known volume of air is drawn through or past a sorbent using pumps. PAS on the other hand, rely on diffusion of a chemical from air into a sorbent. Uptake of chemical in the sorbent occurs at a rate proportional to the chemicals concentration in the atmosphere. Loss of chemical from the sorbent is proportional to the concentration of chemical in the sorbent. According to Wania and Shunthirasingham (2020), the amount (in mol) of target chemical (m_S) in the sorbent thus changes over time according to the following equation:

$$\frac{dm_S}{dt} = V_S(k_u C_G - k_l C_S) \qquad \text{(eq. 1)}$$

Where k_u and k_l are rate constants for uptake and loss per day, V_S is volume of the sorbent in m^3, and C_G and C_S are concentration in the gas-phase and sorbent, respectively in mol/m^3. In PAS theory, it is generally assumed air-side resistance controls uptake and loss in the sorbent. Fick’s first law is applied to molecular diffusion of target chemical through a stagnant air boundary layer of thickness Δz (m):

$$k_u = \frac{DA}{\Delta z V_S} \qquad \text{(eq. 2)}$$

Where D is molecular diffusivity in m^2 pr day and A is the surface area of the sorbent in m^2. The rate constant of loss is dependent on the equilibrium partitioning coefficient between gas-phase and sorbent, K_{SG}:

$$k_l = \frac{DA}{\Delta z V_S K_{SG}} \qquad \text{(eq. 3)}$$

Amount of analyte taken up in the sorbent during deployment time of the PAS is then:

$$\frac{\Delta m_S}{\Delta t} = \frac{DA}{\Delta z}\left(C_G - \frac{C_S}{K_{SG}}\right) = SR(C_G - \frac{C_S}{K_{SG}}) \qquad \text{(eq. 4)}$$

The kinetic parameter, $\frac{DA}{\Delta z}$ or sampling rate (SR) in m^3/day, designates how fast diffusive transport can take place. The concentration difference term $(C_G - \frac{C_S}{K_{SG}})$ describes the driving force of target chemical from the gas-phase to the sorbent, and the thermodynamic parameter

(K_{SG}) determine the maximum uptake capacity of the sorbent (Wania and Shunthirasingham, 2020).

It is worth noting that transport of chemical within the sorbent has been shown to play a role, which is not accounted for in the above equations (Zhang and Wania, 2012).

3.2.1.2 Kinetic versus equilibrium samplers

The uptake of SVOCs in a sorbent goes through three phases, the linear phase, the curvilinear phase, and the equilibrium phase (Figure 2).

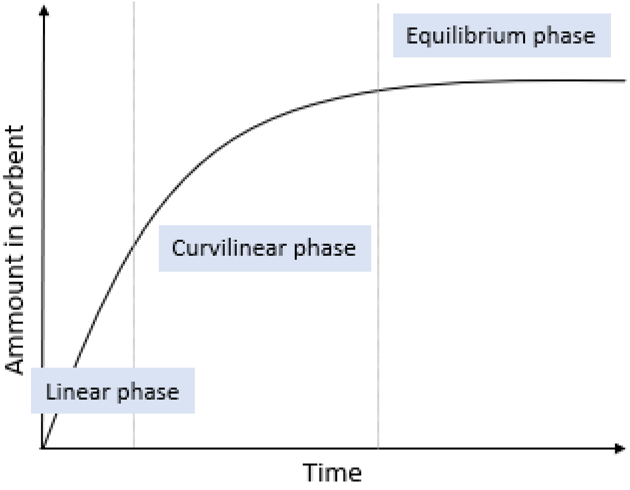

Figure 2: Generic uptake curve of SVOCs in a passive sampling medium (Bartkow et al., 2005).

PAS can be designed to function either as kinetic samplers, operating in the linear phase, or equilibrium samplers, operating in the equilibrium phase. For equilibrium samplers, a high SR, and low (but still large enough to allow for quantification) uptake capacity (low K_{SG}) is desirable. Both PAS used in this thesis (**Paper I** and **Paper III**) are designed as kinetic samplers. For kinetic samplers a high (K_{SG}) is desirable, to keep the term $\frac{C_S}{K_{SG}} \ll C_G$. With this condition met, Δm_S is only dependent on SR, C_G, and deployment length (Δt) (Wania and Shunthirasingham, 2020). However, K_{SG}, which is strongly correlated with K_{OA}, varies over many orders of magnitude for SVOCs. As a consequence, the length of the linear phase may vary widely for SVOCs with different K_{OA}, with shorter linear phase for more volatile chemicals (Farrar et al., 2005), and shorter linear phase at higher temperatures. This is of relevance when sampling CPs, which has a range of K_{OA} spanning at least five orders of magnitude.

3.2.1.3 Uptake rates for kinetic PAS

Given the relatively low concentrations of SVOCs in the ambient atmosphere, PAS for SVOCs depend on SRs which are sufficiently high to capture detectable amounts within deployments of a reasonable length of time (typical deployment times are in the range of a few weeks up to a year). In addition, SRs need to be stable and well defined to result in reliable quantified air concentrations. However, SRs can be affected by both the physicochemical properties of the target chemical and the meteorological parameters during sampling. Wind speed generally has the strongest influence (Klánová et al., 2007; Wania and Shunthirasingham, 2020), though temperature may also play a role (Bohlin-Nizzetto et al., 2020). As a consequence, SRs for PAS for SVOCs have been shown to be highly variable (Melymuk et al., 2014). Most PAS use wind shelters, and strategies involving use of depuration compounds are often used to address this issue (Bartkow et al., 2006). Depuration compounds are e.g., isotopically labelled compounds which are added to the PAS sorbent prior to deployment. The rate of loss of these compounds is assumed to be correlated to the rate of uptake of SVOCs with similar physicochemical properties. Depuration compounds are however not applicable to the SVOCs which are largely partitioned to the particle phase.

In the PAS for GEM developed by McLagan et al. (2015), the issue of variable SRs has been solved by constraining the SR using a diffusive barrier, in addition to using a wind shelter. The addition of a diffusive barrier leads to low SRs, but with this PAS it is possible to sample detectable amounts of GEM as the entire sorbent amount is analysed using thermal desorption. A similar solution is currently unavailable for SVOCs.

3.2.2 Soil

Soil is a complex and heterogeneous environmental media consisting of air, water, mineral matter, and organic matter (Mackay, 2001). Soil represents an important reservoir as historically emitted SVOCs like CPs and dechloranes can accumulate in the soil as a consequence of its retention capacity (Dalla Valle et al., 2005; Ockenden et al., 2003). Soil also represents the largest reservoir for Hg (Obrist et al., 2018). SVOCs and Hg may however also be re-emitted from soils through volatilization, leach to groundwater, or mobilize via erosion. As such, soils can act as storage, sink, and/or secondary source for these chemicals. In addition to the physicochemical properties of the chemical (as described above in section 3.1.1), the properties of the soil affect these processes. Organic matter content plays an important role for sorption of SVOCs (Mackay, 2001; Meijer et al., 2002) and for retention of Hg (O'Connor et al., 2019). For Hg, pH, cation exchange capacity, content of clay, redox potential, and soil moisture may also influence the soils retention capacity and exchange between media for Hg (O'Connor et al., 2019). Clay content is also important for the retention of SVOCs in dry soil with very low organic matter content (Goss et al., 2004).

Soil is highly heterogenic, and both the properties of the soil and the content of contaminants can vary on a scale of just a few metres. This makes it challenging to collect representative soil samples for analysis of these chemicals.

3.2.3 Sediment

Sediments may represent a sink for SVOCs like the studied POPs and chemicals of emerging concern. In aquatic systems, the hydrophobic nature of most SVOCs ensures that they preferentially sorb to suspended particles and organic matter (Figure 1) (Korosi et al., 2015). If sediments are allowed to sequentially settle and remain undisturbed and the chemical is sufficiently persistent, sediment cores can be used to determine the time trends of deposition of the chemicals (Heim and Schwarzbauer, 2013; Korosi et al., 2015). Sediment cores dated using radioisotopes can thus provide an alternative to long-term time trend studies that rely on monitoring of air concentrations. This is highly relevant for regions where air monitoring over time has been limited, as in developing regions in the Global South. Studies on long-term time trends of POPs and chemicals of emerging concern in sediments have been carried out in marine systems (Arp et al., 2011; Combi et al., 2016; Zeng et al., 2013), lakes (Arinaitwe et al., 2016; Sverko et al., 2008; Zennegg et al., 2007), and rivers (Dendievel et al., 2020; Lorgeoux et al., 2016; Vauclin et al., 2021). Analysis of sediment cores has been shown to potentially be a reliable method for evaluating the historical inputs of PCBs, PBDEs, aBFRs, CPs and dechloranes (Korosi et al., 2015).

4. Methods

4.1 Sampling strategy

Figure 3 shows the sampling locations in Dar es Salaam and surrounding areas. The sampling strategy was devised to facilitate assessment of spatial trends of some chemicals of emerging concern (CPs and dechloranes) and Hg (**Paper I** and **Paper III**), and for facilitating the assessment of temporal trends of some POPs (PCBs and PBDEs) and chemicals of emerging concern (aBFRs, CPs, and dechloranes) (**Paper II**). For the assessments of spatial trends, we were particularly interested in the urban environment as a source region, and in the processing of municipal waste and e-waste as potential point sources. Sampling was therefore conducted along two transects, one covering urban Dar es Salaam and areas 40 km upwind and 60 km downwind from the city. For CPs and dechloranes this transect consisted of 19 locations (**Paper I**), while for Hg, an additional five locations were included (**Paper III**). A smaller transect (approximately 12 km, with nine locations) to the southwest of Dar es Salaam, covered Dar es Salaams main municipal waste dumpsite and a commissioned e-waste handler (Figure 4) (**Paper I** and **Paper III**).

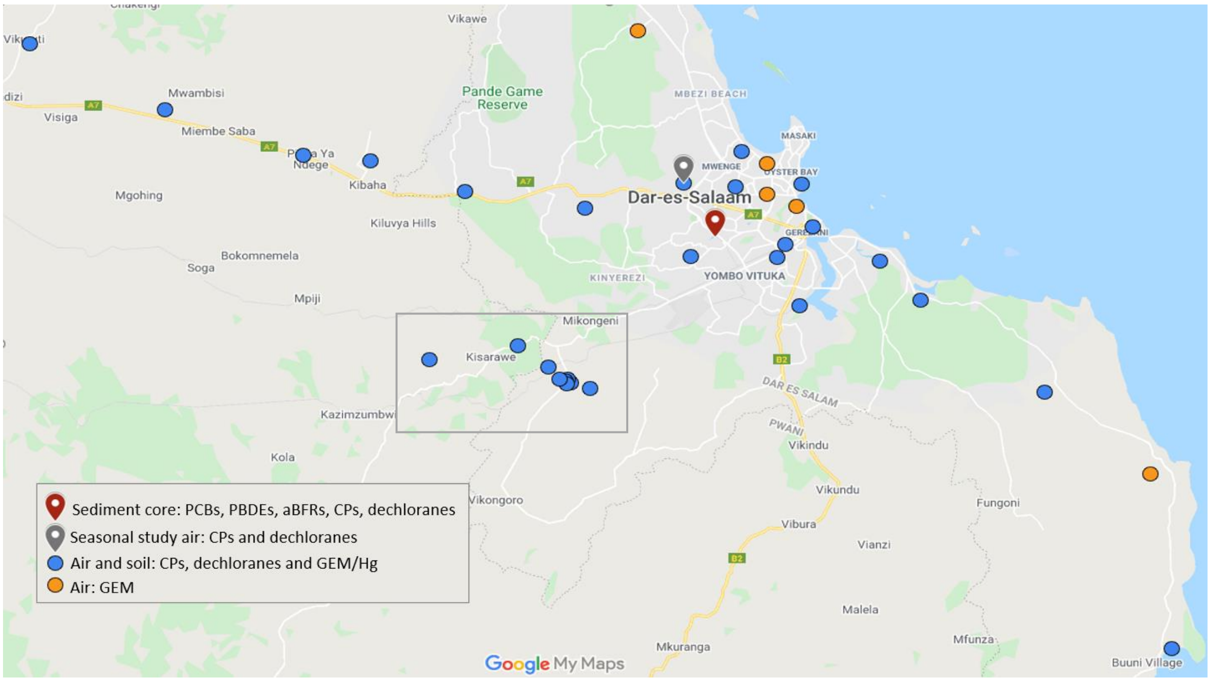

Figure 3: Map of study region showing sampling locations. Outlined box shown in more detail in Figure 4. Map from Google.com/maps.

Figure 4: Map of sampling locations on the municipal waste/e-waste transect. Map from Google.com/maps.

The assessment of temporal trends was based on a dated sediment core (**Paper II**). For this we targeted an urban area, to assess contaminants from local rather than remote sources. We also targeted a site where we would expect regular settling of sediments, which consisted of fine particles, e.g., clay and/or organic matter as this has higher sorption capacity compared to courser textured material like sand. Finding a site suitable for the collection of sediments cores was a challenge as the riverbeds in Dar es Salaam mainly consists of sand. However, a location was found on a floodplain system where sediments were expected to be undisturbed and consisted mainly of clay.

4.2 Sample collection

Two types of PAS were used for sampling targeted chemicals in the air, one aimed at CPs and dechloranes (PUF-PAS), and one for GEM. Deployment of the PAS, sample collection of soil (**Paper I** and **Paper III**), and sampling of sediment (**Paper II**) was carried out in February 2019. PAS were collected in April 2019, after an approximately 60-day sampling period. Six PUF-PAS were also deployed in succession for two-to-three-month periods between January 2018 and April 2019 at one suburban location to assess seasonal variation of CPs and dechloranes in air (**Paper I**). The last deployment in the sequence corresponded with the main sampling campaign.

Two sediment cores were collected, one for analysis of selected POPs and chemicals of emerging concern, and one for dating (**Paper II**). The cores both measured 39 cm and were sectioned on site into 1 cm thick slices (1-15 cm) and 2 cm thick slices (15-39 cm) making a total of 28 sediment core samples.

4.3 Sample preparation

The methods used for extraction and clean-up of air, soil and sediment samples for POPs and chemicals of emerging concern are described in detail in **Paper I** and **Paper II**, and references therein. These analyses were carried out at NILU - Norwegian Institute for Air Research, Kjeller, Norway. The sample preparation methods used on PAS for GEM and soil samples for total Hg are given in **Paper III** and references therein. These analyses were carried out at University of Toronto Scarborough, Canada, and University of Oslo, Norway, respectively. Only a summary of the methods is provided here.

Targeted chemicals in the PUF-discs in the PAS were extracted using soxhlet, while accelerated solvent extraction (ASE) was used for soil and sediment samples. N-hexane and acetone (1:1) was used for all extractions. ^{13}C labelled internal standards were added to all samples prior to extraction. For soil (**Paper I**), approximately 7 g wet weight (ww) of sample was used, while for sediments (**Paper II**) only 2 g ww was used. These amounts of soil and sediment were chosen to minimize matrix related instrumental interferences, while still achieving detectable signals for the targeted chemicals. Given the presence of notable amounts of elemental sulphur in sediments, activated copper powder was added to ASE cells prior to extraction for sediments. This was not necessary for soil.

Extracts from air, soil, and sediment samples were treated with concentrated sulphuric acid for removal of lipids and other acid-labile potential instrumental interferences. Extracts were further cleaned using column chromatography with activated silica eluted with diethyl ether/n-hexane (1:9). The solvent was changed to isooctane, and volume was reduced to 100 µL using a gentle stream of nitrogen. A recovery standard (1,2,3,4-tetrachloronapthalene) was added before instrumental analysis.

The radioisotope analysis and modelling work to provide dating of sediments was outsourced to GEL Laboratories, Charleston, USA.

4.4 Instrumental analysis and quantification

Details for instrumental analysis are given in **Papers I** to **III** and references therein. Briefly, for **Paper II**, concentrations of PCBs, PBDEs, and aBFRs were determined using gas chromatography high-resolution mass spectrometry (GC-HRMS) (AutoSpec, Waters, Manchester, UK). For **Paper I** and **Paper II**, concentrations of CPs and dechloranes were determined using gas chromatography quadrupole time-of-flight high-resolution mass spectrometry (GC/Q-TOF) (Agilent, Santa Clara, USA). Quantification was carried out using the isotope dilution principle. This was also implemented in the pattern deconvolution method which was used for quantification of CPs (Bogdal et al., 2015).

Analysis of PAS for GEM (**Paper III**), was carried out according to US EPA method 7473, using thermal combustion, amalgamation, and atomic absorption spectrometry (USEPA, 2007). Total Hg in soil was analysed using a similar method.

4.5 Statistical analysis

Data processing and statistical analysis was carried out using Microsoft Excel and R Studio. In general, distributions were non-normal, so non-parametric methods were used throughout. The Wilcoxon rank-sum test was used for testing of group differences and the Spearman's rank method was used for the determination of correlations. Results were deemed to be significant if $p < 0.05$. In **Paper I**, detection frequencies of the analysed chemicals of emerging concern were highly variable (14 to 100%). To account for the presence of censored values we used the robust Regression on Order statistical method to determine summary statistics for the chemicals which had detection frequency between 40 and 80%, as recommended by Helsel (2011).

4.6 Evaluation of applied methods

4.6.1 Quality control

Strict quality control measures were followed during the field campaigns and throughout laboratory procedures. A range of standards and standard reference materials (SRMs) were analysed to monitor method performance, which in general provided recoveries close to 100%, showing good method performance. Recovery of internal standard (**Paper I** and **Paper II**) was generally lower than this. However, when seen in the context of the results from spiked standards and SRMs, it is clear that the isotope dilution quantification method adequately accounts for losses during sample preparation.

Some elevated field- and method blank levels were seen in the study, particularly for the chemicals of emerging concern, but also for GEM. For chemicals of emerging concern, notably for the CPs, this is a well-known and relatively common analytical issue, resulting in high detection limits in many studies (Möckel et al., 2020; van Mourik et al., 2020a; van Mourik et al., 2020b). Possible explanations include the presence of CPs in the indoor environment, including laboratories (Fridén et al., 2011), and thus the possibility of contamination during sample preparation through laboratory air/dust. Also, contamination of samples during fieldwork and transport is a common issue, particularly when fieldwork is conducted in distant and remote regions, involving elevated temperatures, dusty conditions, and multiple transportation steps. In the case of GEM, such contamination is likely the explanation for slightly elevated field blank GEM levels. Overall, as the concentrations of the targeted chemicals of emerging concern and GEM were relatively high in the studied region, the blank levels only had a minor effect on analytical data. This is illustrated for CPs and dechloranes in Figures S2 to S4 in the SI for **Paper I**. The LOQ for GEM was in the lower end of the range of Southern Hemisphere background concentrations (**Paper III**). Only three locations had concentrations below the LOQ (reported in italic in the following text).

4.6.2 Calculation of air concentrations

Given the uncertainty associated with SRs for SVOCs (see section 3.2.1.3), there are arguments for presenting spatial data for SVOCs like CPs and dechloranes from PAS on a per sampler basis, rather than as air concentrations on a volume basis (Wania and Shunthirasingham, 2020). However, this limits the possibility of comparing results with other studies. **Paper I** reported CPs in air for the first time from Africa, making comparisons with other regions highly relevant.

To calculate volume-based air concentrations of CPs and dechloranes, we applied two different approaches, including a modelling-based approach with equations gathered from the much-used Harner Template (Harner, 2016), which allows for congener group specific SRs. It also accounts for volatile chemicals entering the curvilinear phase (Figure 2) and partitioning to particles for low volatility SVOCs. The limitation of this approach is that it relies on physicochemical property data for each CP congener group as input. Good quality data of this type was at the time of our study only available for a limited number of congener groups (Glüge et al., 2013), hence this approach only allowed for quantification of a fraction of the CPs analysed in this study. The congener group specific air concentrations were thus only used as input to calculations of soil/air fugacity ratios (see SI **Paper I** for further detail). In the main text of **Paper I**, we chose to present data for total CPs and dechloranes with volume-based air concentrations calculated from generic SRs gathered from literature. These SRs were based on calibration studies on CPs and dechloranes as these allow inclusion of all analysed CP congener groups. Doing so allowed for comparisons with other studies using the same method. The limitations of this approach are however acknowledged, particularly for CPs, which span a wide range of K_{OA}. The modelled ∑SCCPs air concentrations (based on the 24 congener groups where physicochemical property data were available) were on average 28% lower than the

SCCP air concentrations calculated using generic SR (for all 34 congener groups). This indicates that the generic SR provides a reasonable estimate. Recently, the Harner template has been adapted to CPs, including data on the relevant physicochemical properties for a wider range of congener groups (Niu et al., 2021). For future work, use of this template is recommended.

4.6.3 Dating of sediment core

The dating of the sediment core was challenging, given low content of the radioisotopes which the dating process is based on (**Paper II**). Consequently, only sediment layers from the middle and upper section of the core could be dated. The dated sediment layers covered 1962 to 2019, while the layers below were classified as pre-1962. The low content of relevant radioisotopes also caused some uncertainty in the dating, particularly for the older layers. However, the main conclusions derived from the analysis of the sediment layers relate to the upper, more recent sediment layers, and are thus not affected by uncertainty in dating of older layers.

5. Results and discussion

5.1 POPs

In **Paper II**, we demonstrated that there were increasing trends of PCBs and PBDEs in sediments from Dar es Salaam (Figure 5). While long-term time trends of PCBs derived from dated sediment cores have been reported from Uganda (Arinaitwe et al., 2016) and Morocco (Giuliani et al., 2015), no such studies have previously been conducted for PBDEs on the African continent. The time trends of PCBs and PBDEs found in our study were compared with similar studies from other developing and newly industrialized regions, and regions which has been industrialized for an extended time. Several of the studies from developing and newly industrialized regions showed peak concentrations in the uppermost layers of sediment. The overall tendency for POPs in industrialized regions was for concentrations to peak around the year of peak production (~1970 for PCBs, ~2000 for PBDEs). Overall, the findings in our study and the studies we compared with supports the hypothesis expressed by Breivik et al. (2011), that source regions for POPs are shifting geographically away from industrialized regions, where they were produced and more extensively used, towards developing and newly industrialized regions.

The increasing trends of PCBs and PBDEs suggests that unlike in the Global North, international regulatory efforts have not yet been effective in lowering environmental burdens of these chemicals in Dar es Salaam.

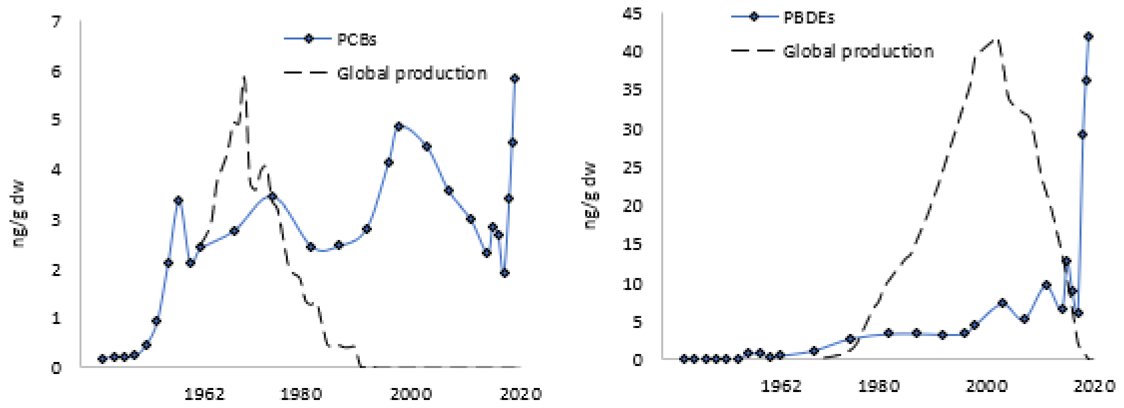

*Figure 5: Concentration of ∑PCBs and ∑PBDEs, respectively, in sediments layers from Dar es Salaam dated from before 1962–2019, along with trend in global production for PCBs from Breivik et al. (2002), and trend in global production for PBDEs from Abbasi et al. (2019) (**Paper II**).*

Time trends in ∑PBDEs showed correlations with parameters relating to socioeconomic development in the region, including growth in gross domestic product (GDP) per capita, urban population, consumption, and waste generation. Time trends in ∑PCBs did not show such correlations. The difference likely reflects the type of products these POPs were used in, where PBDEs to a larger degree are associated with contemporary consumer products (Abbasi et al., 2019). PCBs on the other hand, were mainly used in closed compartments in large electrical equipment, e.g., transformers, in Tanzania (IPEN, 2005). Strong correlations were seen between organic matter content in sediments and concentration of PCBs and PBDEs. Organic matter content was however discounted as a major governing factor for concentrations of these POPs in sediments, as all major features of the time-trends remained when concentrations were normalized to organic matter content. Neither the trends of PCBs nor the trends PBDEs appeared to be driven by secondary sources (re-mobilization of contaminated surface reservoirs). The increase in ∑PCBs in sediments corresponding to the late 2010s therefore remains largely unexplained. Declines in atmospheric concentrations of PCBs is documented in a recent publication regarding long-term trends of atmospheric POPs concentrations at seven locations in Africa, however this was not significant at the three urban sites (White et al., 2020). They attribute slow rate of decline and some elevated concentrations at urban sites to continued PCBs emissions in Africa (White et al., 2020). A study on atmospheric concentrations of PCBs, near an un-regulated e-waste recycling site in Ghana, showed highly elevated concentrations, confirming that e-waste is a source of PCBs in Africa (Hogarh et al., 2018). There are however no comparable large-scale e-waste processing sites located within the watershed of the sediment core collection site in our study.

5.2 Chemicals of emerging concern

5.2.1 Temporal trends of chemicals of emerging concern

Paper II is the first study to report sediment core based long-term temporal trends of aBFRs, CPs, and dechloranes from the African continent. This study showed that the increase of some of these studied chemicals of emerging concern in sediments were dramatic (Figure 6). This was particularly the case for CPs, which also had the highest concentration by two to three orders of magnitude compared to the other analysed chemicals of emerging concern and POPs. Also, the aBFR DBDPE had strongly increasing concentrations during recent years. The dechloranes, on the other hand, showed diverging trends, with DP increasing, while Dec 602 and Dec 603 displayed flat or declining trends.

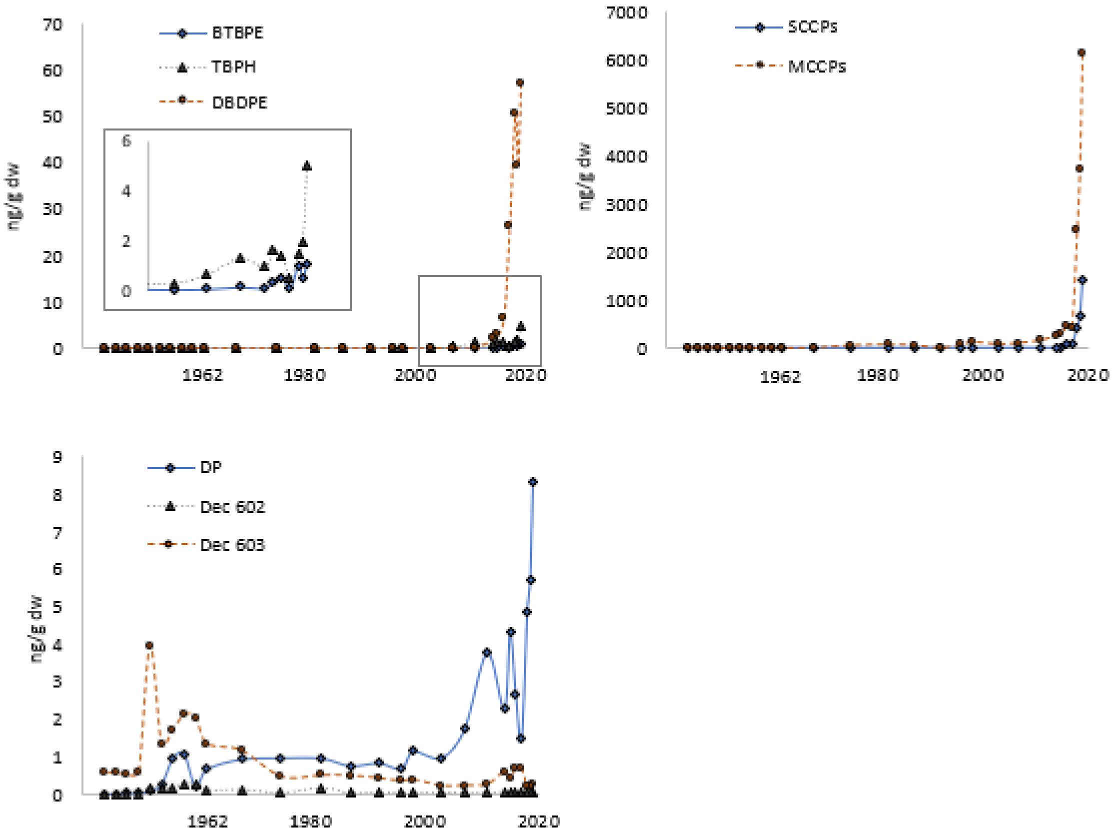

*Figure 6: Concentration of aBFRs, CPs, and dechloranes in sediments layers from Dar es Salaam dated from before 1962–2019 (**Paper II**).*

Significant correlation was found between temporal trends of the studied chemicals of emerging concern with known use in consumer products (aBFRs, CPs, and DP), and factors relating to socioeconomic development in the region. Dec 602 and Dec 603, on the other hand, showed no or negative correlations with socioeconomic factors. Significant correlations were also found between rainfall anomalies and sediment concentrations for CPs and DBDPE. As such, a significant increase in rain amounts during the late 2010s may have contributed to the increases in CPs and DBDPE in sediments, as this may have mobilized these chemicals via erosion of contaminated surface reservoirs.

5.2.2 CPs and dechloranes in air and soil

Paper I documented the concentrations of two groups of chemicals of emerging concern, the CPs and dechloranes, in air and soil along an urban-rural transect across Dar es Salaam, and a transect covering the city's main municipal waste dumpsite and an e-waste handler (Table 2, Table 3). These data represent the first reports of CPs in air and dechloranes in soil from the African continent.

*Table 2: Descriptive statistics of air concentrations of CPs and dechloranes in the Dar es Salaam region. (**Paper I**).*

	SCCPs (ng/m^3)	MCCPs (ng/m^3)	DP (pg/m^3)	Dec 602 (pg/m^3)	Dec 603^a (pg/m^3)
Range	0.3 - 63	<0.4 - 35	<0.4 - 20	<0.007 - 0.2	<0.007 - 0.2
Average	22	9	2	0.05	-
Median	13	5	0.7	0.03	-
Std. dev.	20	11	4	0.06	-
Det. freq.	100%	93%	57%	46%	14%

[a] Detection frequency of Dec 603 too low for determination of descriptive statistics

*Table 3: Descriptive statistics of concentrations of CPs and dechloranes in soil (ng/g dw) (**Paper I**).*

	SCCPs	MCCPs	DP	Dec 602	Dec 603
Range	<11 – 5 300	<19 – 5 100	<0.01 - 6	<0.001 - 0.05	<0.001 - 3
Average	330	640	0.7	0.006	0.2
Median	51	170	0.2	0.003	0.009
Std. dev.	1 000	1 200	1	0.01	0.6
Det. freq.	89%	86%	89%	71%	61%

5.2.2.1 Urban -rural transect

There were significantly higher concentrations of SCCPs and MCCPs in urban air compared to rural air, while suburban locations had intermediate concentrations. Urban/rural ratios were 5 and 10 for SCCPs and MCCPs, respectively. There were similar findings for CPs in soil with urban/rural ratios of 8 and 11 for SCCPs and MCCPs, respectively. Higher urban concentrations are consistent with studies from India, Pakistan, Bangladesh, and China (Chaemfa et al., 2014; Nøst et al., 2015; Wang et al., 2013). However, as China (and some other parts of Asia) are major producers of CPs, it is more difficult to deconvolute their sources related to production of CPs from diffuse urban emissions relating e.g., to use and disposal of CPs containing products in these regions.

Dechloranes were found at much lower concentrations in air and soil compared to CPs. For most of the analysed dechloranes, higher concentrations were found in air and soil in urban compared to rural locations, but not significantly so in all cases. Urban/rural ratios for DP was 5 for air and 14 for soil. For Dec 602 and Dec 603, urban/rural ratios were 2 and 5 for soil, respectively, but urban/rural ratios could not be determined for air given lack of detection of these compounds in air in rural areas.

5.2.2.2 Municipal waste/e-waste transect

Within the municipal waste/e-waste transect, high concentrations of CPs in air were found at both the municipal waste dumpsite and the e-waste handler, with elevated concentrations also in the vicinity of these two locations. In soil, the highest concentrations of CPs were found at the municipal waste dumpsite, followed by the e-waste handler, while the concentrations of CPs were low in the vicinity of these locations. This demonstrates that handling of both municipal waste and e-waste represent significant sources for CPs. This is consistent with the findings of **Paper II**, which showed strong correlations between CPs in sediments and consumption and waste generation.

DP was found at higher concentrations at the e-waste handler compared to the municipal waste dumpsite, suggesting DP is more associated with e-waste compared to municipal waste. This is consistent with the known uses of DP. Dec 602 and Dec 603 did not show any apparent connection with municipal waste or e-waste, suggesting no or minor presence of these chemicals in consumer products/electronics in the region. This is also consistent with the findings in **Paper II**.

5.2.3 Environmental processes and fate

Air concentrations of the less volatile of the studied chemicals of emerging concern, MCCPs and DP, showed significant negative linear association with the amount of rainfall throughout the year in our seasonal study (**Paper I**). For the relatively more volatile SCCPs, the association was also negative, although not significantly so. Most research on seasonal variation of SVOCs like CPs and dechloranes in air has been conducted in temperate and arctic regions. In these regions, seasonal variation is often driven by the large fluctuations in temperatures affecting the volatility of the SVOCs from primary and secondary sources, and in some cases seasonality of emissions from some primary sources (Shunthirasingham et al., 2018; Wong et al., 2021). Seasonal variation in atmospheric SVOCs in the tropics with high and stable temperatures remains largely understudied (Lammel et al., 2018). Our results, although based on limited data, suggests that in the studied region, the monsoonal rain patterns drive seasonal variation by washout of particle associated SVOCs. Heavy rain during monsoon season also increases mobilization of SVOCs via erosion of contaminated surface reservoirs and decreases volatilization of SVOCs in soil (Gillett et al., 2017; Wong and Wania, 2011).

In addition to an urban-rural concentration gradient, we also observed an urban-rural fractionation pattern of CPs in soil (**Paper I**). In soil at the more remote locations the less chlorinated, shorter chain length (i.e., more volatile) CP congener groups dominated, while the higher chlorinated and longer chain length (i.e., less volatile) CP congener groups were found in soil from urban areas (Figure 7). This pattern was not seen for air, where the congener group profile was relatively uniform across location categories. This suggests that the mobility of the less volatile congener groups via atmospheric transport is limited in the region, despite high ambient temperatures and low content of soil organic matter.

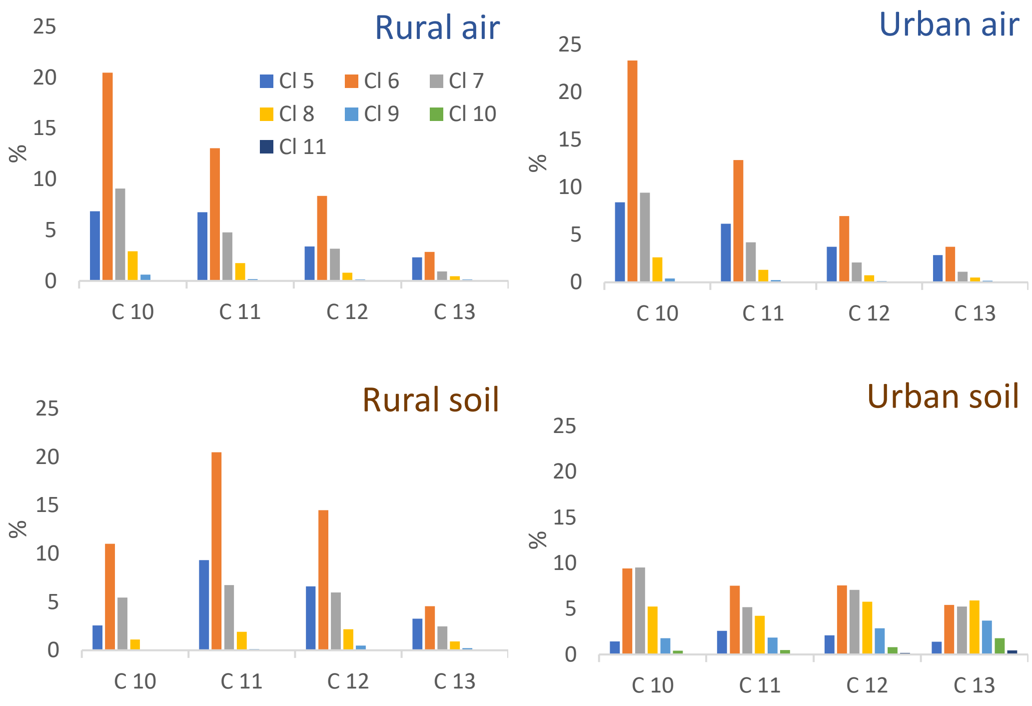

Figure 7: Average relative abundance of SCCP congener groups in air and soil from rural and urban locations. Cl and C denote the number of chlorides and C the number of carbons on the congener groups.

Soil organic matter content was found to be low in the region (median 1.7 %, range <0.01-9.6 %), and overall appeared to have low impact on the spatial distribution of CPs and DP in soil. Dec 602 and Dec 603 did however show significant correlations with organic matter, although the physicochemical partitioning properties of these dechloranes are not very different to DP (Figure 1). This can be rationalized by the lack of current sources for Dec 602 and Dec 603 as compared to DP., For Dec 602 and Dec 603, the historic rather than current nature of sources were shown by the time trends documented in **Paper II**. DP on the other hand, were documented to have current sources by the elevated air concentrations detected near e-waste processing (**Paper I**), and by the increasing trends documented in **Paper II**. Thus, the spatial distribution of DP was likely dominated by proximity to sources, while for Dec 602 and Dec 603, biogeochemical processes, such as sorption to organic matter, have been allowed to play out over time and has come to govern their spatial distribution.

5.3 Mercury

GEM concentrations along the urban-rural transect and the municipal waste/e-waste transect ranged from *0.79* to 5.34 ng/m^3, while total Hg in soil ranged from 0.0067 to 0.098 mg/kg (**Paper III**).

5.3.1 Urban-rural transect

Overall, higher GEM concentrations were found in urban areas and lower concentrations were found in the more remote locations, although the difference between urban and rural/suburban areas was not significant. This was due to a few samples with low concentrations from urban areas, and the presence of some local sources in rural/suburban areas. As for GEM, urban and rural locations were not significantly different in terms of total Hg concentrations in soil.

Annual GEM emissions in the urban area, as estimated from the measured GEM concentrations in our study, suggests that the regional emission estimates given by Streets et al. (2019) may be biased low. Previous studies on Hg emissions have suggested ASGM and coal fires power plants as the dominant sources in Africa (Masekoameng et al., 2010; Pacyna et al., 2010; Streets et al., 2019), although neither of these sources are known to be relevant in Dar es Salaam. Two urban locations in our study showed particularly high GEM concentration (5.13 and 5.34 ng/m^3). We were however unable to identify the sources.

5.3.2 Municipal waste/e-waste transect

GEM concentrations at the municipal waste dumpsite and the e-waste handler were somewhat elevated. However, these sites appeared to be less important sources for GEM than for CPs and DP. Concentrations of total Hg in soil at the municipal waste dumpsite and the e-waste site were only the ninth and fifth highest out of the 28 samples collected, respectively. The comparatively low concentrations of GEM and total Hg at these sites are likely a result of low Hg content in products and waste in the region.

5.3.3 Environmental processes and fate

Soil in the region appeared to have low retention capacity for Hg, compared to studies of Hg in soil from other regions, and as compared to some of the studied chemicals of emerging concern (**Paper I**). For Hg, this is likely explained by the process of photoreduction of Hg(II) to GEM (Carpi and Lindberg, 1997; Eckley et al., 2016; Xin and Gustin, 2007) and the higher volatility of GEM compared to the studied chemicals of emerging concern. The levels of total Hg in soil were found to be significantly correlated to the soil organic matter content. This could be a consequence of higher soil organic matter and low photoreduction being confounding factors, as a high degree of vegetation cover may produce higher levels of soil organic matter through litterfall and also provide shade from intense sunlight. Influence of vegetation cover on soil Hg has been demonstrated previously by e.g., Eckley et al. (2016). Normalizing Hg content in soil to organic matter content overall provided a similar trend as compared to dry weight concentrations, with some exceptions. Total Hg in soil at the municipal waste dumpsite and the e-waste site shifted from ninth to sixth and fifth to fourth highest out of the 28 samples collected, respectively, when normalized to organic matter content. This reflects the presence of sources for Hg and low levels of organic matter along the municipal waste/e-waste transect.

6. Conclusions

This thesis presents an assessment of occurrence, distribution, and sources of some POPs, chemicals of emerging concern, and Hg in and around Dar es Salaam, Tanzania, based on an investigation of their spatial and temporal trends. The following were the main conclusions regarding temporal trends of POPs based on dated sediment layers:

- Moderate increases were found for PCBs and PBDEs in sediment layers corresponding to the late 2010s.
- Time trends of ∑PBDEs showed strong correlations with factors related to socioeconomic development in the region (growth in GDP, population, consumption, and waste generation).
- ∑PCBs did not show such correlations.
- Differences in time trends of selected POPs in the Global North and our results suggest that any impact of global regulatory efforts on the time trends of these POPs in Dar es Salaam is yet to be seen.

The following were the main conclusions regarding chemicals of emerging concern based on their temporal and spatial distributions:

- Strong increases were observed for the studied chemicals of emerging concern, particularly CPs and some aBFRs, in sediment layers corresponding to the late 2010s.
- Of the dechloranes, DP concentrations peaked in the contemporary surface sediment layers, while Dec 602 and Dec 603 concentrations peaked in sediment layers dated to pre-1962.
- Socioeconomic development factors had strong explanatory value for the time trends of chemicals of emerging concern that are commonly used in consumer products (i.e., CPs, aBFRs, and DP), while no or negative correlations were found for Dec 602 and Dec 603.
- Urban-rural gradients were generally observed for concentrations of CPs and dechloranes in air and soil.
- Municipal waste and e-waste handling were important point sources for CPs, while e-waste handling was the most important source for DP.
- Organic matter content in sediment was not a major factor governing temporal trends of CPs or dechloranes, though organic matter content in soil affected the spatial distribution of Dec 602 and Dec 603.

- Spatial trends of dechloranes in air and soil suggested a lack of significant current sources for Dec 602 and Dec 603 within the region.
- The more volatile CPs appeared to be susceptible to atmospheric transport. Less volatile CPs and dechloranes appeared to remain in soil near their source.
- Monsoonal rain patterns affect the environmental fate of the studied chemicals of emerging concern.

The following were the main conclusions regarding Hg based on its spatial distribution in air and soils:

- For GEM and total Hg in soil, urban concentrations were not significantly higher than rural/suburban concentrations because of some elevated concentrations in rural/suburban areas.
- Concentrations of GEM exceeding 5 ng/m^3 in air suggested significant sources in the urban area, however these could not be identified.
- Predicted annual GEM emissions into air, based on observations, suggest existing regional emission estimates may be biased low.
- GEM concentrations near municipal waste and e-waste processing sites were only moderately elevated above Southern Hemisphere background.

7. Future Perspectives

Most locations included in monitoring programs for atmospheric POPs, chemicals of emerging concern, and Hg are situated in the Global North. Expansion of existing global air monitoring programs, by the addition of more locations on the African continent, and implementation of new air monitoring programs for Africa is recommended. This is a prerequisite to understand the potential risk of harmful pollutants to human health and ecosystems in Africa, as input from the atmosphere represents a major pathway for all the studied chemicals to terrestrial and aquatic ecosystems, and thereby also the human food-chain. Further, the inclusion of both urban and background locations in such monitoring efforts could provide insights into local versus distant sources (e.g., LRT) and primary vs. secondary emissions. Long-term monitoring efforts are also encouraged, as this may show how primary emissions respond to regulatory efforts and other emission-reducing measures.

We also encourage the collection and analysis of sediment cores from more sites within Dar es Salaam. This would be useful both to understand how representative the time-trends obtained in this study are for the region, and to follow the development of time trends of the studied POPs and chemicals of emerging concern, i.e., whether they continue to increase, stabilize, or decline. More studies using sediment cores from other developing and newly industrialized regions in the Global South are also recommended, as these are regions where monitoring of environmental contaminants has largely been lacking. The natural archives of sequentially settled sediments constitute an alternative method to assess the long-term time trends. The potential shift in global source regions of POPs could thereby be better documented and understood.

Our investigation into the temporal trends of PCBs and PBDEs, chemicals previously used in consumer products, electronics, and electrical equipment, showed that their concentrations in sediments in Dar es Salaam were increasing. We thus recommend investigations into the spatial distribution of these POPs in the region to identify their sources and emissions.

As elevated concentrations of CPs and DP were observed near municipal waste and e-waste handling sites, we recommend improvements to waste handling practices at a local level to limit emissions. This would also be relevant for limiting emissions of other chemicals extensively used in consumer products, e.g., PBDEs and aBFRs. At an international level, the closing of loopholes and strengthening of existing regulation of trade and export of hazardous products and waste is recommended. In addition, further efforts to address and account for potential transitions in global source regions should be included in international regulatory efforts like the Stockholm Convention on POPs and the Minamata Convention on Hg.

In addition, further studies should be carried out on the effects of monsoonal rain patterns on seasonal trends of contaminant mobility by air and water transport. This could help inform future sampling strategies and increase the understanding of the overall environmental fate of the studied chemicals in regions with monsoonal rain.

References

Abbasi, G., Li, L., Breivik, K., 2019. Global historical stocks and emissions of PBDEs. Environmental science & technology 53, 6330-6340.

Alaee M, Arias P, Sjödin A, Bergman Å. An overview of commercially used brominated flame retardants, their applications, their use patterns in different countries/regions and possible modes of release. Environment international 2003; 29: 683-689.

Arinaitwe K, Rose NL, Muir DC, Kiremire BT, Balirwa JS, Teixeira C. Historical deposition of persistent organic pollutants in Lake Victoria and two alpine equatorial lakes from East Africa: Insights into atmospheric deposition from sedimentation profiles. Chemosphere 2016; 144: 1815-1822.

Arp HPH, Villers F, Lepland A, Kalaitzidis S, Christanis K, Oen AM, et al. Influence of historical industrial epochs on pore water and partitioning profiles of polycyclic aromatic hydrocarbons and polychlorinated biphenyls in Oslo Harbor, Norway, sediment cores. Environmental toxicology and chemistry 2011; 30: 843-851.

Asante, K.A., Amoyaw-Osei, Y., Agusa, T., 2019. E-waste recycling in Africa: risks and opportunities. Current Opinion in Green and Sustainable Chemistry 18, 109-117.

Baldé CP, Forti V, Gray V, Kuehr R, Stegmann P. The global e-waste monitor 2017: Quantities, flows and resources: United Nations University, International Telecommunication Union, and International Solid Waste Association, Bonn/Geneva/Vienna, 2017.

Barber JL, Sweetman AJ, Thomas GO, Braekevelt E, Stern GA, Jones KC. Spatial and temporal variability in air concentrations of short-chain (C10− C13) and medium-chain (C14− C17) chlorinated n-alkanes measured in the UK atmosphere. Environmental science & technology 2005; 39: 4407-4415.

Bartkow ME, Booij K, Kennedy KE, Müller JF, Hawker DW. Passive air sampling theory for semivolatile organic compounds. Chemosphere 2005; 60: 170-176.

Bartkow ME, Jones KC, Kennedy KE, Holling N, Hawker DW, Müller JF. Evaluation of performance reference compounds in polyethylene-based passive air samplers. Environmental Pollution 2006; 144: 365-370.

Bogdal C, Alsberg T, Diefenbacher PS, MacLeod M, Berger U. Fast quantification of chlorinated paraffins in environmental samples by direct injection high-resolution mass spectrometry with pattern deconvolution. Analytical chemistry 2015; 87: 2852-2860.

Bogdal C, Scheringer M, Abad E, Abalos M, Van Bavel B, Hagberg J, et al. Worldwide distribution of persistent organic pollutants in air, including results of air monitoring by passive air sampling in five continents. TrAC Trends in Analytical Chemistry 2013; 46: 150-161.

Bohlin-Nizzetto P, Melymuk L, White KB, Kalina J, Madadi VO, Adu-Kumi S, et al. Field- and model-based calibration of polyurethane foam passive air samplers in different climate regions highlights differences in sampler uptake performance. Atmospheric Environment 2020: 117742.

Bohlin P, Audy O, Škrdlíková L, Kukučka P, Přibylová P, Prokeš R, et al. Outdoor passive air monitoring of semi volatile organic compounds (SVOCs): a critical evaluation of performance and limitations of polyurethane foam (PUF) disks. Environmental Science: Processes & Impacts 2014; 16: 433-444.

Breivik K, Armitage JM, Wania F, Jones KC. Tracking the global generation and exports of e-waste. Do existing estimates add up? Environmental science & technology 2014; 48: 8735-8743.

Breivik K, Armitage JM, Wania F, Sweetman AJ, Jones KC. Tracking the global distribution of persistent organic pollutants accounting for e-waste exports to developing regions. Environmental science & technology 2015; 50: 798-805.

Breivik K, Gioia R, Chakraborty P, Zhang G, Jones KC. Are reductions in industrial organic contaminants emissions in rich countries achieved partly by export of toxic wastes? Environmental science & technology 2011; 45: 9154-9160.

Breivik K, Sweetman A, Pacyna JM, Jones KC. Towards a global historic emission inventory for selected polychlorinated biphenyl congeners–a mass balance approach. Sci. Total Environ. 2002a; 290: 181-224.

Breivik K, Sweetman A, Pacyna JM, Jones KC. Towards a global historical emission inventory for selected PCB congeners—a mass balance approach: 2. Emissions. Science of the Total Environment 2002b; 290: 199-224.

Breivik K, Sweetman A, Pacyna JM, Jones KC. Towards a global historical emission inventory for selected PCB congeners—a mass balance approach: 3. An update. Science of the Total Environment 2007; 377: 296-307.

Carpi A, Lindberg SE. Sunlight-mediated emission of elemental mercury from soil amended with municipal sewage sludge. Environmental Science & Technology 1997; 31: 2085-2091.

Chaemfa C, Xu Y, Li J, Chakraborty P, Hussain Syed J, Naseem Malik R, et al. Screening of atmospheric short-and medium-chain chlorinated paraffins in India and Pakistan using polyurethane foam based passive air sampler. Environmental science & technology 2014; 48: 4799-4808.

Chakraborty P, Selvaraj S, Nakamura M, Prithiviraj B, Cincinelli A, Bang JJ. PCBs and PCDD/Fs in soil from informal e-waste recycling sites and open dumpsites in India: levels, congener profiles and health risk assessment. Science of the Total Environment 2018; 621: 930-938.

Chen S-J, Tian M, Wang J, Shi T, Luo Y, Luo X-J, et al. Dechlorane Plus (DP) in air and plants at an electronic waste (e-waste) site in South China. Environmental Pollution 2011; 159: 1290-1296.

Combi T, Miserocchi S, Langone L, Guerra R. Polychlorinated biphenyls (PCBs) in sediments from the western Adriatic Sea: sources, historical trends and inventories. Science of the Total Environment 2016; 562: 580-587.

Covaci A, Harrad S, Abdallah MA-E, Ali N, Law RJ, Herzke D, et al. Novel brominated flame retardants: a review of their analysis, environmental fate and behaviour. Environment international 2011; 37: 532-556.

Dalla Valle M, Jurado E, Dachs J, Sweetman AJ, Jones KC. The maximum reservoir capacity of soils for persistent organic pollutants: implications for global cycling. Environmental Pollution 2005; 134: 153-164.

de Wit CA, Herzke D, Vorkamp K. Brominated flame retardants in the Arctic environment—trends and new candidates. Science of the Total Environment 2010; 408: 2885-2918.

Dendievel A-M, Mourier B, Coynel A, Evrard O, Labadie P, Ayrault S, et al. Spatio-temporal assessment of the polychlorinated biphenyl (PCB) sediment contamination in four major French river corridors (1945–2018). Earth System Science Data 2020; 12: 1153-1170.

Drage DS, Newton S, de Wit CA, Harrad S. Concentrations of legacy and emerging flame retardants in air and soil on a transect in the UK West Midlands. Chemosphere 2016; 148: 195-203.

Driscoll CT, Mason RP, Chan HM, Jacob DJ, Pirrone N. Mercury as a global pollutant: sources, pathways, and effects. Environmental science & technology 2013; 47: 4967-4983.

Eckley CS, Tate MT, Lin C-J, Gustin M, Dent S, Eagles-Smith C, et al. Surface-air mercury fluxes across Western North America: A synthesis of spatial trends and controlling variables. Science of the Total Environment 2016; 568: 651-665.

EU. Regulation (EC) No 1907/2006 of the European Parliament and of the Council of 18 December 2006 concerning the Registration, Evaluation, Authorisation and Restriction of Chemicals (REACH), establishing a European Chemicals Agency, amending Directive 1999/45/EC and repealing Council Regulation (EEC) No 793/93 and Commission Regulation (EC) No 1488/94 as well as Council Directive 76/769/EEC and Commission Directives 91/155/EEC, 93/67/EEC, 93/105/EC and 2000/21/EC, 2006.

EU. Directive 2011/65/EU of the European Parliament and of the Council of 8 June 2011 on the restriction of the use of certain hazardous substances in electrical and electronic equipment 2011.

EU. Directive 2012/19/EU of the European Parliament and of the Council of 4 July 2012 on waste electrical and electronic equipment (WEEE), 2012.

Farrar N, Harner T, Shoeib M, Sweetman A, Jones KC. Field deployment of thin film passive air samplers for persistent organic pollutants: a study in the urban atmospheric boundary layer. Environmental science & technology 2005; 39: 42-48.

Fiedler H. Short-chain chlorinated paraffins: production, use and international regulations. Chlorinated paraffins. Springer, 2010, pp. 1-40.

Forti V, Baldé C, Kuehr R, Bel G. The Global E-waste Monitor 2020: Quantities, flows and the circular economy potential. United Nations University (UNU)/United Nations Institute for Training and Research (UNITAR) – co-hosted SCYCLE Programme, International Telecommunication Union (ITU) & International Solid Waste Association (ISWA), Bonn/Geneva/Rotterdam., 2020.

Fridén UE, McLachlan MS, Berger U. Chlorinated paraffins in indoor air and dust: concentrations, congener patterns, and human exposure. Environment international 2011; 37: 1169-1174.

Fu J, Zhou Q, Liu J, Liu W, Wang T, Zhang Q, et al. High levels of heavy metals in rice (Oryzasativa L.) from a typical E-waste recycling area in southeast China and its potential risk to human health. Chemosphere 2008; 71: 1269-1275.

Gillett RW, Galbally IE, Keywood MD, Powell JC, Stevenson G, Yates A, et al. Atmospheric short-chain-chlorinated paraffins in Melbourne, Australia–first extensive Southern Hemisphere observations. Environ. Chem. 2017; 14: 106.

Gioia R, Eckhardt S, Breivik K, Jaward FM, Prieto A, Nizzetto L, et al. Evidence for major emissions of PCBs in the West African region. Environmental science & technology 2011; 45: 1349-1355.

Giuliani S, Piazza R, El Moumni B, Polo FP, Vecchiato M, Romano S, et al. Recognizing different impacts of human and natural sources on the spatial distribution and temporal trends of PAHs and PCBs (including PCB-11) in sediments of the Nador Lagoon (Morocco). Science of the Total Environment 2015; 526: 346-357.

Glüge J, Bogdal C, Scheringer M, Buser AM, Hungerbühler K. Calculation of physicochemical properties for short-and medium-chain chlorinated paraffins. Journal of Physical and Chemical Reference Data 2013; 42: 023103.

Glüge J, Wang Z, Bogdal C, Scheringer M, Hungerbühler K. Global production, use, and emission volumes of short-chain chlorinated paraffins–A minimum scenario. Science of the Total Environment 2016; 573: 1132-1146.

Goss K-U, Buschmann J, Schwarzenbach RP. Adsorption of organic vapors to air-dry soils: model predictions and experimental validation. Environmental science & technology 2004; 38: 3667-3673.

Gouin T, Mackay D, Webster E, Wania F. Screening chemicals for persistence in the environment. Environmental science & technology 2000; 34: 881-884.

Gustin MS, Lyman SN, Kilner P, Prestbo E. Development of a passive sampler for gaseous mercury. Atmospheric Environment 2011; 45: 5805-5812.

Halvorsen HL, Bohlin-Nizzetto P, Eckhardt S, Gusev A, Krogseth IS, Moeckel C, et al. Main sources controlling atmospheric burdens of persistent organic pollutants on a national scale. Ecotoxicology and Environmental Safety 2021; 217: 112172.

Harner T. v1 3 Template for Calculating PUF and SIP Disk Sample Air Volumes. March, 2016.

Harner T, Farrar NJ, Shoeib M, Jones KC, Gobas FA. Characterization of polymer-coated glass as a passive air sampler for persistent organic pollutants. Environmental science & technology 2003; 37: 2486-2493.

Harner T, Shoeib M, Diamond M, Stern G, Rosenberg B. Using passive air samplers to assess urban− rural trends for persistent organic pollutants. 1. Polychlorinated biphenyls and organochlorine pesticides. Environmental Science & Technology 2004; 38: 4474-4483.

Heim S, Schwarzbauer J. Pollution history revealed by sedimentary records: a review. Environmental chemistry letters 2013; 11: 255-270.

Helsel DR. Statistics for censored environmental data using Minitab and R. Vol 77: John Wiley & Sons, 2011. ISBN 1118162765.

Hogarh JN, Seike N, Kobara Y, Carboo D, Fobil JN, Masunaga S. Source characterization and risk of exposure to atmospheric polychlorinated biphenyls (PCBs) in Ghana. Environmental Science and Pollution Research 2018; 25: 16316-16324.

Hoh E, Zhu L, Hites RA. Dechlorane Plus, a chlorinated flame retardant, in the Great Lakes. Environmental science & technology 2006; 40: 1184-1189.

Holt E, Bohlin-Nizzetto P, Borůvková J, Harner T, Kalina J, Melymuk L, et al. Using long-term air monitoring of semi-volatile organic compounds to evaluate the uncertainty in polyurethane-disk passive sampler-derived air concentrations. Environmental Pollution 2017; 220: 1100-1111.

Hoornweg, D., and Bhada-Tata, P. (2012). What a waste: a global review of solid waste management. Urban Development Series Knowledge Papers; World Bank: Washington, D.C., 2012, No. 15

Huang J, Choi H-D, Landis MS, Holsen TM. An application of passive samplers to understand atmospheric mercury concentration and dry deposition spatial distributions. Journal of Environmental Monitoring 2012; 14: 2976-2982.

Huang X, Li M, Friedli HR, Song Y, Chang D, Zhu L. Mercury emissions from biomass burning in China. Environmental science & technology 2011; 45: 9442-9448.

Hung H, Kallenborn R, Breivik K, Su Y, Brorström-Lundén E, Olafsdottir K, et al. Atmospheric monitoring of organic pollutants in the Arctic under the Arctic Monitoring and Assessment Programme (AMAP): 1993–2006. Science of the Total Environment 2010; 408: 2854-2873.

Hung H, Katsoyiannis AA, Brorström-Lundén E, Olafsdottir K, Aas W, Breivik K, et al. Temporal trends of Persistent Organic Pollutants (POPs) in arctic air: 20 years of monitoring under the Arctic Monitoring and Assessment Programme (AMAP). Environmental Pollution 2016; 217: 52-61.

Hung H, MacLeod M, Guardans R, Scheringer M, Barra R, Harner T, et al. Toward the next generation of air quality monitoring: Persistent organic pollutants. Atmospheric environment 2013; 80: 591-598.

Iozza S, Müller CE, Schmid P, Bogdal C, Oehme M. Historical profiles of chlorinated paraffins and polychlorinated biphenyls in a dated sediment core from Lake Thun (Switzerland). Environmental science & technology 2008; 42: 1045-1050.

IPEN. Hotspot report for Pattern of Practices: PCBs Sources and Releases in Tanzania. The International POPs Elimination Project, ipen.org, 2005.

Iqbal M, Syed JH, Breivik K, Chaudhry MJI, Li J, Zhang G, et al. E-waste driven pollution in Pakistan: The first evidence of environmental and human exposure to flame retardants (FRs) in Karachi City. Environmental science & technology 2017; 51: 13895-13905.

Jones KC, De Voogt P. Persistent organic pollutants (POPs): state of the science. Environmental pollution 1999; 100: 209-221.

Kierkegaard A, Björklund J, Fridén U. Identification of the flame retardant decabromodiphenyl ethane in the environment. Environmental Science & Technology 2004; 38: 3247-3253.

Klánová J, Čupr P, Holoubek I, Borůvková J, Přibylová P, Kareš R, et al. Monitoring of persistent organic pollutants in Africa. Part 1: Passive air sampling across the continent in 2008. Journal of Environmental Monitoring 2009; 11: 1952-1963.

Klánová J, Èupr P, Kohoutek Ji, Harner T. Assessing the influence of meteorological parameters on the performance of polyurethane foam-based passive air samplers. Environmental science & technology 2007; 42: 550-555.

Korosi JB, Cheng W, Blais JM. Organic pollutants in sediment core archives. Environmental Contaminants. Springer, 2015, pp. 161-185.

Lammel G, Degrendele C, Gunthe SS, Mu Q, Muthalagu A, Audy O, et al. Revolatilisation of soil-accumulated pollutants triggered by the summer monsoon in India. Atmospheric Chemistry and Physics 2018; 18: 11031-11040.

Leslie H, van Bavel B, Abad E, De Boer J. Towards comparable POPs data worldwide with global monitoring data and analytical capacity building in Africa, Central and Latin America, and the South Pacific. TrAC Trends in Analytical Chemistry 2013; 46: 85-97.

Li L, Wania F. Tracking chemicals in products around the world: introduction of a dynamic substance flow analysis model and application to PCBs. Environment international 2016; 94: 674-686.

Li L, Wania F. Occurrence of single-and double-peaked emission profiles of synthetic chemicals. Environmental science & technology 2018; 52: 4684-4693.

Li Q, Li J, Wang Y, Xu Y, Pan X, Zhang G, et al. Atmospheric short-chain chlorinated paraffins in China, Japan, and South Korea. Environmental science & technology 2012; 46: 11948-11954.

Lorgeoux C, Moilleron R, Gasperi J, Ayrault S, Bonté P, Lefèvre I, et al. Temporal trends of persistent organic pollutants in dated sediment cores: chemical fingerprinting of the anthropogenic impacts in the Seine River basin, Paris. Science of the Total Environment 2016; 541: 1355-1363.

Mackay D. Finding fugacity feasible. Environmental Science & Technology 1979; 13: 1218-1223.

Mackay D. Multimedia environmental models: the fugacity approach: CRC press, 2001. ISBN 1420032542.

Mackay D, McCarty LS, MacLeod M. On the validity of classifying chemicals for persistence, bioaccumulation, toxicity, and potential for long-range transport. Environmental Toxicology and Chemistry: An International Journal 2001; 20: 1491-1498.

Mahenge, R.S., Ulanga, P., Malabeja, M., Pilly, J., Massoy, W., 2018. Performance audit report on electronic waste management. Available at ELECTRONIC-WASTE-MANAGEMENT-2018.pdf (nao.go.tz). Accessed March 2021.

Martin LG, Labuschagne C, Brunke E-G, Weigelt A, Ebinghaus R, Slemr F. Trend of atmospheric mercury concentrations at Cape Point for 1995–2004 and since 2007. Atmospheric Chemistry and Physics 2017; 17: 2393-2399.

Masekoameng KE, Leaner J, Dabrowski J. Trends in anthropogenic mercury emissions estimated for South Africa during 2000–2006. Atmospheric Environment 2010; 44: 3007-3014.

McGrath TJ, Morrison PD, Ball AS, Clarke BO. Detection of novel brominated flame retardants (NBFRs) in the urban soils of Melbourne, Australia. Emerging Contaminants 2017; 3: 23-31.

McLagan DS, Hussain BA, Huang H, Lei YD, Wania F, Mitchell CP. Identifying and evaluating urban mercury emission sources through passive sampler-based mapping of atmospheric concentrations. Environmental Research Letters 2018; 13: 074008.

McLagan DS, Mazur ME, Mitchell CP, Wania F. Passive air sampling of gaseous elemental mercury: a critical review. Atmospheric Chemistry and Physics 2016; 16: 3061-3076.

McLagan DS, Mitchell CP, Huang H, Lei YD, Cole AS, Steffen A, et al. A high-precision passive air sampler for gaseous mercury. Environmental Science & Technology Letters 2015; 3: 24-29.

Meijer S, Steinnes E, Ockenden W, Jones KC. Influence of environmental variables on the spatial distribution of PCBs in Norwegian and UK soils: implications for global cycling. Environmental science & technology 2002; 36: 2146-2153.

Meijer SN, Ockenden W, Sweetman A, Breivik K, Grimalt JO, Jones KC. Global distribution and budget of PCBs and HCB in background surface soils: implications for sources and environmental processes. Environmental science & technology 2003; 37: 667-672.

Melymuk L, Bohlin P, Sáňka Oe, Pozo K, Klánová J. Current challenges in air sampling of semivolatile organic contaminants: sampling artifacts and their influence on data comparability. Environmental science & technology 2014; 48: 14077-14091.

Mézière M, Krätschmer K, Pērkons I, Zacs D, Marchand P, Dervilly G, et al. Addressing main challenges regarding short-and medium-chain chlorinated paraffin analysis using GC/ECNI-MS and LC/ESI-MS methods. Journal of the American Society for Mass Spectrometry 2020; 31: 1885-1895.

Muir DC, Howard PH. Are there other persistent organic pollutants? A challenge for environmental chemists. Environmental science & technology 2006; 40: 7157-7166.

Möckel C, Breivik K, Nøst TH, Sankoh A, Jones KC, Sweetman A. Soil pollution at a major West African E-waste recycling site: Contamination pathways and implications for potential mitigation strategies. Environment International 2020; 137: 105563.

Naccarato A, Tassone A, Martino M, Moretti S, Macagnano A, Zampetti E, et al. A field intercomparison of three passive air samplers for gaseous mercury in ambient air. Atmos. Meas. Tech. Discussion 2020: 1-34.

Niu S, Harner T, Chen R, Parnis JM, Saini A, Hageman K. Guidance on the Application of Polyurethane Foam Disk Passive Air Samplers for Measuring Nonane and Short-Chain Chlorinated Paraffins in Air: Results from a Screening Study in Urban Air. Environmental Science & Technology 2021; 55: 11693-11702.

Nøst TH, Halse AK, Randall S, Borgen AR, Schlabach M, Paul A, et al. High concentrations of organic contaminants in air from ship breaking activities in Chittagong, Bangladesh. Environmental science & technology 2015; 49: 11372-11380.

O'Connor D, Hou D, Ok YS, Mulder J, Duan L, Wu Q, et al. Mercury speciation, transformation, and transportation in soils, atmospheric flux, and implications for risk management: A critical review. Environment international 2019; 126: 747-761.

Obrist D, Kirk JL, Zhang L, Sunderland EM, Jiskra M, Selin NE. A review of global environmental mercury processes in response to human and natural perturbations: Changes of emissions, climate, and land use. Ambio 2018; 47: 116-140.

Ockenden WA, Breivik K, Meijer SN, Steinnes E, Sweetman AJ, Jones KC. The global re-cycling of persistent organic pollutants is strongly retarded by soils. Environmental Pollution 2003; 121: 75-80.

Ontiveros-Cuadras JF, Ruiz-Fernández AC, Sanchez-Cabeza J-A, Sericano J, Pérez-Bernal LH, Páez-Osuna F, et al. Recent history of persistent organic pollutants (PAHs, PCBs, PBDEs) in sediments from a large tropical lake. Journal of hazardous materials 2019; 368: 264-273.

Ottar B. The transfer of airborne pollutants to the Arctic region. Atmospheric Environment (1967) 1981; 15: 1439-1445.

Pacyna EG, Pacyna J, Sundseth K, Munthe J, Kindbom K, Wilson S, et al. Global emission of mercury to the atmosphere from anthropogenic sources in 2005 and projections to 2020. Atmospheric Environment 2010; 44: 2487-2499.

Petty JD, Huckins JN, Zajicek JL. Application of semipermeable membrane devices (SPMDs) as passive air samplers. Chemosphere 1993; 27: 1609-1624.

Pirrone N, Cinnirella S, Feng X, Finkelman RB, Friedli HR, Leaner J, et al. Global mercury emissions to the atmosphere from anthropogenic and natural sources. Atmospheric Chemistry and Physics 2010; 10: 5951-5964.

Pozo K, Harner T, Lee SC, Wania F, Muir DC, Jones KC. Seasonally resolved concentrations of persistent organic pollutants in the global atmosphere from the first year of the GAPS study. Environmental Science & Technology 2008; 43: 796-803.

Pozo K, Harner T, Wania F, Muir DC, Jones KC, Barrie LA. Toward a global network for persistent organic pollutants in air: results from the GAPS study. Environmental Science & Technology 2006; 40: 4867-4873.

Qiu X, Marvin CH, Hites RA. Dechlorane plus and other flame retardants in a sediment core from Lake Ontario. Environmental science & technology 2007; 41: 6014-6019.

Rauert C, Schuster JK, Eng A, Harner T. Global atmospheric concentrations of brominated and chlorinated flame retardants and organophosphate esters. Environmental science & technology 2018; 52: 2777-2789.

Ren N, Sverko E, Li Y-F, Zhang Z, Harner T, Wang D, et al. Levels and isomer profiles of Dechlorane Plus in Chinese air. Environmental science & technology 2008; 42: 6476-6480.

Renner R. Government Watch: In US, flame retardants will be voluntarily phased out. ACS Publications, 2004.

Robinson BH. E-waste: an assessment of global production and environmental impacts. Science of the total environment 2009; 408: 183-191.

Rutter AP, Schauer JJ, Shafer MM, Creswell JE, Olson MR, Robinson M, et al. Dry deposition of gaseous elemental mercury to plants and soils using mercury stable isotopes in a controlled environment. Atmospheric Environment 2011; 45: 848-855.

Saini A, Harner T, Chinnadhurai S, Schuster JK, Yates A, Sweetman A, et al. GAPS-Megacities: A new global platform for investigating persistent organic pollutants and chemicals of emerging concern in urban air. Environmental Pollution 2020; 267: 115416.

Schuster JK, Harner T, Sverko E. Dechlorane Plus in the Global Atmosphere. Environmental Science & Technology Letters 2020; 8: 39-45

Selin NE. Global biogeochemical cycling of mercury: a review. Annual Review of Environment and Resources 2009; 34: 43-63.

Shoeib M, Harner T. Characterization and comparison of three passive air samplers for persistent organic pollutants. Environmental science & technology 2002; 36: 4142-4151.

Shoeib M, Harner T, Lee SC, Lane D, Zhu J. Sorbent-impregnated polyurethane foam disk for passive air sampling of volatile fluorinated chemicals. Analytical chemistry 2008; 80: 675-682.

Shunthirasingham C, Alexandrou N, Brice KA, Dryfhout-Clark H, Su K, Shin C, et al. Temporal trends of halogenated flame retardants in the atmosphere of the Canadian Great Lakes Basin (2005–2014). Environmental Science: Processes & Impacts 2018; 20: 469-479.

Skov H, Sørensen BT, Landis MS, Johnson MS, Sacco P, Goodsite ME, et al. Performance of a new diffusive sampler for Hg0 determination in the troposphere. Environmental Chemistry 2007; 4: 75-80.

Slemr F, Martin L, Labuschagne C, Mkololo T, Angot H, Magand O, et al. Atmospheric mercury in the Southern Hemisphere–Part 1: Trend and inter-annual variations in atmospheric mercury at Cape Point, South Africa, in 2007–2017, and on Amsterdam Island in 2012–2017. Atmospheric Chemistry and Physics 2020; 20: 7683-7692.

Snow MA, Darko G, Gyamfi O, Ansah E, Breivik K, Hoang C, et al. Characterization of inhalation exposure to gaseous elemental mercury during artisanal gold mining and e-waste recycling through combined stationary and personal passive sampling. Environmental Science: Processes & Impacts 2021; 23: 569-579.

Sprovieri F, Pirrone N, Bencardino M, D'Amore F, Carbone F, Cinnirella S, et al. Atmospheric mercury concentrations observed at ground-based monitoring sites globally distributed in the framework of the GMOS network. Atmospheric chemistry and physics 2016; 16: 11915-11935.

Sprovieri F, Pirrone N, Ebinghaus R, Kock H, Dommergue A. A review of worldwide atmospheric mercury measurements. Atmospheric Chemistry and Physics 2010; 10: 8245-8265.

Streets DG, Devane MK, Lu Z, Bond TC, Sunderland EM, Jacob DJ. All-time releases of mercury to the atmosphere from human activities. Environmental science & technology 2011; 45: 10485-10491.

Streets DG, Horowitz HM, Lu Z, Levin L, Thackray CP, Sunderland EM. Global and regional trends in mercury emissions and concentrations, 2010–2015. Atmospheric environment 2019; 201: 417-427.

Sverko E, Tomy GT, Marvin CH, Zaruk D, Reiner E, Helm PA, et al. Dechlorane plus levels in sediment of the lower Great Lakes. Environmental science & technology 2008; 42: 361-366.

Sverko E, Tomy GT, Reiner EJ, Li Y-F, McCarry BE, Arnot JA, et al. Dechlorane plus and related compounds in the environment: a review. Environmental science & technology 2011; 45: 5088-5098.

Sweetman AJ, Dalla Valle M, Prevedouros K, Jones KC. The role of soil organic carbon in the global cycling of persistent organic pollutants (POPs): interpreting and modelling field data. Chemosphere 2005; 60: 959-972.

Temme C, Blanchard P, Steffen A, Banic C, Beauchamp S, Poissant L, et al. Trend, seasonal and multivariate analysis study of total gaseous mercury data from the Canadian atmospheric mercury measurement network (CAMNet). Atmospheric Environment 2007; 41: 5423-5441.

UNECE. The 1998 Protocol on Persistent Organic Pollutants, Including the Amendments Adopted by the Parties on 18 December 2009 In: Europe UNECf, editor. United Nations Economic Comission for Europe, https://unece.org/DAM/env/lrtap/full%20text/ece.eb.air.104.e.pdf, 2010. Accessed October 2021.

UNEP. Stockholm Convention on Persistent Organic Pollutants. United Nations Environment Programme, http://chm.pops.int, 2009. Accessed January 2021.

UNEP. Stockholm Convention on Persistent Organic Pollutants (POPs). United Nations Environment Programme, www.pops.int/TheConvention/Overview/TextoftheConvention/tabid/2232/Default.aspx, 2017. Accessed October 2021.

UNEP. Basel Convention on the Control of Transboundary Movements of Hazardous Wastes and their Disposal. In: Programme UNE, editor, www.basel.int, 2019a. Accessed January 2022.

UNEP. Proposal to list Dechlorane Plus (CAS No. 13560-89-9) and its syn-isomer (CAS No. 135821-03-3) and anti-isomer (CAS No. 135821-74-8) in Annexes A, B and/or C to the Stockholm Convention on Persistent Organic Pollutants, www.pops.int, 2019b. Accessed January 2021.

UNEP. Global Monitoring Plan for Persistent Organic Pollutants: Third Regional Monitoring Report - Africa Region, http://chm.pops.int/Implementation/GlobalMonitoringPlan/MonitoringReports/tabid/525/, 2021. Accessed October 2021.

UNEP. Minamata convention on mercury. United Nations Environment Programme, Nairobi, Kenya 2013. Accessed November 2021.

USEPA. Method 7473: Mercury in solids and solutions by thermal decomposition, amalgamation, and atomic absorption spectrophotometry (Vol. 17). Washington: United States Environmental Protection Agency, 2007. Accessed November 2021.

van Mourik L, Lava R, O'Brien J, Leonards P, de Boer J, Ricci M. The underlying challenges that arise when analysing short-chain chlorinated paraffins in environmental matrices. Journal of Chromatography A 2020a; 1610: 460550.

van Mourik LM, Leonards PE, Gaus C, de Boer J. Recent developments in capabilities for analysing chlorinated paraffins in environmental matrices: a review. Chemosphere 2015; 136: 259-272.

van Mourik LM, Wang X, Paxman C, Leonards PE, Wania F, de Boer J, et al. Spatial variation of short-and medium-chain chlorinated paraffins in ambient air across Australia. Environmental Pollution 2020b: 114141.

Vauclin S, Mourier B, Dendievel A-M, Marchand P, Vénisseau A, Morereau A, et al. Temporal trends of legacy and novel brominated flame retardants in sediments along the Rhône River corridor in France. Chemosphere 2021; 271: 129889.

Voogt P, Brinkman U. Production, properties and usage of polychlorinated biphenyls. Halogenated biphenyls, terphenyls, naphthalenes, dibenzodioxins and related products 1989: 3-45.

Wang Y, Li J, Cheng Z, Li Q, Pan X, Zhang R, et al. Short-and medium-chain chlorinated paraffins in air and soil of subtropical terrestrial environment in the Pearl River Delta, South China: distribution, composition, atmospheric deposition fluxes, and environmental fate. Environmental science & technology 2013; 47: 2679-2687.

Wania F, Dugani CB. Assessing the long-range transport potential of polybrominated diphenyl ethers: A comparison of four multimedia models. Environmental Toxicology and Chemistry: An International Journal 2003; 22: 1252-1261.

Wania F, Mackay D. Peer reviewed: tracking the distribution of persistent organic pollutants. Environmental science & technology 1996; 30: 390A-396A.

Wania F, Shen L, Lei YD, Teixeira C, Muir DC. Development and calibration of a resin-based passive sampling system for monitoring persistent organic pollutants in the atmosphere. Environmental science & technology 2003; 37: 1352-1359.

Wania, F., Shunthirasingham, C., 2020. Passive air sampling for semi-volatile organic chemicals. Environmental Science: Processes & Impacts 22, 1925-2002

Webster E, Mackay D, Wania F. Evaluating environmental persistence. Environmental Toxicology and Chemistry: An International Journal 1998; 17: 2148-2158.

White KB, Kalina Jí, Scheringer M, Přibylová P, Kukučka P, Kohoutek Jí, et al. Temporal trends of persistent organic pollutants across Africa after a decade of MONET passive air sampling. Environmental Science & Technology 2020; 55: 9413-9424.

Wong F, Hung H, Dryfhout-Clark H, Aas W, Bohlin-Nizzetto P, Breivik K, et al. Time trends of persistent organic pollutants (POPs) and Chemicals of Emerging Arctic Concern (CEAC) in Arctic air from 25 years of monitoring. Science of the Total Environment 2021; 775: 145109.

Wong F, Wania F. Visualising the equilibrium distribution and mobility of organic contaminants in soil using the chemical partitioning space. Journal of Environmental Monitoring 2011; 13: 1569-1578.

Wong M, Wu S, Deng WJ, Yu X, Luo Q, Leung A, et al. Export of toxic chemicals–a review of the case of uncontrolled electronic-waste recycling. Environmental Pollution 2007; 149: 131-140.

Xin M, Gustin MS. Gaseous elemental mercury exchange with low mercury containing soils: investigation of controlling factors. Applied Geochemistry 2007; 22: 1451-1466.

Xu C, Zhang Q, Gao L, Zheng M, Qiao L, Cui L, et al. Spatial distributions and transport implications of short-and medium-chain chlorinated paraffins in soils and sediments from an e-waste dismantling area in China. Science of The Total Environment 2019; 649: 821-828.

Yhdego M. From a Sanitary Landfill to a Dump Site: Pugu Kinyamwezi Community Curse in Dar es Salaam. Tanzania, 2017. DOI: 10.13140/RG.2.2.27828.04483

Zeng L, Chen R, Zhao Z, Wang T, Gao Y, Li A, et al. Spatial distributions and deposition chronology of short chain chlorinated paraffins in marine sediments across the Chinese Bohai and Yellow Seas. Environmental science & technology 2013; 47: 11449-11456.

Zennegg M, Kohler M, Hartmann PC, Sturm M, Gujer E, Schmid P, et al. The historical record of PCB and PCDD/F deposition at Greifensee, a lake of the Swiss plateau, between 1848 and 1999. Chemosphere 2007; 67: 1754-1761.

Zhang W, Tong Y, Hu D, Ou L, Wang X. Characterization of atmospheric mercury concentrations along an urban–rural gradient using a newly developed passive sampler. Atmospheric environment 2012; 47: 26-32.

Zhang X, Sühring R, Serodio D, Bonnell M, Sundin N, Diamond ML. Novel flame retardants: Estimating the physical–chemical properties and environmental fate of 94 halogenated and organophosphate PBDE replacements. Chemosphere 2016a; 144: 2401-2407.

Zhang X, Wania F. Modeling the uptake of semivolatile organic compounds by passive air samplers: Importance of mass transfer processes within the porous sampling media. Environmental science & technology 2012; 46: 9563-9570.

Zhang Y, Jacob DJ, Horowitz HM, Chen L, Amos HM, Krabbenhoft DP, et al. Observed decrease in atmospheric mercury explained by global decline in anthropogenic emissions. Proceedings of the National Academy of Sciences 2016b; 113: 526-531.

Appendix

Table A1: POPs regulated under the Aarhus Protocol and the Stockholm Convention (marked "V" in the table), and chemicals added in amendments (marked "v" in the table). Chemicals of emerging concern proposed for listing under the Stockholm Convention marked "PFL". POPs and chemicals of emerging concern discussed in this thesis are marked in bold.

Chemicals and chemical groups	Structure	Aarhus Protocol	Stockholm Convention
Aldrin		V	V
1,2-bis (2,4,6 tribromophenoxy) ethane (BTBPE)	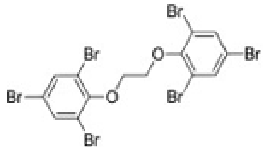		
Bis (2-ethylhexyl)-3,4,5,6-tetrabromo-phthalate (TBPH)	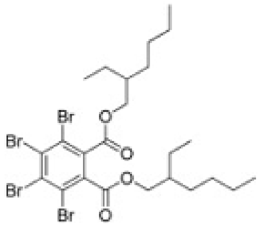		
Chlordane		V	V
Chlordecone		V	v
Decabromodiphenyl ether (Deca-BDE)	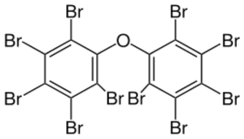		v
Decabromodiphenyl ethane (DBDPE)	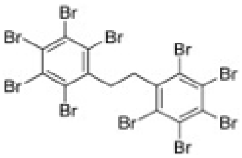		
Dechlorane 602 (Dec 602)	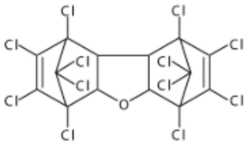		
Dechlorane 603 (Dec 603)	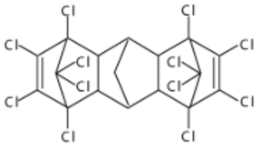		
Dechlorane Plus (DP)	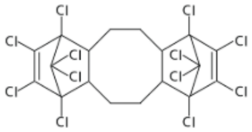		PFL
Dichlorodiphenyltrichloroethane		V	V
Dicofol			v

(Table A1 continued)

Chemicals and chemical groups	Structure	Aarhus Protocol	Stockholm Convention
Dieldrin		V	V
Endosulfan			v
Endrin		V	V
Heptachlor		V	V
Hexabromobiphenyl		V	v
Hexabromocyclododecane			v
Hexachlorobenzene		V	V
Hexachlorobutadiene		v	v
Hexachlorocyclohexanes		V	v
Medium chain chlorinated paraffins (MCCPs)*	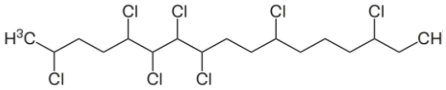		PFL
Mirex		V	V
Octabromodiphenyl ether (Octa-BDE)*	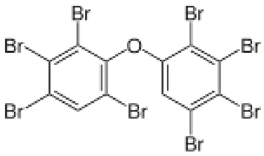	v	v
Pentabromodiphenyl ether (Penta-BDE)*	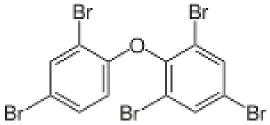	v	v
Pentachlorobenzene		v	v
Pentachlorophenol			v
Perfluorooctanoic acid			v
Perfluorooctylsulfonate		v	v
Polycyclic aromatic hydrocarbons		V	
Polychlorinated biphenyls (PCBs)*	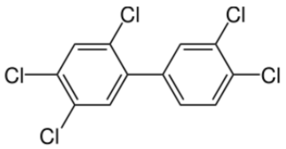	V	V
Polychlorinated dibenzofurans		V	V
Polychlorinated dibenzo-p-dioxins		V	V
Polychlorinated naphthalenes		v	v
Short chain chlorinated paraffins (SCCPs)*	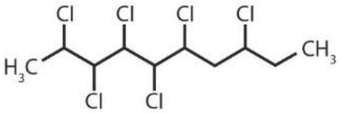	v	v
Toxaphene		V	V

* Example structures: MCCP: 2,5,6,7,8,11,15-heptachloroheptadecane, octa-BDE: BDE-196, penta-BDE: BDE-100, PCB: PCB-118, SCCP: 2,3,4,5,6,8-hexachlorodecane.

Paper I

Environmental Pollution 292 (2022) 118298

Contents lists available at ScienceDirect

Environmental Pollution

journal homepage: www.elsevier.com/locate/envpol

Spatial trends of chlorinated paraffins and dechloranes in air and soil in a tropical urban, suburban, and rural environment☆

Maja Nipen[a,b,*], Rolf David Vogt[a], Pernilla Bohlin-Nizzetto[b], Katrine Borgå[c], Eliezer Brown Mwakalapa[d], Anders Røsrud Borgen[b], Susanne Jøntvedt Jørgensen[a], Samwel Moses Ntapanta[e], Aviti John Mmochi[f], Martin Schlabach[b], Knut Breivik[a,b]

[a] Centre for Biogeochemistry in the Anthropocene, Department of Chemistry, University of Oslo, P.O. Box 1033, 0315 Oslo, Norway
[b] NILU-Norwegian Institute for Air Research, P.O. Box 100, 2027 Kjeller, Norway
[c] Centre for Biogeochemistry in the Anthropocene, Department of Biosciences, University of Oslo, P.O. Box 1066, 0316 Oslo, Norway
[d] Department of Natural Sciences, Mbeya University of Science and Technology, Mbeya, Tanzania
[e] Department of Social Anthropology, University of Oslo, P.O. Box 1091, 0317 Oslo, Norway
[f] Institute for Marine Science, University of Dar Es Salaam, Zanzibar, Tanzania

ARTICLE INFO

Keywords:
E-waste
Urban pulse
Passive air sampling
Environmental fate
SCCPs
MCCPs

ABSTRACT

There are large knowledge gaps concerning environmental levels and fate of many organic pollutants, particularly for chemicals of emerging concern in tropical regions of the Global South. In this study, we investigated the levels of chlorinated paraffins (CPs) and dechloranes in air and soil in rural, suburban, and urban regions in and around Dar es Salaam, Tanzania. Samples were also collected near the city's main municipal waste dumpsite and an electronic waste (e-waste) handling facility. In passive air samples, short chain CPs (SCCPs) dominated, with an average estimated concentration of 22 ng/m^3, while medium chain CPs (MCCPs) had an average estimated concentration of 9 ng/m^3. The average estimated air concentration of $\sum$dechloranes (Dechlorane Plus (DP) + Dechlorane 602 + Dechlorane 603) was three to four orders of magnitudes lower, 2 pg/m^3. In soil samples, MCCPs dominated with an average concentration of 640 ng/g dw, followed by SCCPs with an average concentration of 330 ng/g dw, and $\sum$dechloranes with an average concentration of 0.9 ng/g dw. In both air and soil, DP was the dominating dechlorane compound. Urban pulses were observed for CPs and dechloranes in air and soil. CPs were in addition found in elevated levels at the municipal waste dumpsite and the e-waste handling facility, while DPs were found in elevated levels at the e-waste handling facility. This suggests that waste handling sites represent important emission sources for these pollutants. Investigations into seasonal trends and environmental fate of CPs and dechloranes showed that monsoonal rain patterns play a major role in governing air concentrations and mobility, particularly for the less volatile MCCPs and dechloranes. This study is the first to report levels of CPs in air from sub-Saharan Africa, and DP, Dechlorane 602, and Dechlorane 603 in soil from sub-Saharan Africa.

1. Introduction

A number of organic chemicals and chemical groups have been regulated as persistent organic pollutants (POPs) because they represent a risk for environmental and human health (UNEP, 2017). At the same time, there is considerable scientific and regulatory interest in substances which may have similar hazardous properties as the legacy POPs. Examples include chlorinated paraffins (CPs) and dechloranes. Short chain CPs (SCCPs, C_{10}–C_{13}) are subject to international regulation under the Stockholm Convention on POPs and the Aarhus Protocol of the Convention on Long-Range Transboundary Air Pollution, while medium chained CPs (MCCPs, C_{14}–C_{17}) remain unregulated at the international level (Glüge et al., 2018; UNECE, 2010; UNEP, 2017). The latter also applies to Dechlorane Plus (DP) which is proposed for listing under the Stockholm Convention (UNEP, 2019). While legacy POPs have been extensively studied in terms of their environmental levels and fate, our

---

☆ This paper has been recommended for acceptance by Charles Wong.

* Corresponding author. Centre for Biogeochemistry in the Anthropocene, Department of Chemistry, University of Oslo, P.O. Box 1033, 0315 Oslo, Norway.
E-mail address: majanip@kjemi.uio.no (M. Nipen).

https://doi.org/10.1016/j.envpol.2021.118298
Received 14 July 2021; Received in revised form 30 September 2021; Accepted 4 October 2021
Available online 6 October 2021

understanding of the environmental occurrence and behaviour of CPs and dechloranes remains fragmented and incomplete. There is therefore considerable interest and need for further research into these two substance groups to support chemical management strategies.

CPs and dechloranes are added as flame retardants or plasticizers in a range of consumer products. More than a million tonnes of CPs are produced annually, mainly in China, and used in plastics, paints, sealants, rubber, and leather products, as well as in metalworking applications (Glüge et al., 2016). DP is used in electronics and plastic roofing materials (Hoh et al., 2006; UNEP, 2019). Production volumes of DP are lower compared to CPs, at 750–6000 tonnes annually (Hansen et al., 2020), while use categories and production volumes are less well described for Dechlorane 602 (Dec 602) and Dechlorane 603 (Dec 603).

Most studies on sources and fate of chemicals of emerging concern (CECs) like CPs and dechloranes have been conducted in developed economies of the Global North, where effective regulatory efforts to some extent have reduced production, use and trade of these chemicals. Countries in the Global South may on the other hand be experiencing increasing environmental burdens of CPs and dechloranes due to a range of socioeconomic factors. These factors include increased consumption and limited waste handling systems, limited capacity to enforce environmental regulations, as well as being on the receiving end of transboundary trade of used products and waste (Abbasi et al., 2019; Breivik et al., 2011; Li and Wania, 2016; Robinson, 2009). In addition, differences in climate between these regions will likely lead to differences in environmental fate of CPs and dechloranes. For example, higher temperatures in tropical regions increase the volatility of both substance groups (Wania and Mackay, 1996) and cause more rapid environmental degradation in various environmental compartments, including air and soil (Webster et al., 1998).

Tanzania is a sub-Saharan African country with a tropical climate, and an emerging economy with an annual average increase in gross domestic product of 6 % since the turn of the century (WorldBank, 2021). With a population of 6.4 million, Tanzania's largest city Dar es Salaam suffers from insufficient waste handling systems, notably including electronic waste (e-waste) (Mahenge et al., 2018; Yhdego, 2017). Dar es Salaam is not known as a major recipient in the illegal e-waste trade, but the amount of e-waste generated is growing (NBS, 2019). These factors combined suggest that the Tanzanian environment, particularly urban Dar es Salaam, may be experiencing increasing burdens of CPs and dechloranes. But to our knowledge, there are no previous studies reporting concentrations of CPs and dechloranes in the Tanzanian environment in peer reviewed scientific literature. However, the NGO network IPEN recently reported high concentrations of SCCPs in free-range chicken eggs collected near a municipal waste dumpsite in Dar es Salaam (Petrlik et al., 2020). This shows that these CECs are present in consumer products and waste in the region. Elsewhere, studies have shown elevated levels of CPs and DP near e-waste recycling sites (Chen et al., 2011; Möckel et al., 2020; Someya et al., 2016; Xu et al., 2019), and CPs near a municipal waste site (Möckel et al., 2020). In addition, elevated levels of both CPs and dechloranes have been found in urban environments (Barber et al., 2005; Saini et al., 2020).

The main objective of this study was to determine concentrations of CPs and dechloranes in the physical environment within and around Dar es Salaam, representing an urban tropical environment. We selected ambient air and soil as sampling media as atmospheric inputs represents the key pathway of environmental contaminants into terrestrial ecosystems, including the terrestrial part of the human food-chain (McLachlan, 1995). By choosing air and soil we wanted to gain insights into contemporary emissions and historical accumulation of these two substance groups in the physical environment, respectively. Our aim was furthermore to study to what extent environmental burdens of CPs and dechloranes are associated with contemporary use and/or disposal, as well as to evaluate potential dispersion of these chemicals from assumed source areas. Additional motivations for this study were to rationalize the main factors governing the spatial distribution, air-soil exchange, and environmental fate of CPs and dechloranes in a tropical urban region.

2. Materials and methods

2.1. Sample collection

2.1.1. Sampling locations

Dar es Salaam has an average temperature of 26°*C*, with only minor temperature fluctuations throughout the year, February being the warmest month (average 29°*C*) and July the coldest (average 24°*C*). The annual precipitation of more than 1000 mm is monsoonal, with most rainfall in April (~250 mm/month) and least in June, July, August, and September (~30 mm/month).

Air and soil samples were collected from 19 locations along a transect covering 40 km southeast of Dar es Salaam, the city of Dar es Salaam, and 60 km northwest of the city (Fig. 1). This transect comprised different settlement regions, including densely populated and industrialized urban areas (U), suburban areas (S), and rural areas (R) with little anthropogenic activity. Air and soil samples were also collected from 9 locations along a shorter (12 km), waste-source transect (W) targeting specifically the city's main municipal waste dumpsite and an e-waste handling facility on the outskirts of Dar es Salaam. The e-waste facility is by Tanzanian standards a large-scale facility, mainly handling electronics from domestic use. Being part of the formalized sector, crude recycling techniques (e.g., cable burning, acid leaching) commonly practiced in some East Asian and West African countries (Alabi et al., 2012; Wong et al., 2007) are not known to be carried out at this facility.

2.1.2. Air samples

Air samples were collected using polyurethane foam (PUF) based passive samplers (Shoeib and Harner, 2002) of the type used in the MONET monitoring network (Klánová et al., 2009; Klánová et al., 2006). PUF disks and sampler metal components were pre-cleaned and stored dust-free before deployment, and PUF disks were also kept refrigerated. Air samplers were deployed at least 2 m above ground level for approximately two months, between February and April 2019.

In addition to investigating spatial trends, seasonal fluctuations in levels of CPs and dechloranes in air were also monitored for more than a year (January 2018 to April 2019) at location S-13. Samplers were deployed for two-to three-month periods, with a total of six samples being collected.

2.1.3. Soil samples

Achieving representability and comparability of soils sampled in areas affected by local anthropogenic activities is challenging. To promote representability, samples from each site were composed of three pooled subsamples, collected within a range of three to five square metres using a stainless-steel handheld corer to a depth of approximately 5 cm. Comparability was optimized by collecting samples below the canopies of mature trees. This minimizes the risk for collecting displaced soils, although it might lead to overall higher soil concentrations of CPs and dechloranes compared to soil in open areas due to the forest filter effect and higher throughfall and litterfall deposition (Horstmann and Mclachlan, 1998). At the e-waste facility, soil was collected from the courtyard used for storing electrical components. At the municipal dumpsite, soil was collected within ~30 m of the waste piles. Soil samples were collected in February 2019.

2.2. Sample preparation and analysis

Details on sample preparation and analysis are given in the SI and a summary is presented here. Soil samples (~7 g) were dried and homogenized with sodium sulphate in a mortar until a free-flowing powder was achieved. The air samples (PUF disks) and soil samples were

Fig. 1. Locations for air and soil sampling in Dar es Salaam and surrounding areas (R: Rural, S: Suburban, U: Urban, W: Waste). Predominant wind direction shown by arrow. Map from Google.com/maps.

extracted in acetone/n-hexane (1:1) using soxhlet extraction and accelerated solvent extraction, respectively, after the addition of internal standards (^{13}C labelled 1,5,5,6,6,10-hexachlorodecane, DP syn, and Dec 602). Extracts from both air and soil samples were volume reduced using a Turbovap system (Zymark) before being treated with concentrated sulphuric acid for the removal of lipids and polymeric impurities. Further, the extracts were cleaned using a dry packed column with 4 g activated silica covered by a 1 cm layer of sodium sulphate eluted with diethyl ether in n-hexane (1:9). Solvent was changed to isooctane, volume reduced to 100 μL, and 1,2,3,4-tetrachloronaphthalene was added as a recovery standard.

Extracts were analysed for SCCPs, MCCPs, DP (syn- and anti-isomers), Dec 602, and Dec 603 using gas chromatography quadrupole time-of-flight high resolution mass spectrometry (GC/Q-TOF) (Agilent, Santa Clara, USA) in electron capture negative ionization (ECNI) mode. A total of 34 SCCPs and 28 MCCPs congener groups (groups of CPs that share molecular formula) were identified and quantified in all samples. In addition, 14 very short chain CPs (vSCCPs, C_7–C_9) congener groups were identified in air samples, although due to lack of available quantification standards these were not quantified.

2.2.1. Quantification of CPs

CPs in industrial products and environmental samples potentially consist of thousands of structurally similar isomers, causing a level of complexity that makes quantification of CPs challenging (van Mourik et al., 2020a). In this study, a pattern deconvolution method developed by Bogdal et al. (2015) was used to quantify CPs. This method applies an algorithm to reconstruct the congener group patterns in the analysed samples using a linear combination of congener group patterns from multiple CPs quantification standards. SCCPs standards with 51 %, 55 %, and 63 % Cl (w/w), and single chain length standards of C_{10}, C_{11}, C_{12}, and C_{13} (50 % and 65 % Cl) were used, and for MCCPs, standards of 42 %, 52 %, and 57 % Cl, and single chain C_{14} with 52 % Cl were used. Close match between sample and quantification standard is important as instrument response factors are dependent on chlorination degree (Mézière et al., 2020). The deconvolution method accounts for this by including standards with different chlorination degrees. Match between sample pattern and reconstructed pattern was assessed using the coefficient of determination (R^2), where R^2 of above 0.5 was deemed acceptable. Average R^2 were 0.96 and 0.90 for SCCPs, and 0.99 and 0.76 for MCCPs for air and soil, respectively. Details are given in the SI.

2.2.2. Determining ambient air concentrations of CPs and dechloranes

Volume-based air concentrations of CPs were estimated using a sampling rate of 4.2 m^3/day (Li et al., 2012). For dechloranes, which to a large extent are sorbed to particles in air, a sampling rate of 2.3 m^3/day was applied (Drage et al., 2016). This reflects the lower uptake efficiency of particle-associated compounds compared to gas-phase compounds with the MONET type sampler (Markovic et al., 2015). We note that estimated volume-based air concentrations are associated with larger uncertainty compared to the sequestered amount per sample (Wania and Shunthirasingham, 2020). However, volume-based results are presented in this study to allow for comparisons with other studies.

2.3. Quality control/quality assurance

Method blanks (N = 12) and field blanks (N = 8) were analysed along with every batch of air and soil samples. The average blank levels compared to the levels in samples were 0.8, 3.6, 28, and 17 % for air samples, and 8.6, 2.7, 16, and 14 % in soil samples for SCCPs, MCCPs, DP syn, and DP anti respectively. All samples were blank corrected for CPs and DP content based on blanks prepared and analysed alongside each batch of samples. For CPs, blank correction was performed using the integrated area for each individual congener group from the blank samples, which was subtracted from the corresponding integrated area for the samples. This procedure corrects the total CPs concentration but also acts to prevent the congener group patterns in samples from being skewed by blank contributions.

Method Limits of Detection (LODs) were set at three times the standard deviation of the blanks (normalized by the average sample amount/volume). No significant difference was seen between method blanks and field blanks ($p > 0.05$), so both were used in the determination of LODs. For air samples, the LODs were 0.2 and 0.4 ng/m^3 for SCCPs and MCCPs, and 0.4 and 0.6 pg/m^3 for DP syn and DP anti, respectively. The LODs for soil samples were 11 and 19 ng/g dw for SCCPs and MCCPs, and 0.01 and 0.02 ng/g dw for DP syn and DP anti, respectively. Dec 602 and Dec 603 were not detected in blanks, so instrument LODs were used (0.001 ng/g dw for soil samples, 0.007 pg/m^3 for air samples). LODs for CPs in air were high despite measures to prevent blank contamination, although this is not uncommon (van Mourik et al., 2020b). However, the high levels of CPs in exposed air samples in this study ensured that the high LODs only had a minor effect on the analytical data (Fig. S2). The much lower levels of DP in blanks for air had a larger effect on analytical data, as the DP levels in air were low (Fig. S4). Larger sample volumes would help address this issue. In addition, the use of controlled clean-room laboratories is recommendable for the analysis of CECs which may be present in indoor environments.

Air samplers were deployed in duplicate at three locations. These gave an average deviation in results of less than 20 % for CPs and dechloranes, while four soil samples analysed in duplicate gave an average deviation of less than 30 %. A spike recovery test using CPs standards was performed to assess differences in performance of the sample preparation method for individual congener groups. For total CPs concentrations, the test showed a recovery of 103 ± 3 % for SCCPs and 105 ± 10 % for MCCPs. Only minute differences could be seen in congener group profiles of the spiked samples having been through extraction and clean-up, and the congener group profiles of the applied CPs standards analysed directly ($R^2 = 0.998$). Recovery of CPs internal standards were 65 ± 14 and 73 ± 17 % for air and soil samples respectively, while recovery of Dechlorane internal standards were 67 ± 13 and 64 ± 13 % in air samples, and 61 ± 22 % in soil samples (Tables S5–S8). The quantification procedures for both CPs and dechloranes were based on ^{13}C labelled internal standards added before sample extraction and clean-up, and thus intrinsically corrects for recovery.

2.4. Mechanistic assessments of environmental processes and fate

Processes governing distribution and mobility of CPs and dechloranes in the environment were assessed using chemical partitioning space plots and mobility plots, as developed by Gouin et al. (2000) and Wong and Wania (2011). These plots visualize the degree to which individual CPs congener groups and dechloranes associate with the different soil compartments (pore air, pore water, and organic solids), and the relative importance of their mobility by volatilization, leaching, and erosion. The modelled distribution and mobility uses partitioning coefficients based on physicochemical property data from Glüge et al. (2013) for CPs, and Sverko et al. (2011) for dechloranes. CPs and dechloranes concentrations in air and soil were used to determine soil/air fugacity ratios (f_{soil}/f_{air}) to assess to which degree soils in the studied region serve as a temporary reservoir or secondary source. Fugacity calculations were done using equations from Mackay (2001), and parameters relevant for local conditions if available. Further details are provided in the SI.

2.5. Statistical analysis

Data treatment and statistical tests were performed using R studio 3.4.3 and Microsoft Excel. Summary statistics for compounds with detection between 40 % and 80 % were determined using the robust regression on order statistics method as described in Helsel (2011). The non-parametric Wilcoxon rank sum test was used for group comparisons, while correlation between compounds were determined using Spearman rank correlations. Principal component analysis (PCA) was used to investigate if there were systematic spatial differences in congener group profiles. Compounds with detection frequency <40 % were excluded from statistical analysis.

3. Results and discussion

3.1. CPs and dechloranes in air and soil

3.1.1. General overview

Descriptive statistics for CPs and dechloranes in air and soil are given in Table 1, while concentrations at individual locations are provided in Tables S5–S8. Median estimated concentrations of CPs and dechloranes in air had the following order: SCCPs > MCCPs ≫ DP > Dec 602. The MCCP/SCCP ratios in air ranged from 0.14 to 0.76, with a median value of 0.35. SCCPs were detected in all air samples collected, while MCCPs were detected in 93 % of air samples.

Although not quantified, vSCCPs were also detected in all air samples. C_7 CPs were only found in minor amounts, while C_8 and C_9 CPs combined comprised on average 9 % of total analysed CPs on an integrated signal basis. Their ubiquitous presence and relatively large contribution to total CPs underlines the importance of making vSCCPs quantification standards available, so their environmental presence can be quantified and reported along with other CPs.

In soil samples, median concentrations of CPs and dechloranes were ordered as follows: MCCPs > SCCPs ≫ DP > Dec 603 > Dec 602. Of the CPs, MCCPs dominated in soil, giving an MCCP/SCCP ratio above 1 (0.5–11) at most sites, with a median value of 3.1. Correlations between concentrations in air and soil were seen for SCCPs, MCCPs, DP, and Dec 602 (Spearman's rho: 0.45–0.71, $p < 0.05$) (Table S10).

Air and soil concentrations of CPs and dechloranes from other studies are compiled in Tables S11 and S12 for comparison. Our study is as far as we are aware the first to report CPs in air from sub-Saharan Africa. The concentrations of CPs in air and soil in the studied region were comparable or even higher than CPs concentrations in countries with a high degree of industrialization. For example, the concentrations of SCCPs in air at the highly industrialized Pearl River Delta in China (18 ng/m^3) were similar to our study (22 ng/m^3). The average soil concentrations of SCCPs and MCCPs (330 and 640 ng/g dw, respectively) were even an order of magnitude higher than the Chinese study (18 and 59 ng/g dw, respectively) (Wang et al., 2013). The range of air concentrations of SCCPs and MCCPs (0.3–63 and < 0.4–35 ng/m^3, respectively) were also comparable to urban areas in India and Pakistan (<LOD-47 and <LOD-38 ng/m^3, for SCCPs and MCCPs respectively) (Chaemfa et al., 2014). We caution that comparisons of CPs concentrations between studies are associated with significant uncertainties given analytical challenges and lack of certified reference materials (van Mourik et al., 2018).

Concentrations of dechloranes in air and soil were in the mid-to high range of concentrations reported in studies from elsewhere in the world (Table S11, Table S12). The Global Atmospheric Passive Sampling (GAPS) Megacities study (Saini et al., 2020) recently reported air concentrations of DP and Dec 602 in 19 large cities worldwide. In that study, Lagos, Nigeria, showed the highest DP air concentration of all megacities. The highest concentrations of DP and Dec 602 in Tanzanian air (20 and 0.2 pg/m^3, respectively) were comparable to the concentrations reported for Lagos (DP: 28 pg/m^3, Dec 602: 0.2 pg/m^3). Despite low detection frequency, the highest estimated concentrations of Dec 603 in air (0.2 pg/m^3) were an order of magnitude higher than in urban air in Spain (0.01 pg/m^3) (De la Torre et al., 2018). The highest Dec 603 concentration in soil (3 ng/g dw) were higher than any found in the

Table 1
Descriptive statistics and detection frequency of CPs and dechloranes in air and soil.

	CPs Air (ng/m^3)		CPs Soil (ng/g dw)		Dechloranes air (pg/m^3)			Dechloranes Soil (ng/g dw)		
	SCCPs	MCCPs	SCCPs	MCCPs	DP	Dec 602	Dec 603[a]	DP	Dec 602	Dec 603
Range	0.3–63	<0.4–35	<11–5300	<19–5100	<0.4–20	<0.007-0.2	<0.007-0.2	<0.01–6	<0.001-0.05	<0.001–3
Average	22	9	330	640	2	0.05	–	0.7	0.006	0.2
Median	13	5	51	170	0.7	0.03	–	0.2	0.003	0.009
Std. dev.	20	11	1000	1200	4	0.06	–	1	0.01	0.6
Det. freq.	100 %	93 %	89 %	86 %	57 %	46 %	14 %	89 %	71 %	61 %

[a] Detection frequency too low for determination of descriptive statistics.

literature. Concentrations of DP, Dec 602, and Dec 603 in soil has to our knowledge not previously been reported from sub-Saharan Africa. Neither CPs nor dechloranes are known to be produced in Tanzania (Glüge et al., 2016; Hansen et al., 2020). The levels of primary industrial use are expected to be low, although there are little data available to confirm this. The relatively high concentrations of CPs and dechloranes in air and soil in the study area despite lack of production may be linked to issues with the handling of municipal waste and e-waste.

3.1.2. *Seasonal fluctuations of CPs and dechloranes in air*

Monitoring of seasonal fluctuations of CPs and dechloranes in air at location S-13 showed that the highest concentrations occurred during colder, dry months (June–November). This contrasts with seasonal trends of CPs in air in temperate and sub-tropical regions of China and Australia, where concentrations were higher during warmer summer months (Gillett et al., 2017; Niu et al., 2020; Wang et al., 2012; Wang et al., 2013). This differs also from DP in air in temperate North America, which showed no seasonal trend (Shunthirasingham et al., 2018). While temperature may be a driver for seasonal trends of semi-volatile compounds in air (Wania and Mackay, 1996), this is not the case in our study given the relatively low annual temperature fluctuations and the inverse relationship with air concentrations of CPs and dechloranes. Amount of rainfall was investigated as an alternative explanatory factor. This was done by plotting air concentrations of SCCPs, MCCPs, and DP against cumulative rainfall during each sampling period. Dec 602 and Dec 603 were omitted as concentrations were near or below LOD. Rainfall data was gathered from the Tanzanian Meteorological Authority (TMA, 2021). Results showed negative liner association between SCCPs, MCCPs, and DP concentrations and amount of rainfall (Fig. S6), which was significant for MCCPs and DP ($p < 0.05$), but not for SCCPs ($p > 0.05$). This can be explained by a higher degree of washout of compounds associated with particles (e.g., DP and MCCPs) compared to gas-phase compounds (e.g., SCCPs) (Bidleman, 1988). A model and field-based study from India has shown comparable results for some legacy POPs, although in general, the effect of monsoonal rain patterns on both POPs and CECs in air remain understudied (Lammel et al., 2018). The observed seasonal fluctuations indicate that annual average levels of CPs and dechloranes in air may be higher than those reported in this study since the main sampling campaign for air samples (February to April) coincided with the rain-season. This is particularly relevant for the less volatile dechloranes, but potentially also for higher chlorinated, longer chain MCCPs congener groups, which to some extent may be sorbed to particles in air.

3.2. *Spatial pattern and potential sources*

3.2.1. *Urban pulse and waste related sources for CPs*

An urban pulse was seen for CPs in air and soil. Concentrations of SCCPs and MCCPs in air and MCCPs in soil were significantly higher in urban compared to rural locations ($p < 0.05$) (Fig. 2). For SCCPs in soil,

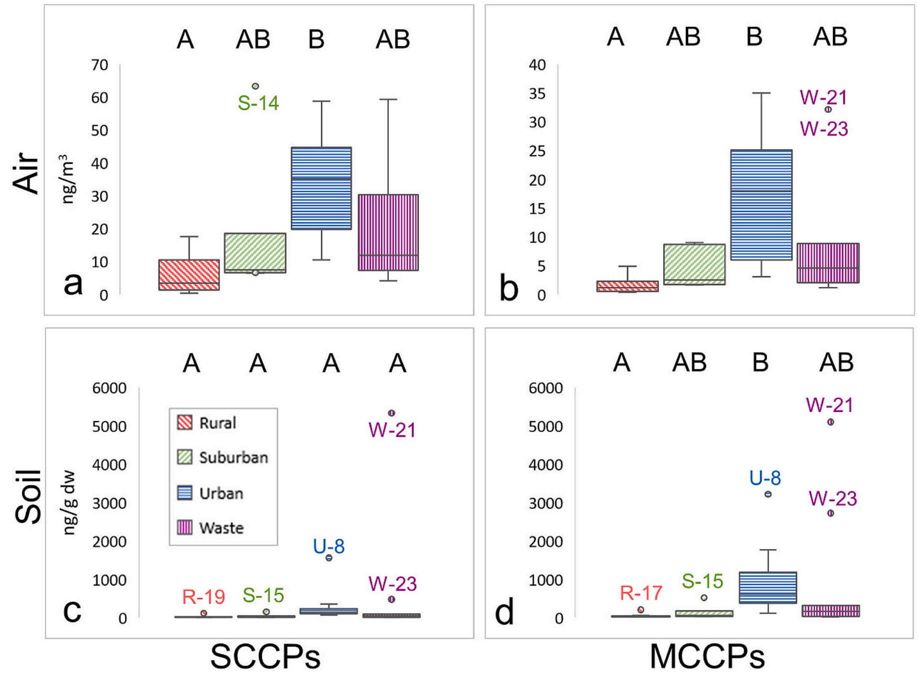

Fig. 2. Concentrations of SCCPs and MCCPs in air (top) and soil (lower) in different settlement categories. The median value is represented by the line inside the box, the upper and lower sections of the box show the upper and lower quartiles. Whiskers represent minimum and maximum values. Outliers are marked as points outside the whiskers. Groups not significantly different from each other (Wilcoxon rank sum test) share letter code (A, B).

there was no significant difference ($p > 0.05$), caused by one high concentration at a rural location (R-19, 120 ng/g). The corresponding air sample at R-19 did however not show elevated concentration of SCCPs (2 ng/m^3), indicating historic emissions at this location. The highest individual concentrations of CPs in air were found within the waste-source transect and at urban locations, in addition to one suburban location which had high concentration of SCCPs (S-14, 63 ng/m^3). In soil, the highest individual concentrations of CPs were found within the waste-source transect, followed by urban locations. The lowest concentrations of CPs in air and soil were found at the rural southeastern end of the transect, upwind from the city, where there is minor anthropogenic influence. SCCPs were strongly correlated with MCCPs in both air and soil (Spearman's rho: 0.95 and 0.91, respectively, $p < 0.001$).

Concentrations of CPs in air and soil within the waste-source transect showed large variability. Concentrations were generally low, except at the dumpsite (W-21, SCCPs: 59 ng/m^3 and 5300 ng/g dw, MCCPs: 33 ng/m^3 and 5100 ng/g dw) and the e-waste facility (W-23, SCCPs: 55 ng/m^3 and 480 ng/g dw, MCCPs: 32 ng/m^3 and 2700 ng/g dw). Considering the elevated concentrations of CPs in air and soil at these two locations, it appears clear that both municipal waste and e-waste represent important point sources for CPs. MCCP/SCCP ratios at the dumpsite (soil: 1.0, air: 0.55) and the e-waste facility (soil: 5.7, air: 0.60) imply that municipal waste is the dominant source for SCCPs, while both municipal waste and e-waste are important sources of MCCPs. This is likely related to differences in CPs content in products in the two waste streams.

Concentrations of CPs in African soils are previously reported for an e-waste site in Ghana (SCCPs: 150-28 000 ng/g dw, MCCPs: <LOD-1300 ng/g dw) and a municipal waste dumpsite in Sierra Leone (SCCPs: 69-1600 ng/g dw, MCCPs: <LOD-1400 ng/g dw) (Möckel et al., 2020). These MCCPs concentrations are two to four times lower than the concentrations found in soil at the dumpsite and e-waste facility in our study, while SCCPs concentrations are higher at the site in Ghana. Results also differ in two additional ways. Firstly, in the Möckel et al. (2020) study, concentrations of SCCPs were an order of magnitude higher at the e-waste site than at the dumpsite, while in our study we found the opposite. Secondly, the MCCP/SCCP ratio in soil at the e-waste site was $\ll 1$ in Ghana, compared to 5.7 at the e-waste facility in this study. The higher total CPs concentrations at the e-waste site in Ghana are likely related to i) Higher volume of e-waste processed, as Ghana is a major recipient in the global e-waste trade (Asante et al., 2019); and ii) Cruder processing methods in Ghana, including low temperature burning of cables and plastics. The higher MCCP/SCCP ratio in Tanzania is potentially also a consequence of socioeconomic factors, as Tanzania is more economically developed, and more modern electronics are therefore consumed. Modern electronics likely contain relatively more MCCPs due to recent production shifts from SCCPs towards MCCPs governed by international regulation (Glüge et al., 2018). This however also makes the year of sample collection a relevant factor (Ghana: 2015, this study: 2019).

Although both municipal waste and e-waste clearly act as important sources of CPs, also the urban environment, with its use of products containing CPs, contributes to local CPs pollution. However, widespread informal disposal of waste and small-scale informal e-waste processing are known to occur, making it difficult to separate the contributions of waste/e-waste compared to emissions from products in use based on CPs concentrations alone. Congener group profiles in soil (PCA, Fig. S11) does however suggest differences in sources between the e-waste facility, dumpsite, and urban areas, indicating that urban CPs contamination cannot be specifically or at least exclusively tied to waste and e-waste in the urban environment.

3.2.2. *Urban pulse and waste related sources for dechloranes*

Urban pulses were also observed for the dechloranes (Fig. 3). For concentrations of Dec 602 in air, and DP and Dec 603 in soil, differences between urban and rural locations were significant ($p < 0.05$). Although for Dec 603 in soil, the highest individual concentration by an order of magnitude was found in a suburban area (S-13, 3 ng/g dw). There were no significant differences between urban and rural locations for concentrations of DP in air and Dec 602 in soil ($p > 0.05$), however, detection frequencies were higher in urban areas.

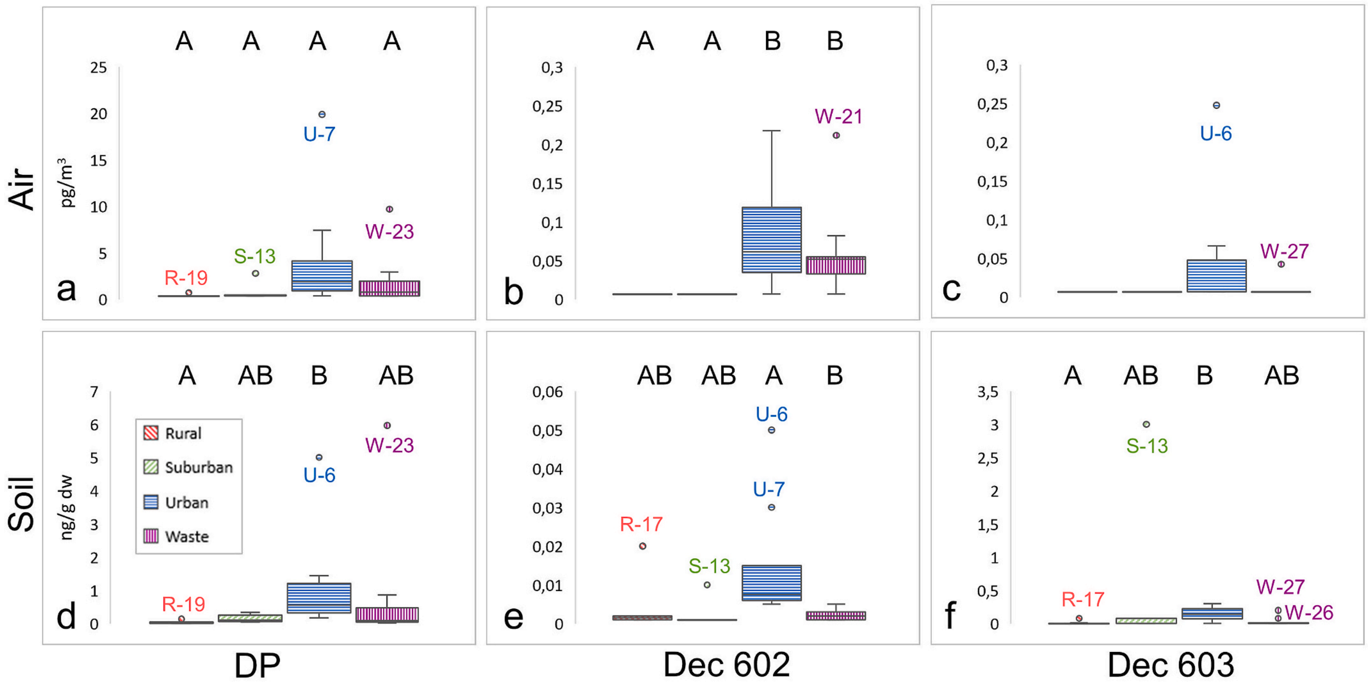

Fig. 3. Dechloranes concentrations in air (top) and soil (lower) in different settlement categories. The median value is represented by the line inside the box, the upper and lower sections of the box show the upper and lower quartiles. Whiskers represent minimum and maximum values. Outliers are marked as point outside the whiskers. Groups not significantly different from each other (Wilcoxon rank sum test) share letter code (A, B).

The concentration of DP in air and soil at the e-waste facility (9 pg/m^3 and 6 ng/g dw, respectively) was higher compared to the dumpsite (3 pg/m^3 and 0.9 ng/g dw). This suggests that unlike for CPs, the release of DP to the regional environment is greater from e-waste than municipal waste. Elevated levels of DP in the environment near e-waste recycling sites have also been documented in e.g., China and Vietnam (Chen et al., 2011; Someya et al., 2016). The concentration of DP in soil at the e-waste facility was comparable to the highest urban concentration (U-6, 5 ng/g dw), while the concentration of DP in air at the e-waste facility was a factor two lower compared to the highest urban location U-7 (20 pg/m^3). U-6 is located within ~500 m of an urban e-waste handler, and U-7 is located in the vicinity of a market where trade and repair of used electronics are taking place. It is thus possible that the high DP levels found at these locations are connected to electronics and e-waste. Any similar associations with electronics are not known for the other urban locations included in this study. Despite some apparent differences in primary sources, strong correlations were found between DP, SCCPs, and MCCPs in both air and soil (Spearman's rho: 0.66–0.88, $p < 0.001$).

Dec 603 generally showed weak correlations with the other analysed CECs (Table S10). This is also seen in a study from North America where the authors pointed to the occurrence of Dec 603 as an impurity in the historically used pesticides Aldrin and Dieldrin as the cause of these differences (Shen et al., 2010). The low concentrations and low detection frequency of Dec 603 in air samples compared to soil, and the lack of association with domestic waste or e-waste could comply with Dec 603 sources being of a legacy rather than contemporary nature. Combined, these factors suggest that the Dec 603 found in soils may be from past pesticide use. Spatial trends of Dec 602 did not allow any conclusions to be drawn regarding its sources.

3.3. *Environmental processes and fate of CPs and dechloranes*

3.3.1. *Correlations of CPs and dechloranes with SOM*

The SOM content was typically low in the studied region with a median value of 1.7 % (<0.01–10 %), and no significant correlations were found between SOM and soil concentrations of total SCCPs or MCCPs, nor individual congener groups ($p > 0.05$). This is consistent with other studies on CPs (Halse et al., 2015; Wang et al., 2014; Wang et al., 2017). The correlation between SOM and soil concentration of DP was also not significant ($p > 0.05$). This suggests that proximity to sources is the main governing factor for the spatial variation in soil concentrations of CPs and DP in this study region. Correlations for SOM versus Dec 602 and Dec 603 in soil were significant (Spearman's rho: 0.47 for both, $p < 0.05$), further supporting legacy rather than current sources for Dec 603 in the region.

3.3.2. *Distribution of CPs and dechloranes in soil and environmental fate*

Soil consists of solids of minerogenic and organic nature, in addition to pore space filled with air and water. For organic compounds like CPs and dechloranes, distribution within the various soil compartments and associated loss/mobility processes are key factors in determining their environmental fate. These distributions and processes are governed by soil properties and the physicochemical properties of the compound, in addition to climatic conditions, and have here been assessed using a simple soil model (Fig. 4) (Gouin et al., 2000; Wong and Wania, 2011).

The studied CPs congener groups and dechloranes are predicted to be mainly associated with organic solids, rather than pore air or pore water (Fig. 4, left). This is also predicted to be the case when the soils are very dry (as during dry months) and very wet (as during rain-season) (Fig. S12), and within most (>90 %) of the range of SOM found in the studied soil. In dry soils with very low SOM content the area of mineral surfaces, thus the content of clay minerals (not included in the model), likely play a significant role in sorption (Goss et al., 2004).

CPs and dechloranes in soil are subject to diffusive and advective loss processes, mainly by erosion due to surface runoff, evaporation, and leaching to groundwater (Wong and Wania, 2011). Most of the studied CECs, particularly the dechloranes and longer chain, highly chlorinated CPs, are predicted to be mobilized mainly by erosion (Fig. 4, right). Evaporation may be an important loss process for more volatile short chained and low chlorinated congener groups. These predictions correspond well with congener group profiles of CPs found in air and soil. Air samples from all location categories were dominated by the congener groups shown by the soil model to be more mobile via evaporation (Fig. S8 and Fig. S9), while congener groups in soil showed an urban fractionation pattern (Fig. S10). Congener groups with relatively low volatility that are emitted in source areas appear to be deposited in soil locally. Congener groups in rural soil on the other hand are less

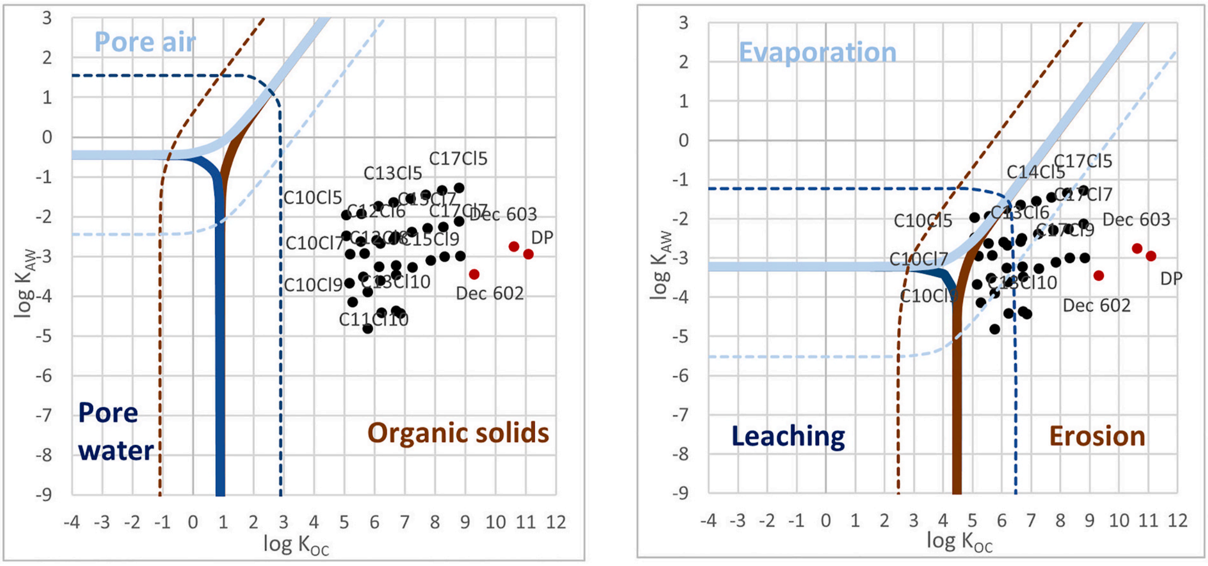

Fig. 4. Chemical partitioning space plot and mobility plot for CPs and dechloranes in soil with characteristics typical of the study area. CPs in black, dechloranes in red. Left: Predicted distribution of selected CPs congener groups and dechloranes in soil organic solids, soil pore air and soil pore water. Thick and dotted lines represent 50 % and 1 % in the phase, respectively. Right: Predicted relative importance of mobility processes (evaporation, leaching, and erosion). Thick and dotted lines represent 50 % and 1 % relevance of process, respectively. (For interpretation of the references to colour in this figure legend, the reader is referred to the Web version of this article.)

chlorinated and have shorter chain lengths (i.e., are more volatile), and are likely transported there via air from source areas. The model also corresponds well with spatial patterns for dechloranes in air and soil and fugacity calculations (see SI Text S3). Strong air to soil flux of dechloranes indicate that soil functions as a temporary storage reservoir for these compounds. This is a consequence of their physicochemical properties (low K_{AW}, high K_{OC}), suggesting that once in soil, dechloranes will not return to the gas phase. The model further predicts that leaching from soil to groundwater may be a relevant loss process for short chained CPs congener groups, while chlorination degree is not predicted to affect potential for leaching. This differs from a study on soil profiles in China, where both chain length and chlorination degree of CPs were seen to affect potential for leaching through soil (Zeng et al., 2011). Degradation processes may however have influenced these results. The soil moisture content, and by extension the monsoonal rain patterns, are predicted to affect the relative importance of mobility processes (Fig. S13). Less evaporation from soil due to soil pore-space being occupied by water could contribute to lower air concentrations of the more volatile SCCPs during periods of heavy rain. This has been observed in Australia (Gillett et al., 2017), and could help explain the seasonal trend seen for SCCPs. Also, the magnitude of mobility of the studied CECs will be affected by rainfall, particularly mobility via erosion which will increase with increased rainfall. Overall, the monsoonal rain patterns in the region seem to have significant effects on the environmental fate of CPs and dechloranes.

4. Conclusions

The levels of CPs and dechloranes in air and soil in the Dar es Salaam region presented in this study adds to the knowledge on CECs in tropical environments and in the Global South. Urban pulses and spatial association with general waste and e-waste indicate that consumption and waste handling practices contribute to local pollution of CPs and dechloranes. This should be addressed at a regional level through improved waste management. It should also be addressed in international regulatory efforts relating to international trade of products, used products, and waste containing these compounds, as the situation is likely to be similar in other countries with comparable socioeconomic conditions.

The relatively high levels of CPs and dechloranes reported in this study underlines the importance of expanding environmental monitoring of CECs in economically developing tropical regions, particularly in urban areas where large populations potentially are exposed to high CECs concentrations. More data on CECs in these regions is also of importance to improve the understanding of environmental distribution and fate of these compounds.

This study showed that the monsoonal rain in the region affects the environmental fate of the studied CECs. For air concentrations, differences were seen compared to seasonal trends in temperate and subtropical regions. These findings have implications for future air monitoring strategies in regions with monsoonal rain. However, our results are based on limited data, and we therefore suggest future studies on CPs and dechloranes in air in the region include studies of seasonal variation at multiple sites.

Credit author statement

Maja Nipen: Conceptualization, Investigation, Formal analysis, Writing – Original Draft. Rolf David Vogt: Conceptualization, Supervision, Investigation, Writing – Review and Editing. Pernilla Bohlin-Nizzetto: Conceptualization, Supervision, Writing – Review and Editing. Katrine Borgå: Conceptualization, Supervision, Project Administration, Writing – Review and Editing. Eliezer Brown Mwakalapa: Investigation. Anders Røsrud Borgen: Supervision, Investigation, Writing – Review and Editing. Susanne Jøntvedt Jørgensen: Investigation. Samwel Moses Ntapanta: Investigation. Aviti John Mmochi: Resources, Writing – Review and Editing. Martin Schlabach: Supervision, Resources. Knut Breivik: Conceptualization, Supervision, Writing – Review and Editing.

Declaration of competing interest

The authors declare that they have no known competing financial interests or personal relationships that could have appeared to influence the work reported in this paper.

Acknowledgements

This study was conducted as part of the AnthroTox project, a convergence environment combining social and natural sciences to study anthropogenic toxicants. The AnthroTox project is funded through the University of Oslo Life:Science initiative and the Norwegian Ministry of Education and Research. We thank Ane Haarr, Franziska Klaas, and Signe Mikkelsen for their contributions during fieldwork, and we thank local authorities for their cooperation and contributions. We also thank the residents and businesses of Dar es Salaam and the Coastal Region who allowed us to deploy air samplers and collect soil samples on their properties.

Appendix A. Supplementary data

Supplementary data to this article can be found online at https://doi.org/10.1016/j.envpol.2021.118298.

References

Abbasi, G., Li, L., Breivik, K., 2019. Global historical stocks and emissions of PBDEs. Environ. Sci. Technol. 53, 6330–6340.

Alabi, O.A., Bakare, A.A., Xu, X., Li, B., Zhang, Y., Huo, X., 2012. Comparative evaluation of environmental contamination and DNA damage induced by electronic-waste in Nigeria and China. Sci. Total Environ. 423, 62–72.

Asante, K.A., Amoyaw-Osei, Y., Agusa, T., 2019. E-waste recycling in Africa: risks and opportunities. Curr. Opin. Green Sustain. Chem. 18, 109–117.

Barber, J.L., Sweetman, A.J., Thomas, G.O., Braekevelt, E., Stern, G.A., Jones, K.C., 2005. Spatial and temporal variability in air concentrations of short-chain (C10– C13) and medium-chain (C14– C17) chlorinated n-alkanes measured in the UK atmosphere. Environ. Sci. Technol. 39, 4407–4415.

Bidleman, T.F., 1988. Atmospheric processes. Environ. Sci. Technol. 22, 361–367.

Bogdal, C., Alsberg, T., Diefenbacher, P.S., MacLeod, M., Berger, U., 2015. Fast quantification of chlorinated paraffins in environmental samples by direct injection high-resolution mass spectrometry with pattern deconvolution. Anal. Chem. 87, 2852–2860.

Breivik, K., Gioia, R., Chakraborty, P., Zhang, G., Jones, K.C., 2011. Are reductions in industrial organic contaminants emissions in rich countries achieved partly by export of toxic wastes? Environ. Sci. Technol. 45, 9154–9160.

Chaemfa, C., Xu, Y., Li, J., Chakraborty, P., Hussain Syed, J., Naseem Malik, R., Wang, Y., Tian, C., Zhang, G., Jones, K.C., 2014. Screening of atmospheric short-and medium-chain chlorinated paraffins in India and Pakistan using polyurethane foam based passive air sampler. Environ. Sci. Technol. 48, 4799–4808.

Chen, S.-J., Tian, M., Wang, J., Shi, T., Luo, Y., Luo, X.-J., Mai, B.-X., 2011. Dechlorane Plus (DP) in air and plants at an electronic waste (e-waste) site in South China. Environ. Pollut. 159, 1290–1296.

De la Torre, A., Barbas, B., Sanz, P., Navarro, I., Artíñano, B., Martínez, M., 2018. Traditional and novel halogenated flame retardants in urban ambient air: gas-particle partitioning, size distribution and health implications. Sci. Total Environ. 630, 154–163.

Drage, D.S., Newton, S., de Wit, C.A., Harrad, S., 2016. Concentrations of legacy and emerging flame retardants in air and soil on a transect in the UK West Midlands. Chemosphere 148, 195–203.

Gillett, R.W., Galbally, I.E., Keywood, M.D., Powell, J.C., Stevenson, G., Yates, A., Borgen, A.R., 2017. Atmospheric short-chain-chlorinated paraffins in Melbourne, Australia–first extensive Southern Hemisphere observations. Environ. Chem. 14, 106.

Glüge, J., Bogdal, C., Scheringer, M., Buser, A.M., Hungerbühler, K., 2013. Calculation of physicochemical properties for short-and medium-chain chlorinated paraffins. J. Phys. Chem. Ref. Data 42, 023103.

Glüge, J., Schinkel, L., Hungerbühler, K., Cariou, R., Bogdal, C., 2018. Environmental risks of medium-chain chlorinated paraffins (MCCPs): a review. Environ. Sci. Technol. 52, 6743–6760.

Glüge, J., Wang, Z., Bogdal, C., Scheringer, M., Hungerbühler, K., 2016. Global production, use, and emission volumes of short-chain chlorinated paraffins–A minimum scenario. Sci. Total Environ. 573, 1132–1146.

Goss, K.-U., Buschmann, J., Schwarzenbach, R.P., 2004. Adsorption of organic vapors to air-dry soils: model predictions and experimental validation. Environ. Sci. Technol. 38, 3667–3673.

Gouin, T., Mackay, D., Webster, E., Wania, F., 2000. Screening chemicals for persistence in the environment. Environ. Sci. Technol. 34, 881–884.

Halse, A.K., Schlabach, M., Schuster, J.K., Jones, K.C., Steinnes, E., Breivik, K., 2015. Endosulfan, pentachlorobenzene and short-chain chlorinated paraffins in background soils from Western Europe. Environ. Pollut. 196, 21–28.

Hansen, K.M., Fauser, P., Vorkamp, K., Christensen, J.H., 2020. Global Emissions of Dechlorane Plus. Science of The Total Environment, 140677.

Helsel, D.R., 2011. Statistics for Censored Environmental Data Using Minitab and R. John Wiley & Sons, ISBN 1118162765.

Hoh, E., Zhu, L., Hites, R.A., 2006. Dechlorane plus, a chlorinated flame retardant, in the Great Lakes. Environ. Sci. Technol. 40, 1184–1189.

Horstmann, M., Mclachlan, M.S., 1998. Atmospheric deposition of semivolatile organic compounds to two forest canopies. Atmos. Environ. 32, 1799–1809.

Klánová, J., Čupr, P., Holoubek, I., Borůvková, J., Přibylová, P., Kareš, R., Tomšej, T., Ocelka, T., 2009. Monitoring of persistent organic pollutants in Africa. Part 1: passive air sampling across the continent in 2008. J. Environ. Monit. 11, 1952–1963.

Klánová, J., Kohoutek, J., Hamplová, L., Urbanová, P., Holoubek, I., 2006. Passive air sampler as a tool for long-term air pollution monitoring: Part 1. Performance assessment for seasonal and spatial variations. Environ. Pollut. 144, 393–405.

Lammel, G., Degrendele, C., Gunthe, S.S., Mu, Q., Muthalagu, A., Audy, O., Biju, C.V., Kukučka, P., Mulder, M.D., Octaviani, M., 2018. Revolatilisation of soil-accumulated pollutants triggered by the summer monsoon in India. Atmos. Chem. Phys. 18, 11031–11040.

Li, L., Wania, F., 2016. Tracking chemicals in products around the world: introduction of a dynamic substance flow analysis model and application to PCBs. Environ. Int. 94, 674–686.

Li, Q., Li, J., Wang, Y., Xu, Y., Pan, X., Zhang, G., Luo, C., Kobara, Y., Nam, J.-J., Jones, K. C., 2012. Atmospheric short-chain chlorinated paraffins in China, Japan, and South Korea. Environ. Sci. Technol. 46, 11948–11954.

Mackay, D., 2001. Multimedia Environmental Models: the Fugacity Approach. CRC press, ISBN 1420032542.

Mahenge, R.S., Ulanga, P., Malabeja, M., Pilly, J., Massoy, W., 2018. Performance Audit Report on Electronic Waste Management. Available at: ELECTRONIC-WASTE-MANAGEMENT-2018.pdf (nao.go.tz). Accessed March 2021.

Markovic, M.Z., Prokop, S., Staebler, R.M., Liggio, J., Harner, T., 2015. Evaluation of the particle infiltration efficiency of three passive samplers and the PS-1 active air sampler. Atmos. Environ. 112, 289–293.

McLachlan, M.S., 1995. Bioaccumulation of hydrophobic chemicals in agricultural food chains. Environ. Sci. Technol. 30, 252–259.

Mézière, M., Krätschmer, K., Perkons, I., Zacs, D., Marchand, P., Dervilly, G., Le Bizec, B., Schächtele, A., Cariou, R., Vetter, W., 2020. Addressing main challenges regarding short-and medium-chain chlorinated paraffin analysis using GC/ECNI-MS and LC/ESI-MS methods. J. Am. Soc. Mass Spectrom. 31, 1885–1895.

Möckel, C., Breivik, K., Nøst, T.H., Sankoh, A., Jones, K.C., Sweetman, A., 2020. Soil pollution at a major West African E-waste recycling site: contamination pathways and implications for potential mitigation strategies. Environ. Int. 137, 105563.

NBS, 2019. National E-waste statistics report. In: National Bureau of Statistics and United Nations University, V.S. United Nations University, ViE – SCYCLE, Bonn, Germany. National Bureau Statistics, Dodoma, Tanzania.

Niu, S., Chen, R., Zou, Y., Dong, L., Hai, R., Huang, Y., 2020. Spatial distribution and profile of atmospheric short-chain chlorinated paraffins in the Yangtze River Delta. Environ. Pollut. 259, 113958.

Petrlik, J., Ochola, G.O., Mng'anya, S., 2020. POPs in Eggs from Kenya and Tanzania - Plastic Waste Poisons the Food Chain in Kenya and Tanzania. Retrieved from ResearchGate. https://doi.org/10.13140/RG.2.2.28526.02885, 2020.

Robinson, B.H., 2009. E-waste: an assessment of global production and environmental impacts. Sci. Total Environ. 408, 183–191.

Saini, A., Harner, T., Chinnadhurai, S., Schuster, J.K., Yates, A., Sweetman, A., Aristizabal-Zuluaga, B.H., Jiménez, B., Manzano, C.A., Gaga, E.O., 2020. GAPS-Megacities: a new global platform for investigating persistent organic pollutants and chemicals of emerging concern in urban air. Environ. Pollut. 267, 115416.

Shen, L., Reiner, E.J., MacPherson, K.A., Kolic, T.M., Helm, P.A., Richman, L.A., Marvin, C.H., Burniston, D.A., Hill, B., Brindle, I.D., 2010. Dechloranes 602, 603, 604, dechlorane plus, and Chlordene plus, a newly detected analogue, in tributary sediments of the Laurentian Great Lakes. Environ. Sci. Technol. 45, 693–699.

Shoeib, M., Harner, T., 2002. Characterization and comparison of three passive air samplers for persistent organic pollutants. Environ. Sci. Technol. 36, 4142–4151.

Shunthirasingham, C., Alexandrou, N., Brice, K.A., Dryfhout-Clark, H., Su, K., Shin, C., Park, R., Pajda, A., Noronha, R., Hung, H., 2018. Temporal trends of halogenated flame retardants in the atmosphere of the Canadian Great Lakes Basin (2005–2014). Environ. Sci.: Processes & Impacts 20, 469–479.

Someya, M., Suzuki, G., Ionas, A.C., Tue, N.M., Xu, F., Matsukami, H., Covaci, A., Viet, P. H., Takahashi, S., Tanabe, S., 2016. Occurrence of emerging flame retardants from e-waste recycling activities in the northern part of Vietnam. Emerg. Contam. 2, 58–65.

Sverko, E., Tomy, G.T., Reiner, E.J., Li, Y.-F., McCarry, B.E., Arnot, J.A., Law, R.J., Hites, R.A., 2011. Dechlorane plus and related compounds in the environment: a review. Environ. Sci. Technol. 45, 5088–5098.

Tma, T.M.A., 2021. Climate analysis. Tanzanian meteorological authority TMA. Available at: http://maproom.meteo.go.tz. (Accessed August 2021). Accessed.

UNECE, 2010. In: Europe, U.N.E.C.f. (Ed.), The 1998 Protocol on Persistent Organic Pollutants, Including the Amendments Adopted by the Parties on 18 December 2009. UNECE, 2010. https://unece.orµDAM/env/lrtap/full%20text/ece.eb.air.104.e.pdf. (Accessed January 2021).

UNEP, 2017. Stockholm convention on persistent organic pollutants (POPs). In: Convention, S.o.T.S, (Ed.). UNEP. 2017. Accessed. www.pops.int/TheConvention/Overview/TextoftheConvention/tabid/2232/Default.aspx. (Accessed January 2021).

UNEP, 2019. Proposal to List Dechlorane Plus (CAS No. 13560-89-9) and its Syn-Isomer (CAS No. 135821-03-3) and Anti-isomer (CAS No. 135821-74-8) in Annexes A, B And/or C to the Stockholm Convention on Persistent Organic Pollutants, Available at: www.pops.int, 2019. Accessed January 2021.

van Mourik, L., Lava, R., O'Brien, J., Leonards, P., de Boer, J., Ricci, M., 2020a. The underlying challenges that arise when analysing short-chain chlorinated paraffins in environmental matrices. J. Chromatogr. A 1610, 460550.

van Mourik, L., Van Der Veen, I., Crum, S., De Boer, J., 2018. Developments and interlaboratory study of the analysis of short-chain chlorinated paraffins. Trac. Trends Anal. Chem. 102, 32–40.

van Mourik, L.M., Wang, X., Paxman, C., Leonards, P.E., Wania, F., de Boer, J., Mueller, J.F., 2020b. Spatial variation of short-and medium-chain chlorinated paraffins in ambient air across Australia. Environ. Pollut., 114141

Wang, T., Han, S., Yuan, B., Zeng, L., Li, Y., Wang, Y., Jiang, G., 2012. Summer–winter concentrations and gas-particle partitioning of short chain chlorinated paraffins in the atmosphere of an urban setting. Environ. Pollut. 171, 38–45.

Wang, X.-T., Wang, X.-K., Zhang, Y., Chen, L., Sun, Y.-F., Li, M., Wu, M.-H., 2014. Short-and medium-chain chlorinated paraffins in urban soils of Shanghai: spatial distribution, homologue group patterns and ecological risk assessment. Sci. Total Environ. 490, 144–152.

Wang, X.-T., Xu, S.-Y., Wang, X.-K., Hu, B.-P., Jia, H.-H., 2017. Occurrence, homologue patterns and source apportionment of short-and medium-chain chlorinated paraffins in suburban soils of Shanghai, China. Chemosphere 180, 302–311.

Wang, Y., Li, J., Cheng, Z., Li, Q., Pan, X., Zhang, R., Liu, D., Luo, C., Liu, X., Katsoyiannis, A., 2013. Short-and medium-chain chlorinated paraffins in air and soil of subtropical terrestrial environment in the Pearl River Delta, South China: distribution, composition, atmospheric deposition fluxes, and environmental fate. Environ. Sci. Technol. 47, 2679–2687.

Wania, F., Mackay, D., 1996. Peer reviewed: tracking the distribution of persistent organic pollutants. Environ. Sci. Technol. 30, 390A–396A.

Wania, F., Shunthirasingham, C., 2020. Passive air sampling for semi-volatile organic chemicals. Environ. Sci.: Processes & Impacts 22, 1925–2002.

Webster, E., Mackay, D., Wania, F., 1998. Evaluating environmental persistence. Environ. Toxicol. Chem.: Int. J. 17, 2148–2158.

Wong, F., Wania, F., 2011. Visualising the equilibrium distribution and mobility of organic contaminants in soil using the chemical partitioning space. J. Environ. Monit. 13, 1569–1578.

Wong, M., Wu, S., Deng, W.J., Yu, X., Luo, Q., Leung, A., Wong, C., Luksemburg, W., Wong, A., 2007. Export of toxic chemicals–a review of the case of uncontrolled electronic-waste recycling. Environ. Pollut. 149, 131–140.

WorldBank, 2021. The World Bank in Tanzania. The World Bank, 2021. http://www.worldbank.org/en/country/tanzania/overview. (Accessed January 2021).

Xu, C., Zhang, Q., Gao, L., Zheng, M., Qiao, L., Cui, L., Wang, R., Cheng, J., 2019. Spatial distributions and transport implications of short-and medium-chain chlorinated paraffins in soils and sediments from an e-waste dismantling area in China. Sci. Total Environ. 649, 821–828.

Yhdego, M., 2017. From a Sanitary Landfill to a Dump Site: Pugu Kinyamwezi Community Curse in Dar Es Salaam. Tanzania. https://doi.org/10.13140/RG.2.2.27828.04483.

Zeng, L., Wang, T., Han, W., Yuan, B., Liu, Q., Wang, Y., Jiang, G., 2011. Spatial and vertical distribution of short chain chlorinated paraffins in soils from wastewater irrigated farmlands. Environ. Sci. Technol. 45, 2100–2106.

Supporting information

For

Spatial trends of chlorinated paraffins and dechloranes in air and soil in a tropical urban, suburban, and rural environment

Maja Nipen[a,b,*], Rolf David Vogt[a], Pernilla Bohlin-Nizzetto[b], Katrine Borgå[c], Eliezer Brown Mwakalapa[d], Anders Røsrud Borgen[b], Susanne Jøntvedt Jørgensen[a], Samwel Moses Ntapanta[e], Aviti John Mmochi[f], Martin Schlabach[b], Knut Breivik[a,b]

[a]Centre for Biogeochemistry in the Anthropocene, Department of Chemistry, University of Oslo (UiO), NO-0315 Oslo, Norway, [b]NILU-Norwegian Institute for Air Research, NO-2027 Kjeller, Norway, [c]Centre for Biogeochemistry in the Anthropocene, Department of Biosciences, UiO, NO-0316 Oslo, Norway, [d]Department of Natural Sciences, Mbeya University of Science and Technology, Mbeya, Tanzania, [e]Department of Social Anthropology, UiO, NO-0317 Oslo, Norway, [f]Institute for Marine Science, University of Dar es Salaam, Zanzibar, Tanzania,

* Corresponding author. Centre for Biogeochemistry in the Anthropocene, Department of Chemistry, University of Oslo (UiO), NO-0315 Oslo, Norway.

Email address: majanip@kjemi.uio.no

Table of Content

Table S1: Sampling locations

Location	Coordinates	Category	Sampling time (air)
R-1	-7.12267,39.5335	Rural	08.02.19-11.04.19
R-2	-6.93477,39.44751	Rural	09.02.19-11.04.19
R-3	-6.86737,39.36371	Rural	09.02.19-11.04.19
S-4	-6.8384,39.33624	Suburban	08.02.19-11.04.19
U-5	-6.87142,39.28221	Urban	12.02.19-11.04.19
U-6	-6.82964,39.27505	Urban	13.02.19-10.04.19
U-7	-6.82543,39.27159	Urban	13.02.19-10.04.19
U-8	-6.81301,39.29107	Urban	12.02.19-12.04.19
U-9	-6.78262,39.28333	Urban	12.02.19-12.04.19
U-10	-6.75804,39.24283	Urban	11.02.19-12.04.19
U-11	-6.78428,39.23887	Urban	12.02.19-12.04.19
U-12	-6.83541,39.20857	Urban	12.02.19-14.04.19
S-13	-6.78127,39.20413	Suburban/Season	11.02.19-12.04.19
S-13 Season 1	-6.78127,39.20413	Season	26.01.18-12.04.18
S-13 Season 2	-6.78127,39.20413	Season	12.04.18-18.06.18
S-13 Season 3	-6.78127,39.20413	Season	18.06.18-23.08.18
S-13 Season 4	-6.78127,39.20413	Season	23.08.18-19-11.19
S-13 Season 5	-6.78127,39.20413	Season	19-11.18-11.02.19
S-14	-6.79938,39.13767	Suburban	10.02.19-13.04.19
S-15	-6.788330,39.0524	Suburban	10.02.19-13.04.19
S-16	-6.76502,38.99271	Suburban	10.02.19-13.04.19
R-17	-6.76059 38.94704	Rural	10.02.19.13.04.19
R-18	-6.72717,38.854	Rural	10.02.19-13.04.19
R-19	-6.67864,38.76234	Rural	11.02.19-13.04.19
W-20	-6.9317,39.14074	Waste	06.02.19-10.04.19
W-21	-6.9278,39.12785	Waste	06.02.19-10.04.19
W-22	-6.92825,39.12506	Waste	06.02.19-10.04.19
W-23	-6.92644,39.12468	Waste	06.02.19-10.04.19
W-24	-6.92525,39.12572	Waste	06.02.19-10.04.19
W-25	-6.92526,39.12017	Waste	07.02.19-10.04.19
W-26	-6.91611,39.11291	Waste	06.02.19-10.04.19
W-27	-6.90065,39.09197	Waste	07.02.19-10.04.19
W-28	-6.91072,39.03234	Waste	07.02.19-10.04.19

Text S1: Method

Sampling

The soil samples were wrapped in minimum two layers of aluminium foil and Ziplock bags, transported in cooler bags, and subsequently frozen.

Polyurethane foam (PUF) disks were cleaned prior to deployment by soxhlet extraction in toluene (24 hours), acetone (8 hours) and n-hexane (8 hours), before drying in a desiccator under vacuum. Cleaned PUF discs were wrapped in two layers of aluminium foil and two Ziploc bags and stored cool. The metal components of the air sampling unit were pre cleaned by soaking overnight in alkaline soap, before rinsing in water, acetone, and n-hexane. After cleaning, the metal components of the air samplers were stored dust free until deployment. Prior to deployment, during the field campaign, and during transport the PUF discs were kept cool, and after arrival at the laboratory, they were stored at freezer temperatures.

Sample preparation

Soil sample results were evaluated on both a dry weight (dw) and organic matter (OM) basis, where the OM content was determined by loss on ignition (LOI) using previously air-dried subsamples. LOI values were corrected for structural water loss according to Hoogsteen et al. (2015).

Procedural blank samples were prepared and analysed alongside air and soil samples, and in addition, field blanks were included. In this study, field blanks consisted of blanks where the sampling material was briefly exposed on location during sample collection (N = 5), and travel blanks (N = 3). One procedural blank sample for DPs in air was eliminated from LOD calculation as an outlier.

For the sample preparation, all glassware was heated at 450 ℃ overnight and rinsed with acetone and n-hexane before use, and high-purity grade solvents were used throughout. Prior to extraction, soil samples were dried and homogenized by mixing approximately 7 g soil with sodium sulphate in a mortar until a free-flowing powder was achieved. ^{13}C labelled internal standards of 1,5,5,6,6,10-hexachlorodecane and Dechlorane Plus (DP) Syn were added to the samples, and extraction was performed using Accelerated Solvent Extraction (ASE) (Dionex), with 1:1 acetone/n-hexane, two extraction cycles, 1500 psi and 100 ℃. Extraction cells were packed (from bottom to top) with three cellulose filters, 5 g precleaned

Florisil, filter, sample, filter. For the air samples, the PUF disks had ^{13}C labelled internal standards of 1,5,5,6,6,10-hexachlorodecane, DP Syn, and Dechlorane 602 (Dec 602) added before soxhlet extraction with acetone/ n-hexane (1:1) for a minimum of eight hours.

The extracts from soil samples and air samples were volume reduced to approximately 0.5 mL using a Turbovap system (Zymark). Solvent was changed to n-hexane, before the extracts were treated with approximately 2 mL concentrated sulfuric acid (four repetitions for soil samples, three repetitions for air samples), to remove acid labile matrix interferences. To remove potential interferences of a more polar nature, including remaining break down products from acid treatment, samples were subsequently put through a 15 mm internal diameter column containing 4 g activated silica and a 1 cm layer of sodium sulphate. The column was dry packed and conditioned with 30 mL diethyl ether in n-hexane (1:9) and eluted with 30 mL diethyl ether in n-hexane (1:9). Solvent was changed to isooctane, and volume reduced to approximately 100 µL using a gentle stream of nitrogen. 1,2,3,4-tetrachloronaphthalene (TCN) was added to extracts as a recovery standard. The ratios of TCN and internal standards in samples were compared against the ratios of TCN and internal standards in quantification mixtures (which were not subject to extraction and clean-up) to determine the recovery of internal standards.

Instrumental analysis

The samples were analysed using gas chromatography quadrupole time-of-flight high resolution mass spectrometry (7200B GC/Q-TOF) (Agilent, Santa Clara, USA). The gas chromatographic separation was done using a two-part column, where the analytical column was a 15 m HP-5ms Ultra Inert stationary phase with inner diameter 250 µm, and film thickness 0.25 µm. The second column was a 1.8 m fused silica column with no stationary phase and an inner diameter of 150 µm for the purpose of restriction. Flow rates were 1.2 mL/min on the first section of the column, and 1.4 mL/min on the second section. Samples were introduced using a programmed temperature vaporization (PTV) inlet in solvent vent mode, starting at 60 ℃, holding for 0.35 min, increasing by 500 ℃/min to 320 ℃, holding for 3 minutes, before changing by 10 ℃/min to 290 ℃, and holding for 20 min and finally at 500℃/min to 320℃. The GC oven temperature program was as follows: initial temperature 55 ℃, hold time 2 min. Change rate 70 ℃/min to 200 ℃, hold for 1 min. Change rate 10 ℃/min to 280 ℃, hold for 1 min, then change rate 10 ℃/min to 310 ℃ and finally at 70℃/min to 325℃, hold for 4 min. The Q-TOF was run in Electron Capture Negative

Ionization (ECNI) mode using methane as a moderating gas. The ion source was kept at 120℃ to minimize fragmentation and thus optimize the formation of the $[M-Cl]^-$ or the $[M-HCl]^-$ ion for the chlorinated paraffins (CPs) and $[M]^-$ for the dechloranes. The electron energy was set to 250 electron volts in the source, with an emission current of 12 µA.

Quantification of Chlorinated paraffins

All chromatograms were manually inspected using the MassHunter software. Manual integration was performed where necessary to avoid potential interferences. CPs were quantified using a pattern deconvolution procedure based on the method presented in Bogdal et al. (2015). Briefly, for short chain CPs (SCCPs), C_{10} - C_{13} standards with 51%, 55% and 63% Cl (w/w), and single chain length standards of C_{10}, C_{11}, C_{12}, and C_{13} (50% and 65% Cl) were analysed, and for medium chain CPs (MCCPs), C_{14} - C_{17} standards of 42%, 52%, and 57% Cl, and single chain C_{14} with 52% Cl were analysed, and the resulting congener patterns were used to reconstruct the congener pattern of the sample. The pattern reconstruction was done using the nnls package in R studio, which applies the Lawson-Hanson algorithm to provide non-negative least squares estimates for the contribution of the various standards to the sample pattern. A R^2 between sample pattern and reconstructed pattern of 0.5 or above was considered satisfactory (Bogdal et al., 2015). Given the large number of standards involved in quantification, only a smaller number of standards were analysed alongside each batch of samples to confirm stability of the instrument response (typically SCCPs with 51%, 55%, and 63% Cl, and MCCPs with 42% Cl). The instrument stability and quantification procedure were also monitored by the regular analysis of known concentration in-house standard mixtures. Quantification of sample CPs content was achieved by constructing separate calibration curves using areas from each standard at four concentration levels, from which sample areas were compared, and concentration calculated. R^2 for the calibration curves were above 0.99, except C_{13} 50% Cl where R^2 was above 0.98. Calculated sample concentration based on each standard was subsequently weighted by the non-negative least squares estimate for contribution of each standard to the sample, and contributions from all standards were summarized. All sample and standard areas were normalized using ^{13}C labelled internal standard. In addition, areas were normalized by natural abundance of the measured m/z, enabling extension of the instruments linear range.

Spike recovery test

The recovery calculation of CPs after the laboratory procedure is based on the ratio of internal standard and recovery standard in the sample, compared to the same ratio in a quantification standard consisting of a known amount of both internal standard and recovery standard. As the recovery rate is based on one single CP congener, it was of interest to assess whether the different SCCP and MCCP congener groups have similar levels of recovery from the laboratory procedure. PUF disks were spiked with 100 µL technical mixture of SCCPs (51% Cl by weight), and 100 µL technical mixture of MCCPs (52% Cl by weight), in addition to 20 µL internal standard. The PUF discs were subsequently extracted using soxhlet and cleaned using concentrated sulfuric acid and silica as described above. The recovery test samples were volume reduced using N_2 gas to 120 µL, before addition of 20 µL TCN as recovery standard. A quantification standard for the recovery test samples was prepared by mixing 100 µL of each of the technical mixtures mentioned above, and 20 µL of internal standard. The quantification standard mix was volume reduced using N_2 gas to 120 µL and given 20 µL TCN as a recovery standard.

Table S2: Congener groups of SCCPs included in the analytical process, analysed ion, accurate mass, and natural abundance. Congener groups in italic only identified, not quantified, congener groups in bold included in distribution and fugacity analysis.

Congener group	Ion	m/z	Natural abundance
$C_7H_{10}Cl_6$	$[M-Cl]^-$	270.9201	0.37
$C_7H_9Cl_7$	$[M-Cl]^-$	304.8811	0.34
$C_8H_{13}Cl_5$	$[M-HCl]^-$	249.9669	0.39
$C_8H_{12}Cl_6$	$[M-Cl]^-$	284.9358	0.37
$C_8H_{11}Cl_7$	$[M-Cl]^-$	318.8968	0.33
$C_8H_{10}Cl_8$	$[M-Cl]^-$	352.8578	0.30
$C_8H_9Cl_9$	$[M-Cl]^-$	388.8159	0.29
$C_9H_{15}Cl_5$	$[M-HCl]^-$	263.9826	0.38
$C_9H_{14}Cl_6$	$[M-HCl]^-$	297.9436	0.36
$C_9H_{13}Cl_7$	$[M-Cl]^-$	332.9124	0.33
$C_9H_{12}Cl_8$	$[M-Cl]^-$	366.8735	0.29
$C_9H_{11}Cl_9$	$[M-Cl]^-$	402.8315	0.28
$C_9H_{10}Cl_{10}$	$[M-Cl]^-$	436.7926	0.28
$C_{10}H_{18}Cl_4$	$[M-HCl]^-$	242.0401	0.39

$C_{10}H_{17}Cl_5$	$[M-HCl]^-$	277.9982	0.38
$C_{10}H_{16}Cl_6$	$[M-HCl]^-$	311.9592	0.36
$C_{10}H_{15}Cl_7$	$[M-Cl]^-$	346.9281	0.33
$C_{10}H_{14}Cl_8$	$[M-Cl]^-$	380.8891	0.29
$C_{10}H_{13}Cl_9$	$[M-Cl]^-$	416.8472	0.28
$C_{10}H_{12}Cl_{10}$	$[M-Cl]^-$	450.8082	0.27
$C_{11}H_{20}Cl_4$	$[M-HCl]^-$	256.0558	0.39
$C_{11}H_{19}Cl_5$	$[M-HCl]^-$	292.0139	0.38
$C_{11}H_{18}Cl_6$	$[M-HCl]^-$	325.9749	0.36
$C_{11}H_{17}Cl_7$	$[M-Cl]^-$	360.9437	0.32
$C_{11}H_{16}Cl_8$	$[M-Cl]^-$	394.9048	0.29
$C_{11}H_{15}Cl_9$	$[M-Cl]^-$	430.8628	0.28
$C_{11}H_{14}Cl_{10}$	$[M-Cl]^-$	464.8239	0.27
$C_{11}H_{13}Cl_{11}$	$[M-Cl]^-$	498.7849	0.26
$C_{11}H_{12}Cl_{12}$	$[M-Cl]^-$	532.7459	0.24
$C_{11}H_{11}Cl_{13}$	$[M-Cl]^-$	568.7040	0.23
$C_{12}H_{22}Cl_4$	$[M-HCl]^-$	270.0714	0.38
$C_{12}H_{21}Cl_5$	$[M-HCl]^-$	306.0295	0.37
$C_{12}H_{20}Cl_6$	$[M-HCl]^-$	339.9905	0.35
$C_{12}H_{19}Cl_7$	$[M-Cl]^-$	374.9594	0.32
$C_{12}H_{18}Cl_8$	$[M-Cl]^-$	408.9204	0.28
$C_{12}H_{17}Cl_9$	$[M-Cl]^-$	444.8785	0.28
$C_{12}H_{16}Cl_{10}$	$[M-Cl]^-$	478.8395	0.27
$C_{12}H_{15}Cl_{11}$	$[M-Cl]^-$	512.8006	0.25
$C_{13}H_{24}Cl_4$	$[M-HCl]^-$	284.0871	0.38
$C_{13}H_{23}Cl_5$	$[M-HCl]^-$	320.0452	0.37
$C_{13}H_{22}Cl_6$	$[M-HCl]^-$	354.0062	0.35
$C_{13}H_{21}Cl_7$	$[M-Cl]^-$	388.9750	0.32
$C_{13}H_{20}Cl_8$	$[M-Cl]^-$	422.9361	0.28
$C_{13}H_{19}Cl_9$	$[M-Cl]^-$	458.8941	0.27
$C_{13}H_{18}Cl_{10}$	$[M-Cl]^-$	492.8552	0.27
$C_{13}H_{17}Cl_{11}$	$[M-Cl]^-$	526.8162	0.25
$C_{13}H_{16}Cl_{12}$	$[M-Cl]^-$	560.7772	0.23

Table S3: Congener groups of MCCPs included in the analytical process, analysed ion, accurate mass, and natural abundance. Congener groups in bold included in distribution and fugacity analysis.

Congener group	**Ion**	**m/z**	**Natural abundance**
$C_{14}H_{26}Cl_4$	$[M-HCl]^-$	298.1027	0.37
$C_{14}H_{25}Cl_5$	$[M-HCl]^-$	334.0608	0.37
$C_{14}H_{24}Cl_6$	$[M-HCl]^-$	368.0218	0.35
$C_{14}H_{23}Cl_7$	$[M-Cl]^-$	402.9907	0.32
$C_{14}H_{22}Cl_8$	$[M-Cl]^-$	436.9517	0.28
$C_{14}H_{21}Cl_9$	$[M-Cl]^-$	472.9098	0.27
$C_{14}H_{20}Cl_{10}$	$[M-Cl]^-$	506.8708	0.27
$C_{15}H_{27}Cl_4$	$[M-HCl]^-$	312.1183	0.37
$C_{15}H_{27}Cl_5$	$[M-HCl]^-$	348.0765	0.37
$C_{15}H_{26}Cl_6$	$[M-HCl]^-$	382.0375	0.34
$C_{15}H_{25}Cl_7$	$[M-Cl]^-$	417.0063	0.31
$C_{15}H_{24}Cl_8$	$[M-Cl]^-$	450.9674	0.28
$C_{15}H_{23}Cl_9$	$[M-Cl]^-$	486.9254	0.27
$C_{15}H_{22}Cl_{10}$	$[M-Cl]^-$	520.8865	0.26
$C_{16}H_{30}Cl_4$	$[M-HCl]^-$	326.1340	0.36
$C_{16}H_{29}Cl_5$	$[M-HCl]^-$	362.0921	0.36
$C_{16}H_{28}Cl_6$	$[M-HCl]^-$	396.0531	0.34
$C_{16}H_{27}Cl_7$	$[M-Cl]^-$	431.0219	0.31
$C_{16}H_{26}Cl_8$	$[M-Cl]^-$	464.9830	0.28
$C_{16}H_{25}Cl_9$	$[M-Cl]^-$	500.9411	0.27
$C_{16}H_{24}Cl_{10}$	$[M-Cl]^-$	534.9021	0.26
$C_{17}H_{32}Cl_4$	$[M-HCl]^-$	340.1497	0.36
$C_{17}H_{31}Cl_5$	$[M-HCl]^-$	367.1078	0.36
$C_{17}H_{30}Cl_6$	$[M-HCl]^-$	410.0688	0.34
$C_{17}H_{29}Cl_7$	$[M-Cl]^-$	445.0376	0.31
$C_{17}H_{28}Cl_8$	$[M-Cl]^-$	478.9987	0.27
$C_{17}H_{27}Cl_9$	$[M-Cl]^-$	514.9576	0.26
$C_{17}H_{26}Cl_{10}$	$[M-Cl]^-$	548.9178	0.26

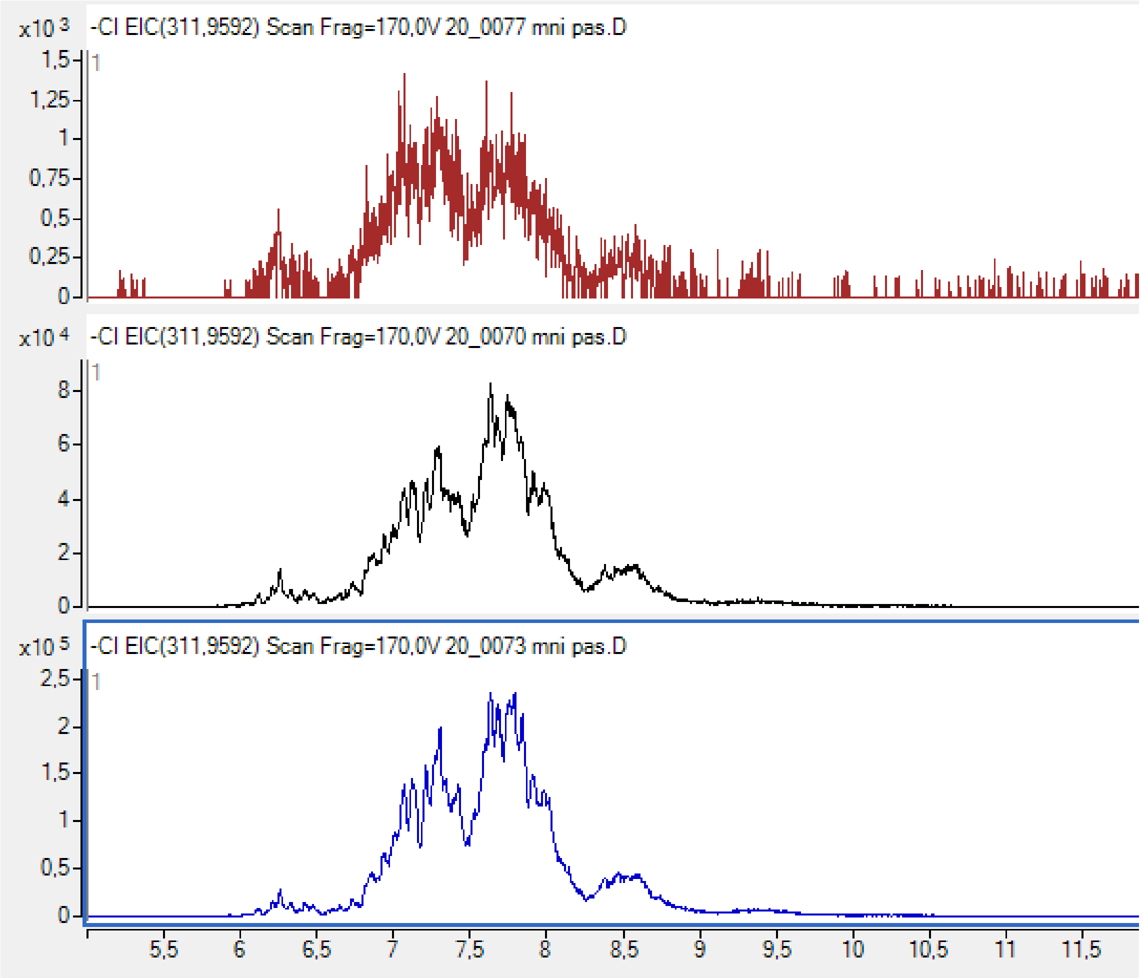

Figure S1: Example chromatograms for $C_{10}H_{16}Cl_6$ in air samples from location S-15 (lower), location S-13 (middle), and blank analysed alongside samples (top).

Table S4: Results from spike recovery test

	SCCPs (ng)	**MCCPs (ng)**	**Diff. SCCP (%)**	**Diff. MCCP (%)**
P1	10 520	11 338	5.2	13.4
P2	9 969	9 517	0.3	4.8
P3	10 423	10 265	4.2	2.7
P4	10 718	12 100	7.2	21.0
P5	10 026	9 825	0.3	1.7
P6	10 067	10 184	0.7	1.8
Average	10 288	10 539	3.0	7.6
Stand. dev.	309	983	3.0	7.9
Expected amount	10 000	10 000		

Table S5: Sequestered amount in air sample and estimated concentration, chlorination degree, goodness of fit in deconvolution, ratio MCCP/SCCP, and recovery of internal standard for CPs in air samples.

Location	**SCCPs** µg/sample (ng/m^3)	**SCCP** Cl (% w/w)	**SCCP R^2**	**MCCPs** µg/sample (ng/m^3)	**MCCP** Cl (% w/w)	**MCCP R^2**	**MCCP/ SCCP**	**Recovery** (%)
R-1	0.09 (0.3)	60.4	0.95	<0.1 (<0.4)	52.6	0.94	-	66
R-2	0.3 (1)	60.1	0.95	<0.1 (<0.4)	54.6	0.98	-	61
R-3	5 (18)	60.2	0.95	1 (5)	53.5	0.99	0.28	15
S-4	2 (7)	59.9	0.99	0.5 (2)	53.8	0.99	0.27	58
U-5	8 (33)	59.1	0.97	6 (25)	51.6	0.98	0.76	65
U-6	11 (45)	60.5	0.95	6 (26)	53.8	0.99	0.57	56
U-7	11 (45)	60.6	0.96	5 (21)	55.8	0.99	0.48	75
U-8	5 (22)	59.5	0.98	1 (5)	53.4	0.99	0.25	69
U-9	4 (14)	59.5	0.98	2 (6)	52.2	0.98	0.43	68
U-10	3 (11)	59.9	0.97	0.7 (3)	53.0	0.99	0.29	69
U-11	15 (59)	58.9	0.93	9 (35)	52.9	0.99	0.61	68
U-12	10 (38)	60.0	0.95	4 (14)	53.7	0.99	0.39	64
S-13	5 (19)	60.3	0.95	2 (9)	54.5	0.99	0.48	64
S-13 Season 1	4 (15)	60.4	0.93	2 (9)	54.0	0.99	0.60	83
S-13 Season 2	4 (16)	60.5	0.93	3 (10)	54.0	0.99	0.62	76
S-13 Season 3	6 (22)	60.6	0.94	4 (15)	54.6	0.99	0.66	69
S-13 Season 4	5 (21)	60.6	0.93	4 (15)	54.6	0.99	0.71	72
S-13 Season 5	4 (16)	60.5	0.93	3 (12)	54.9	0.99	0.81	82
S-14	16 (63)	59.2	0.97	2 (9)	53.5	0.98	0.14	65
S-15	2 (7)	60.1	0.98	0.4 (2)	53.9	0.99	0.22	59
S-16	2 (7)	60.2	0.96	0.7 (3)	53.7	0.99	0.38	60
R-17	1 (5)	60.3	0.96	0.4 (1)	55.0	0.99	0.31	76
R-18	3 (13)	59.2	0.97	0.7 (3)	54.8	0.99	0.20	78
R-19	0.5 (2)	60.6	0.96	0.2 (0.8)	56.3	0.97	0.39	76
W-20	8 (30)	59.8	0.98	1 (5)	53.7	0.99	0.18	63
W-21	16 (59)	60.5	0.95	9 (33)	53.4	0.99	0.55	26
W-22	8 (29)	60.8	0.92	2 (9)	53.9	0.99	0.31	59
W-23	15 (55)	59.6	0.98	9 (32)	53.7	0.97	0.60	*
W-24	2 (9)	60.4	0.95	1 (4)	55.0	0.99	0.43	85
W-25	2 (7)	60.3	0.97	0.6 (2)	53.9	0.99	0.28	68
W-26	3 (12)	60.5	0.95	1 (5)	54.4	0.99	0.39	73
W-27	1 (6)	60.2	0.97	0.4 (2)	53.7	0.99	0.27	75
W-28	1 (4)	60.6	0.95	0.3 (1)	54.3	0.99	0.28	52

* Recovery calculation not possible due to an instrumental interference affecting the recovery standard (1,2,3,4-Tetrachloronapthalene). Internal standard used for quantification (^{13}C labelled 1,5,5,6,6,10-Hexachlorodecane) not affected.

- MCCP/SCCP not determined

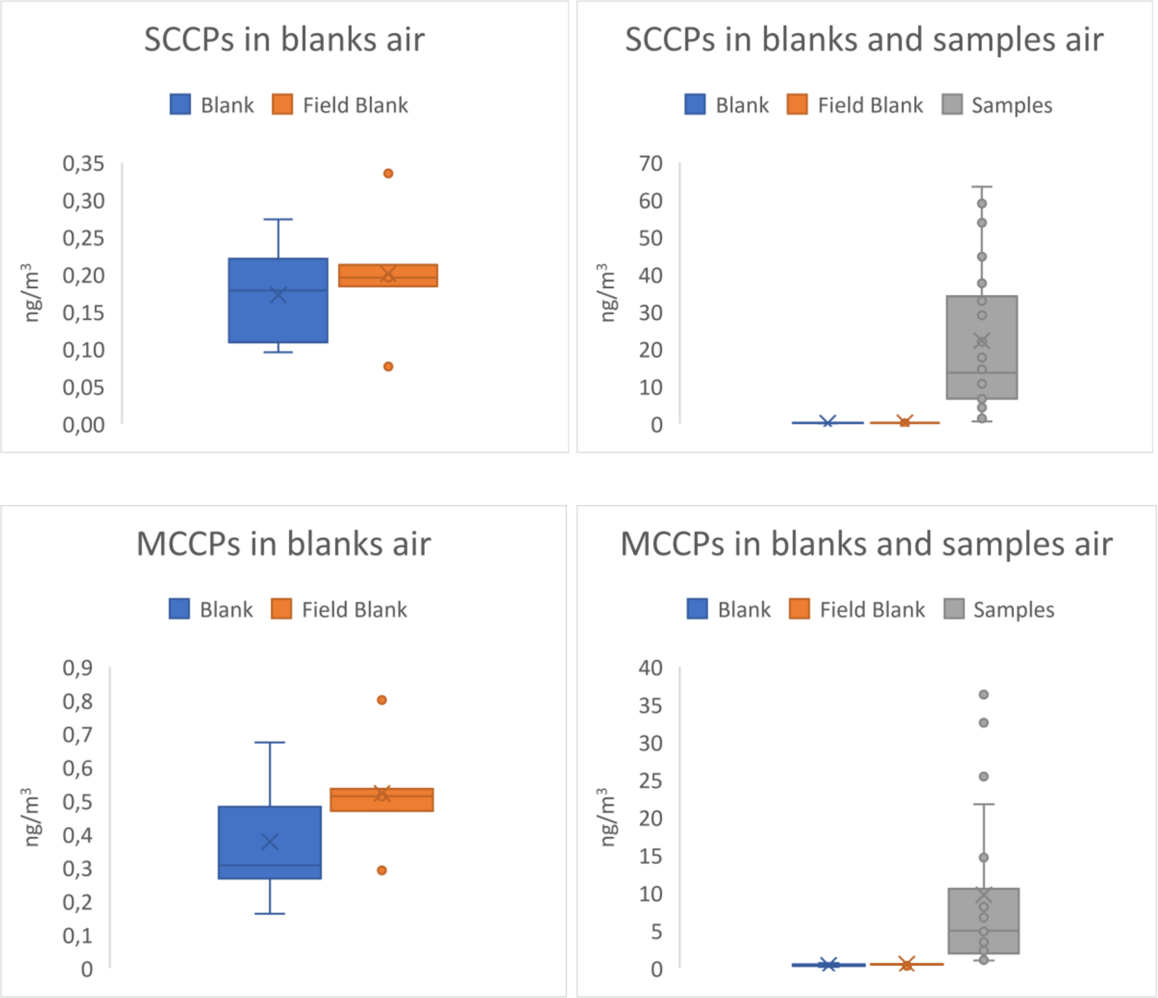

Figure S2: Boxplots illustrating relative levels of CPs in blanks, field blanks, and air samples. Blank concentrations converted to ng/m^3.

Table S6: Concentration, chlorination degree, goodness of fit in deconvolution, ratio MCCP/SCCP, content of OM, sample amount, and recovery of internal standard for CPs in soil samples.

Location	**SCCPs** ng/g dw	**SCCP Cl** (% w/w)	**SCCP R^2**	**MCCPs** ng/g dw	**MCCP Cl** (% w/w)	**MCCP R^2**	**MCCP/ SCCP**	**Recovery** (%)	**OM** (%)	**Sample amount** g dw
R-1	<11	60.1	*0.41*	<19	54.0	0.93	-	89	8.6	6.053
R-2	15	59.5	0.94	<19	53.9	0.96	-	93	1.4	6.705
R-3	12	60.2	0.94	20	56.7	0.91	1.4	82	0.4	7.195
S-4	14	60.0	0.87	31	58.3	0.87	2.3	85	2.2	5.594
U-5	80	61.8	0.96	370	58.1	0.80	4.6	79	3.3	5.240
U-6	360	64.1	0.97	1 800	59.7	*0.33*	4.9	68	2.1	6.405
U-7	120	62.4	0.95	730	58.0	0.97	5.9	82	1.9	5.526
U-8	1 600	61.5	0.85	3 200	57.0	0.53	2.1	38	3.0	5.745
U-9	190	62.0	0.86	990	57.4	0.88	5.3	81	7.4	5.020
U-10	67	61.7	0.91	120	57.3	0.80	1.8	76	1.7	5.541
U-11	160	63.7	0.95	500	58.3	0.81	3.1	72	0.3	5.507
U-12	110	63.1	0.96	380	58.1	0.82	3.4	79	1.7	6.494
S-13	25	62.4	0.91	180	57.3	0.63	7.0	67	9.6	5.196
S-14	50	59.8	0.96	53	58.5	0.92	1.1	45	0.2	5.208
S-15	150	62.8	0.97	520	58.8	0.71	3.4	75	1.5	5.868
S-16	<11	62.2	0.77	30	58.8	0.73	-	78	0.9	5.238
R-17	19	61.4	0.76	210	57.8	*0.33*	11	75	2.3	5.774
R-18	<11	58.6	0.84	<19	57.2	0.66	-	74	3.6	5.327
R-19	120	58.2	0.95	59	55.6	0.95	0.49	38	1.8	5.265
W-20	15	62.1	0.86	26	57.4	0.66	1.8	72	0.8	7.156
W-21	5 300	63.4	0.91	5 100	58.4	0.91	1.0	57	1.5	6.421
W-22	11	62.5	0.86	33	58.4	0.82	3.0	102	1.0	7.091
W-23	480	63.0	0.93	2 700	59.7	0.65	5.7	59	1.1	7.682
W-24	40	62.4	0.93	99	58.5	0.80	2.5	93	0.9	7.123
W-25	52	58.9	0.97	160	55.2	0.71	3.1	36	<0.01	7.155
W-26	91	61.5	0.94	240	59.0	0.83	2.7	82	<0.01	7.131
W-27	30	62.3	0.96	320	56.8	0.64	11	85	7.4	6.125
W-28	15	59.1	0.94	<19	57.7	0.83	-	72	2.4	7.289

Coefficient of determination (R^2) for the deconvolution quantification below 0.5 given in italic, indicating that the reported value is indicative.

- MCCP/SCCP not determined

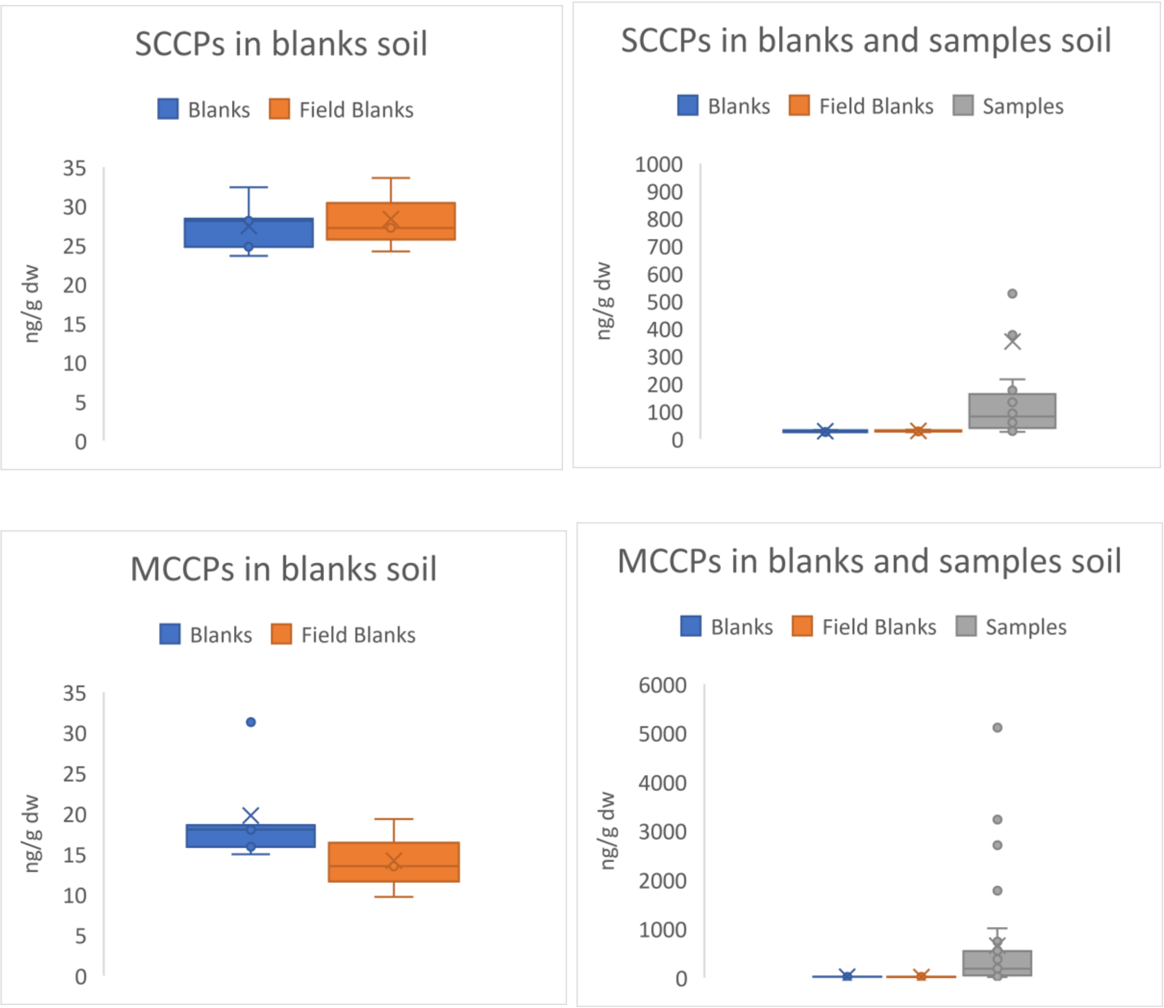

Figure S3: Boxplots illustrating relative levels of CPs in blanks, field blanks, and soil samples. For SCCPs in soil samples, four samples have concentrations higher than the illustrated range. Blank concentrations converted to ng/g dw.

Table S7: Sequestered amount in air sample and estimated concentration, fraction of DP anti isomer, and recovery of internal standard for dechloranes in air samples

Location	**Dec 602** ng/sample (pg/m^3)	**Dec 603** ng/sample (pg/m^3)	**DP syn** ng/sample (pg/m^3)	**DP anti** ng/sample (pg/m^3)	**Recovery Dec 602** (%)	**Recovery DP syn** (%)	***f* anti**
R-1	<0.001 (<0.007)	<0.001 (<0.007)	<0.06 (<0.4)	<0.09 (<0.6)	74	74	-
R-2	<0.001 (<0.007)	<0.001 (<0.007)	<0.06 (<0.4)	<0.09 (<0.6)	70	68	-
R-3	<0.001 (<0.007)	<0.001 (<0.007)	<0.06 (<0.4)	0.1 (0.7)	18	18	-
S-4	<0.001 (<0.007)	<0.001 (<0.007)	<0.06 (<0.4)	<0.09 (<0.6)	69	73	-
U-5	0.009 (0.07)	<0.001 (<0.007)	0.08 (0.6)	0.2 (2)	58	62	0.73
U-6	0.02 (0.2)	0.03 (0.2)	0.3 (2)	0.7 (5)	51	60	0.71
U-7	0.03 (0.2)	0.009 (0.07)	0.5 (4)	2 (16)	68	80	0.80
U-8	0.007 (0.05)	<0.001 (<0.007)	<0.06 (<0.4)	0.1 (0.8)	66	68	-
U-9	<0.001 (<0.007)	<0.001 (<0.007)	<0.06 (<0.4)	<0.09 (<0.6)	71	72	-
U-10	0.006 (0.04)	<0.001 (<0.007)	<0.06 (<0.4)	0.1 (1)	63	66	-
U-11	0.01 (0.1)	0.006 (0.04)	<0.06 (<0.4)	0.2 (1)	65	65	-
U-12	<0.001 (<0.007)	<0.001 (<0.007)	0.2 (1)	0.2 (2)	73	75	0.59
S-13	<0.001 (<0.007)	<0.001 (<0.007)	0.1 (0.8)	0.3 (2)	72	73	0.71
Season 1	0.01 (0.1)	<0.001 (<0.007)	0.1 (0.8)	0.4 (3)	68	68	0.77
Season 2	0.01 (0.1)	0.01 (0.08)	0.1 (0.9)	0.4 (3)	63	70	0.74
Season 3	0.02 (0.1)	0.01 (0.08)	0.2 (2)	0.6 (4)	54	61	0.73
Season 4	0.01 (0.1)	<0.001 (<0.007)	0.2 (1)	0.5 (4)	54	63	0.74
Season 5	0.02 (0.1)	0.01 (0.09)	0.1 (1)	0.5 (3)	66	71	0.78
S-14	<0.001 (<0.007)	<0.001 (<0.007)	<0.06 (<0.4)	<0.09 (<0.6)	75	78	-
S-15	<0.001 (<0.007)	<0.001 (<0.007)	0.06 (0.5)	<0.09 (<0.6)	70	70	-
S-16	<0.001 (<0.007)	<0.001 (<0.007)	<0.06 (<0.4)	<0.09 (<0.6)	70	71	-
R-17	<0.001 (<0.007)	<0.001 (<0.007)	<0.06 (<0.4)	<0.09 (<0.6)	73	73	-
R-18	<0.001 (<0.007)	<0.001 (<0.007)	<0.06 (<0.4)	<0.09 (<0.6)	73	77	-
R-19	<0.001 (<0.007)	<0.001 (<0.007)	<0.06 (<0.4)	0.1 (1)	75	75	-
W-20	0.008 (0.05)	<0.001 (<0.007)	<0.06 (<0.4)	0.1 (0.8)	63	67	-
W-21	0.03 (0.2)	<0.001 (<0.007)	0.1 (1)	0.3 (2)	21	28	0.67
W-22	0.01 (0.08)	<0.001 (<0.007)	0.09 (0.6)	0.2 (1)	57	62	0.71
W-23	0.008 (0.05)	<0.001 (<0.007)	0.3 (2)	1 (7)	*	*	0.77
W-24	0.005 (0.03)	<0.001 (<0.007)	<0.06 (<0.4)	0.2 (1)	73	91	-
W-25	<0.001 (<0.007)	<0.001 (<0.007)	<0.06 (<0.4)	<0.09 (<0.6)	72	73	-
W-26	0.008 (0.05)	<0.001 (<0.007)	<0.06 (<0.4)	<0.09 (<0.6)	72	74	-
W-27	0.005 (0.03)	0.006 (0.04)	<0.06 (<0.4)	<0.09 (<0.6)	71	73	-
W-28	<0.001 (<0.007)	<0.001 (<0.007)	<0.06 (<0.4)	<0.09 (<0.6)	70	71	-

* Recovery calculation not possible due to an instrumental interference affecting the recovery standard (1,2,3,4-Tetrachloronapthalene). Internal standard used for quantification (^{13}C labelled 1,5,5,6,6,10-Hexachlorodecane) not affected.

- *f* anti not determined

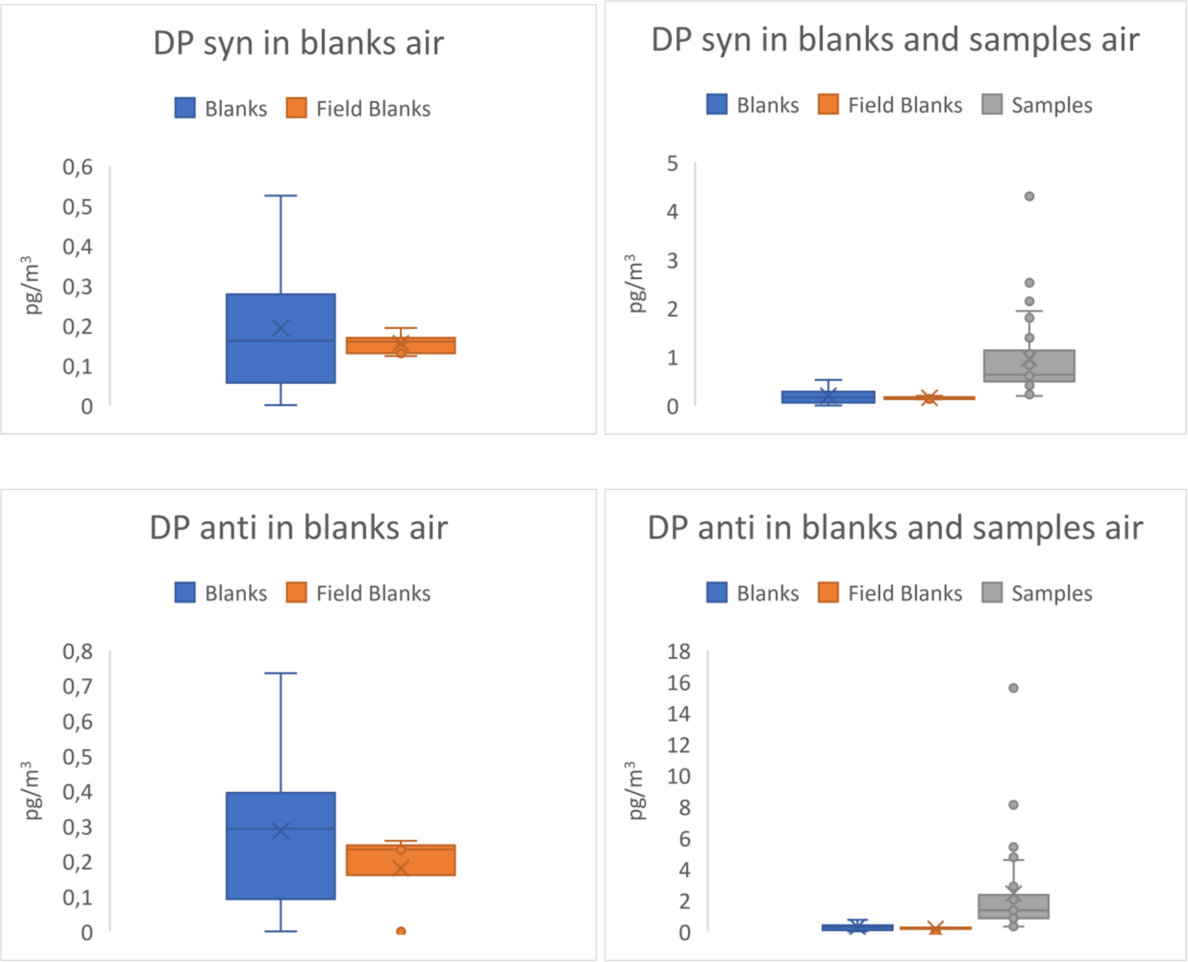

Figure S4: Boxplots illustrating relative levels of DP in blanks, field blanks, and air samples. Blank concentrations converted to pg/m^3.

Table S8: Concentration of dechloranes, recovery of internal standard, and fraction of DP anti isomer in soil samples.

Location	**Dec 602** ng/g dw	**Dec 603** ng/g dw	**DP syn** ng/g dw	**DP anti** ng/g dw	**Recovery DP syn** (%)	***f* anti**
R-1	0.002	<0.001	<0.01	<0.02	74	-
R-2	0.001	<0.001	<0.01	<0.02	76	-
R-3	<0.001	0.008	<0.01	0.06	71	-
S-4	<0.001	<0.001	0.01	0.05	72	0.82
U-5	0.005	0.2	0.07	0.2	78	0.77
U-6	0.05	0.2	3	2	110	0.47
U-7	0.03	0.09	0.3	1	62	0.77
U-8	0.007	0.3	0.09	0.5	32	0.83
U-9	0.006	0.3	0.1	0.2	65	0.71
U-10	0.01	0.04	0.05	0.1	58	0.72
U-11	0.008	0.004	0.2	0.8	59	0.80
U-12	0.006	0.08	0.2	0.4	63	0.73
S-13	0.01	3	0.06	0.2	49	0.77
S-14	<0.001	0.08	0.04	0.08	14	0.68
S-15	<0.001	<0.001	0.06	0.3	51	0.81
S-16	<0.001	<0.001	0.01	0.04	57	0.78
R-17	0.02	0.08	0.02	0.03	53	0.66
R-18	0.002	0.002	<0.01	<0.02	53	-
R-19	<0.001	<0.001	0.03	0.1	10	0.76
W-20	<0.001	<0.001	<0.01	0.03	83	-
W-21	0.004	0.01	0.3	0.6	79	0.64
W-22	0.002	<0.001	0.02	0.05	89	0.76
W-23	0.003	<0.001	2	4	70	0.74
W-24	0.003	<0.001	0.07	0.2	76	0.74
W-25	<0.001	<0.001	0.02	0.04	34	0.70
W-26	0.001	0.08	0.02	0.07	82	0.77
W-27	0.005	0.2	0.08	0.4	76	0.84
W-28	0.001	0.01	<0.01	0.03	52	-

\- *f* anti not determined

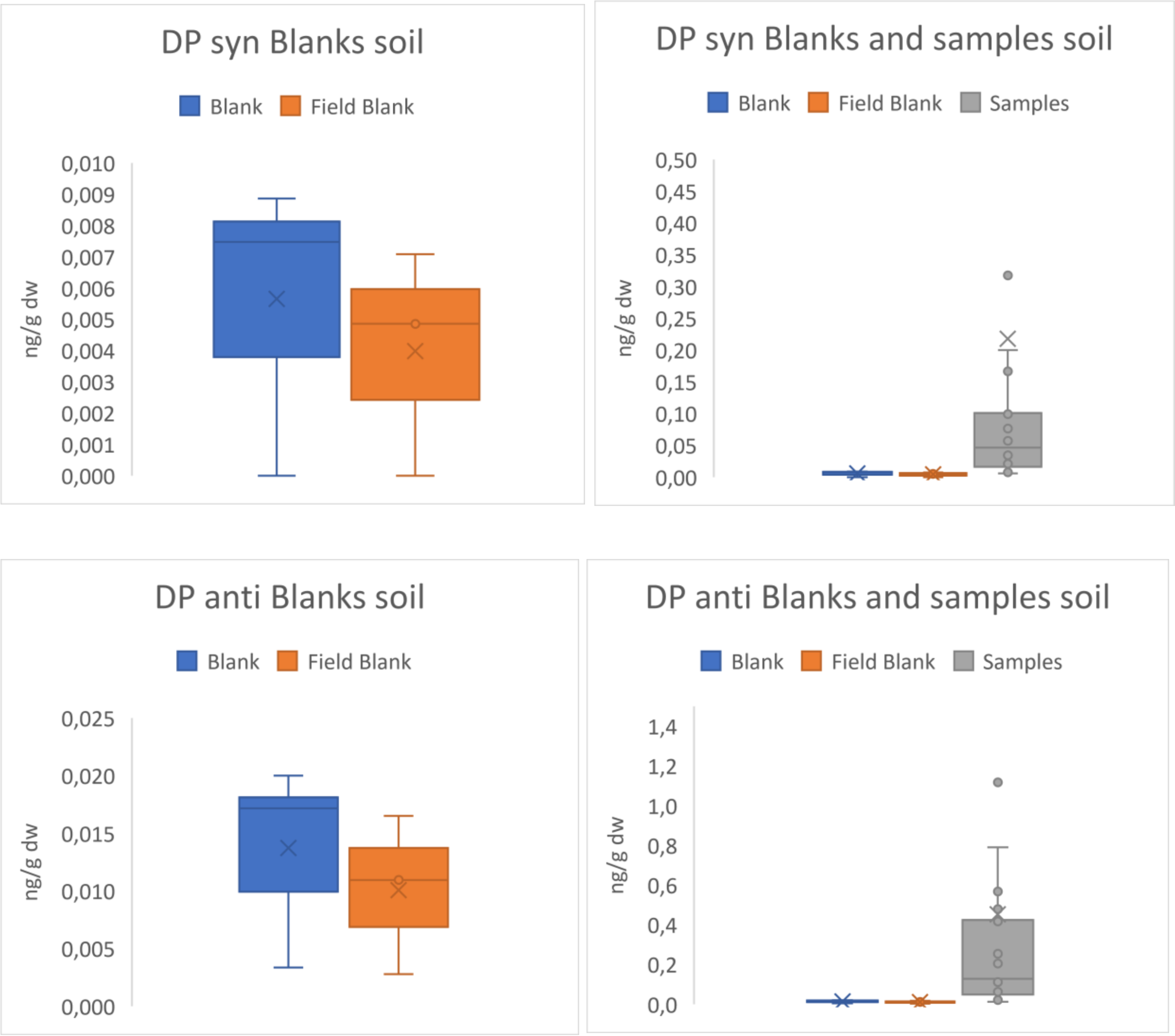

Figure S5: Boxplots illustrating relative levels of DP in blanks, field blanks, and samples. For both DP syn and DP anti in soil samples, two samples have concentrations higher than the illustrated range. Blank concentrations converted to ng/g dw.

Table S9: Average percent deviation for air samples deployed in duplicate (N=3), and soil samples analysed in parallel (N=4).

Compound	**Air**	**Soil**
SCCPs	7%	17%
MCCPs	15%	15%
DP syn	11%	14%
DP anti	19%	26%
Dec 602	7%	2%
Dec 603	ND	8%

ND: Dec 603 not detected in any of the air samples analysed in parallel.

Table S10: Correlations between analysed compounds and soil organic matter (SOM). Dec 603 in air omitted given low detection frequency.

	DP air	***Dec 602 air***	***SCCP air***	***MCCP air***	***DP soil***	***Dec 602 soil***	***Dec 603 soil***	***SCCP soil***	***MCCP soil***
Dec 602 air	0,64***	1							
SCCP air	0,66***	0,61***	1						
MCCP air	0,74***	0,69***	0,95***	1					
DP soil	0,71***	0,59**	0,63***	0,71***	1				
Dec 602 soil	0,53**	0,45*	0,37	0,49**	0,60***	1			
Dec 603 soil	0,17	0,21	0,34	0,38	0,45*	0,66***	1		
SCCP soil	0,52**	0,49**	0,51**	0,54**	0,84***	0,44*	0,40*	1	
MCCP soil	0,53**	0,55**	0,53**	0,61***	0,88***	0,62***	0,50**	0,91***	1
SOM	-0,03	-0,17	-0,27	-0,19	0,04	0,47*	0,47*	-0,04	0,11

*p < 0.05, **p < 0.01, ***p < 0.001

Table S11: Reported concentrations of CPs and dechloranes in air from selected studies. CPs air concentrations in ng/m^3, Dechlorane air concentrations in pg/m^3.

Country/ region	**Location type**	**Sampling**	**SCCPs (ng/m^3)**	**MCCPs (ng/m^3)**	**DP (pg/m^3)**	**Dec 602 (pg/m^3)**	**Dec 603 (pg/m^3)**	**Ref.**
Tanzania	urban/rural/(e-)waste	Passive	0.3-63	<0.4-35	<0.4-20	<0.007-0.2	<0.007-0.2	this study
Australia	urban/rural	Passive	<LOD-1	<LOD-2				(van Mourik et al., 2020)
India/ Pakistan	urban/rural	Passive	<LOD-47	<LOD-38				(Chaemfa et al., 2014)
UK		Active	<LOD-3	<LOD-14				(Barber et al., 2005)
Antarctica	remote	Active	0.01-0.02	0.004-0.005				(Ma et al., 2014)
Australia	urban	Active	2-82					(Gillett et al., 2017)
Tibet	remote	Passive	0.1-1					(Wu et al., 2017)
Tibet	urban	Passive	1-14					(Wu et al., 2017)
Switzerland	urban	Passive	1-42					(Diefenbacher et al., 2015)
China	industrial	Passive	6-63					(Niu et al., 2020)
China	urban	Active	2-330					(Wang et al., 2012)
China	industrial	Passive	1-110					(Wang et al., 2013)
China	urban	Active	15-91					(Zhu et al., 2017)
China	urban/rural	Passive	14-520					(Li et al., 2012)
Japan	urban/rural	Passive	0.3-14					(Li et al., 2012)

South Korea	urban/rural	Passive	0.6-9					(Li et al., 2012)
Bangladesh	shipbreaking/ urban	Passive	8-580					(Nøst et al., 2015)
Tibet	remote	Passive		0.05-0.7				(Wu et al., 2019)
Tibet	urban	Passive		0.8-7				(Wu et al., 2019)
Africa	rural/ background	Passive			<LOD-0.6			(Schuster et al., 2020)
Global (excl. Africa)	background/ urban	Passive			<LOD-30			(Schuster et al., 2020)
Uganda	suburban	Active			<LOD-6			(Arinaitwe et al., 2014)
North Sea	marine	Active			0.1-22			(Möller et al., 2012)
Southeast Asia	marine	Active			0.3-11			(Möller et al., 2012)
Atlantic Ocean	marine	Active			0.05-4			(Möller et al., 2010)
Greenland		Active			<LOD-42			(Vorkamp et al., 2015)
China	urban/rural	Passive			<LOD-66			(Ren et al., 2008)
China	e-waste	Active			13-1800			(Chen et al., 2011)
China	urban	Passive			5-9			(Ma et al., 2011)
Tibet		Passive			<LOD-12			(Liu et al., 2018)
UK	urban/rural	Passive			0.6-21*			(Drage et al., 2016)
US	urban/rural	Active			<LOD-490			(Hoh et al., 2006)
US	urban/rural	Active			0.3-5*			(Liu et al., 2016)
US	urban/rural	Active			<LOD-4*			(Olukunle et al., 2018)
Africa	urban	Passive			2-28	0.08-0.2		(Saini et al., 2020)
Global (excl. Africa)	urban	Passive			0.02-14	<LOD-0.5		(Saini et al., 2020)
Africa	background	Passive			<LOD	<LOD-0.07		(Rauert et al., 2018)
Global (excl. Africa)	background/ urban	Passive			<LOD-116	<LOD-2		(Rauert et al., 2018)
East Asia	marine	Active			0.01-1	0.01-0.2	0.4	(Möller et al., 2011)
Spain	urban	Active/ passive			0.01-7	<LOD-0.02	<LOD-0.01	(De la Torre et al., 2018)

* Range of means

Table S12: Reported concentrations of CPs and dechloranes in soil from selected studies.

Country/ region	**Location type**	**SCCPs (ng/g dw)**	**MCCPs (ng/g dw)**	**DP (ng/g dw)**	**Dec 602 (ng/g dw)**	**Dec 603 (ng/g dw)**	
Tanzania	urban/rural/ (e-)waste	<11-5 300	<19-5 100	<0.01-6	<0.001-0.05	<0.001-3	this study
Ghana/ Sierra Leone	e-waste	69-28 000	<LOD-1 400				(Möckel et al., 2020)
Switzerland		3-35	5-160				(Bogdal et al., 2017)
China	urban	<LOD-620	2-190				(Wang et al., 2014)
China	suburban	<LOD-700	<LOD-670				(Wang et al., 2017)
China	Industrial	2-240	2-1 500				(Wang et al., 2013)
China		79-950	20-1 200				(Wang et al., 2020)
China	e-waste	69-220 000	510-4 400 000				(Xu et al., 2019)
China	suburban	160-1 500					(Zeng et al., 2011)
UK/Norway	background	<LOD-280					(Halse et al., 2015)
UK	urban/rural			<LOD-5*			(Drage et al., 2016)
Vietnam	e-waste			<LOD-65			(Someya et al., 2016)
Tibet				<LOD-0.05			(Liu et al., 2018)
China	urban			0.01			(Ma et al., 2011)
China	industrial			0.03-5			(Yu et al., 2010)
China	e-waste			<LOD-47			(Yu et al., 2010)
China	e-waste			4-2100			(Li et al., 2018)
China	e-waste			<LOD-160	<LOD-0.4	<LOD-0.3	(Tao et al., 2015)
Antarctica	remote			0.06-0.3	<LOD-0.007	<LOD-0.07	(Gao et al., 2018)

* Organic matter normalized soil concentration

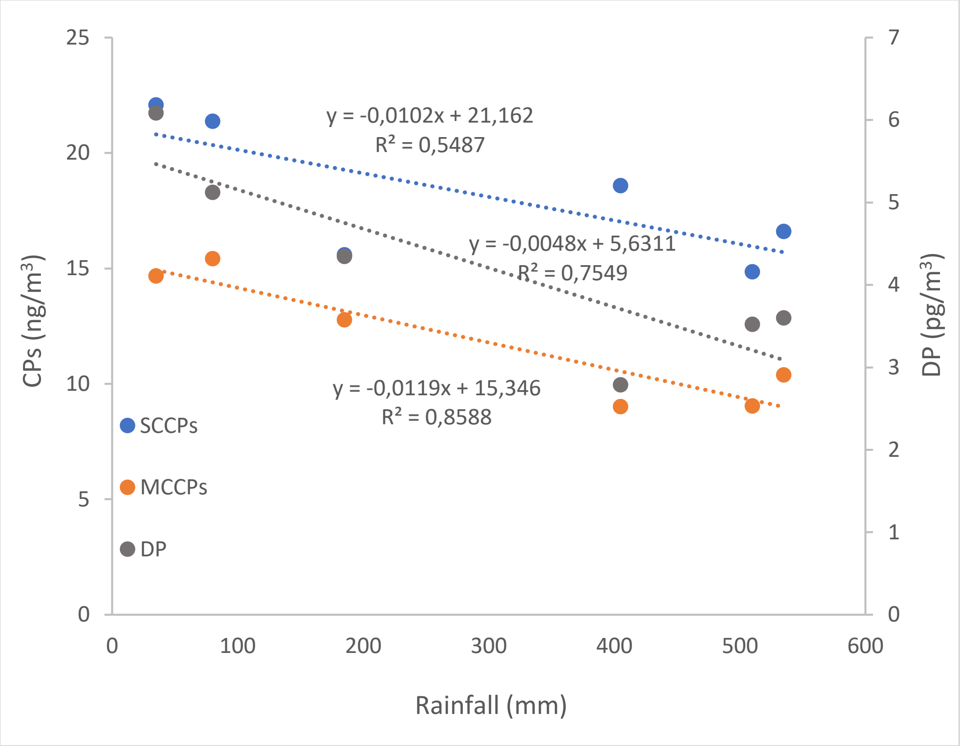

Figure S6: Air concentrations of SCCPs, MCCPs, and DP plotted against cumulative rainfall during air sample deployment.

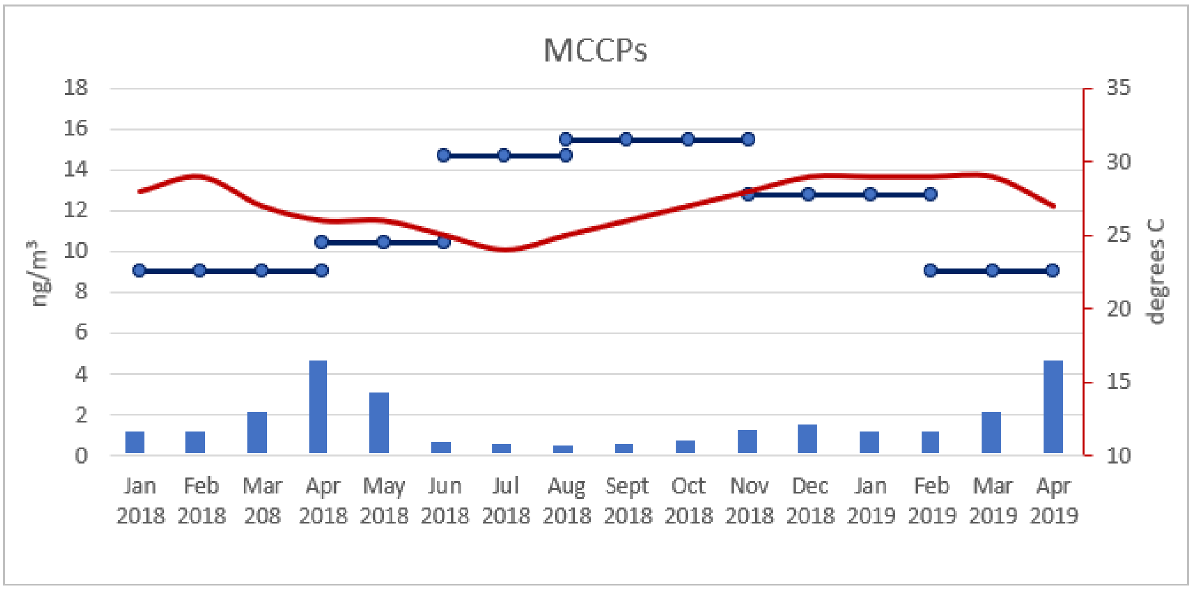

Figure S7: Seasonal variation in air concentrations of MCCPs at location S-13(horizontal lines). Temperature in red (left scale), rainfall as vertical blue bars (relative scale).

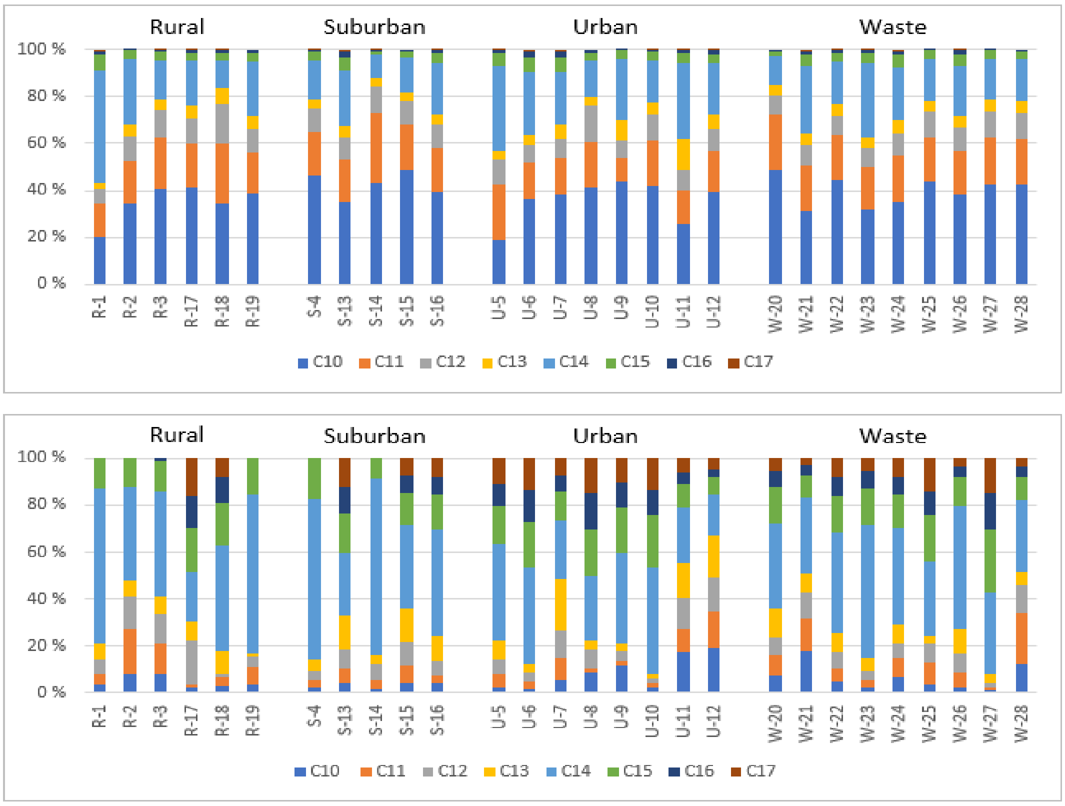

Figure S8: Chain length distribution of CPs in air samples (above) and soil samples (lower).

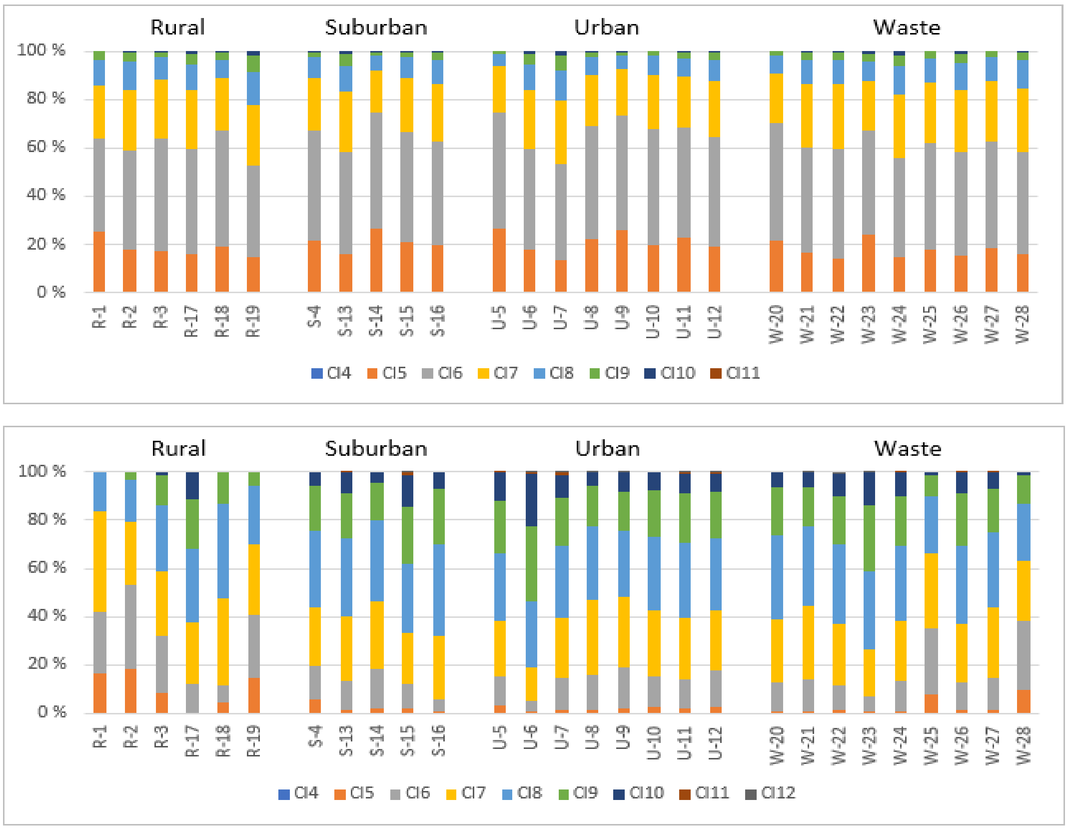

Figure S9: Chlorination degree of CPs in air samples (above) and soil samples (lower).

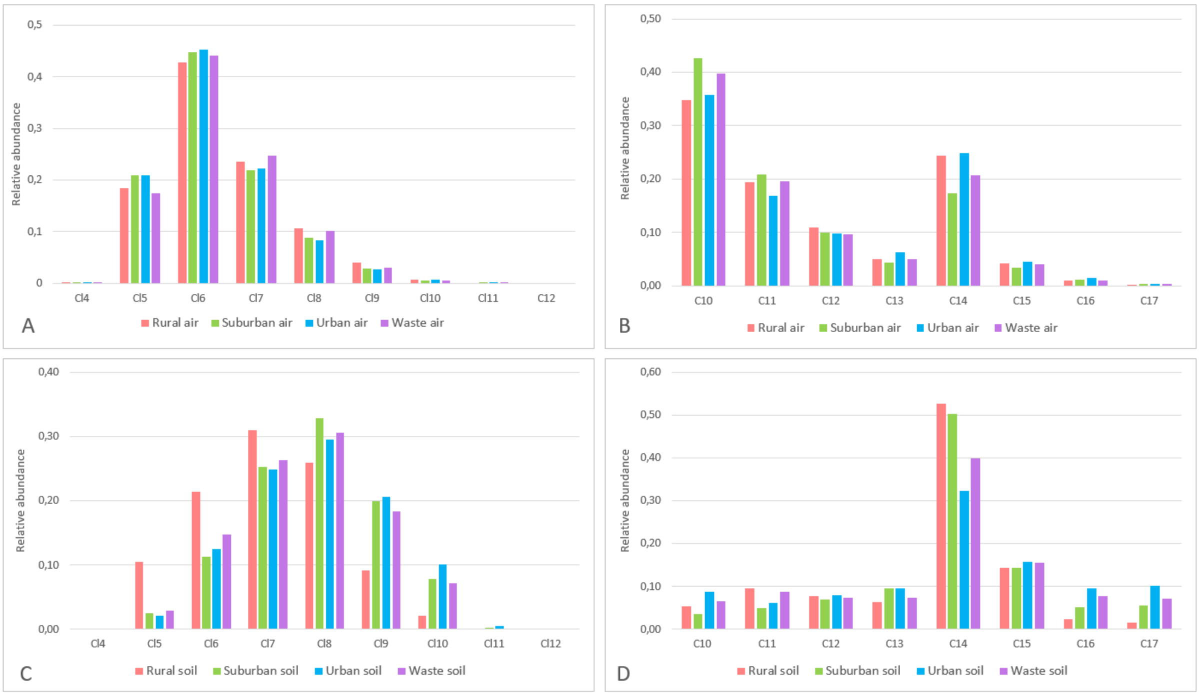

Figure S10: Chlorination degree in air samples (A) and soil samples (C), and chain length distribution in air samples (B) and soil samples (D).

Text S2: Congener group profiles

A larger degree of spatial variation in CPs congener group profiles was observed in soil compared to air (Figure S10). This was particularly notable for chlorination degree, where the distribution of the number of chlorines was centered around Cl_7 congener groups for rural locations, as opposed to Cl_8 congener groups which dominated at suburban, urban, and waste-source transect locations. A Wilcoxon rank sum test on chlorination degree of soil samples (Table S6) showed a significant difference between urban and rural locations ($p < 0.05$) for both SCCPs and MCCPs. Within rural locations, air and soil congener group profiles showed some similarity, both characterized by low chlorination degree, although the distributions of the number of chlorines in air were dominated by Cl_6. Overall, soil showed a higher chlorination degree, and a larger contribution of longer chain lengths compared to air. The lack of spatial variation in congener group profiles in air as opposed to soil reflect that air is a well-mixed medium, and congener group profiles in air therefore represent an “average” of nearby sources during the sampling period, in addition to the physicochemical properties of the congener groups.

Principal component analysis (PCA) was applied to CPs congener group profiles for air samples and soil samples. In the PCA on air sample congener profiles, distinction between settlement categories was low (data not shown), reflecting the findings Figure S10 (and Figure S8 and S9), where high similarity of congener group profiles of the different settlement categories was seen.

Figure S11 shows a PCA score plot from soil sample congener group profiles. Differences in congener group profiles between urban soil, and rural soil mirror the differences also seen in Figure S10. The PCA score plot also show a separation between urban locations, the e-waste location (W-23), and the dumpsite (W-21). The separation between these hot spots for CPs contamination suggests differences in sources, implying materials handled at the dumpsite and at the e-waste site differ, and that the urban CPs contamination found in Dar es Salaam cannot be tied specifically or at least exclusively to waste or e-waste in the urban environment.

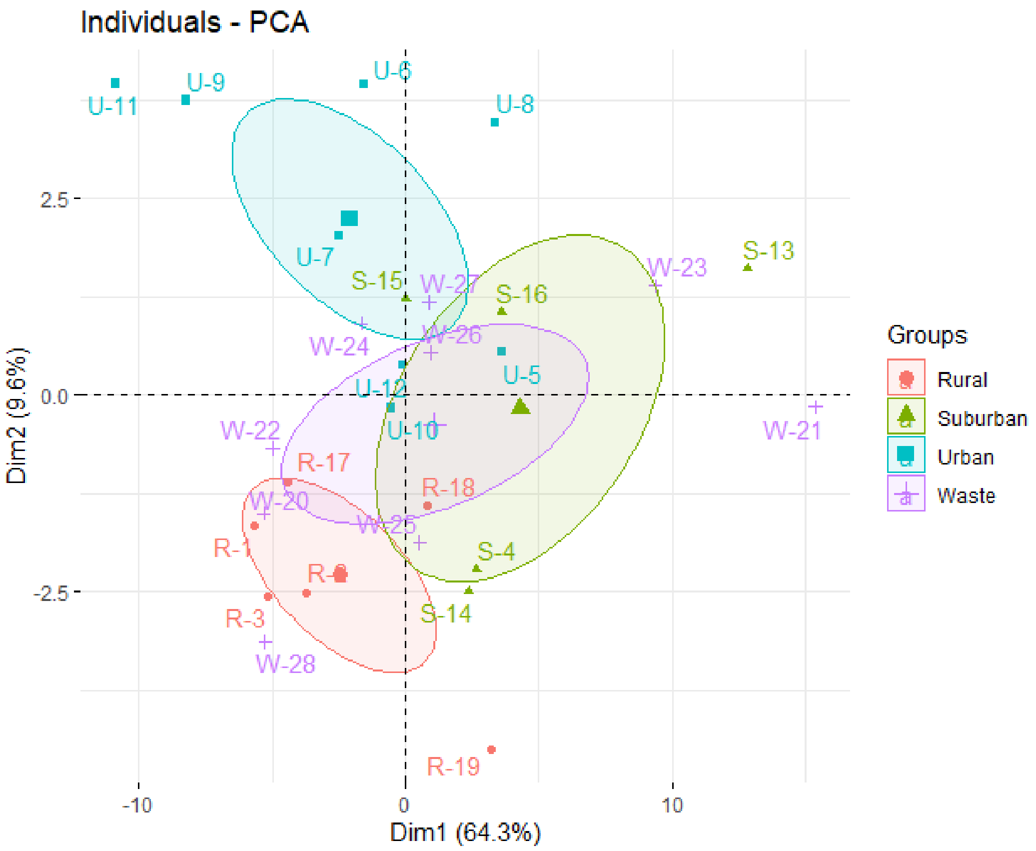

Figure S11: PCA biplot on CPs congener group profiles from soil samples.

Table S13: Values and equations used in mechanistic assessments and fugacity calculations.

Symbol	Value	Unit	Description	Equation
ρoc	1000000	g/m3	Density of organic matter	
ρw	1000000	g/m3	Density of water	
ρmm	2400000	g/m3	Density of minerals	
φ	0,5		Porosity of soil	
VFw			Volume fraction water	
VFa			Volume fraction air	
VFe			Volume fraction soil solids	
VFeoc			Volume fraction organic solids	
MFoc			Mass fraction of organic carbon in dry soil	
MFw			Mass fraction of water in soil	
Fa			Relative importance evaporation	Fa = De/(De + Dew + Der)
Few			Relative importance leaching	Few = Dew/(De + Dew + Der)
Fer			Relative importance erosion	Fer = Der/(De + Dew + Der)
De		mol/h Pa	D-value for evaporation	Ae/((1/U7e Za) + (1/(U5e Za)+(U6e Zw))
Dew		mol/h Pa	D-value for leching	(1-frUe)Uew Ae Zw
Der		mol/h Pa	D-value for erosion	Ae Uer Zeoc
Za		mol/m^3 Pa	Fugacity capacity in air	1/(RT)
Zw		mol/m^3 Pa	Fugacity capacity in water	1/(R T Kaw)
Zeoc		mol/m^3 Pa	Fugacity capacity in organic solids	Zw Koc VFeoc (ρoc/10^6)
Zs		mol/m^3 Pa	Fugacity capacity in soil	MFoc K_{OC} Zw (ρmm/10^6)
U5e		m/h	MTC for air filled pore space	(Ba/ln2h) ((VFa^10/3)/(VFa + VFw)^2
U6e		m/h	MTC for diffusion in the water filled pore space	(Bw/ln2h) ((VFw^10/3)/(VFa + VFw)^2
Ue7	2,08	m/h	MTC through air boundary layer over soil	
Ba	0,018	m2/h	Molecular diffusivity in air	
Bw	0,0000018	m2/h	Molecular diffusivity in water	
h	0,1	m	Soil depth	
Ae	1	m2	Soil area	
frUe	0,43		Fraction of water evaporation from soil	
Uew	0,000039	m/h	Leaching rate of water from soil	
Uer	0,000000023	m/h	Solid runoff rate from soil	
T	298	K	Temperature	
R	8,134	m3Pa/Kmol	Gas constant	
K_{AW}			Air water partition coefficient	
K_{OC}			Organic solids water partition coefficient	
f_A		Pa	Fugacity in air	C_A/Za
f_S		Pa	Fugacity in soil	C_S/Zs

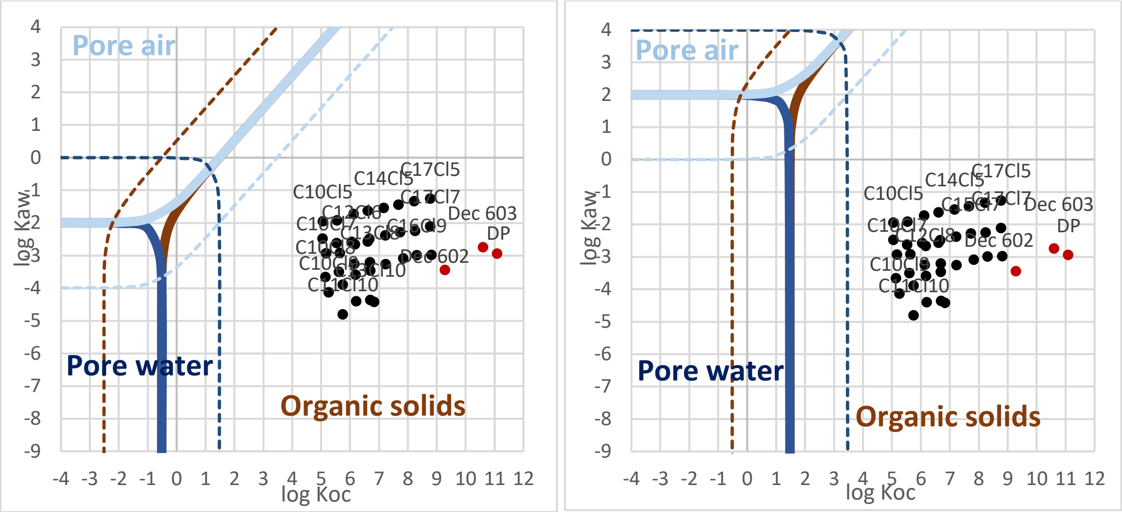

Figure S12: Distribution plots for CPs (black) and dechloranes (red) in soil compartments. Left: dry soil (pore space 1% water). Right: wet soil (pore space 99% water). Thick line represents 50% in phase, dotted line represents 1% in phase.

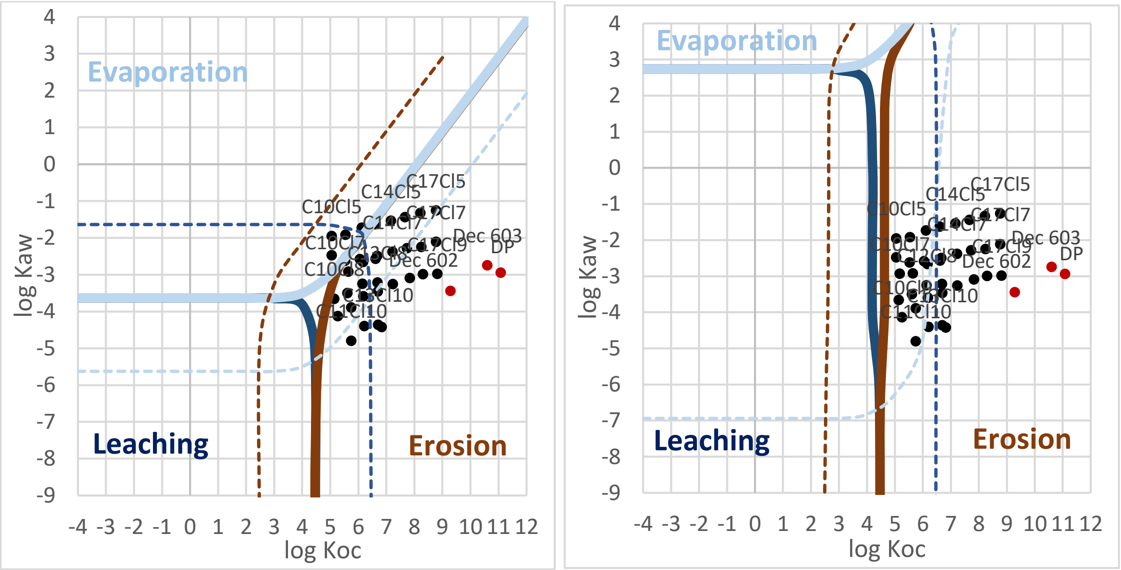

Figure S13: Mobility plots for CPs (black) and dechloranes (red) in soil compartments. Left: dry soil (pore space 1% water). Right: wet soil (pore space 99% water). Thick line represents 50% relevance of process, dotted line represents 1% relevance of process.

Text S3: Soil air fugacity ratios

Physicochemical property data is required to perform fugacity calculations. For CPs, congener group specific physicochemical property data were available for 24 SCCPs and 12 MCCPs congener groups from Glüge et al. (2013) (congener groups in bold in Table S2 and

Table S3), so only these congener groups were included in fugacity calculations. For dechloranes, physicochemical property data from Sverko et al. (2011) was used.

Congener group specific air sample volumes for fugacity calculations

For the results of fugacity calculations to better account for the wide range of physicochemical properties of CPs, congener group specific sample volumes for the passive air sampling were calculated for the included congener groups, using the physicochemical property data from Glüge et al. (2013) and the following equations from Harner (2016):

$$V_{air}(m^3) = K_{PUF-A}\, V_{PUF}(1 - e^{(-Dt\, MTC\, /\, K_{PUF-A}\, / D_{film})} \qquad \text{(eq. S1)}$$

And

$$\log K_{PUF-A} = d\ 10^{(0.6366 \log K_{OA} - 3.1744)} \qquad \text{(eq. S2)}$$

Where d is PUF density (g/m^3) and V_{PUF} is the volume of the PUF disk (m^3), Dt is deployment time (days), MTC is air-side mass transfer coefficient (m/day) and D_{film} is effective film thickness (m).

The K_{OA} values used in eq. S2 are for 25℃. As this is close to the average temperature in the studied region (26℃), no temperature adjustment of these values was carried out.

The fraction of compound bound to particles vs. the fraction in gas phase is important for the MONET type passive sampler, which has been shown to be less effective at uptake of particle associated compounds compared to alternative sampler configurations (Bohlin et al., 2014; Klánová et al., 2007; Markovic et al., 2015). Highly chlorinated, longer chain length CPs have high log K_{OA} values (>11), indicating association with particles in air even in climate zones with elevated temperature. Thus, the particle fraction correction equations from Harner (2016) were used to adjust sample volumes.

$$V_{air,} particle\ corrected = V_{air}((1 - \varphi) + (\varphi \varphi_{R.P})) \qquad \text{(eq. S3)}$$

Where φ is the fraction of analyte associated with particles:

$$\varphi = K_P\, TSP / (K_P\, TSP + 1) \qquad \text{(eq. S4)}$$

And

$$\log K_P = logK_{OA} + \log fOM - 11.91 \qquad \text{(eq. S5)}$$

$\varphi_{R.P}$ is the particle phase sampling rate as a fraction of the gas phase sampling rate. Here we used 0.54 for $\varphi_{R.P}$ (Markovic et al., 2015).

Concentration of analyte in air (C_{air}) then equals:

$$C_{air} = m/V_{air,}particle\ corrected \qquad \text{(eq. S6)}$$

Where m is amount of analyte in the analysed sample.

The modelled SCCPs air concentrations from these calculations (based on sum of the 24 congener groups where physicochemical property data were available) were on average 28% lower than the SCCP air concentrations calculated using generic sampling rates as described in the main text (as sum of all 34 congener groups). This indicates that the generic sampling rates provides a reasonable estimate.

Fugacity ratios

The f_{soil}/f_{air} ratio was calculated for locations where any CPs congener groups or dechloranes were detected in both air and soil. The f_{soil}/f_{air} ratio indicates the direction of the net diffusive flux of CPs and dechloranes, thus indicating whether soils act as a net temporary reservoir or a secondary source.

There are always uncertainties associated with fugacity calculations, and for this specific study there are additional uncertainties, notably related to i) SOM content, which is likely to be higher in sampled locations compared to regional average given the choice of sampling locations under tree canopies, ii) the LOI method used for SOM determination, iii) depth of the sampled soil, which is likely to be deeper than the layer most active in air-soil exchange, iv) uncertainties associated with the physical chemical properties of CPs and the quantification method, which are carried through to fugacity calculations. Consequently, f_{soil}/f_{air} should be interpreted with these uncertainties in mind, and here we only consider deviation from equilibrium probable if f_{soil}/f_{air} differ from unity by an order of magnitude or more.

On average, SCCPs and MCCPs congener groups had $f_{soil}/f_{air} > 1$, indicating soil to air flux, while dechloranes had $f_{soil}/f_{air} << 1$ indicating a clear air to soil flux. The strong air to soil flux of dechloranes in combination with lower frequencies of detection of dechloranes in air outside source regions indicate that soil functions as a net temporary storage reservoir for these compounds in the studied region (Figure S20). This is consistent with our soil model and is a consequence of their physicochemical properties (low K_{AW}, high K_{OC}), suggesting that once in soil, dechloranes will not return to the gas phase irrespective of SOM content and season. Resuspension sorbed to aeolian dust is however a possibility. Some highly chlorinated CPs congener groups (Cl_9 to Cl_{11}) also showed f_{soil}/f_{air} <1 in rural and urban areas. For low chlorinated SCCPs congener groups, soil was seen to act as a secondary source, particularly in rural areas (Figure S16). In urban areas, this effect was likely outcompeted by the prevalent presence of primary sources.

Urban locations overall showed few CPs congener groups deviating from equilibrium status. Exceptions were high chlorinated and longer chain length congener groups, which showed air to soil flux. The analysed dechloranes also showed strong air to soil flux at all urban locations where detected.

Locations on the waste-source transect showed on average soil to air flux for most of the C_{10}, C_{11} and C_{12} congener groups. This average was strongly influenced by high soil to air flux at the dumpsite, W-21, with an average SCCPs congener group f_{soil}/f_{air} of 49. In comparison, the e-waste facility, W-23, showed an average SCCPs congener group f_{soil}/f_{air} of only 7. Locations in the vicinity, W-20 and W-22 showed air to soil flux for highly chlorinated congener groups.

Rural locations had particularly high f_{soil}/f_{air} for low chlorinated congener groups (e.g., $C_{10}Cl_5$: 176, $C_{11}Cl_5$: 728, $C_{12}Cl_5$: 542). This indicates soils in these areas act as secondary sources for these compounds. Some higher chlorinated CPs on the other hand have f_{soil}/f_{air} showing air to soil flux, e.g., $C_{13}Cl_{10}$: 0.03.

W-25 and W-26 were excluded from fugacity calculations given the lack of SOM in soil from these locations.

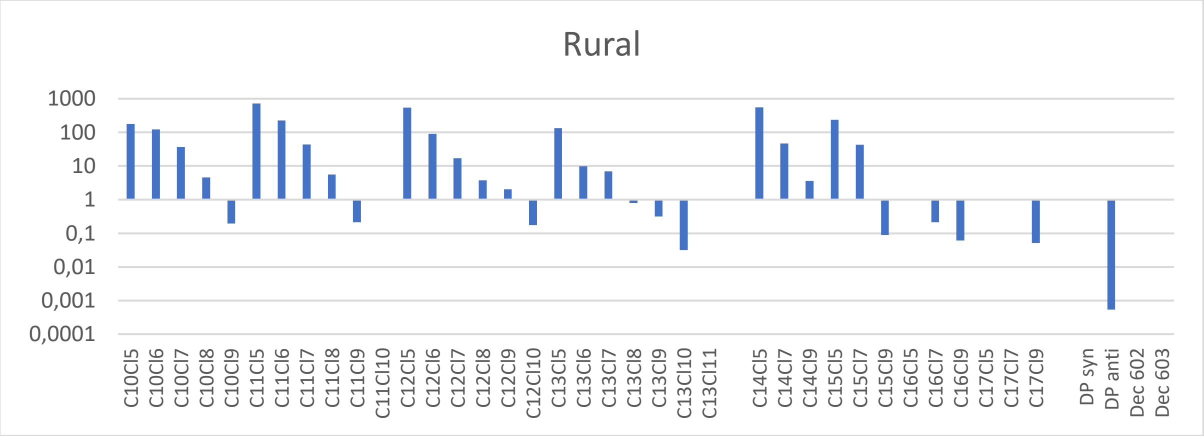

Figure S14: Average f_{soil}/f_{air} for CPs congener groups and dechloranes at rural locations.

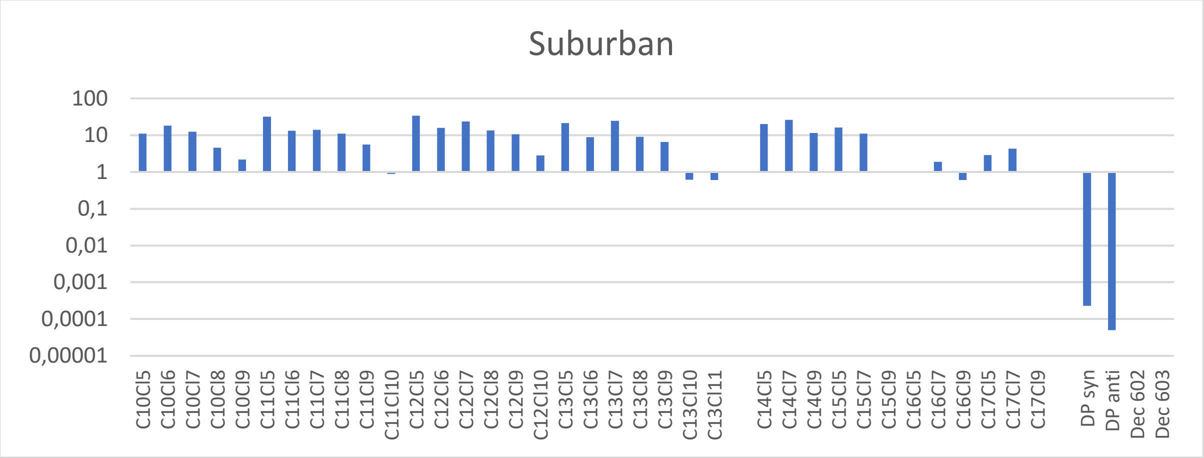

Figure S15: Average f_{soil}/f_{air} for CPs congener groups and dechloranes at suburban locations.

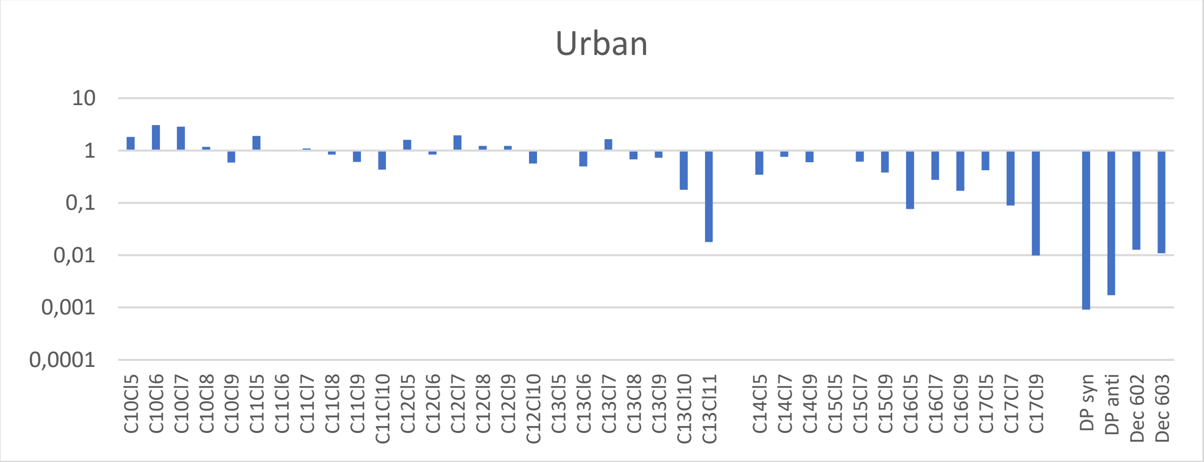

Figure S16: Average f_{soil}/f_{air} for CPs congener groups and dechloranes at urban locations.

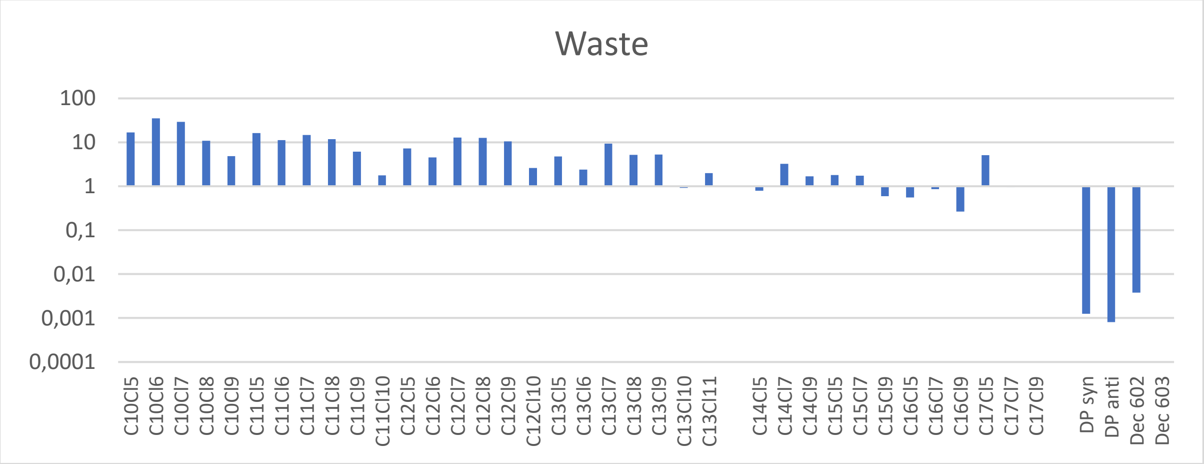

Figure S17: Average f_{soil}/f_{air} for CPs congener groups and dechloranes within the waste-source transect.

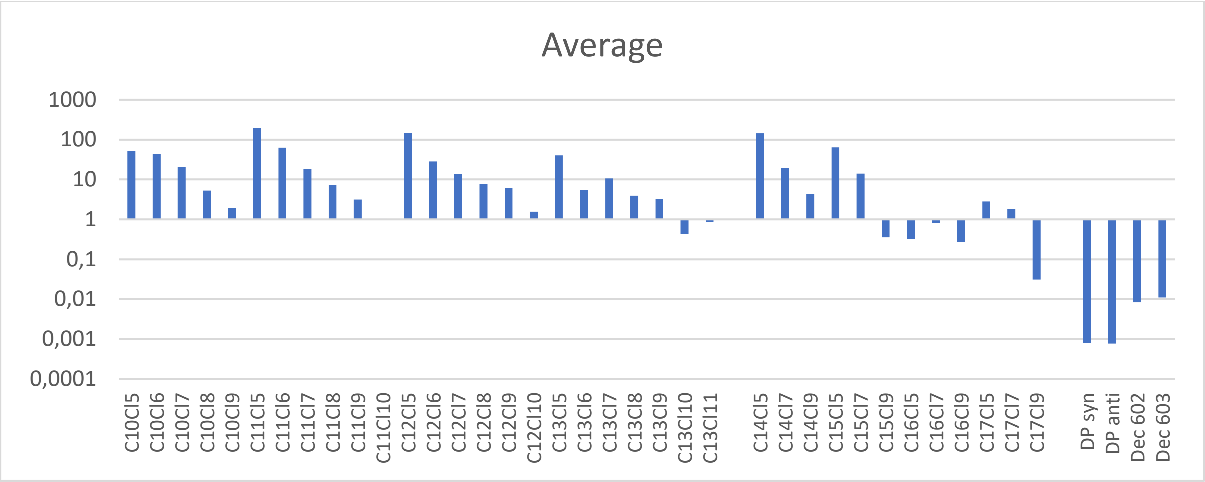

Figure S18: Average f_{soil}/f_{air} for CPs congener groups and dechloranes at all locations.

References

Arinaitwe K, Muir DC, Kiremire BT, Fellin P, Li H, Teixeira C. Polybrominated diphenyl ethers and alternative flame retardants in air and precipitation samples from the Northern Lake Victoria Region, East Africa. Environmental science & technology 2014; 48: 1458-1466.

Barber JL, Sweetman AJ, Thomas GO, Braekevelt E, Stern GA, Jones KC. Spatial and temporal variability in air concentrations of short-chain (C10– C13) and medium-chain (C14– C17) chlorinated n-alkanes measured in the UK atmosphere. Environmental science & technology 2005; 39: 4407-4415.

Bogdal C, Alsberg T, Diefenbacher PS, MacLeod M, Berger U. Fast quantification of chlorinated paraffins in environmental samples by direct injection high-resolution mass spectrometry with pattern deconvolution. Analytical chemistry 2015; 87: 2852-2860.

Bogdal C, Niggeler N, Glüge J, Diefenbacher PS, Wächter D, Hungerbühler K. Temporal trends of chlorinated paraffins and polychlorinated biphenyls in Swiss soils. Environmental pollution 2017; 220: 891-899.

Bohlin P, Audy O, Škrdlíková L, Kukučka P, Přibylová P, Prokeš R, et al. Outdoor passive air monitoring of semi volatile organic compounds (SVOCs): a critical evaluation of performance and limitations of polyurethane foam (PUF) disks. Environmental Science: Processes & Impacts 2014; 16: 433-444.

Chaemfa C, Xu Y, Li J, Chakraborty P, Hussain Syed J, Naseem Malik R, et al. Screening of atmospheric short-and medium-chain chlorinated paraffins in India and Pakistan using polyurethane foam based passive air sampler. Environmental science & technology 2014; 48: 4799-4808.

Chen S-J, Tian M, Wang J, Shi T, Luo Y, Luo X-J, et al. Dechlorane Plus (DP) in air and plants at an electronic waste (e-waste) site in South China. Environmental Pollution 2011; 159: 1290-1296.

De la Torre A, Barbas B, Sanz P, Navarro I, Artíñano B, Martínez M. Traditional and novel halogenated flame retardants in urban ambient air: gas-particle partitioning, size distribution and health implications. Science of the Total Environment 2018; 630: 154-163.

Diefenbacher PS, Bogdal C, Gerecke AC, Glüge J, Schmid P, Scheringer M, et al. Short-Chain Chlorinated Paraffins in Zurich, Switzerland Atmospheric Concentrations and Emissions. Environmental science & technology 2015; 49: 9778-9786.

Drage DS, Newton S, de Wit CA, Harrad S. Concentrations of legacy and emerging flame retardants in air and soil on a transect in the UK West Midlands. Chemosphere 2016; 148: 195-203.

Gao H, Na G, Yao Y, Li R, Gao Y, Zhang Z, et al. Distribution Characteristics and Source of Dechloranes in Soil and Lichen of the Fildes Peninsula (Antarctica). International journal of environmental research and public health 2018; 15: 2312.

Gillett RW, Galbally IE, Keywood MD, Powell JC, Stevenson G, Yates A, et al. Atmospheric short-chain-chlorinated paraffins in Melbourne, Australia–first extensive Southern Hemisphere observations. Environ. Chem. 2017; 14: 106.

Glüge J, Bogdal C, Scheringer M, Buser AM, Hungerbühler K. Calculation of physicochemical properties for short-and medium-chain chlorinated paraffins. Journal of Physical and Chemical Reference Data 2013; 42: 023103.

Halse AK, Schlabach M, Schuster JK, Jones KC, Steinnes E, Breivik K. Endosulfan, pentachlorobenzene and short-chain chlorinated paraffins in background soils from Western Europe. Environmental pollution 2015; 196: 21-28.

Harner T. v1 3 Template for Calculating PUF and SIP Disk Sample Air Volumes. March, 2016.

Hoh E, Zhu L, Hites RA. Dechlorane Plus, a chlorinated flame retardant, in the Great Lakes. Environmental science & technology 2006; 40: 1184-1189.

Hoogsteen MJ, Lantinga EA, Bakker EJ, Groot JC, Tittonell PA. Estimating soil organic carbon through loss on ignition: effects of ignition conditions and structural water loss. European Journal of Soil Science 2015; 66: 320-328.

Klánová J, Èupr P, Kohoutek Ji, Harner T. Assessing the influence of meteorological parameters on the performance of polyurethane foam-based passive air samplers. Environmental science & technology 2007; 42: 550-555.

Li N, Chen X-W, Deng W-J, Giesy JP, Zheng H-L. PBDEs and Dechlorane Plus in the environment of Guiyu, Southeast China: A historical location for E-waste recycling (2004, 2014). Chemosphere 2018; 199: 603-611.

Li Q, Li J, Wang Y, Xu Y, Pan X, Zhang G, et al. Atmospheric short-chain chlorinated paraffins in China, Japan, and South Korea. Environmental science & technology 2012; 46: 11948-11954.

Liu L-Y, Salamova A, Venier M, Hites RA. Trends in the levels of halogenated flame retardants in the Great Lakes atmosphere over the period 2005–2013. Environment international 2016; 92: 442-449.

Liu X, Bing H, Chen Y, Li J, Wu Y, Zhang G. Brominated flame retardants and dechlorane plus on a remote high mountain of the eastern Tibetan Plateau: implications for regional sources and environmental behaviors. Environmental geochemistry and health 2018; 40: 1887-1897.

Ma W-L, Liu L-Y, Qi H, Sun D-Z, Shen J-M, Wang D-G, et al. Dechlorane plus in multimedia in northeastern Chinese urban region. Environment international 2011; 37: 66-70.

Ma X, Zhang H, Zhou H, Na G, Wang Z, Chen C, et al. Occurrence and gas/particle partitioning of short-and medium-chain chlorinated paraffins in the atmosphere of Fildes Peninsula of Antarctica. Atmospheric Environment 2014; 90: 10-15.

Markovic MZ, Prokop S, Staebler RM, Liggio J, Harner T. Evaluation of the particle infiltration efficiency of three passive samplers and the PS-1 active air sampler. Atmospheric Environment 2015; 112: 289-293.

Möckel C, Breivik K, Nøst TH, Sankoh A, Jones KC, Sweetman A. Soil pollution at a major West African E-waste recycling site: Contamination pathways and implications for potential mitigation strategies. Environment International 2020; 137: 105563.

Möller A, Xie Z, Caba A, Sturm R, Ebinghaus R. Occurrence and air-seawater exchange of brominated flame retardants and Dechlorane Plus in the North Sea. Atmospheric environment 2012; 46: 346-353.

Möller A, Xie Z, Cai M, Sturm R, Ebinghaus R. Brominated flame retardants and dechlorane plus in the marine atmosphere from Southeast Asia toward Antarctica. Environmental science & technology 2012; 46: 3141-3148.

Möller A, Xie Z, Cai M, Zhong G, Huang P, Cai M, et al. Polybrominated diphenyl ethers vs alternate brominated flame retardants and dechloranes from East Asia to the Arctic. Environmental science & technology 2011; 45: 6793-6799.

Möller A, Xie Z, Sturm R, Ebinghaus R. Large-scale distribution of dechlorane plus in air and seawater from the Arctic to Antarctica. Environmental science & technology 2010; 44: 8977-8982.

Niu S, Chen R, Zou Y, Dong L, Hai R, Huang Y. Spatial distribution and profile of atmospheric short-chain chlorinated paraffins in the Yangtze River Delta. Environmental Pollution 2020; 259: 113958.

Nøst TH, Halse AK, Randall S, Borgen AR, Schlabach M, Paul A, et al. High concentrations of organic contaminants in air from ship breaking activities in Chittagong, Bangladesh. Environmental science & technology 2015; 49: 11372-11380.

Olukunle OI, Lehman DC, Salamova A, Venier M, Hites RA. Temporal trends of Dechlorane Plus in air and precipitation around the North American Great Lakes. Science of the total environment 2018; 642: 537-542.

Rauert C, Schuster JK, Eng A, Harner T. Global atmospheric concentrations of brominated and chlorinated flame retardants and organophosphate esters. Environmental science & technology 2018; 52: 2777-2789.

Ren N, Sverko E, Li Y-F, Zhang Z, Harner T, Wang D, et al. Levels and isomer profiles of Dechlorane Plus in Chinese air. Environmental science & technology 2008; 42: 6476-6480.

Saini A, Harner T, Chinnadhurai S, Schuster JK, Yates A, Sweetman A, et al. GAPS-Megacities: A new global platform for investigating persistent organic pollutants and chemicals of emerging concern in urban air. Environmental Pollution 2020; 267: 115416.

Schuster JK, Harner T, Sverko E. Dechlorane Plus in the Global Atmosphere. Environmental Science & Technology Letters 2020; 8: 39-45.

Someya M, Suzuki G, Ionas AC, Tue NM, Xu F, Matsukami H, et al. Occurrence of emerging flame retardants from e-waste recycling activities in the northern part of Vietnam. Emerging Contaminants 2016; 2: 58-65.

Sverko E, Tomy GT, Reiner EJ, Li Y-F, McCarry BE, Arnot JA, et al. Dechlorane plus and related compounds in the environment: a review. Environmental science & technology 2011; 45: 5088-5098.

Tao W, Zhou Z, Shen L, Zhao B. Determination of dechlorane flame retardants in soil and fish at Guiyu, an electronic waste recycling site in south China. Environmental pollution 2015; 206: 361-368.

van Mourik LM, Wang X, Paxman C, Leonards PE, Wania F, de Boer J, et al. Spatial variation of short- and medium-chain chlorinated paraffins in ambient air across Australia. Environmental Pollution 2020: 114141.

Vorkamp K, Bossi R, Rigét FF, Skov H, Sonne C, Dietz R. Novel brominated flame retardants and dechlorane plus in Greenland air and biota. Environmental Pollution 2015; 196: 284-291.

Wang D-G, Yang M, Qi H, Sverko E, Ma W-L, Li Y-F, et al. An Asia-specific source of dechlorane plus: concentration, isomer profiles, and other related compounds. Environmental science & technology 2010; 44: 6608-6613.

Wang K, Gao L, Zhu S, Cui L, Qiao L, Xu C, et al. Spatial distributions and homolog profiles of chlorinated nonane paraffins, and short and medium chain chlorinated paraffins in soils from Yunnan, China. Chemosphere 2020: 125855.

Wang T, Han S, Yuan B, Zeng L, Li Y, Wang Y, et al. Summer–winter concentrations and gas-particle partitioning of short chain chlorinated paraffins in the atmosphere of an urban setting. Environmental pollution 2012; 171: 38-45.

Wang X-T, Wang X-K, Zhang Y, Chen L, Sun Y-F, Li M, et al. Short-and medium-chain chlorinated paraffins in urban soils of Shanghai: spatial distribution, homologue group patterns and ecological risk assessment. Science of the total environment 2014; 490: 144-152.

Wang X-T, Xu S-Y, Wang X-K, Hu B-P, Jia H-H. Occurrence, homologue patterns and source apportionment of short-and medium-chain chlorinated paraffins in suburban soils of Shanghai, China. Chemosphere 2017; 180: 302-311.

Wang Y, Li J, Cheng Z, Li Q, Pan X, Zhang R, et al. Short-and medium-chain chlorinated paraffins in air and soil of subtropical terrestrial environment in the Pearl River Delta, South China: distribution, composition, atmospheric deposition fluxes, and environmental fate. Environmental science & technology 2013; 47: 2679-2687.

Wu J, Cao D, Gao W, Lv K, Liang Y, Fu J, et al. The atmospheric transport and pattern of Medium chain chlorinated paraffins at Shergyla Mountain on the Tibetan Plateau of China. Environmental Pollution 2019; 245: 46-52.

Wu J, Gao W, Liang Y, Fu J, Gao Y, Wang Y, et al. Spatiotemporal distribution and alpine behavior of short chain chlorinated paraffins in air at Shergyla Mountain and Lhasa on the Tibetan Plateau of China. Environmental Science & Technology 2017; 51: 11136-11144.

Xu C, Zhang Q, Gao L, Zheng M, Qiao L, Cui L, et al. Spatial distributions and transport implications of short-and medium-chain chlorinated paraffins in soils and sediments from an e-waste dismantling area in China. Science of The Total Environment 2019; 649: 821-828.

Yu Z, Lu S, Gao S, Wang J, Li H, Zeng X, et al. Levels and isomer profiles of Dechlorane Plus in the surface soils from e-waste recycling areas and industrial areas in South China. Environmental Pollution 2010; 158: 2920-2925.

Zeng L, Wang T, Han W, Yuan B, Liu Q, Wang Y, et al. Spatial and vertical distribution of short chain chlorinated paraffins in soils from wastewater irrigated farmlands. Environmental science & technology 2011; 45: 2100-2106.

Zhu X, Bai H, Gao Y, Chen J, Yuan H, Wang L, et al. Concentrations and inhalation risk assessment of short-chain polychlorinated paraffins in the urban air of Dalian, China. Environmental Science and Pollution Research 2017; 24: 21203-21212.

Paper II

frontiers
in Environmental Science

ORIGINAL RESEARCH
published: 07 January 2022
doi: 10.3389/fenvs.2021.805544

Increasing Trends of Legacy and Emerging Organic Contaminants in a Dated Sediment Core From East-Africa

Maja Nipen[1,2]*, *Rolf David Vogt*[3], *Pernilla Bohlin-Nizzetto*[2], *Katrine Borgå*[4,5], *Eliezer Brown Mwakalapa*[6], *Anders Røsrud Borgen*[2], *Martin Schlabach*[2], *Guttorm Christensen*[7], *Aviti John Mmochi*[8] and *Knut Breivik*[1,2]

[1]Centre for Biogeochemistry in the Anthropocene, Department of Chemistry, University of Oslo, Oslo, Norway, [2]NILU-Norwegian Institute for Air Research, Kjeller, Norway, [3]Norwegian Institute for Water Research, Oslo, Norway, [4]Centre for Biogeochemistry in the Anthropocene, Department of Biosciences, University of Oslo, Oslo, Norway, [5]Aquatic Biology and Toxicology, Department of Biosciences, University of Oslo, Oslo, Norway, [6]Department of Natural Sciences, Mbeya University of Science and Technology, Mbeya, Tanzania, [7]Akvaplan-niva, Tromsø, Norway, [8]Institute for Marine Science, University of Dar es Salaam, Zanzibar, Tanzania

Edited by:
Jabir Hussain Syed,
COMSATS University Islamabad
Pakistan, Pakistan

Reviewed by:
Begoña Jiménez,
Spanish National Research Council
(CSIC), Spain
Qinghui Huang,
Tongji University, China

***Correspondence:**
Maja Nipen
majanip@kjemi.uio.no
mni@nilu.no

Specialty section:
This article was submitted to
Toxicology, Pollution and the
Environment,
a section of the journal
Frontiers in Environmental Science

Received: 30 October 2021
Accepted: 20 December 2021
Published: 07 January 2022

Citation:
Nipen M, Vogt RD, Bohlin-Nizzetto P,
Borgå K, Mwakalapa EB, Borgen AR,
Schlabach M, Christensen G,
Mmochi AJ and Breivik K (2022)
Increasing Trends of Legacy and
Emerging Organic Contaminants in a
Dated Sediment Core From East-
Africa.
Front. Environ. Sci. 9:805544.
doi: 10.3389/fenvs.2021.805544

Temporal trends of industrial organic contaminants can show how environmental burdens respond to changes in production, regulation, and other anthropogenic and environmental factors. Numerous studies have documented such trends from the Northern Hemisphere, while there is very limited data in the literature from sub-Saharan Africa. We hypothesized that the temporal trends of legacy and contemporary industrial contaminants in sub-Saharan Africa could greatly differ from the regions in which many of these chemicals were initially produced and more extensively used. For this purpose, a dated sediment core covering six decades from a floodplain system in urban Dar es Salaam, Tanzania, was analysed. The samples were analysed for selected legacy persistent organic pollutants (POPs) [polychlorinated biphenyls (PCBs) and polybrominated biphenyl ethers (PBDEs)] and chemicals of emerging concern (CECs) [alternative brominated flame retardants (aBFRs), chlorinated paraffins (CPs), and dechloranes]. All groups of chemicals showed a steep increase in concentrations towards the uppermost sediment layers reflecting the more recent years. Concentrations of the individual compound groups in surface sediment were found in the order CPs >> aBFRs ~ $\sum_{25}$PBDEs > dechloranes ~ $\sum_{32}$PCBs. Time trends for the individual compounds and compound groups differed, with $\sum_{32}$PCBs showing presence in sediments since at least the early 1960s, while some CECs first occurred in sediments corresponding to the last decade. Investigations into potential drivers for the observed trends showed that socioeconomic factors related to growth in population, economy, and waste generation have contributed to increasing concentrations of PBDEs, aBFRs, CPs, and Dechlorane Plus. Further monitoring of temporal trends of industrial organic contaminants in urban areas in the Global South is recommended.

Keywords: temporal trends, urban environment, PCBs, PBDEs, flame retardants, dechloranes, chlorinated paraffins

INTRODUCTION

Legacy persistent organic pollutants (POPs), like polychlorinated biphenyls (PCBs) and polybrominated diphenyl ethers (PBDEs), have physicochemical properties which makes them persistent, bioaccumulative, toxic, and have a potential for long-range environmental transport. Some chemicals of emerging concern (CECs), like alternative brominated flame-retardants (aBFRs), chlorinated paraffins (CPs), and dechloranes, also share some of these properties. Time trends for production of these contaminants vary. PCBs and CPs have been produced since the 1930s, Dechlorane Plus (DP) from the 1960s, and PBDEs from the 1970s, while some aBFRs were not produced before the 1980s and 1990s (Breivik et al., 2002; Hoh et al., 2006; Covaci et al., 2011; Glüge et al., 2016; Abbasi et al., 2019). International regulation ensured an end to production of PCBs by the 1990s and PBDEs by the 2010s (Breivik et al., 2002; UNEP, 2017; Abbasi et al., 2019), while the CECs largely remain unregulated at an international level and production remains high or is increasing (Glüge et al., 2016; Xiong et al., 2019; Hansen et al., 2020). Both legacy POPs and CECs have been and are still used extensively in consumer products with different functions and user lifetimes. PCBs were applied in long-life electrical equipment, such as capacitors and transformers (Voogt and Brinkman, 1989), while PBDEs, aBFRs, CPs, and dechloranes have been, or still are used as flame retardants in e.g., electronics, building materials, and textiles. Many of the contemporary products containing CECs have shorter use lifetimes. Emissions to the environment may occur during production, but also during use of products containing legacy POPs and CECs, and from their disposal and recycling when these products reach their end of life.

Different histories for legacy POPs and CECs in terms of production, use, regulation, and waste disposal are thus likely to be reflected in long-term time trends of contaminant burdens in the physical environment. Research on time trends of these contaminants is therefore important to assess the effects of regulation and other emission-reducing measures, and to identify compounds that may merit further attention. Most studies on long-term temporal trends of POPs and CECs are from the Northern Hemisphere, where most of these chemicals have been more extensively produced and used. For instance, PCBs were mainly produced and/or used in North America, Europe, and Japan (Breivik et al., 2002). In these regions, environmental burdens peak around the time of peak production (Bogdal et al., 2008; Arp et al., 2011). Monitoring of atmospheric concentrations have documented declining primary emissions in recent decades (Schuster et al., 2010; Hung et al., 2016; Halvorsen et al., 2021; Wong et al., 2021).

However, elevated atmospheric concentrations of PCBs in some developing and newly industrialized regions in the Global South, including sub-Saharan Africa, indicate ongoing emissions (Klánová et al., 2009; Gioia et al., 2011). Unfortunately, studies on environmental levels of legacy POPs and CECs from sub-Saharan Africa are limited, particularly involving monitoring of long-term time trends (UNEP, 2021). The population and consumption is growing in urban areas in sub-Saharan Africa, though there is a low capacity for environmentally sound waste and e-waste handling. These regions are thus conceived to receive disproportionally large burdens of emissions at the end of the lifetime of products containing legacy POPs and CECs (Hoornweg and Bhada-Tata, 2012). Furthermore, elevated ambient temperatures may lead to enhanced emission of semi-volatile POPs and CECs from products in use and from waste (Breivik et al., 2011). These factors are likely to result in diverging long-term time trends compared to temperate regions in the industrialized Northern Hemisphere, indicating a need for further research in sub-Saharan Africa.

FIGURE 1 | Sampling location for sediment cores marked with arrow. Map from Google Earth.

Studies assessing time trends are often based on monitoring of atmospheric levels. However, assessments of long-term time trends require monitoring over decades, yet atmospheric monitoring programs have only recently included CECs (Wong et al., 2021). Instead, sequentially settled and undisturbed sediments in e.g., fluvial floodplain systems may serve as archives documenting how levels of persistent contaminants in the physical environment have changed in response to changing emissions. This is possible as sediments function as a sink for legacy POPs and CECs, and individual sediment layers can be dated using radioisotopes (Korosi et al., 2015). The collection and analysis of sediment cores is therefore a relevant technique to assess long-term temporal trends of both legacy POPs and CECs in regions where long-term monitoring has been lacking.

The main objective of this study is to describe long-term temporal trends of selected legacy POPs and CECs in a dated sediment core from a sub-Saharan African urban region. Dar es Salaam, Tanzania, was chosen as the study area. This city has experienced growing consumption and population yet suffers from a limited capacity for handling municipal waste and e-waste (Yhdego, 2017; Mahenge et al., 2018). PCBs, PBDEs, aBFRs, CPs, and dechloranes were selected as target analytes as they represent divergent histories related to production, use, and international regulation. None of the selected chemicals are known to have been produced in the region. Their long-term trends in the dated sediment core are compared with results from similar studies from other parts of the world, with particular attention to potential differences between industrialized and developing regions. Finally, the likely socioeconomic and biogeochemical drivers affecting the observed trends are assessed.

MATERIALS AND METHODS

Sampling Site

An urban area was targeted for sampling as the aim was to assess contaminants from local sources rather than contaminants from e.g., long-range transport. Sediment cores were thus collected from a tributary to the Msimbazi River in Tabata ward in Dar es Salaam (6° 49′ 17″ S, 39° 13′ 29″ E) (**Figure 1**) in February 2019. The size of the tributary river watershed is approximately 30 km^2. Soil textures within the catchment are mainly sand and sandy clay (Igulu and Mshiu, 2020) while the sampled section of the riverbed mainly consisted of clay. A floodplain area was chosen for sampling since such terrains favour gravitational settling. The sediments are also less prone to be eroded due to the slow water movement (Heim and Schwarzbauer, 2013). Dar es Salaam has a wet tropical climate, with an annual rainfall of more than 1000 mm, mainly occurring during two rain seasons; the “long rains” in April-May and the “short rains” in October-November. Within the watershed, sources of legacy POPs and CECs to sediments are expected to include surface runoff, untreated wastewater, atmospheric deposition, and seepage from unsolicited scattered dumping of domestic waste.

Sample Collection

Two sediment cores, one for dating and one for legacy POPs and CECs analysis, were collected within ~30 cm of each other using the inner tube (inner diameter 65 mm) of a gravity corer. Both cores were 39 cm in length, of which the top 15 cm were cut in 1 cm layers, while the lower sections were cut into 2 cm layers. Sectioning was done on-site, and slicing tools were rinsed in stream water between each slicing. Sediment layers were placed in pre-cleaned glass containers with aluminium foil-lined lids, transported in cooling bags, and subsequently stored in freezer after arrival at the laboratory.

Dating of Sediments

Layers from the sediment core collected for dating were shipped to GEL Laboratories, Charleston SC, United States, for radioisotope analysis and dating. ^{210}Pb was determined by Alpha spectrometric analysis of its granddaughter in the ^{238}U series, ^{210}Po, which provide more accurate estimates of ^{210}Pb compared to its direct analysis. ^{226}Ra and ^{137}Cs were determined using gamma spectrometry (Kim and Burnett, 1986). Sedimentation rate was modelled based on ^{210}Pb that was not from the decay of ^{226}Ra in the sediments (i.e., excess ^{210}Pb) using the constant rate of supply (CRS) model and the constant flux: constant sedimentation (CF:CS) model as detailed in Appleby and Oldfield (1992).

Sample Preparation and Instrumental Analysis

Methods used for sample preparation and chemical analysis are detailed in the supplementary information (SI) and previously described for soils in Nipen et al. (2021). Only a summary is provided here. Approximately 2 g of wet sediment from each layer of the sediment core collected for legacy POPs and CECs analysis were dried and homogenized by mixing with sodium sulphate in a mortar. ^{13}C labelled internal standards were added to each sediment layer before accelerated solvent extraction (ASE) using acetone/n-hexane (1:1). Approximately 2 g of activated copper powder was added to the extraction cells to remove elemental sulphur. Extracts were volume reduced, before concentrated sulphuric acid was added to remove lipids and other acid-labile potential instrumental interferences, followed by column chromatography clean-up with activated silica eluted with diethyl ether/n-hexane (1:9). The solvent was changed to isooctane, and volume reduced to 100 µl using a gentle stream of N_2. A recovery standard of 1,2,3,4-tetrachloronapthalene was added before instrumental analysis.

Sediment concentrations of 32 PCBs, 25 PBDEs, and 14 aBFRs were determined using gas chromatography high-resolution mass spectrometry (GC-HRMS) (AutoSpec, Waters, Manchester, United Kingdom). Concentrations of 34 short chain CPs (SCCPs) congener groups, 28 medium chain CPs (MCCPs) congener groups, and nine dechlorane compounds were analysed using gas chromatography quadrupole time-of-flight high-resolution mass spectrometry (GC/Q-TOF) (Agilent, Santa Clara, United States). CPs were quantified using a pattern deconvolution procedure (Bogdal et al., 2015). A full inventory of congeners, congener groups, and acronyms used in the text is provided in **Supplementary Table S1**.

Water and organic matter (OM) content in sediment layers were determined gravimetrically by loss on drying at 110°C and loss on ignition (LOI) at 550°C, respectively. OM was determined by LOI followed by correction for loss of structural water in clay (Hoogsteen et al., 2015). Water content, which varied from 31% in the lowest sediment layer to 75% in the top layer, was used to calculate dry weight (dw) concentrations and bulk density.

Quality Assurance

All glassware were baked overnight at 450°C and rinsed with acetone and n-hexane before use. Components for ASE cells were sonicated in acetone twice, followed by sonication in n-hexane. High purity grade solvents were used throughout laboratory procedures. Field blanks ($N = 3$) and method blanks ($N = 5$) were analysed along with the sediment samples. Average blank levels were typically low, except for DBDPE, SCCPs, and MCCPs. High concentrations of these compounds in sediment samples ensured average blank concentrations only represented 6, 9, and 4% of average detected sample concentrations, respectively. Detailed information on blank levels is provided in **Supplementary Table S2**. Sample concentrations were blank corrected based on field and method blanks run with each sample batch. No significant difference was detected between field and method blanks ($p < 0.05$), so both were used to determine method detection limits (LODs). LODs were determined as three times the standard deviation of the blanks normalized to the average sample amount. LODs ranged between 0.0028 and 0.069 ng/g dw for PCBs, 0.0002 and 0.19 ng/g dw for PBDEs, and 0.0011 and 0.043 ng/g dw for aBFRs other than DBDPE. DBDPE had a higher detection limit of 1.7 ng/g dw. LOD for both SCCPs and MCCPs were 22 ng/g dw. No dechloranes were detected in blanks. Instrument detection limits, which ranged from 0.0041 to 0.083 ng/g dw, were therefore used for these compounds. For PCBs, PBDEs, and aBFRs two isotope m/z ratios were analysed for each compound, and results were to be excluded if the ratio diverged from the theoretical isotope ratio by more than 20%. However, no diverging ratios were found in samples with concentrations above the LODs.

Recoveries of internal standards were acceptable for the methods used. They varied between 48 ± 13% and 59 ± 6% for PCBs, 29 ± 7% and 51 ± 10% for PBDEs, 35 ± 11% and 48 ± 11% for aBFRs, 79 ± 15% and 90 ± 21% for dechloranes, and 71 ± 18% for CPs. Samples with internal standard recovery <15% were re-analysed. All legacy POPs and CECs were quantified using the isotope dilution principle, hence intrinsically correcting for recovery. The standard reference material SRM 1944 of an urban marine sediment, from the National Institute for Standards and Technology, was analysed for PCBs and PBDEs with 92 ± 14% and 89 ± 14% compliance, respectively.

RESULTS AND DISCUSSION

Sediment Core Dating

The sediment layers contained low activities of excess ^{210}Pb, rendering core dating challenging. However, a reasonably good exponential decay of ^{210}Pb was measured in a mid-section of the core (8–20 cm depth). For this section, the sediment accumulation rate (SAR) was determined to be 0.27 ± 0.07 cm/year using the CRS model. This corresponds well with SAR determined using the CF:CS model (0.18 ± 0.03 cm/year). Dates for the top- and mid-section of the core were thus assigned based on the rate of sedimentation (CRS model) in the mid-section of the core, covering the time interval 1962 to 2019. Sediment layers below the mid-section of the core did not show exponential decay of ^{210}Pb. This section could therefore not be dated with any confidence and is thus referred to as pre-1962. Activities of ^{137}Cs were generally below or near detection limits and could thus not confirm the dating.

Concentrations and Time Trends of Legacy POPs and CECs

Temporal trends in concentrations of $\sum_{32}$PCBs, $\sum_{25}$PBDEs, aBFRs, CPs, and dechloranes with estimated age of sediment layers are shown in **Figure 2**. Concentrations and congener profiles in each sediment layer are provided in **Supplementary Table S6** and **Supplementary Figures S4–S8**. All analysed PCBs and PBDEs congeners, and both SCCPs and MCCPs, were detected in one or more sediment layer. Of the 14 analysed aBFRs, the following were detected in one or more sediment layers: DBDPE, BTBPE, TBPH, ATE, a-TBECH, b-TBECH, g/d-TBECH, HBB, and PBBZ. Of these, only three (DBDPE, BTBPE, and TBPH) were detected in notable amounts (concentrations >0.1 ng/g dw) and with discernible time trends and are therefore included in further discussions. Of the nine analysed dechloranes, only DP (syn- and anti-isomers), Dec 602, and Dec 603 were detected. Overall, the highest concentrations were found for CPs, followed by aBFRs and $\sum_{25}$PBDEs with concentrations two orders of magnitude lower than CPs, and dechloranes and $\sum_{32}$PCBs with concentrations three orders of magnitude lower than CPs.

Most of the legacy POPs and CECs showed steep increases in concentrations in sediment layers corresponding to the late 2010s. This trend was particularly notable for the CECs, with CPs and aBFRs showing 10–15 times increase from sediment layers corresponding to 2016/2017 to 2019. Of the dechloranes, DP increased five times in the same layers, but the levels of Dec 602 and Dec 603 remained relatively constant. Of the legacy POPs, $\sum_{25}$PBDEs concentrations increased seven times, while $\sum_{32}$PCBs concentrations tripled. Although the increase in $\sum_{32}$PCBs in the late 2010s was small compared to some CECs, it is notable considering that the global production of PCBs peaked five decades ago (Breivik et al., 2002).

Tables 1, **2** lists the approximate year of peak concentration in sediment cores from this study and other studies for comparison, organized by region (developing and newly industrialized countries (**Table 1**) and industrialized countries (**Table 2**)). Temporal trends for the compound groups are discussed below, followed by a discussion of potential drivers for the observed increasing trends.

Legacy POPs

$\sum_{32}$PCB concentrations varied between 0.19 ng/g dw in the deepest sediment layer and 5.8 ng/g dw in the surface sediment layer (**Figure 2A**). Subsurface peaks of $\sum_{32}$PCBs were found in layers corresponding to pre-1962 (3.4 ng/g dw), the 1970s (3.5 ng/g dw), and the late-1990s (4.9 ng/g dw). The dominating congeners in the sediments were PCB-138 (on

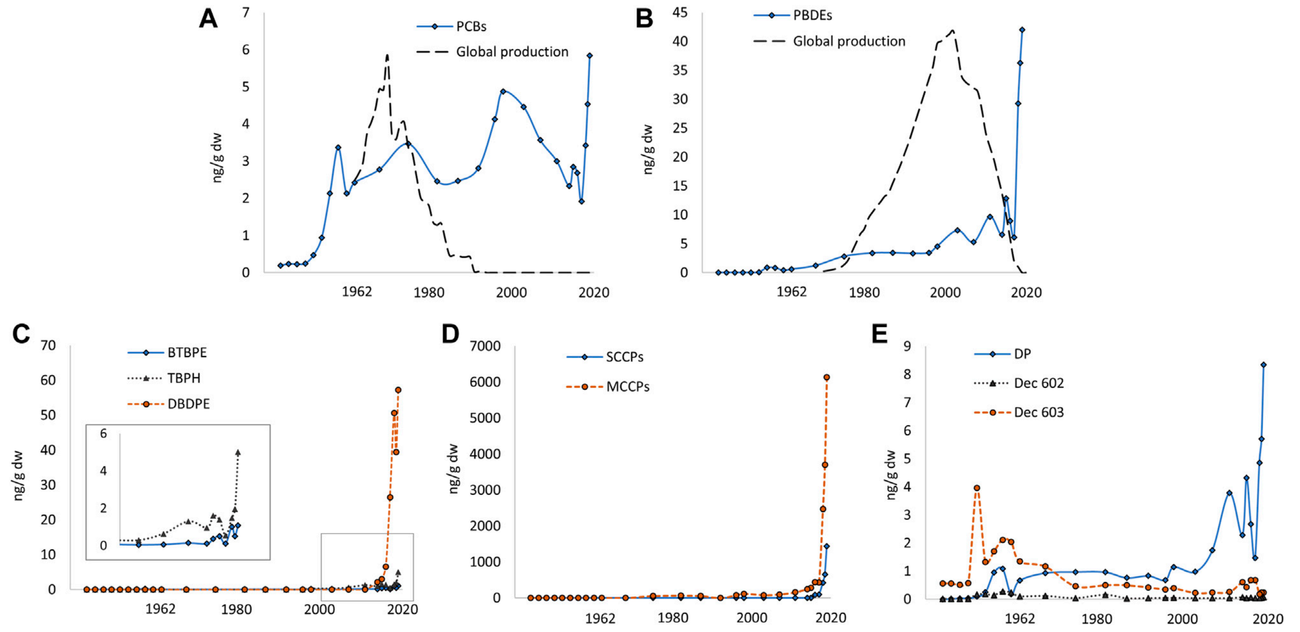

FIGURE 2 | A,B) Concentration of $\sum_{32}$PCBs and $\sum_{25}$PBDEs, respectively, in sediments layers dated from before 1962–2019, along with trend in global production for PCBs from Breivik et al. (2002), and trend in global production for PBDEs from Abbasi et al. (2019). **(C–E)** Concentration of aBFRs, CPs, and dechloranes, respectively, in sediments layers dated from before 1962–2019.

average 15%), PCB-153 (13%), PCB-149 (9.3%), PCB-101 (8.3%), PCB-118 (7.8%), PCB-180 (7.4%), PCB-28 (4.2%), and PCB-31 (3.0%). Individual PCB congeners had temporal trends which differed from each other (Illustrated for PCB-28 and PCB-180 in **Figure 3**). Concentrations of PCB-118, PCB-138, and PCB-180 peaked in subsurface layers, and the increase between 2017 and 2019 was less than factor 2. Lower chlorinated (e.g., PCB-28 and PCB-52) and higher chlorinated (e.g., PCB-206 and PCB-209) congeners peaked instead in the upper layers of the core, where concentrations increased by factors between 3 and 5 from layers corresponding to 2017–2019. The contribution of higher chlorinated congeners to $\sum_{32}$PCB was however minor (**Supplementary Figure S4**). Lower chlorinated congeners are less persistent, and they reached peak production later compared to higher chlorinated congeners (Breivik et al., 2002). Both these factors may affect comparative time trends.

The temporal trend in $\sum_{32}$PCBs (**Figure 2A**) in the studied sediment core was not consistent with trends found in sediment cores from industrialized countries. The PCBs loading in industrialized regions generally peak around 1970 (**Table 2**), reflecting the trends in global PCBs production (**Figure 2A**). In Tanzania, PCBs were mainly used in closed systems (e.g., electrical transformers) (IPEN, 2005) where emissions are likely to occur during or after decommissioning. This, in combination with long use-lives of transformers, may explain the comparatively low peak in PCBs concentrations observed in the 1970s followed by a higher peak in the late 1990s (**Figure 2A**). In this study, as in several other studies from developing and newly industrialized regions (**Table 1**), the highest PCBs concentrations are found in upper most recent layers of sediments. We attribute this to emissions from products and waste containing PCBs, causing delayed emissions compared to industrialized regions. For example, a Chinese study reported a bimodal peak in PCBs in a dated sediment core, with the first peak corresponding to the 1970s, and the second (higher) peak to the 2000s. These peaks were explained by PCBs production and e-waste processing, respectively (Yang H. et al., 2012).

$\sum_{25}$PBDE concentrations ranged from below LOD in the deeper sediment layers to 42 ng/g dw in the surface layer (**Figure 2B**). Concentrations increased from the 1970s to around 3 ng/g dw in the 1980s, where it remained relatively constant until it increased again from the 2000s. From its first detection onwards, BDE-209, the main congener of the decaBDE mixture, dominated the $\sum_{25}$PBDE concentrations, comprising on average 81% of the total (range 71–90%). The relative contribution of BDE-209 increased with sediment depth ($p < 0.05$). This was an unexpected trend considering that penta- and octaBDE were regulated and phased out of production a decade earlier than decaBDE (Abbasi et al., 2019). Time trends for congeners associated with pentaBDE mixtures and octaBDE mixtures were relatively similar (**Supplementary Figure S5**). $\sum_{25}$PBDEs and $\sum_{32}$PCBs were strongly correlated ($p < 0.001$), and several individual PBDE and PCB congeners were also correlated (**Supplementary Table S7**). PBDEs are not known to have been produced before around 1970. Nevertheless, several PBDE congeners were detected in pre-1962 layers, though at low levels. Similar findings have been reported for PBDEs in sediment cores collected in China, the UK, and North America, with

TABLE 1 | Approximate year of peak concentration of PCBs, PBDEs, aBFRs, CPs, and dechloranes in the studied sediment core and in sediment cores from developing and newly industrialized regions, compiled from literature.

Location	System	PCBs	PBDEs	aBFRs	SCCPs	MCCPs	DP	Dec 602	Dec 603	Ref
Dar es Salaam, Tanzania	River	*2019*	*2019*	*2019*	*2019*	*2019*	*2019*	<1962	<1962	This study
Nador Lagoon, Morocco	Lagoon	*2009*								Giuliani et al. (2015)
Lake Victoria, Uganda	Lake	1986								Arinaitwe et al. (2016)
Lake Bujuku and Mahoma, Uganda	Lakes	*2003*								Arinaitwe et al. (2016)
East China Sea, China	Marine	2000								Yang et al. (2012a)
Bay of Manila, Philippines	Marine	*2009*	*2009*							Kwan et al. (2014)
Gulf of Thailand	Marine	1965	1995							Kwan et al. (2014)
Lake Chapala, Mexico	Lake	*2010*	*2010*							Ontiveros-Cuadras et al. (2019)
Nhat Le and Cua Dai, Vietnam	Estuaries	1968	*2015*							Tham et al. (2020)
East China Sea, Yellow Sea, China	Marine		*2010*							Li et al. (2016)
Thane Creek, Mumbai, India	Estuary		2005							Tiwari et al. (2018)
12 Chinese lakes	Lakes		*2006*	*2006*						Wu et al. (2012)
Dongjiang, China	River		sub-surface	*surface*						Zhang et al. (2009)
Daya Bay, China	Marine		2005	*2012*			*2012*			Liu et al. (2014)
Pearl River estuary, China	Estuary/ mangrove			*surface*						Zhang et al. (2015)
Dongjiang, China	River						sub-surface			He et al. (2014)
Yellow Sea, China	Marine						*2010*			Wang et al. (2017)
East China Seas	Marine						1980			Wang et al. (2016)
Pearl River estuary, China	Estuary/ mangrove						*surface*			Sun et al. (2016)
Beijing, China	Lake				*surface*					Zeng et al. (2011)
Dongjiang, China	River				*surface*	*surface*				Chen et al. (2011)
Nine Chinese lakes	Lakes				*2019*	*2019*				Zhang et al. (2019)
South China Sea, China	Marine				*2004*	*2004*				Zeng et al. (2017)
Yellow Sea, China	Marine				2005	2005				Zeng et al. (2013)

Years in italic indicate peak concentration in surface layer of the sediment core.

PBDEs detected in sediments dated to the 1960s and earlier (Wu et al., 2012; Liu et al., 2014; Yang et al., 2016; Da et al., 2019; Guo et al., 2020). The reason for detection of PBDEs in sediment layers corresponding to dates prior to its production is unknown. Potential explanations include contamination during core extrusion, uncertainty in dating of the older layers, or bioturbation of the sediments. These factors are also of relevance to the other analysed compound groups.

According to sediment core data from Western Europe, the environmental levels of PBDEs levelled off or decreased from the late 1990s and early 2000s (Bogdal et al., 2008; Vauclin et al., 2021). On the other hand, some studies from other industrialized countries conducted in the early 2000s and 2010s, documented increasing sediment concentrations of PBDEs (**Table 2**). This may reflect the continued presence of PBDEs in the anthroposphere. Contrary to flattening trends of PBDEs in Western Europe, and similarly to our study, Ontiveros-Cuadras et al. (2019) found increasing PBDEs concentrations in sediment cores from Mexico (**Table 1**). Li et al. (2016) also found increasing trends of PBDEs in sediment cores from the East China Sea. They explain this with shifts in industrial production towards China and import of waste containing PBDEs. The recent steep increase in PBDEs is therefore likely best explained by increasing disposal and recycling of waste products containing PBDEs.

CECs

The concentrations of DBDPE, BTBPE and TBPH ranged from <1.7 to 57, <0.01 to 1.1, and <0.06–5.0 ng/g dw, respectively (**Figure 2C**). DBDPE was first detected in sediment layers corresponding to 2014 and increased up to 57 ng/g dw in the surface layer. Studies on sediment cores from North America (Yang R. et al., 2012), Japan (Hoang et al., 2021), and China (Zhang et al., 2009; Wu et al., 2012; Zhang et al., 2015) show similar increasing concentrations of DBDPE (**Tables 1**, **2**), though DBDPE was generally detected in layers down to deposits from the 1980s or 1990s. BTBPE was detectable in the sediment down to layers corresponding to the early 1980s, though concentrations increased from the late 1990s, and reached the highest concentration in layers corresponding to the late 2010s. Sediment cores from North America show BTBPE concentrations increasing from the 1970s, and levelling off between the mid-1980s and the early 2000s (Hoh et al., 2005; Yang R. et al., 2012). In a study from China, however, BTBPE concentrations were generally found to continue increasing to the upper sediment layers (Zhang et al., 2015). TBPH was detected down to sediment layers corresponding to the late 1990s. Concentrations

TABLE 2 | Approximate year of peak concentration of PCBs, PBDEs, aBFRs, CPs, and dechloranes in sediment cores from regions which have remained industrialized for an extended time, compiled from literature.

Location	System	PCBs	PBDEs	aBFRs	SCCPs	MCCPs	DP	Dec 602	Dec 603	Ref
Baltic Sea, Sweden	Marine				1940	*2016*				Yuan et al. (2017)
Tokyo Bay, Japan	Marine				1990	1990				Zeng et al. (2017)
Lake Ontario, North America	Lake				1970					Marvin et al. (2003)
Lake Thun, Switzerland	Lake	1969			1986	*2004*				Iozza et al. (2008)
Oslo Harbour, Norway	Marine	1970								Arp et al. (2011)
Beppu Bay, Japan	Marine	1970								Takahashi et al. (2020)
Greifensee, Switzerland	Lake	1960								Zennegg et al. (2007)
Adriatic Sea, Italy	Marine	1985								Combi et al. (2016)
Rhone, France	River	1990								Desmet et al. (2012)
Seine, France	River	1970								Dendievel et al. (2020)
Five lakes, Texas, USA	Lakes/ reservoirs	1970								Van Metre and Mahler (2004)
Lake Superior, North America	Lake	1985	*2002*							Song et al. (2004)
Lake Thun, Switzerland	Lake	1965	*2004*							Bogdal et al. (2008)
Rhone, France	River		1995							Vauclin et al. (2021)
Drammensfjord, Norway	Marine		1999							Zegers et al. (2003)
Wadden Sea, Netherlands	Marine		1989							Zegers et al. (2003)
Lake Woserin, Germany	Lake		1990							Zegers et al. (2003)
Lake Erie, North America	Lake		1999							Zhu and Hites, (2005)
Lake Michigan, USA	Lake		1995							Zhu and Hites, (2005)
Sidney estuary, Australia	Estuary		*2014*							Drage et al. (2015)
Lake Ontario, North America	Lake		*2004*				1994			Qiu et al. (2007)
Lake Michigan, North America	Lake						1976			Hoh et al. (2006)
Lake Erie, North America	Lake						sub-surface			Sverko et al. (2008)
Five Great Lakes, North America	Lakes						1980	1990[a]	1990[a]	Yang et al. (2011)
Lake Ontario, North America	Lake						1980	1995	1980	Shen et al. (2011)
Lake Ontario, North America	Lake						1980	1980	1990	Shen et al. (2010b)
Three Great Lakes, North America	Lakes		2000	*2010*			1980			Guo et al. (2020)
Lake Michigan, North America	Lake		1995	1986						Hoh et al. (2005)
Five Great Lakes, North America	Lakes			*2007*						Yang et al. (2012b)
Beppu Bay, Japan	Marine			*2011*						Hoang et al. (2021)

Years in italic indicate peak concentration in surface layer of the sediment core.

[a] *Dec 602 and Dec 603 reported together.*

remain relatively constant between 1 and 2 ng/g dw through the 2010s and increase to 5 ng/g dw in the surface sediment layer. A study from South China reported similar increasing concentrations of TBPH in sediments (Liu et al., 2014). The delayed appearance of DBDPE, BTBPE, and TBPH in the sediments from Dar es Salaam, compared to studies from North America and China, is likely due to differences in industrial activity. DBDPE, BTBPE, and TBPH all correlated strongly with $\sum_{25}$PBDEs and individual PBDEs congeners. BTBPE and TBPH also showed strong correlations to $\sum_{32}$PCBs ($p < 0.001$) (**Supplementary Table S7**).

MCCPs dominated over SCCPs with concentrations varying from <22 to 6,200 and to 1,400 ng/g dw, respectively. The highest CPs concentrations were found in the surface sediment layer, with strongest increase occurring between 2017 and 2019 (**Figure 2D**). MCCPs were detected in all sediment layers corresponding to the mid-1990s onwards, while SCCPs were first detected in layers corresponding to the mid-2010s. Time trends of SCCPs and MCCPs were strongly correlated to $\sum_{25}$PBDEs and aBFRs ($p < 0.001$) (**Supplementary Table S7**). In sediment cores from Western Europe, SCCPs concentrations peaked around the 1980s and 1990s, while MCCPs generally show continued increasing trends (Iozza et al., 2008; Yuan et al., 2017). In sediment cores from China, which has sustained high CPs production, both SCCPs and MCCPs concentrations in general show the highest concentrations in surface layers (Zeng et al., 2012; Zhang et al., 2019) (**Tables 1**, **2**). There is no known production of CPs in Tanzania, so the continued increasing trend is likely connected to the increased use and disposal of CPs containing products, possibly in combination with increased applications of CPs in metal industry. Elevated levels of CPs have been measured in air and soil in and around Dar es Salaam. Spatial trends suggested that municipal waste and e-waste were important sources (Nipen et al., 2021). Surface sediment concentrations of SCCPs and MCCPs were comparable to or higher than the highest soil concentration found in urban areas (1600 and 3200 ng/g dw, respectively, (Nipen et al., 2021). Moreover, congener group profiles of CPs in sediments were more comparable to urban soil than to urban air (SI Text 2).

DP was the dominant dechlorane compound in the sediment (**Figure 2E**), with concentrations ranging from <0.02 to 8.4 ng/g dw. Dec 602 and Dec 603 concentrations ranged from <0.01 to

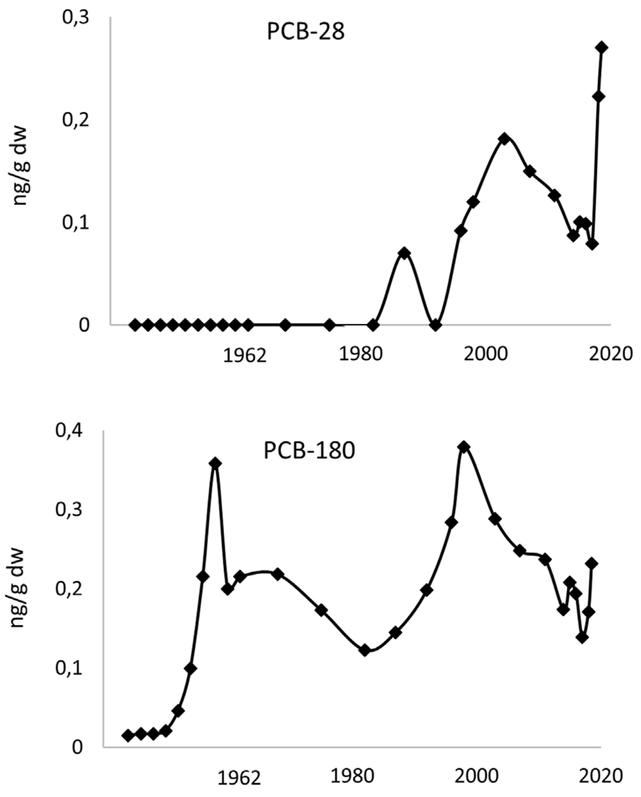

FIGURE 3 | Concentration of PCB-28 and PCB-180 in sediments layers dated from before 1962–2019.

0.27, and 0.18–4.0 ng/g dw, respectively. DP was detected in pre-1962 layers and remained stable at around 1 ng/g dw until the early 2000s. From the mid-2000s, concentrations fluctuated over a general increase to peak concentration in the surface layer. As far as we are aware, this study is the first to report sediment core based long-term time trends for dechloranes from outside regions where they are produced (the North American Great Lakes region and China). In the Great Lakes region, DP concentrations have generally increased from the 1960s or 1970s, usually peaking in the 1980s or 1990s, although some sediment cores showed continued increasing trends into the upper layers (Qiu et al., 2007; Shen et al., 2010b; Shen et al., 2011; Yang et al., 2011) (**Table 2**). In China, the vertical profile of DP in sediments show increasing trends towards the surface layers (**Table 1**). Dec 603 concentration in the studied sediment peaked in layers corresponding to pre-1962 (**Figure 2E**), followed by comparatively low concentrations in subsequent sediment layers. In sediment cores from the Great Lakes region, Dec 603 increased from the 1950s or 1960s, and peaked around the 1980s or 1990s (Shen et al., 2010b; Shen et al., 2011) (**Table 2**). Shen et al. (2010a) describe Dec 603 as an impurity in the historically used pesticides Aldrin and Dieldrin. They observed spatial trends of Dec 603 in sediments in the Great Lakes corresponding to pesticide use. Historic pesticide use is also a plausible explanation for the trends for Dec 603 in this study (SI Text 3). The levels of Dec 602 also peaked in pre-1962 sediment layers (**Figure 2E**). The Dec 602 peak was followed by declining concentrations, with stable low concentrations around or just below 0.05 ng/g dw from the mid-1980s up to the surface sediment layer. In sediment cores from the Great Lakes region, Dec 602 concentrations increased from the 1960s or 1970s and peaked around the 1980s and 1990s (Shen et al., 2010b; Shen et al., 2011). Dec 602 only showed a significant correlation with Dec 603 ($p < 0.01$), while correlations between Dec 603 and other CECs and legacy POPs were generally negative. Although DP showed strong positive correlations with both the legacy POPs ($\sum_{32}$PCBs and $\sum_{25}$PBDEs) and the other CECs (aBFRs and CPs) ($p < 0.001$ for all), the continued presence of DP in sediments over decades demonstrate that it is not a “new” contaminant in this region.

Spatial trends and elevated levels of DP in air and soil in Dar es Salaam suggest e-waste as an important source (Nipen et al., 2021). The levels of DP in the surface sediment layer were higher than the highest concentrations found in urban soil (5.0 ng/g dw). Dec 602 and Dec 603 concentrations in surface sediment (0.07 and 0.2 ng/g dw, respectively) were comparable to the highest soil concentrations found in urban areas (0.05 and 0.3 ng/g dw, respectively). Moreover, the study by Nipen et al. suggested that the Dec 603 sources were of a historic nature, which is consistent with the findings in this study.

Potential Drivers for Time Trends of Legacy POPs and CECs

There are several conceptual explanations for the recent increasing trends in POPs and CECs, both in terms of the socioeconomic development in the region and due to shifts in environmental pressures on biogeochemical processes.

Growth in urban population and especially in per capita Gross Domestic Product (GDP) (**Figure 4A**) imply growth in consumption and general waste generation (Hoornweg and Bhada-Tata, 2012). Further, the very strong growth in mobile and broadband subscriptions, along with the amount of e-waste generated in the region, show that consumption has been particularly strong for electronics during the last decade. Strong correlations were found between these socioeconomic parameters and sediment concentrations of $\sum_{25}$PBDEs, aBFRs, DP, and CPs ($p < 0.001$). Dec 602, Dec 603, and $\sum_{32}$PCBs were not correlated with any of the socioeconomic parameters, although some individual congeners (PCB-28 and PCB-206, $p < 0.001$) were (**Supplementary Table S8**). Strong temporal correlations between socioeconomic parameters and the level of flame retardants (PBDEs, aBFRs, DP, along with CPs) in the sediment layers, suggest that increases in consumption and waste generation of consumer goods containing these additives contribute to the increase in these pollutants during the late 2010s. PCB-28 and PCB-206 have been reported to occur as unintentional by-products in pigment production (Anh et al., 2020). Consequently, use and disposal of pigment-containing consumer products may be a contributing factor for the increasing trend for these congeners in the 2010s. These findings suggest that

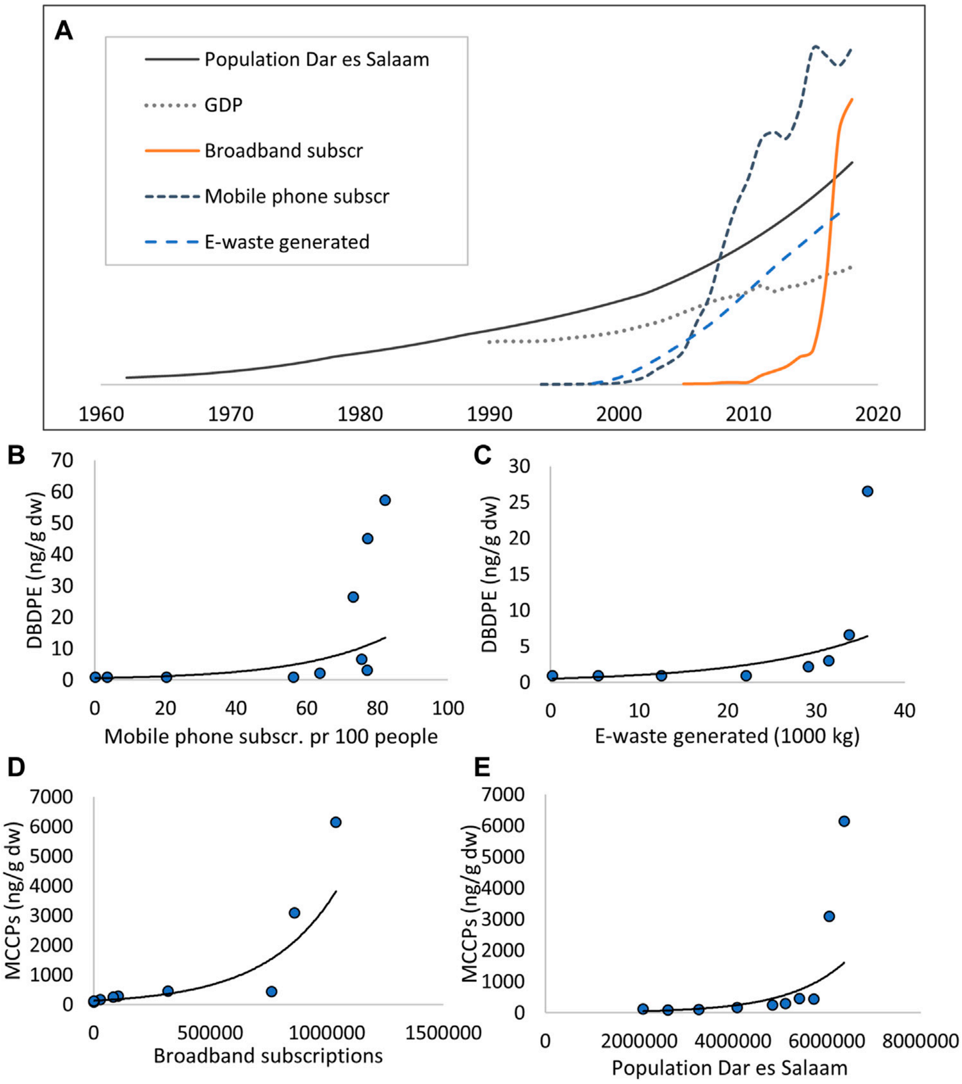

FIGURE 4 | (A) Time trends of some socioeconomic factors in Tanzania (GDP, broadband subscriptions, mobile phone subscriptions, e-waste generated) and Dar es Salaam (population). For comparison purposes data have been converted to unitless numbers by normalizing using the mean. Original data for population, GDP per capita, Broadband subscriptions, and mobile phone subscriptions are gathered from the World Bank (WorldBank, 2021). E-waste data are from the Tanzanian National Beaureu of Statistics (NBS, 2019). **(B,C)** Concentrations of DBDPE plotted against mobile phone subscriptions and e-waste from 1998 to 2019 (e-waste data only available to 2017). **(D,E)**: Concentrations of MCCPs plotted against broadband subscriptions and population in Dar es Salaam from 1998 to 2019.

inadequate handling and recycling of waste has led to increasing pollutant levels in the urban environment.

The exponential rather than linear relationship between CECs and socioeconomic factors (**Figures 4B–E**) suggests that additional factors may contribute synergistically to increasing concentrations. Elevated concentrations of organic pollutants in sediment layers may be due to erosion of contaminated topsoil or other contaminated surface reservoirs within the watershed caused by intense rainfall and flooding events (Lu et al., 2016). Correlations of rainfall versus legacy POPs and CECs were investigated for two different time intervals (1983–2018 and 2010–2018), using rainfall data from the Tanzanian Meteorological Authority (TMA, 2021). The longer and shorter time intervals were chosen based on the likelihood of legacy POPs and CECs being present in topsoil, respectively. No significant correlations were found for the time interval 1983–2018 (**Supplementary Table S9**). For the time interval 2010 to 2018, the rainfall episodes between 2010 and 2012 were less intense, around average between 2013 and 2016, and stronger than average in 2017 and 2018. For the time interval 2010 to 2018, CPs and DBDPE were significantly correlated with rainfall ($p < 0.05$ and $p < 0.01$, respectively). Similarities in CPs congener group profiles in soil from urban areas and sediment, as well as comparable concentrations, support that increased erosion of contaminated soil has contributed to the increasing trend of CPs in sediments.

Strong associations are expected between OM content and the hydrophobic legacy POPs and CECs (**Supplementary Figure**

S11). OM content in the sediment varied between 1% in the lowest sediment layer to 9% in the top layer. The OM content was strongly positively correlated to sediment concentration of most PCB and PBDE congeners, $\sum_{32}$PCBs, $\sum_{25}$PBDE, TBPH, BTBPE, DP, and MCCPs ($p < 0.001$). OM content was also significantly correlated to PCB-209, DBDPE, and SCCPs ($p < 0.05$), while there were no or negative correlations between OM and Dec 602 and Dec 603. However, the main features of trends of legacy POPs and CECs, including strong increases in the late 2010s and subsurface peaks for PCBs, remain when concentrations are normalized to OM content (**Supplementary Figure S12**). If OM content was the main explanatory factor governing the time trends, there would have been a "smoothing out" of the concentration differences between the sediment layers. The trend in OM content is therefore not likely to be the main driver for the observed temporal trends.

Overall, these findings suggest that the increasing trends in legacy POPs and CECs in sediment layers corresponding to the late 2010s are mainly a consequence of increased primary emissions from products and waste in connection with the rapid socioeconomic development in the region. However, secondary emissions in the form of remobilized surface reservoirs of legacy POPs and CECs are likely to have contributed to the increasing trends, particularly for CPs and DBDPE.

CONCLUDING REMARKS

This study showed that concentrations of both legacy POPs and CECs, particularly CPs and DBDPE, have increased notably in sediment layers corresponding to the late 2010s. Other studies from industrialized regions, as well as other developing and newly industrialized regions, in general also show increasing trends for these CECs. This suggests that particular attention should be given to these compounds in future monitoring studies, both regionally and internationally. Comparisons of time trends of legacy POPs showed that the flattening and declining trends seen in most industrialized regions, as a response to regulation and emission controls, are not reflected in the studied region, nor in most other developing and newly industrialized regions. This underlines the importance of improved emissions controls in waste handling and recycling in these regions. This should be further prioritized at a regional level, but also in international regulatory efforts relating to trade in products, used products, and waste that contain these compounds.

More studies of sediment cores are needed to further document historical emission trends in developing and newly industrialized regions. Monitoring of atmospheric concentrations of legacy POPs and CECs in urban areas in these regions may also be an important additional asset to assess the effect of emissions reductions, as atmospheric concentrations respond more rapidly to changes in emissions.

DATA AVAILABILITY STATEMENT

The raw data supporting the conclusions of this article will be made available by the authors, without undue reservation.

AUTHOR CONTRIBUTIONS

MN, RV, PB-N, KBo, and KBr conceptualized the study, MN wrote the original draft, while RV, PB-N, KBo, EM, AB, MS, GC, AM, and KBr contributed to review and editing of the manuscript. Formal analysis was conducted by MN. Investigation was conducted by MN, EM, AB, and GC. Supervision was provided by RV, PB-N, KBo, MS, and KBr, and KBo was project administrator.

FUNDING

The AnthroTox project is funded through the University of Oslo Life:Science initiative and the Norwegian Ministry of Education and Research.

ACKNOWLEDGMENTS

This study was conducted as part of the AnthroTox project, a convergence environment combining social and natural sciences to study anthropogenic toxicants. We thank Signe Mikkelsen for contributions during fieldwork. Modelling work for sediment dating was carried out by W. C. Burnett, Florida State University, for GEL Laboratories.

SUPPLEMENTARY MATERIAL

The Supplementary Material for this article can be found online at: https://www.frontiersin.org/articles/10.3389/fenvs.2021.805544/full#supplementary-material

REFERENCES

Abbasi, G., Li, L., and Breivik, K. (2019). Global Historical Stocks and Emissions of PBDEs. *Environ. Sci. Technol.* 53, 6330–6340. doi:10.1021/acs.est.8b07032

Anh, H. Q., Watanabe, I., Minh, T. B., and Takahashi, S. (2020). Unintentionally Produced Polychlorinated Biphenyls in Pigments: An Updated Review on Their Formation, Emission Sources, Contamination Status, and Toxic Effects. *Sci. Total Environ.* 755, 142504. doi:10.1016/j.scitotenv.2020.142504

Appleby, P., and Oldfield, F. (1992). "Applications of lead-210 to Sedimentation Studies," in *Uranium-Series Disequilibrium: Applications to Earth, Marine, and Environmental Sciences*. 2nd Edn. Oxford: Clarendon Press.

Arinaitwe, K., Rose, N. L., Muir, D. C. G., Kiremire, B. T., Balirwa, J. S., and Teixeira, C. (2016). Historical Deposition of Persistent Organic Pollutants in Lake Victoria and Two Alpine Equatorial Lakes from East Africa: Insights into

Atmospheric Deposition from Sedimentation Profiles. *Chemosphere* 144, 1815–1822. doi:10.1016/j.chemosphere.2015.10.061

Arp, H. P. H., Villers, F., Lepland, A., Kalaitzidis, S., Christanis, K., Oen, A. M. P., et al. (2011). Influence of Historical Industrial Epochs on Pore Water and Partitioning Profiles of Polycyclic Aromatic Hydrocarbons and Polychlorinated Biphenyls in Oslo Harbor, Norway, Sediment Cores. *Environ. Toxicol. Chem.* 30 (4), 843–851. doi:10.1002/etc.466

Bogdal, C., Alsberg, T., Diefenbacher, P. S., MacLeod, M., and Berger, U. (2015). Fast Quantification of Chlorinated Paraffins in Environmental Samples by Direct Injection High-Resolution Mass Spectrometry with Pattern Deconvolution. *Anal. Chem.* 87 (5), 2852–2860. doi:10.1021/ac504444d

Bogdal, C., Schmid, P., Kohler, M., Müller, C. E., Iozza, S., Bucheli, T. D., et al. (2008). Sediment Record and Atmospheric Deposition of Brominated Flame Retardants and Organochlorine Compounds in Lake Thun, Switzerland: Lessons from the Past and Evaluation of the Present. *Environ. Sci. Technol.* 42 (18), 6817–6822. doi:10.1021/es800964z

Breivik, K., Gioia, R., Chakraborty, P., Zhang, G., and Jones, K. C. (2011). Are Reductions in Industrial Organic Contaminants Emissions in Rich Countries Achieved Partly by Export of Toxic Wastes? *Environ. Sci. Technol.* 45 (21), 9154–9160. doi:10.1021/es202320c

Breivik, K., Sweetman, A., Pacyna, J., and Jones, K. (2002). Towards a Global Historical Emission Inventory for Selected PCB Congeners - A Mass Balance Approach1. Global Production and Consumption. *Sci. Total Environ.* 290, 181–198. doi:10.1016/s0048-9697(01)01075-0

Chen, M.-Y., Luo, X.-J., Zhang, X.-L., He, M.-J., Chen, S.-J., and Mai, B.-X. (2011). Chlorinated Paraffins in Sediments from the Pearl River Delta, South China: Spatial and Temporal Distributions and Implication for Processes. *Environ. Sci. Technol.* 45 (23), 9936–9943. doi:10.1021/es202891a

Combi, T., Miserocchi, S., Langone, L., and Guerra, R. (2016). Polychlorinated Biphenyls (PCBs) in Sediments from the Western Adriatic Sea: Sources, Historical Trends and Inventories. *Sci. Total Environ.* 562, 580–587. doi:10.1016/j.scitotenv.2016.04.086

Da, C., Wang, R., Ye, J., and Yang, S. (2019). Sediment Records of Polybrominated Diphenyl Ethers (PBDEs) in Huaihe River, China: Implications for Historical Production and Household Usage of PBDE-Containing Products. *Environ. Pollut.* 254, 112955. doi:10.1016/j.envpol.2019.07.123

Dendievel, A.-M., Mourier, B., Coynel, A., Evrard, O., Labadie, P., Ayrault, S., et al. (2020). Spatio-Temporal Assessment of the Polychlorinated Biphenyl (PCB) Sediment Contamination in Four Major French River Corridors (1945-2018). *Earth Syst. Sci. Data* 12 (2), 1153–1170. doi:10.5194/essd-12-1153-2020

Desmet, M., Mourier, B., Mahler, B. J., Van Metre, P. C., Roux, G., Persat, H., et al. (2012). Spatial and Temporal Trends in PCBs in Sediment Along the Lower Rhône River, France. *Sci. Total Environ.* 433, 189–197. doi:10.1016/j.scitotenv.2012.06.044

Drage, D., Mueller, J. F., Birch, G., Eaglesham, G., Hearn, L. K., and Harrad, S. (2015). Historical Trends of PBDEs and HBCDs in Sediment Cores from Sydney Estuary, Australia. *Sci. Total Environ.* 512-513, 177–184. doi:10.1016/j.scitotenv.2015.01.034

Gioia, R., Eckhardt, S., Breivik, K., Jaward, F. M., Prieto, A., Nizzetto, L., et al. (2011). Evidence for Major Emissions of PCBs in the West African Region. *Environ. Sci. Technol.* 45 (4), 1349–1355. doi:10.1021/es1025239

Giuliani, S., Piazza, R., El Moumni, B., Polo, F. P., Vecchiato, M., Romano, S., et al. (2015). Recognizing Different Impacts of Human and Natural Sources on the Spatial Distribution and Temporal Trends of PAHs and PCBs (Including PCB-11) in Sediments of the Nador Lagoon (Morocco). *Sci. Total Environ.* 526, 346–357. doi:10.1016/j.scitotenv.2015.04.057

Glüge, J., Wang, Z., Bogdal, C., Scheringer, M., and Hungerbühler, K. (2016). Global Production, Use, and Emission Volumes of Short-Chain Chlorinated Paraffins - A Minimum Scenario. *Sci. Total Environ.* 573, 1132–1146. doi:10.1016/j.scitotenv.2016.08.105

Guo, J., Li, Z., Ranasinghe, P., Rockne, K. J., Sturchio, N. C., Giesy, J. P., et al. (2020). Halogenated Flame Retardants in Sediments from the Upper Laurentian Great Lakes: Implications to Long-Range Transport and Evidence of Long-Term Transformation. *J. Hazard. Mater.* 384, 121346. doi:10.1016/j.jhazmat.2019.121346

Hansen, K. M., Fauser, P., Vorkamp, K., and Christensen, J. H. (2020). Global Emissions of Dechlorane Plus. *Sci. Total Environ.* 742, 140677. doi:10.1016/j.scitotenv.2020.140677

He, M.-J., Luo, X.-J., Wu, J.-P., Chen, S.-J., Wei, S.-Q., and Mai, B.-X. (2014). Isomers of Dechlorane Plus in an Aquatic Environment in a Highly Industrialized Area in Southern China: Spatial and Vertical Distribution, Phase Partition, and Bioaccumulation. *Sci. Total Environ.* 481, 1–6. doi:10.1016/j.scitotenv.2014.02.025

Heim, S., and Schwarzbauer, J. (2013). Pollution History Revealed by Sedimentary Records: A Review. *Environ. Chem. Lett.* 11 (3), 255–270. doi:10.1007/s10311-013-0409-3

Hoang, A. Q., Aono, D., Watanabe, I., Kuwae, M., Kunisue, T., and Takahashi, S. (2021). Contamination Levels and Temporal Trends of Legacy and Current-Use Brominated Flame Retardants in a Dated Sediment Core from Beppu Bay, Southwestern Japan. *Chemosphere* 266, 129180. doi:10.1016/j.chemosphere.2020.129180

Hoh, E., Zhu, L., and Hites, R. A. (2006). Dechlorane Plus, a Chlorinated Flame Retardant, in the Great Lakes. *Environ. Sci. Technol.* 40 (4), 1184–1189. doi:10.1021/es051911h

Hoh, E., Zhu, L., and Hites, R. A. (2005). Novel Flame Retardants, 1,2-Bis(2,4,6-Tribromophenoxy)ethane and 2,3,4,5,6-Pentabromoethylbenzene, in United States' Environmental Samples. *Environ. Sci. Technol.* 39 (8), 2472–2477. doi:10.1021/es048508f

Hoogsteen, M. J. J., Lantinga, E. A., Bakker, E. J., Groot, J. C. J., and Tittonell, P. A. (2015). Estimating Soil Organic Carbon Through Loss on Ignition: Effects of Ignition Conditions and Structural Water Loss. *Eur. J. Soil Sci.* 66 (2), 320–328. doi:10.1111/ejss.12224

Hoornweg, D., and Bhada-Tata, P. (2012). *What a Waste: A Global Review of Solid Waste Management*. Urban Development Series Knowledge Papers2012, No. 15. Washington, D.C.: World Bank.

Hung, H., Katsoyiannis, A. A., Brorström-Lundén, E., Olafsdottir, K., Aas, W., Breivik, K., et al. (2016). Temporal Trends of Persistent Organic Pollutants (POPs) in Arctic Air: 20 Years of Monitoring under the Arctic Monitoring and Assessment Programme (AMAP). *Environ. Pollut.* 217, 52–61. doi:10.1016/j.envpol.2016.01.079

Igulu, B., and Mshiu, E. (2020). The Impact of an Urbanizing Tropical Watershed to the Surface-Runoff. *Glob. J. Environ. Sci. Manage.* 6 (2), 245–260. doi:10.22034/gjesm.2020.02.09

Iozza, S., Müller, C. E., Schmid, P., Bogdal, C., and Oehme, M. (2008). Historical Profiles of Chlorinated Paraffins and Polychlorinated Biphenyls in a Dated Sediment Core from Lake Thun (Switzerland). *Environ. Sci. Technol.* 42 (4), 1045–1050. doi:10.1021/es702383t

IPEN (2005). *Hotspot Report for Pattern of Practices: PCBs Sources and Releases in Tanzania*. Dar es Salaam: The International POPs Elimination Project.

Kim, K. H., and Burnett, W. C. (1986). Uranium-Series Growth History of a Quaternary Phosphatic Crust from the Peruvian continental Margin. *Chem. Geology. Isotope Geosci. section* 58 (3), 227–244. doi:10.1016/0168-9622(86)90012-6

Klánová, J., Čupr, P., Holoubek, I., Borůvková, J., Přibylová, P., Kareš, R., et al. (2009). Monitoring of Persistent Organic Pollutants in Africa. Part 1: Passive Air Sampling Across the Continent in 2008. *J. Environ. Monit.* 11 (11), 1952–1963. doi:10.1039/b913415h

Korosi, J. B., Cheng, W., and Blais, J. M. (2015). "Organic Pollutants in Sediment Core Archives," in *Environmental Contaminants*. Editors J. Blais, M. Rosen, and J Smol (Dordrecht: Springer), 161–185. doi:10.1007/978-94-017-9541-8_8

Kwan, C. S., Takada, H., Boonyatumanond, R., Kato, Y., Mizukawa, K., Ito, M., et al. (2014). Historical Occurrences of Polybrominated Diphenyl Ethers and Polychlorinated Biphenyls in Manila Bay, Philippines, and in the Upper Gulf of Thailand. *Sci. total Environ.* 470-471, 427–437. doi:10.1016/j.scitotenv.2013.09.076

Li, Y., Lin, T., Hu, L., Feng, J., and Guo, Z. (2016). Time Trends of Polybrominated Diphenyl Ethers in East China Seas: Response to the Booming of PBDE Pollution Industry in China. *Environ. Int.* 92-93, 507–514. doi:10.1016/j.envint.2016.04.033

Liu, H.-H., Hu, Y.-J., Luo, P., Bao, L.-J., Qiu, J.-W., Leung, K. M. Y., et al. (2014). Occurrence of Halogenated Flame Retardants in Sediment off an Urbanized Coastal Zone: Association with Urbanization and Industrialization. *Environ. Sci. Technol.* 48 (15), 8465–8473. doi:10.1021/es500660z

Lu, Q., Futter, M. N., Nizzetto, L., Bussi, G., Jürgens, M. D., and Whitehead, P. G. (2016). Fate and Transport of Polychlorinated Biphenyls (PCBs) in the River Thames Catchment - Insights from a Coupled Multimedia Fate and Hydrobiogeochemical Transport Model. *Sci. Total Environ.* 572, 1461–1470. doi:10.1016/j.scitotenv.2016.03.029

Lunder Halvorsen, H., Bohlin-Nizzetto, P., Eckhardt, S., Gusev, A., Krogseth, I. S., Moeckel, C., et al. (2021). Main Sources Controlling Atmospheric Burdens of Persistent Organic Pollutants on a National Scale. *Ecotoxicology Environ. Saf.* 217, 112172. doi:10.1016/j.ecoenv.2021.112172

Mahenge, R. S., Ulanga, P., Malabeja, M., Pilly, J., and Massoy, W. (2018). Performance Audit Report on Electronic Waste Management. Available at: https://www.nao.go.tz/uploads/ELECTRONIC-WASTE-MANAGEMENT-2018.pdf. (Accessed March, 2021).

Marvin, C. H., Painter, S., Tomy, G. T., Stern, G. A., Braekevelt, E., and Muir, D. C. G. (2003). Spatial and Temporal Trends in Short-Chain Chlorinated Paraffins in Lake Ontario Sediments. *Environ. Sci. Technol.* 37 (20), 4561–4568. doi:10.1021/es0345064

NBS (2019). in *National E-Waste Statistics Report* (Dodoma, Tanzania, Bonn, Germany: V.S. National Bureau of Statistics and United Nations University. National Bureau StatisticsUnited Nations University, ViE – SCYCLE).

Nipen, M., Vogt, R. D., Bohlin-Nizzetto, P., Borgå, K., Mwakalapa, E. B., Borgen, A. R., et al. (2021). Spatial Trends of Chlorinated Paraffins and Dechloranes in Air and Soil in a Tropical Urban, Suburban, and Rural Environment. *Environ. Pollut.* 292, 118298. doi:10.1016/j.envpol.2021.118298

Ontiveros-Cuadras, J. F., Ruiz-Fernández, A. C., Sanchez-Cabeza, J.-A., Sericano, J., Pérez-Bernal, L. H., Páez-Osuna, F., et al. (2019). Recent History of Persistent Organic Pollutants (PAHs, PCBs, PBDEs) in Sediments from a Large Tropical lake. *J. Hazard. Mater.* 368, 264–273. doi:10.1016/j.jhazmat.2018.11.010

Qiu, X., Marvin, C. H., and Hites, R. A. (2007). Dechlorane Plus and Other Flame Retardants in a Sediment Core from Lake Ontario. *Environ. Sci. Technol.* 41 (17), 6014–6019. doi:10.1021/es070810b

Schuster, J. K., Gioia, R., Breivik, K., Steinnes, E., Scheringer, M., and Jones, K. C. (2010). Trends in European Background Air Reflect Reductions in Primary Emissions of PCBs and PBDEs. *Environ. Sci. Technol.* 44 (17), 6760–6766. doi:10.1021/es101009x

Shen, L., Reiner, E. J., Helm, P. A., Marvin, C. H., Hill, B., Zhang, X., et al. (2011). Historic Trends of Dechloranes 602, 603, 604, Dechlorane Plus and Other Norbornene Derivatives and Their Bioaccumulation Potential in Lake Ontario. *Environ. Sci. Technol.* 45 (8), 3333–3340. doi:10.1021/es104328r

Shen, L., Reiner, E. J., MacPherson, K. A., Kolic, T. M., Helm, P. A., Richman, L. A., et al. (2010a). Dechloranes 602, 603, 604, Dechlorane Plus, and Chlordene Plus, a Newly Detected Analogue, in Tributary Sediments of the Laurentian Great Lakes. *Environ. Sci. Technol.* 45 (2), 693–699. doi:10.1021/es1027844

Shen, L., Reiner, E. J., MacPherson, K. A., Kolic, T. M., Sverko, E., Helm, P. A., et al. (2010b). Identification and Screening Analysis of Halogenated Norbornene Flame Retardants in the Laurentian Great Lakes: Dechloranes 602, 603, and 604. *Environ. Sci. Technol.* 44 (2), 760–766. doi:10.1021/es902482b

Song, W., Ford, J. C., Li, A., Mills, W. J., Buckley, D. R., and Rockne, K. J. (2004). Polybrominated Diphenyl Ethers in the Sediments of the Great Lakes. 1. Lake Superior. *Environ. Sci. Technol.* 38 (12), 3286–3293. doi:10.1021/es035297q

Sun, Y.-X., Zhang, Z.-W., Xu, X.-R., Hao, Q.-W., Hu, Y.-X., Zheng, X.-B., et al. (2016). Spatial and Vertical Distribution of Dechlorane Plus in Mangrove Sediments of the Pearl River Estuary, South China. *Arch. Environ. Contam. Toxicol.* 71 (3), 359–364. doi:10.1007/s00244-016-0296-2

Sverko, E., Tomy, G. T., Marvin, C. H., Zaruk, D., Reiner, E., Helm, P. A., et al. (2008). Dechlorane Plus Levels in Sediment of the Lower Great Lakes. *Environ. Sci. Technol.* 42 (2), 361–366. doi:10.1021/es0710104

Takahashi, S., Anh, H. Q., Watanabe, I., Aono, D., Kuwae, M., and Kunisue, T. (2020). Characterization of Mono- to Deca-Chlorinated Biphenyls in a Well-Preserved Sediment Core from Beppu Bay, Southwestern Japan: Historical Profiles, Emission Sources, and Inventory. *Sci. Total Environ.* 743, 140767. doi:10.1016/j.scitotenv.2020.140767

Tham, T. T., Anh, H. Q., Phuong, B. T., Trinh, L. T., Thuy, N. T. T., Yen, N. T. H., et al. (2020). Contamination Status and Temporal Trends of Persistent Toxic Substances in Sediment Cores from Coastal Areas of central Vietnam. *Mar. Pollut. Bull.* 156, 111222. doi:10.1016/j.marpolbul.2020.111222

Tiwari, M., Sahu, S. K., Bhangare, R. C., Ajmal, P. Y., and Pandit, G. G. (2018). Polybrominated Diphenyl Ethers (PBDEs) in Core Sediments from Creek Ecosystem: Occurrence, Geochronology, and Source Contribution. *Environ. Geochem. Health* 40 (6), 2587–2601. doi:10.1007/s10653-018-0125-9

TMA (2021). Rainfall Anomalies Between 1983 and 2018. Available at: http://maproom.meteo.go.tz/maproom/ (Accessed September 2021).

UNEP (2021). Global Monitoring Plan for Persistent Organic Pollutants: Third Regional Monitoring Report - Africa Region. Available at: http://chm.pops.int/Implementation/GlobalMonitoringPlan/MonitoringReports/tabid/525/ (Accessed October 29, 2021).

UNEP (2017). Stockholm Convention on Persistent Organic Pollutants (POPs). Available at: www.pops.int/TheConvention/Overview/TextoftheConvention/tabid/2232/Default.aspx: UNEP (Accessed September 02, 2021).

Van Metre, P. C., and Mahler, B. J. (2004). Contaminant Trends in Reservoir Sediment Cores as Records of Influent Stream Quality. *Environ. Sci. Technol.* 38 (11), 2978–2986. doi:10.1021/es049859x

Vauclin, S., Mourier, B., Dendievel, A.-M., Marchand, P., Vénisseau, A., Morereau, A., et al. (2021). Temporal Trends of Legacy and Novel Brominated Flame Retardants in Sediments along the Rhône River Corridor in France. *Chemosphere* 271, 129889. doi:10.1016/j.chemosphere.2021.129889

Voogt, P., and Brinkman, U. (1989). Production, Properties and Usage of Polychlorinated Biphenyls. *Halogenated biphenyls, terphenyls, naphthalenes, dibenzodioxins Relat. Prod.* (2nd edn) 3–45. doi:10.1016/b978-0-444-81029-8.50005-9

Wang, G., Peng, J., Hao, T., Feng, L., Liu, Q., and Li, X. (2017). Effects of Terrestrial and Marine Organic Matters on Deposition of Dechlorane Plus (DP) in Marine Sediments from the Southern Yellow Sea, China: Evidence from Multiple Biomarkers. *Environ. Pollut.* 230, 153–162. doi:10.1016/j.envpol.2017.06.061

Wang, G., Peng, J., Hao, T., Liu, Y., Zhang, D., and Li, X. (2016). Distribution and Region-specific Sources of Dechlorane Plus in Marine Sediments from the Coastal East China Sea. *Sci. Total Environ.* 573, 389–396. doi:10.1016/j.scitotenv.2016.08.090

Wong, F., Hung, H., Dryfhout-Clark, H., Aas, W., Bohlin-Nizzetto, P., Breivik, K., et al. (2021). Time Trends of Persistent Organic Pollutants (POPs) and Chemicals of Emerging Arctic Concern (CEAC) in Arctic Air from 25 Years of Monitoring. *Sci. Total Environ.* 775, 145109. doi:10.1016/j.scitotenv.2021.145109

WorldBank (2021). The World Bank in Tanzania [Online]. Available at: http://www.worldbank.org/en/country/tanzania/overview (Accessed January 2021).

Wu, F., Guo, J., Chang, H., Liao, H., Zhao, X., Mai, B., et al. (2012). Polybrominated Diphenyl Ethers and Decabromodiphenylethane in Sediments from Twelve Lakes in China. *Environ. Pollut.* 162, 262–268. doi:10.1016/j.envpol.2011.11.014

Xiong, P., Yan, X., Zhu, Q., Qu, G., Shi, J., Liao, C., et al. (2019). A Review of Environmental Occurrence, Fate, and Toxicity of Novel Brominated Flame Retardants. *Environ. Sci. Technol.* 53 (23), 13551–13569. doi:10.1021/acs.est.9b03159

Yang, C., Rose, N. L., Turner, S. D., Yang, H., Goldsmith, B., Losada, S., et al. (2016). Hexabromocyclododecanes, Polybrominated Diphenyl Ethers, and Polychlorinated Biphenyls in Radiometrically Dated Sediment Cores from English Lakes, ~ 1950-present. *Sci. Total Environ.* 541, 721–728. doi:10.1016/j.scitotenv.2015.09.102

Yang, H., Zhuo, S., Xue, B., Zhang, C., and Liu, W. (2012a). Distribution, Historical Trends and Inventories of Polychlorinated Biphenyls in Sediments from Yangtze River Estuary and Adjacent East China Sea. *Environ. Pollut.* 169, 20–26. doi:10.1016/j.envpol.2012.05.003

Yang, R., Wei, H., Guo, J., and Li, A. (2012b). Emerging Brominated Flame Retardants in the Sediment of the Great Lakes. *Environ. Sci. Technol.* 46 (6), 3119–3126. doi:10.1021/es204141p

Yang, R., Wei, H., Guo, J., McLeod, C., Li, A., and Sturchio, N. C. (2011). Historically and Currently Used Dechloranes in the Sediments of the Great Lakes. *Environ. Sci. Technol.* 45 (12), 5156–5163. doi:10.1021/es201019m

Yhdego, M. (2017). *From a Sanitary Landfill to a Dump Site: Pugu Kinyamwezi Community Curse in Dar Es Salaam, Tanzania*. Dar es Salaam, Tanzania: ERC-Environmental Resources Consultancy. doi:10.13140/RG.2.2.27828.04483

Yuan, B., Brüchert, V., Sobek, A., and de Wit, C. A. (2017). Temporal Trends of C8-C36 Chlorinated Paraffins in Swedish Coastal Sediment Cores Over the Past 80 Years. *Environ. Sci. Technol.* 51 (24), 14199–14208. doi:10.1021/acs.est.7b04523

Zegers, B. N., Lewis, W. E., Booij, K., Smittenberg, R. H., Boer, W., De Boer, J., et al. (2003). Levels of Polybrominated Diphenyl Ether Flame Retardants in

Sediment Cores from Western Europe. *Environ. Sci. Technol.* 37 (17), 3803–3807. doi:10.1021/es034226o

Zeng, L., Chen, R., Zhao, Z., Wang, T., Gao, Y., Li, A., et al. (2013). Spatial Distributions and Deposition Chronology of Short Chain Chlorinated Paraffins in Marine Sediments Across the Chinese Bohai and Yellow Seas. *Environ. Sci. Technol.* 47 (20), 11449–11456. doi:10.1021/es402950q

Zeng, L., Lam, J. C. W., Horii, Y., Li, X., Chen, W., Qiu, J.-W., et al. (2017). Spatial and Temporal Trends of Short- and Medium-Chain Chlorinated Paraffins in Sediments off the Urbanized Coastal Zones in China and Japan: A Comparison Study. *Environ. Pollut.* 224, 357–367. doi:10.1016/j.envpol.2017.02.015

Zeng, L., Wang, T., Wang, P., Liu, Q., Han, S., Yuan, B., et al. (2011). Distribution and Trophic Transfer of Short-Chain Chlorinated Paraffins in an Aquatic Ecosystem Receiving Effluents from a Sewage Treatment Plant. *Environ. Sci. Technol.* 45 (13), 5529–5535. doi:10.1021/es200895b

Zeng, L., Zhao, Z., Li, H., Wang, T., Liu, Q., Xiao, K., et al. (2012). Distribution of Short Chain Chlorinated Paraffins in Marine Sediments of the East China Sea: Influencing Factors, Transport and Implications. *Environ. Sci. Technol.* 46 (18), 9898–9906. doi:10.1021/es302463h

Zennegg, M., Kohler, M., Hartmann, P. C., Sturm, M., Gujer, E., Schmid, P., et al. (2007). The Historical Record of PCB and PCDD/F Deposition at Greifensee, A Lake of the Swiss Plateau, Between 1848 and 1999. *Chemosphere* 67 (9), 1754–1761. doi:10.1016/j.chemosphere.2006.05.115

Zhang, C., Chang, H., Wang, H., Zhu, Y., Zhao, X., He, Y., et al. (2019). Spatial and Temporal Distributions of Short-, Medium-, and Long-Chain Chlorinated Paraffins in Sediment Cores from Nine Lakes in China. *Environ. Sci. Technol.* 53 (16), 9462–9471. doi:10.1021/acs.est.8b07296

Zhang, X.-L., Luo, X.-J., Chen, S.-J., Wu, J.-P., and Mai, B.-X. (2009). Spatial Distribution and Vertical Profile of Polybrominated Diphenyl Ethers, Tetrabromobisphenol A, and Decabromodiphenylethane in River Sediment from an Industrialized Region of South China. *Environ. Pollut.* 157 (6), 1917–1923. doi:10.1016/j.envpol.2009.01.016

Zhang, Z.-W., Sun, Y.-X., Sun, K.-F., Xu, X.-R., Yu, S., Zheng, T.-L., et al. (2015). Brominated Flame Retardants in Mangrove Sediments of the Pearl River Estuary, South China: Spatial Distribution, Temporal Trend and Mass Inventory. *Chemosphere* 123, 26–32. doi:10.1016/j.chemosphere.2014.11.042

Zhu, L. Y., and Hites, R. A. (2005). Brominated Flame Retardants in Sediment Cores from Lakes Michigan and Erie. *Environ. Sci. Technol.* 39 (10), 3488–3494. doi:10.1021/es048240s

Conflict of Interest: The authors declare that the research was conducted in the absence of any commercial or financial relationships that could be construed as a potential conflict of interest.

Supplementary Material

1 Method

1.1 Sample preparation

Procedural blanks (N = 5) and field blanks (N = 3) were analysed along with sediment samples. Field blanks consisted of precleaned (baked overnight at 450℃) sodium sulphate packed in the same way as sediment samples. The containers used were glass jars with aluminium foil lined metal lids. Field blanks were opened briefly on-site during extrusion and sectioning of the sediment cores. Procedural blanks consisted of precleaned sodium sulphate being brought through every step of extraction, clean-up, and analysis in the same manner as samples.

Prior to sample preparation all glassware was baked overnight at 450℃ and rinsed with acetone and n-hexane. High purity grade solvents were used throughout. All components for Accelerated Solvent Extraction (ASE) cells were sonicated twice in acetone (15 min) followed by sonication in n-hexane (15 min). Prior to extraction, sediment samples (4 g wet weight) were dried and homogenized by mortaring with precleaned sodium sulphate until a free-flowing powder was achieved. ASE cells (30 mL) were packed (from bottom to top) with 3 cellulose filters, 5 g precleaned (baked overnight at 550℃) Florisil, cellulose filter, the sample/sodium sulphate mix with 2 g activated copper powder mixed in, ^{13}C labelled internal standards, followed by filter. The following ^{13}C labelled internal standards were used for the different analyte groups:

- ^{13}C labelled PCBs: PCB-28, PCB-52, PCB-101, PCB-105, PCB-114, PCB-118, PCB-123, PCB-153, PCB-138, PCB-167, PCB-157, PCB-180, PCB-189, and PCB-209.
- ^{13}C labelled PBDEs: BDE-28, BDE-47, BDE-99, BDE-153, BDE-183, BDE-197, BDE-206, and BDE-209.
- ^{13}C labelled aBFRs: ATE, PBBZ, HBB, DPTE, EHTBB, BTBPE and DBDPE.
- ^{13}C labelled dechloranes: DP syn and Dec 602.
- ^{13}C labelled CPs: 1,5,5,6,6,10-Hexachlorodecane.

Extraction was performed using ASE (Dionex) with acetone/n-hexane (1:1) and three extraction cycles at 1500 psi and 100℃. Collection vials had a 0.5 cm layer of sodium sulphate added to retain any water from sediments being co-extracted in the process.

Extracted samples were volume reduced to 0.5 mL using a Turbovap system (Zymark), and solvent was changed to n-hexane. Samples were transferred to glass centrifuge tubes and had 2 mL concentrated sulphuric acid added for the removal of potential acid labile matrix interferences. This was repeated by removing the n-hexane phase to a clean centrifuge tube adding new sulphuric acid, until a clear extract was achieved (four repetitions). To remove more polar potential interferences, including break-down products from the sulphuric acid treatment still present in the n-hexane phase, samples were further cleaned using activated silica. 4 g of activated silica (baked overnight at 550℃) was dry packed in a 15 mm internal diameter glass column and topped with a 1 cm layer of sodium sulphate. The column was conditioned with 30 mL diethyl ether/n-hexane (1:9) before the sample was added and eluted by 30 mL diethyl ether/n-hexane (1:9). Solvent was changed to isooctane, and volume reduced to 100 µL using a gentle stream of high purity nitrogen. A recovery standard of 1,2,3,4-Tetrachloronaphthalene was added, before transfer to gas chromatography (GC)-vials.

1.2 Instrumental analysis, quantification, and data analysis

For Chlorinated paraffins (CPs) and dechloranes, the samples were analysed using GC quadrupole time-of-flight high resolution mass spectrometry (MS) (7200B GC/Q-TOF, Agilent, Santa Clara, USA). The GC separation was performed using a two-part column. The analytical section was a 15 m HP-5ms Ultra Inert stationary phase with inner diameter 250 µm, and film thickness 0.25 µm, while the second column was a 1.8 m fused silica column with no stationary phase and an inner diameter of 150 µm for the purpose of restriction. Flow rates were 1.2 mL/min on the first section, and 1.4 mL/min on the second section. A programmed temperature vaporization (PVT) inlet in solvent vent mode was used for the introduction of samples. The PTV program was starting at 60°C, holding for 0.35 min, increasing by 500°C/min to 320°C, holding for 3 minutes, before 10°C/min ramp to 290°C, and holding for 20 min and finally 500°C/min ramp to 320°C. The GC oven temperature program was as follows: initial temperature 55°C, hold time 2 min, 70°C/min ramp to 200°C, hold for 1 min. 10°C/min ramp to 280°C, hold for 1 min, then10°C/min ramp to 310°C and finally 70°C/min ramp to 325°C, hold for 4 min. The Q-TOF was run using an electron capture negative ionization (ECNI) source with methane as a moderating gas. Source temperature was kept at 120°C to minimize fragmentation and optimize for the formation of $[M{-}Cl]^-$ or the $[M{-}HCl]^-$ ion for the Chlorinated Paraffins (CPs) and $[M]^-$ for the Dechloranes. The electron energy was set to 250 electron volts in the source, with an emission current of 12 µA.

For PCBs, PBDEs, and aBFRs, analysis was performed using GC-high resolution MS (AutoSpec, Waters, Manchester, UK). PBDEs and aBFRs were both separated on a Restek 1614, 15 m, 250 µm inner diameter column with 0.1 µm film thickness. PTV was used in solvent vent mode starting at 45°C, holding for 0.55 min, before ramping at 250°C/min to 300°C. The GC oven program was as follows: initial temperature 45°C, hold time 2.5 min, followed by 22°C/min ramp to 220°C, 7°C/min ramp to 280°C, and 40°C/min ramp to 300°C and hold for 6.6 min. PCBs were separated on a HT-8, 50 m, 220 µm inner diameter column with 0.25 µm film thickness. PTV was used in solvent vent mode starting at 48°C, holding for 0.35 min, before ramping at 300°C/min to 285°C and holding for 3 min, and ramping at 300°C/min to 310°C, holding for 20 min. The GC oven program was as follows: initial temperature 45°C, hold time 2.65 min followed by a 70°C/min ramp to 170°C, hold for 0.5 min. Further at 3°C/min ramp to 210°C, hold for 0 min, then ramping by 4°C/min to 285°C and hold for 0.5 min. Finally, ramp 20°C/min to 320°C and hold for 4.7 min. For PBDEs, aBFRs, and PCBs, MS was run in electron impact ionization (EI) mode.

Quantification of CPs was performed using a deconvolution method, as described by Bogdal et al. (2015). Briefly, C_{10} - C_{13} standards with 51%, 55% and 63% Cl (w/w), and single chain length standards of C_{10}, C_{11}, C_{12}, and C_{13} (50% and 65% Cl) were analysed for short chain CPs (SCCPs), and for medium chain CPs (MCCPs), C_{14} - C_{17} standards of 42%, 52%, and 57% Cl, and single chain C_{14} with 52% Cl were analysed, and the resulting congener patterns were used to reconstruct the congener pattern of the sample. This was done using the nnls package in R studio, which applies the Lawson-Hanson algorithm to obtain non-negative least squares estimates for the contribution of individual standards to the sample pattern. An R^2 between sample pattern and reconstructed pattern of 0.5 was deemed acceptable. Separate calibration curves at four concentration levels were prepared for each standard, and quantification of total SCCPs and MCCPs content was done based on each standard by using the non-negative least squares estimate for contribution of each standard to the sample and summarizing contributions from all standards. All sample and standard areas were normalized using ^{13}C labelled internal standard. Areas were also normalized by natural abundance of the measured m/z, enabling extension of the instruments linear range.

Statistical analysis was conducted using R studio, version 4.0.5, and Microsoft Excel. Correlations were calculated using the non-parametric rank-based Spearman procedure as the dataset contains censored values and some non-normal distributions (Helsel, 2011). For correlations with socioeconomic parameters sediment data with estimated age from 1962 to 2019 was used. E-waste data (NBS, 2019) only contained data to 2017, and here we assumed continued linear increase to 2019 for correlation analysis. Differences between CPs congener group profiles in urban sediment, soil, and air (as reported in Nipen et al. (2021)) was assessed using the Wilcoxon rank sum test. Compositional changes with depth (fraction of BDE-209, CPs chlorination degree) were assessed using linear regression.

2 Congener groups

SCCPs and MCCPs congener group profiles in urban air and soils in Nipen et al. (2021) were compared with the sediment congener group profiles. This revealed that congener group profiles in sediment were more chlorinated and were dominated by longer chain lengths than air but had similar chain length composition to the soil (Figure S7 and S8). MCCPs in sediment had significantly ($p < 0.05$) lower chlorination degree compared to soils. This was not seen for SCCPs, a consequence of large variation in chlorination degree of SCCPs in soil. The lower chlorination degree of MCCPs in sediment compared to soil is likely caused by a higher tendency for volatilization of lower chlorinated congener groups from soils compared to sediments (Figure S11).

Chlorination degree of SCCPs (61.5-62.7% w/w) decreased towards the lower sediment layers, while no trends in chlorination degree with depth were found for MCCPs. Similar observations were made for both SCCPs and MCCPs in sediments in China (Chen et al., 2011). For MCCPs, longer chain length dominance was found with depth of sediment (Figure S9). Trends towards longer chain lengths and lower chlorination degree with increasing sediment depth is consistent with studies from China and North America (Tomy et al., 1999; Marvin et al., 2003; Chen et al., 2011; Zeng et al., 2011), although it remains unclear whether this is related to degradation processes or shifts in production.

3 Dechlorane 603

Aldrin and Dieldrin have been used in Tanzania, although temporal information is lacking (NIP, 2005). Dieldrin has also previously been detected in sediments of the (main) Msimbazi river in the Tabata area of Dar es Salaam (Mwevura et al., 2002) and the Dar es Salaam coast (Kishimba et al., 2004). A small subset of the sediment layers was analysed for Aldrin and Dieldrin to assess the role of these pesticides as potential sources for Dec 603. Dieldrin was detected with a similar trend pattern to Dec 603, supporting that the source of Dec 603 is the previous use of this pesticide (Figure S10). However, the relative amounts of Dieldrin and Dec 603 did not support this, as Dec 603 concentrations were approximately four times higher than Dieldrin concentrations. This could however be a consequence of higher persistence in sediment of Dec 603 compared to Dieldrin. Aldrin was not detected in sediment layers. However, Aldrin is known to convert to Dieldrin in the environment (Jorgenson, 2001).

4 Supplementary Tables and Figures

4.1 Supplementary Tables

Table S1: Compounds analysed in sediment core samples and abbreviations used in the main text.

Compound class	**Compound**	**Abbreviation**
PCBs	2,2',5-TriCB	PCB-18
	2,4,4'-TriCB	PCB-28
	2,4',5-TriCB	PCB-31
	2',3,4-TriCB	PCB-33
	3,4,4'-TriCB	PCB-37
	2,2',4,4'-TetCB	PCB-47
	2,2',5,5'-TetCB	PCB-52
	2,3',4,4'-TetCB	PCB-66
	2,4,4',5-TetCB	PCB-74
	2,2',4,4',5-PenCB	PCB-99
	2,2',4,5,5'-PenCB	PCB-101
	2,3,3',4,4'-PenCB	PCB-105
	2,3,4,4',5-PenCB	PCB-114
	2,3',4,4',5-PenCB	PCB-118
	2'3,3',4,5-PenCB	PCB-122
	2',3,4,4',5-PenCB	PCB-123
	2,2',3,3',4,4'-HexCB	PCB-128
	2,2',3,4,4',5'-HexCB	PCB-138
	2,2',3,4,5,5'-HexCB	PCB-141
	2,2',3,4',5',6-HexCB	PCB-149
	2,2',4,4',5,5'-HexCB	PCB-153
	2,3,3',4,4',5-HexCB	PCB-156
	2,3,3',4,4',5'-HexCB	PCB-157
	2,3',4,4',5,5'-HexCB	PCB-167
	2,2',3,3',4,4',5-HepCB	PCB-170
	2,2',3,4,4',5,5'-HepCB	PCB-180
	2,2',3,4,4',5',6-HepCB	PCB-183
	2,2',3,4',5,5',6-HepCB	PCB-187
	2,3,3',4,4',5,5'-HepCB	PCB-189
	2,2',3,3',4,4',5,5'-OctCB	PCB-194
	2,2',3,3',4,4',5,5',6-NonCB	PCB-206
	DecaCB	PCB-209
PBDEs	2,2',4-TriBDE	BDE-17
	2,4,4'-TriBDE	BDE-28
	2,2',4,4'-TetBDE	BDE-47
	2,2',4,5'-TetBDE	BDE-49

	2,3',4,4'-TetBDE	BDE-66
	2,3',4',6-TetBDE	BDE-71
	3,3',4,4'-TetBDE	BDE-77
	2,2',3,4,4'-PenBDE	BDE-85
	2,2',4,4',5-PenBDE	BDE-99
	2,2',4,4',6-PenBDE	BDE-100
	2,3',4,4',6-PenBDE	BDE-119
	3,3',4,4',5-PenBDE	BDE-126
	2,2',3,4,4',5'-HexBDE	BDE-138
	2,2',4,4',5,5'-HexBDE	BDE-153
	2,2',4,4',5,6'-HexBDE	BDE-154
	2,3,3',4,4',5-HexBDE	BDE-156
	2,2',3,4,4',5',6-HepBDE	BDE-183
	2,2',3,4,4',6,6'-HepBDE	BDE-184
	2,3,3',4,4',5',6-HepBDE	BDE-191
	2,2',3,3',4,4',5,6'-OctBDE	BDE-196
	2,2',3,3',4,4',6,6'-OctBDE	BDE-197
	2,2',3,3',5,5',6,6'-OctBDE	BDE-202
	2,2',3,3',4,4',5,5',6-NonBDE	BDE-206
	2,2',3,3',4,4',5,6,6'-NonBDE	BDE-207
	DecaBDE	BDE-209
aBFRs	1,3,5-tribromo-2-(2-propen-yloxy) benzene	ATE
	1,2-dibromo-4-(1,2dibromoethyl) cyclohexane (alfa)	a-TBECH
	1,2-dibromo-4-(1,2dibromoethyl) cyclohexane (beta)	b-TBECH
	1,2-dibromo-4-(1,2dibromoethyl) cyclohexane (gamma/delta)	g/d-TBECH
	2-Bromoallyl-2,4,6-tribromophenyl ether	BATE
	Pentabromotoluene	PBT
	1,2,3,4,5-pentabromo-6-etylbenzene	PBEB
	Pentabromobenzene	PBBZ
	Hexabromobenzene	HBB
	2,3-dibromopropyl 2,4,6-tribromophenyl ether	DPTE
	2-ethylhexyl-2,3,4,5-tetrabromobenzoate	EHTBB
	1,2-bis (2,4,6 tribromophenoxy) ethane	BTBPE
	bis(2-ethylhexyl)-3,4,5,6-tetrabromo-phthalate	TBPH
	decabromodiphenyl ethane	DBDPE
Dechloranes	Dibromoaldrin	DBALD
	Dechlorane 602	Dec 602
	Dechlorane 603	Dec 603
	Dechlorane 604	Dec 604
	Dechlorane 601	Dec 601
	Dechlorane plus syn	DP syn
	Dechlorane plus anti	DP anti
	1,3-Dechlorane Plus mono adduct	1,3-DPMA

	1,5-Dechlorene Plus mono adduct	1,5-DPMA
SCCPs	$C_{10}H_{18}Cl_4$	
	$C_{10}H_{17}Cl_5$	
	$C_{10}H_{16}Cl_6$	
	$C_{10}H_{15}Cl_7$	
	$C_{10}H_{14}Cl_8$	
	$C_{10}H_{13}Cl_9$	
	$C_{10}H_{12}Cl_{10}$	
	$C_{11}H_{20}Cl_4$	
	$C_{11}H_{19}Cl_5$	
	$C_{11}H_{18}Cl_6$	
	$C_{11}H_{17}Cl_7$	
	$C_{11}H_{16}Cl_8$	
	$C_{11}H_{15}Cl_9$	
	$C_{11}H_{14}Cl_{10}$	
	$C_{11}H_{13}Cl_{11}$	
	$C_{11}H_{12}Cl_{12}$	
	$C_{11}H_{11}Cl_{13}$	
	$C_{12}H_{22}Cl_4$	
	$C_{12}H_{21}Cl_5$	
	$C_{12}H_{20}Cl_6$	
	$C_{12}H_{19}Cl_7$	
	$C_{12}H_{18}Cl_8$	
	$C_{12}H_{17}Cl_9$	
	$C_{12}H_{16}Cl_{10}$	
	$C_{12}H_{15}Cl_{11}$	
	$C_{13}H_{24}Cl_4$	
	$C_{13}H_{23}Cl_5$	
	$C_{13}H_{22}Cl_6$	
	$C_{13}H_{21}Cl_7$	
	$C_{13}H_{20}Cl_8$	
	$C_{13}H_{19}Cl_9$	
	$C_{13}H_{18}Cl_{10}$	
	$C_{13}H_{17}Cl_{11}$	
	$C_{13}H_{16}Cl_{12}$	
MCCPs	$C_{14}H_{26}Cl_4$	
	$C_{14}H_{25}Cl_5$	
	$C_{14}H_{24}Cl_6$	
	$C_{14}H_{23}Cl_7$	
	$C_{14}H_{22}Cl_8$	
	$C_{14}H_{21}Cl_9$	
	$C_{14}H_{20}Cl_{10}$	
	$C_{15}H_{27}Cl_4$	

	$C_{15}H_{27}Cl_5$
	$C_{15}H_{26}Cl_6$
	$C_{15}H_{25}Cl_7$
	$C_{15}H_{24}Cl_8$
	$C_{15}H_{23}Cl_9$
	$C_{15}H_{22}Cl_{10}$
	$C_{16}H_{30}Cl_4$
	$C_{16}H_{29}Cl_5$
	$C_{16}H_{28}Cl_6$
	$C_{16}H_{27}Cl_7$
	$C_{16}H_{26}Cl_8$
	$C_{16}H_{25}Cl_9$
	$C_{16}H_{24}Cl_{10}$
	$C_{17}H_{32}Cl_4$
	$C_{17}H_{31}Cl_5$
	$C_{17}H_{30}Cl_6$
	$C_{17}H_{29}Cl_7$
	$C_{17}H_{28}Cl_8$
	$C_{17}H_{27}Cl_9$
	$C_{17}H_{26}Cl_{10}$

Table S2: Average blank concentration (ng/sample) and LOD (ng/g dw) for sediment samples. LOD values in parenthesis are instrument based LODs.

Compound	Average blank	LOD
PCB-18	0.028	0.041
PCB-28	0.048	0.069
PCB-31	0.044	0.060
PCB-33	0.035	0.046
PCB-37	0.019	0.014
PCB-47	0.031	0.034
PCB-52	0.047	0.043
PCB-66	0.036	0.015
PCB-74	0.023	0.011
PCB-99	0.014	0.0060
PCB-101	0.029	0.014
PCB-105	0.011	0.0050
PCB-114	0.0047	0.0035
PCB-118	0.020	0.0081
PCB-122	0.0032	0.0035
PCB-123	0.0043	0.0033
PCB-128	0.0058	0.0042
PCB-138	0.014	0.0073
PCB-141	0.0067	0.0034
PCB-149	0.014	0.0061
PCB-153	0.017	0.0066
PCB-156	0.0041	0.0030
PCB-157	0.0034	0.0029
PCB-167	0.0040	0.0038
PCB-170	0.0049	0.0037
PCB-180	0.0078	0.0055
PCB-183	0.0064	0.0045
PCB-187	0.0056	0.0030
PCB-189	0.0033	0.0045
PCB-194	0.0012	(0.0028)
PCB-206	0.0018	(0.0031)
PCB-209	0.0046	0.0069
BDE-17	0.0030	0.00052
BDE-28	0.0040	0.0029
BDE-47	0.045	0.046
BDE-49	0.0022	0.00087
BDE-66	0.0016	0.00086
BDE-71	0.0022	(0.0012)
BDE-77	ND	(0.0011)

BDE-85	0.0012	0.00037
BDE-99	0.0088	0.0050
BDE-100	0.0033	0.0025
BDE-119	0.00073	0.00024
BDE-126	0.00066	0.00047
BDE-138	ND	(0.0040)
BDE-153	0.0034	0.0020
BDE-154	0.0019	0.00063
BDE-156	ND	(0.0053)
BDE-183	0.0033	0.0010
BDE-184	0.0017	(0.0027)
BDE-191	ND	(0.0048)
BDE-196	ND	(0.0054)
BDE-197	ND	(0.0046)
BDE-202	ND	(0.0072)
BDE-206	0.017	0.0078
BDE-207	0.012	0.0060
BDE-209	0.20	0.19
ATE	0.020	0.0026
a-TBECH	0.044	(0.024)
b-TBECH	0.050	0.022
g/d-TBECH	0.033	0.0011
BATE	0.021	0.017
PBT	0.018	0.013
PBEB	0.018	0.022
PBBZ	0.022	0.015
HBB	0.060	0.027
DPTE	0.013	0.011
EHTBB	0.035	0.0098
BTBPE	0.029	0.011
TBPH	ND	(0.043)
DBDPE	1.7	1.7
DBALD	ND	(0.016)
Dec 602	ND	(0.0041)
Dec 603	ND	(0.0041)
Dec 604	ND	(0.083)
Dec 601	ND	(0.021)
DP syn	ND	(0.0075)
DP anti	ND	(0.011)
1,3-DPMA	ND	(0.020)
1,5-DPMA	ND	(0.040)
SCCPs	46	22
MCCPs	33	22

Table S3: Recovery of internal standards in samples and blanks

Internal standard	**Average**	**Standard deviation**	**Minimum**	**Maximum**
^{13}C PCB-28	58	6	46	75
^{13}C PCB-52	53	4	43	62
^{13}C PCB-101	59	6	48	70
^{13}C PCB-105	59	9	35	73
^{13}C PCB-114	59	9	37	75
^{13}C PCB-118	53	11	34	82
^{13}C PCB-123	58	10	34	75
^{13}C PCB-153	53	9	31	71
^{13}C PCB-138	57	9	33	73
^{13}C PCB-167	56	10	30	75
^{13}C PCB-156	57	9	35	74
^{13}C PCB-157	57	10	33	74
^{13}C PCB-180	51	12	25	73
^{13}C PCB-189	48	13	20	72
^{13}C PCB-209	50	13	24	75
^{13}C BDE-28	47	9	31	63
^{13}C BDE-47	42	10	27	60
^{13}C BDE-99	51	10	32	71
^{13}C BDE-153	51	11	31	75
^{13}C BDE-183	50	9	35	72
^{13}C BDE-197	45	8	32	69
^{13}C BDE-206	29	7	19	54
^{13}C BDE-209	32	8	15	52
^{13}C ATE	46	11	28	64
^{13}C PBBZ	48	11	19	68
^{13}C HBB	38	10	24	61
^{13}C DPTE	45	16	24	83
^{13}C EHTBB	35	11	19	64
^{13}C BTBPE	48	16	18	81
^{13}C DBDPE	38	23	17	96
^{13}C Dec 602	79	15	60	123
^{13}C DP syn	90	21	66	153
^{13}C 1,5,5,6,6,10-Hexachlorodecane	71	18	46	120

Table S4: Measured and certified concentrations (ng/g dw) from PCB analysis of CRM 1944, urban sediments.

Congener	measured	Certified
PCB-18	51.9	51±2.6
PCB-28	85.3	80.8±2.7
PCB-31	76.6	78.7±1.6
PCB-52	76.6	79.4±2
PCB-66	56.6	71.9±4.3
PCB-99	27.3	37.5±2.4
PCB-101	67.9	73.4±2.5
PCB-105	23.0	24.5±1.1
PCB-118	48.8	58±4.3
PCB-128	10.4	8.47±0.28
PCB-138	54.4	62.1±3
PCB-149	48.9	49.7±1.2
PCB-153	61.8	74±2.9
PCB-156	6.33	6.52±0.66
PCB-170	12.8	22.6±1.4
PCB-180	41.7	44.3±1.2
PCB-183	9.76	12.19±0.57
PCB-187	24.1	26.1±1.
PCB-194	10.6	11.2±1.4
PCB-206	9.96	9.21±0.51
PCB-209	6.87	6.81±0.33

Table S5: Measured and certified concentrations (ng/g dw) of PBDEs in CRM 1944, urban sediments.

Congener	measured	certified
BDE-47	1.96	1.72±0.28
BDE-99	1.59	1.98±0.26
BDE-100	0.42	0.447±0.027
BDE-153	4.64	6.44±0.37
BDE-154	1.1	1.06±0.08
BDE-183	25.7	31.8±0.1
BDE-206	5.3	6.2±1
BDE-209	73.9	93.5±4.4

Table S6: Concentrations (ng/g dw) of ∑PCBs and selected congeners, ∑PBDEs and selected congeners, aBFRs, CPs, and dechloranes in sediment layers.

Depth (cm)	**0-1**	**1-2**	**2-3**	**3-4**	**4-5**	**5-6**	**6-7**	**7-8**	**8-9**	**9-10**	**10-11**	**11-12**	**12-13**	**13-14**
Estimated age	2019	2018	2018	2017	2016	2015	2014	2011	2007	2003	1998	1996	1992	1987
PCB-28	0.39	0.27	0.22	0.08	0.10	0.10	0.09	0.13	0.15	0.18	0.12	0.09	<0.07	0.07
PCB-52	0.25	0.19	0.14	0.06	0.08	0.07	0.06	0.07	0.09	0.12	0.11	0.11	0.08	0.07
PCB-118	0.46	0.36	0.29	0.16	0.21	0.23	0.18	0.22	0.27	0.32	0.36	0.33	0.24	0.20
PCB-138	0.69	0.54	0.41	0.28	0.40	0.44	0.36	0.43	0.53	0.63	0.75	0.64	0.45	0.36
PCB-180	0.30	0.23	0.17	0.14	0.19	0.21	0.17	0.24	0.25	0.29	0.38	0.28	0.20	0.14
PCB-206	0.03	0.02	0.02	0.01	0.02	0.02	0.01	0.02	0.02	0.02	0.02	0.02	0.01	0.01
PCB-209	<0.007	0.02	0.01	0.01	0.01	0.01	0.01	<0.007	0.01	0.01	0.01	0.01	0.01	0.01
$\sum_{32}$PCBs	5.8	4.5	3.4	1.9	2.7	2.9	2.3	3.0	3.6	4.46	4.88	4.13	2.81	2.47
BDE-47	1.2	0.79	0.61	0.15	0.19	0.23	0.12	0.16	0.09	0.10	0.10	0.09	0.09	0.05
BDE-99	0.85	0.55	0.43	0.11	0.14	0.15	0.07	0.08	0.05	0.05	0.06	0.05	0.04	0.03
BDE-183	0.68	0.34	0.31	0.09	0.11	0.17	0.05	0.13	0.05	0.04	0.04	0.04	0.02	0.04
BDE-209	30	28	23	4.5	7.1	10	5.3	7.7	4.2	6.41	3.63	2.73	2.73	2.79
$\sum_{25}$PBDE	42	36	29	6.1	9.0	13	6.6	9.7	5.3	7.32	4.56	3.45	3.32	3.44
BTBPE	1.1	0.51	1.0	0.11	0.51	0.36	0.11	0.14	0.06	0.04	0.06	0.02	0.02	0.03
TBPH	5.0	2.0	1.5	0.54	1.4	1.6	0.95	1.3	0.64	0.29	0.28	<0.11	<0.11	<0.18
DBDPE	57	39	51	26	6.6	3.0	2.1	<1.7	<1.7	<1.7	<1.7	<1.7	<1.7	<1.7
DP	8.4	5.7	4.9	1.5	2.7	4.3	2.3	3.8	1.7	0.97	1.14	0.68	0.83	0.76
Dec 602	0.07	0.05	0.04	0.04	0.06	0.04	0.07	0.03	0.03	0.03	0.04	0.04	0.03	0.03
Dec 603	0.24	0.23	0.18	0.68	0.68	0.43	0.61	0.26	0.23	0.23	0.39	0.35	0.42	0.50
SCCP	1 400	660	420	93	85	<22	<22	<22	<22	<22	<22	<22	<22	<22
MCCP	6 100	3 700	2 500	430	440	280	250	160	98	80	120	71	<22	54

Table S6 Continued: Concentrations (ng/g dw) of ∑PCBs and selected congeners, ∑PBDEs and selected congeners, aBFRs, CPs, and dechloranes in sediment layers.

Depth (cm)	**14-15**	**15-17**	**17-19**	**19-21**	**21-23**	**23-25**	**25-27**	**27-29**	**29-31**	**31-33**	**33-35**	**35-37**	**37-39**
Estimated age	1982	1975	1968	1962	pre-1962	pre-1962	pre-1962	pre-1962	pre-1962	pre-1962	pre-1962	pre-1962	pre-1962
PCB-28	<0.07	<0.07	<0.07	<0.07	<0.07	<0.07	<0.07	<0.07	<0.07	<0.07	<0.07	<0.07	<0.07
PCB-52	0.09	0.09	0.09	0.07	0.06	0.09	0.07	<0.04	<0.04	<0.04	<0.04	<0.04	<0.04
PCB-118	0.25	0.36	0.19	0.15	0.12	0.18	0.12	0.05	0.03	0.02	0.02	0.02	0.02
PCB-138	0.36	0.60	0.43	0.38	0.33	0.55	0.35	0.16	0.08	0.04	0.03	0.04	0.03
PCB-180	0.12	0.17	0.22	0.22	0.20	0.36	0.22	0.10	0.05	0.02	0.02	0.02	0.01
PCB-206	0.01	0.01	0.01	0.009	0.01	0.01	0.008	0.006	0.005	<0.002	<0.003	0.003	0.002
PCB-209	0.01	0.01	<0.007	<0.007	<0.007	<0.007	<0.007	<0.007	<0.007	<0.007	<0.007	<0.007	<0.007
∑32PCBs	2.5	3.5	2.8	2.4	2.1	3.4	2.1	0.94	0.47	0.25	0.23	0.23	0.19
BDE-47	0.06	<0.05	<0.05	<0.05	<0.05	<0.05	<0.05	<0.05	<0.05	<0.05	<0.05	<0.05	<0.05
BDE-99	0.04	0.02	0.02	0.01	0.005	0.01	0.01	0.01	<0.0008	<0.0008	<0.0008	<0.0008	<0.0008
BDE-183	0.01	<0.001	0.009	0.004	0.002	<0.001	<0.001	0.009	<0.001	<0.001	<0.001	<0.001	<0.001
BDE-209	2.9	2.5	1.0	0.48	0.34	0.75	0.71	<0.19	<0.19	<0.19	<0.19	<0.19	<0.19
∑25PBDE	3.4	2.8	1.2	0.59	0.39	0.83	0.87	0.07	0.005	0.002	0.003	0.003	ND
BTBPE	0.02	<0.01	0.004	<0.01	<0.01	0.19	<0.01	<0.01	<0.01	<0.01	<0.01	<0.01	<0.01
TBPH	<0.11	<0.14	<0.08	<0.11	<0.09	<0.08	<0.06	<0.06	<0.06	<0.04	<0.04	<0.03	<0.03
DBDPE	<1.7	<1.7	<1.7	<1.7	<1.7	<1.7	<1.7	<1.7	<1.7	<1.7	<1.7	<1.7	<1.7
DP	0.96	0.97	0.93	0.67	0.18	1.1	0.95	0.25	0.07	<0.02	<0.02	<0.02	<0.02
Dec 602	0.16	0.04	0.11	0.10	0.24	0.27	0.14	0.17	0.16	0.01	<0.006	<0.008	<0.01
Dec 603	0.50	0.46	1.2	1.3	2.0	2.1	1.7	1.3	4.0	0.57	0.51	0.56	0.56
SCCP	<22	<22	<22	<22	<22	<22	<22	<22	<22	<22	<22	<22	<22
MCCP	66	53	<22	<22	<22	<22	<22	<22	<22	<22	<22	<22	<22

ND: No PBDE congeners detected

Table S7: Spearman rank correlations for selected congeners, legacy POPs, and CECs concentrations in sediments.

	PCB-28	**PCB-52**	**PCB-118**	**PCB-138**	**PCB-180**	**PCB-206**	**PCB-209**	**$\sum_{32}$PCBs**	**BDE-47**	**BDE-99**	**BDE-183**	**BDE-209**	**$\sum_{25}$PBDE**	**BTBPE**	**TBPH**	**DBDPE**	**DP**	**Dec 602**	**Dec 603**	**SCCP**	**MCCP**
PCB-52	0.58^{**}	1.00																			
PCB-118	0.69^{***}	0.87^{***}	1.00																		
PCB-138	0.59^{**}	0.88^{***}	0.90^{***}	1.00																	
PCB-180	0.54^{**}	0.74^{***}	0.66^{***}	0.87^{***}	1.00																
PCB-206	0.89^{***}	0.77^{***}	0.87^{***}	0.82^{***}	0.72^{***}	1.00															
PCB-209	0.60^{***}	0.66^{***}	0.78^{***}	0.60^{***}	0.30	0.65^{***}	1.00														
$\sum_{32}$PCBs	0.72^{***}	0.91^{***}	0.94^{***}	0.97^{***}	0.84^{***}	0.89^{***}	0.66^{***}	1.00													
BDE-47	0.88^{***}	0.52^{**}	0.66^{***}	0.50^{**}	0.42^{*}	0.83^{***}	0.64^{***}	0.61^{***}	1.00												
BDE-99	0.87^{***}	0.65^{***}	0.78^{***}	0.64^{***}	0.53^{**}	0.92^{***}	0.66^{***}	0.73^{***}	0.95^{***}	1.00											
BDE-183	0.88^{***}	0.50^{**}	0.64^{***}	0.49^{**}	0.42^{*}	0.83^{***}	0.59^{**}	0.60^{***}	0.93^{***}	0.94^{***}	1.00										
BDE-209	0.88^{***}	0.66^{***}	0.78^{***}	0.64^{***}	0.54^{**}	0.92^{***}	0.65^{***}	0.74^{***}	0.94^{***}	0.98^{***}	0.92^{***}	1.00									
$\sum_{25}$PBDE	0.90^{***}	0.66^{***}	0.79^{***}	0.66^{***}	0.56^{**}	0.94^{***}	0.65^{***}	0.76^{***}	0.94^{***}	0.98^{***}	0.93^{***}	0.99^{***}	1.00								
BTBPE	0.81^{***}	0.57^{**}	0.64^{***}	0.57^{**}	0.48^{*}	0.84^{***}	0.56^{**}	0.66^{***}	0.87^{***}	0.89^{***}	0.83^{***}	0.89^{***}	0.88^{***}	1.00							
TBPH	0.88^{***}	0.59^{**}	0.77^{***}	0.63^{***}	0.52^{**}	0.92^{***}	0.64^{***}	0.73^{***}	0.90^{***}	0.97^{***}	0.93^{***}	0.96^{***}	0.97^{***}	0.88^{***}	1.00						
DBDPE	0.64^{***}	0.30	0.35	0.18	0.09	0.60^{**}	0.35	0.29	0.77^{***}	0.76^{***}	0.75^{***}	0.72^{***}	0.72^{***}	0.74^{***}	0.73^{***}	1.00					
DP	0.80^{***}	0.63^{***}	0.72^{***}	0.64^{***}	0.58^{**}	0.91^{***}	0.51^{**}	0.73^{***}	0.86^{***}	0.93^{***}	0.83^{***}	0.94^{***}	0.94^{***}	0.89^{***}	0.92^{***}	0.72^{***}	1.00				
Dec 602	-0.19	0.20	0.05	0.14	0.30	0.05	-0.18	0.10	-0.08	0.03	-0.03	-0.02	0.02	0.00	0.02	0.07	0.15	1.00			
Dec 603	-0.75^{***}	-0.57^{**}	-0.73^{***}	-0.56^{**}	-0.32	-0.67^{***}	-0.69^{***}	-0.67^{***}	-0.64^{***}	-0.62^{***}	-0.61^{***}	-0.66^{***}	-0.64^{***}	-0.53^{**}	-0.61^{***}	-0.28	-0.50^{**}	0.55^{**}	1.00		
SCCP	0.59^{**}	0.42^{*}	0.36	0.19	0.11	0.50^{**}	0.33	0.32	0.67^{***}	0.66^{***}	0.64^{***}	0.61^{***}	0.61^{***}	0.65^{***}	0.61^{***}	0.88^{***}	0.61^{***}	0.08	-0.29	1.00	
MCCP	0.90^{***}	0.52^{**}	0.69^{***}	0.50^{**}	0.37	0.86^{***}	0.63^{***}	0.62^{***}	0.93^{***}	0.94^{***}	0.91^{***}	0.93^{***}	0.93^{***}	0.87^{***}	0.93^{***}	0.81^{***}	0.88^{***}	-0.08	-0.63^{***}	0.71^{***}	1.00
OM	0.67^{***}	0.71^{***}	0.71^{***}	0.78^{***}	0.80^{***}	0.79^{***}	0.47^{*}	0.80^{***}	0.68^{***}	0.78^{***}	0.67^{***}	0.75^{***}	0.74^{***}	0.78^{***}	0.73^{***}	0.43^{*}	0.77^{***}	0.20	-0.41^{*}	0.47^{*}	0.65^{***}

$^{*}p < 0.05$, $^{**}p < 0.01$, $^{***}p < 0.001$

Table S8: Spearman rank correlations between development factors and POPs and CECs concentrations in sediment. Based on data from 1962 to 2019.

	GDP	**e-waste**	**Mobile Subscr.**	**Broadb. subscr.**	**Population Dar**
GDP	1.00				
e-waste	0.97^{***}	1.00			
Mobile subscr.	0.97^{***}	0.98^{***}	1.00		
Broadb. subscr.	0.94^{***}	0.96^{***}	0.94^{***}	1.00	
Population Dar	1.00^{***}	0.97^{***}	0.97^{***}	0.94^{***}	1.00
PCB-28	0.80^{***}	0.78^{***}	0.82^{***}	0.66^{**}	0.80^{***}
PCB-52	0.16	0.13	0.17	0.06	0.16
PCB-118	0.22	0.15	0.21	0.07	0.22
PCB-138	0.05	0.00	0.09	-0.12	0.05
PCB-180	0.11	0.10	0.18	-0.04	0.11
PCB-206	0.76^{***}	0.74^{***}	0.81^{***}	0.63^{**}	0.76^{***}
PCB-209	0.09	-0.04	0.00	-0.11	0.09
$\sum_{32}$**PCBs**	0.28	0.23	0.31	0.11	0.28
BDE-47	0.95^{***}	0.92^{***}	0.94^{***}	0.87^{***}	0.95^{***}
BDE-99	0.98^{***}	0.95^{***}	0.97^{***}	0.90^{***}	0.98^{***}
BDE-183	0.95^{***}	0.91^{***}	0.94^{***}	0.91^{***}	0.95^{***}
BDE-209	0.93^{***}	0.92^{***}	0.93^{***}	0.85^{***}	0.93^{***}
$\sum_{25}$**PBDE**	0.94^{***}	0.92^{***}	0.95^{***}	0.85^{***}	0.94^{***}
BTBPE	0.96^{***}	0.95^{***}	0.95^{***}	0.92^{***}	0.96^{***}
TBPH	0.93^{***}	0.93^{***}	0.95^{***}	0.89^{***}	0.93^{***}
DBDPE	0.88^{***}	0.91^{***}	0.89^{***}	0.94^{***}	0.88^{***}
DP	0.89^{***}	0.93^{***}	0.92^{***}	0.89^{***}	0.89^{***}
Dec 602	-0.10	0.00	-0.01	0.08	-0.10
Dec 603	-0.47	-0.38	-0.44	-0.27	-0.47
SCCP	0.79^{***}	0.81^{***}	0.76^{***}	0.84^{***}	0.79^{***}
MCCP	0.97^{***}	0.96^{***}	0.97^{***}	0.92^{***}	0.97^{***}

$^{*}p < 0.05$, $^{**}p < 0.01$, $^{***}p < 0.001$

Table S9: Spearman rank correlations between rainfall and legacy POPs and CECs during 1983-2018 and 2010-2018.

	rain (1983-2018)	**rain (2010-2018)**
PCB-28	0.14	-0.02
PCB-52	0.43	0.38
PCB-118	0.48	0.05
PCB-138	0.45	-0.20
PCB-180	0.35	-0.61
PCB-206	0.11	-0.04
PCB-209	0.44	0.59
$\sum_{32}$PCBs	0.43	-0.02
BDE-47	0.15	0.34
BDE-99	0.16	0.56
BDE-183	0.00	0.23
BDE-209	0.07	0.05
$\sum_{25}$PBDE	0.07	0.05
BTBPE	0.08	0.38
TBPH	-0.24	0.07
DBDPE	0.26	0.88^{**}
DP	-0.22	0.05
Dec 602	0.17	0.18
Dec 603	0.02	0.09
SCCP	0.20	0.84^{*}
MCCP	0.18	0.77^{*}

*$p < 0.05$, **$p < 0.01$, ***$p < 0.001$

4.2 Supplementary Figures

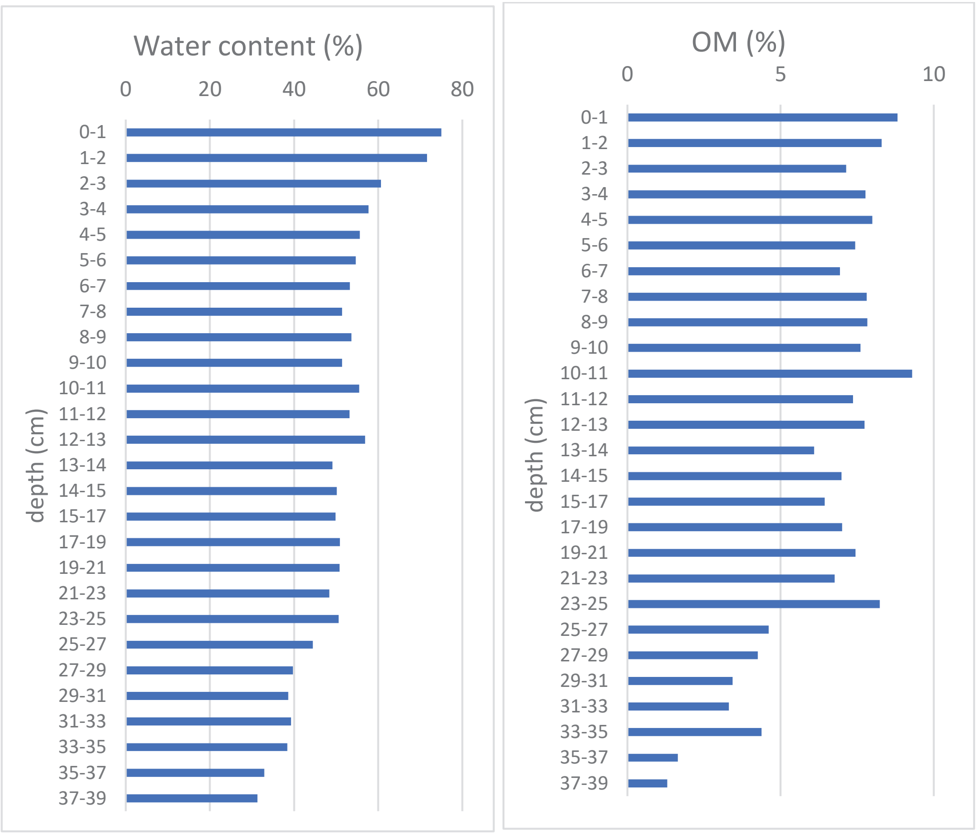

Figure S1: Water content and organic matter content of sediment layers.

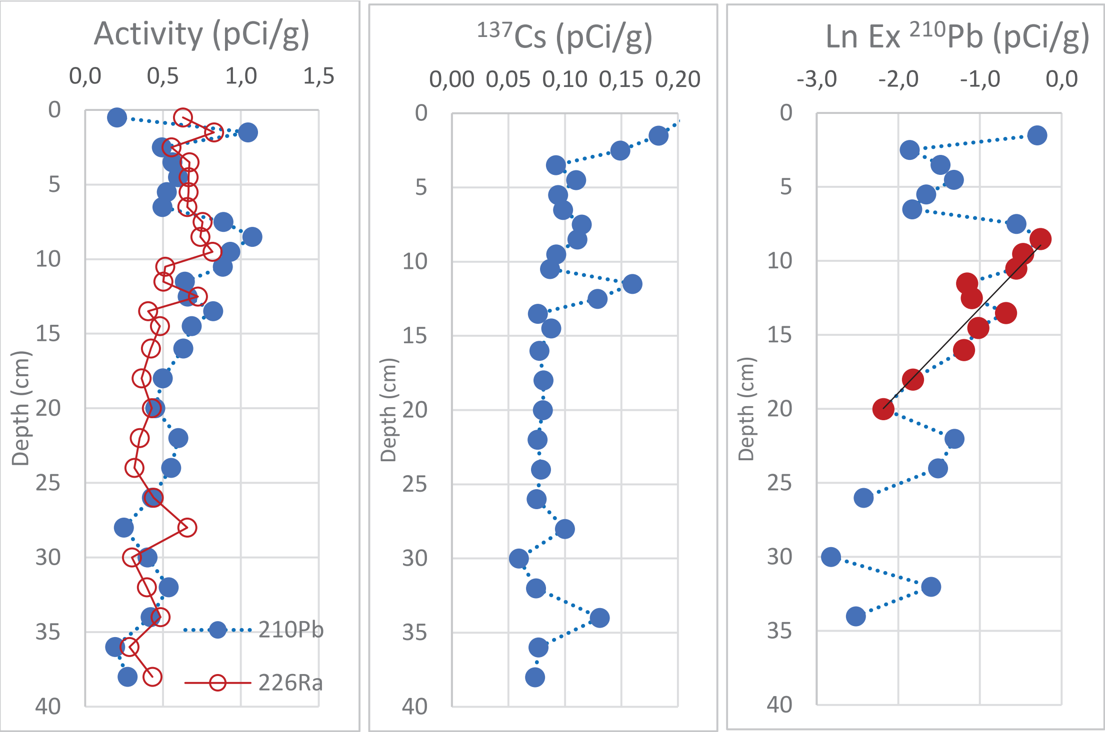

Figure S2: Activity of ^{210}Pb and ^{226}Ra (left), ^{137}Cs (middle), and excess ^{210}Pb (right) at different depts in the sediment core.

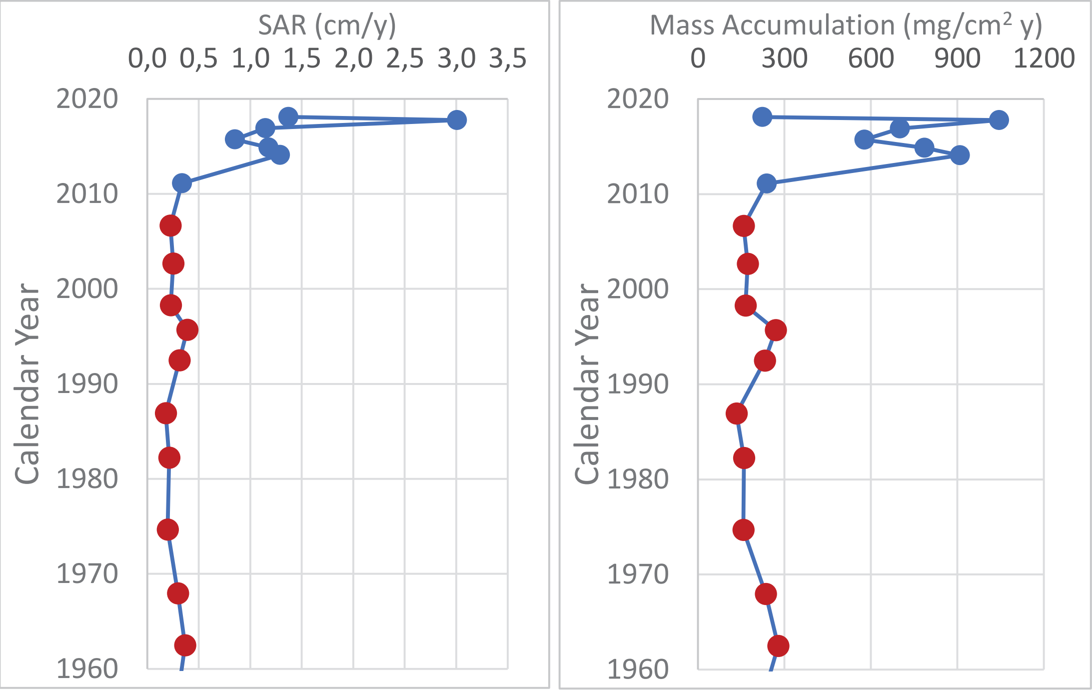

Figure S3: Sediment accumulation rate and mass accumulation in dated section of the sediment core.

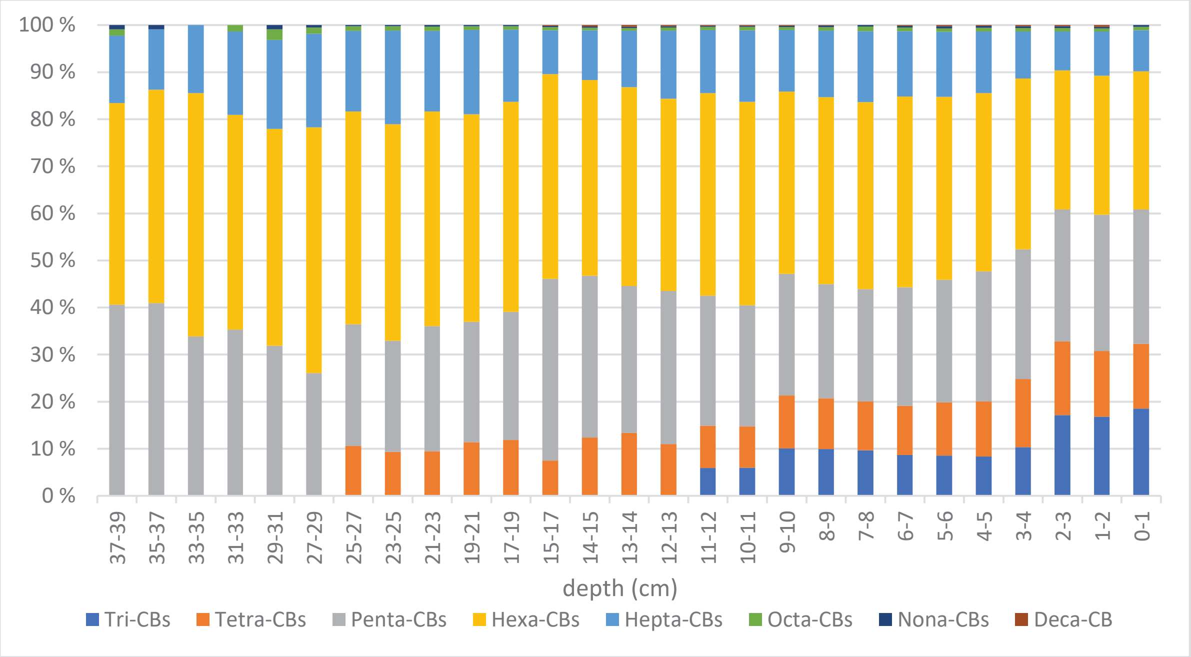

Figure S4: Distribution of PCBs homologues at different sediment depths.

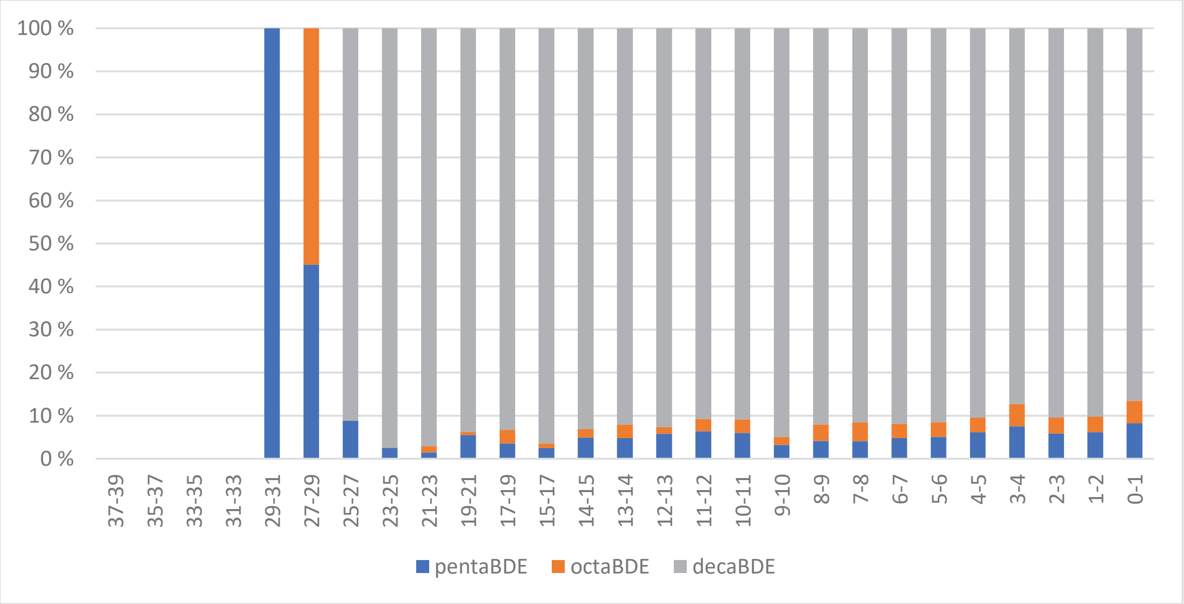

Figure S5: Distribution of PBDEs at different sediment depths. PentaBDE sum of BDE-47, BDE-99, BDE-100, BDE-153, and BDE-154. OctaBDE sum of BDE-183, BDE-196, and BDE-197. DecaBDE equal to BDE-209.

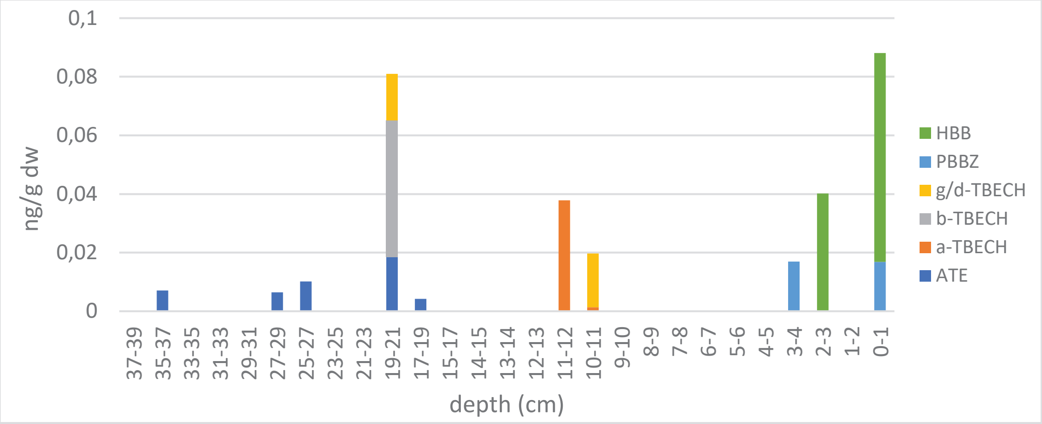

Figure S6: Concentrations of the aBFRs detected in sediments but not discussed in main text.

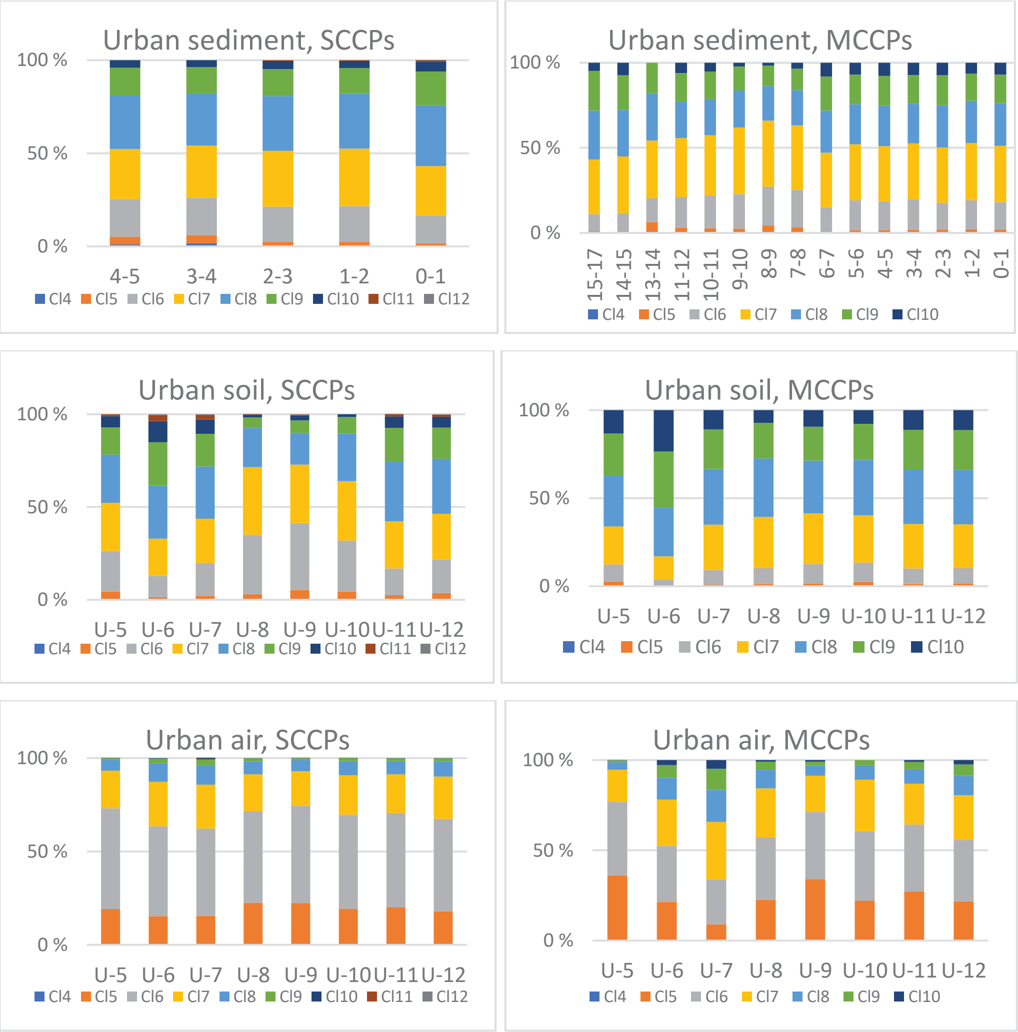

Figure S7: Distribution of chlorination degree in sediment, soil, and air samples from Dar es Salaam. For location references for soil and air see Nipen et al. (2021)).

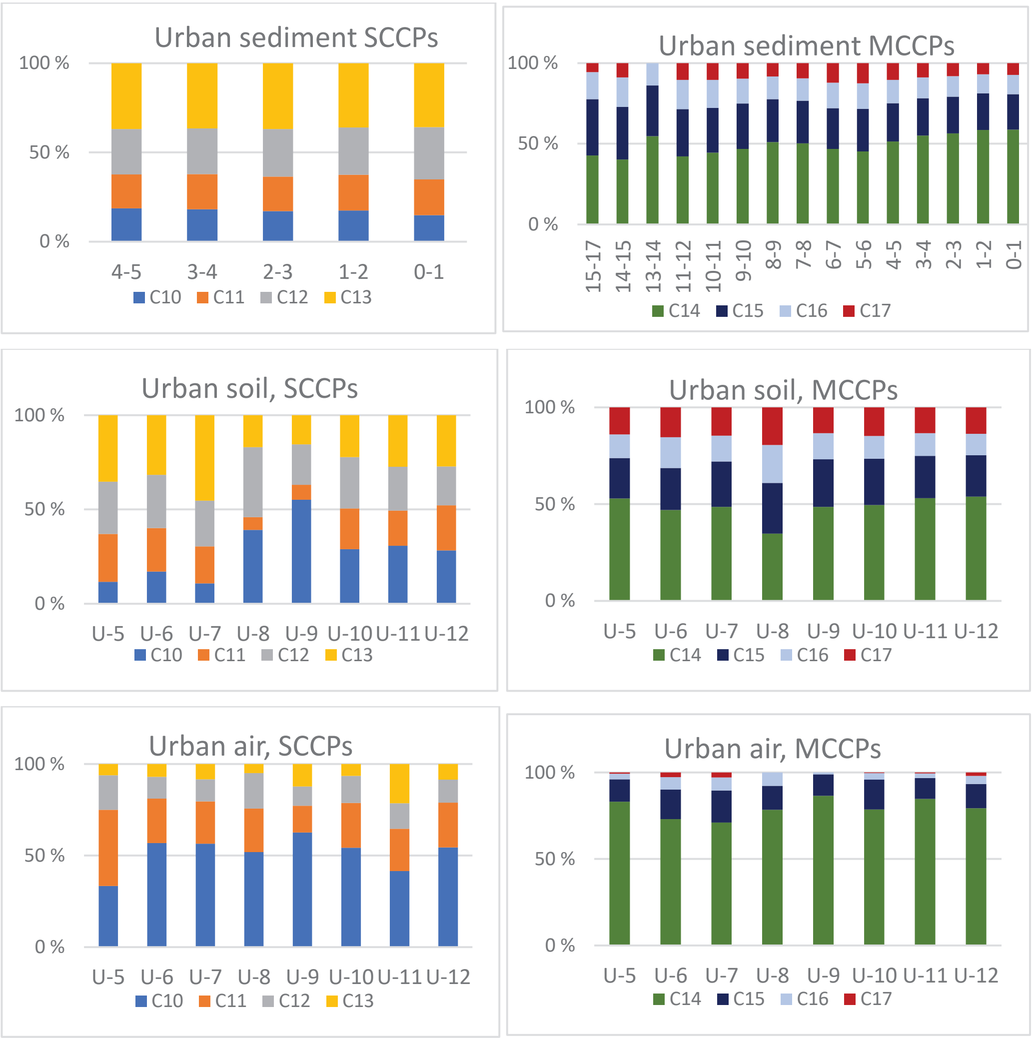

Figure S8: Distribution of chain length in urban sediments, urban soil, and urban air in Dar es Salaam. For location references for soil and air see Nipen et al. (2021))

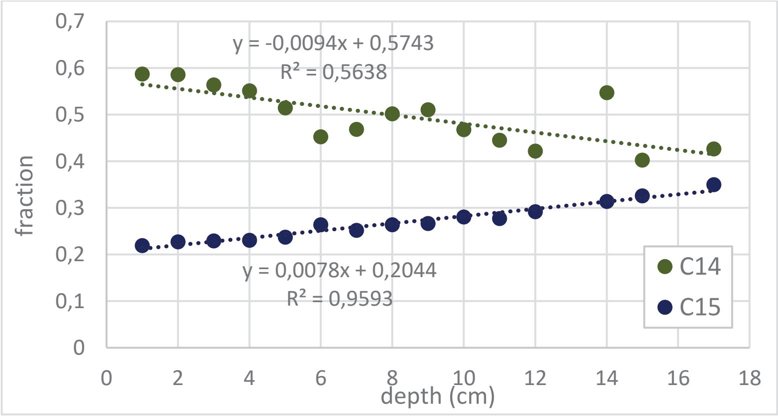

Figure S9: C_{14} and C_{15} MCCPs versus sediment depth.

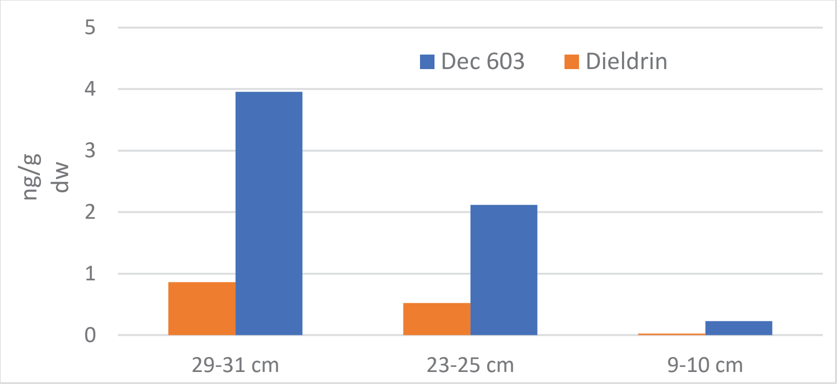

Figure S10: Concentration of Dec 603 and Dieldrin in selected sediment layers.

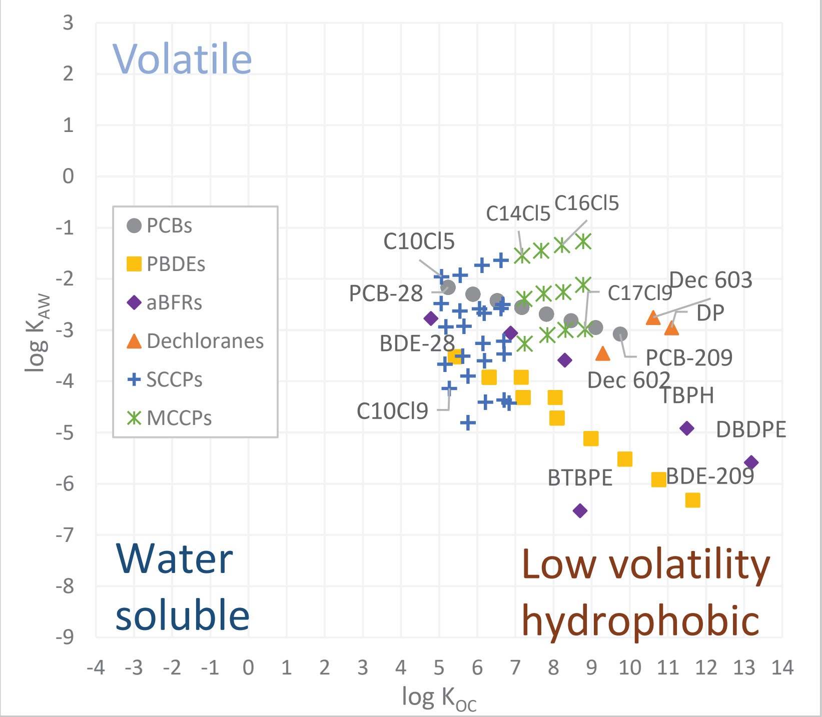

Figure S11: Chemical space plot showing PCBs, PBDEs, aBFRs, Dechloranes and CPs plotted according to their log K_{OC} (water/organic carbon) and log K_{AW} (air/water) distribution coefficients.

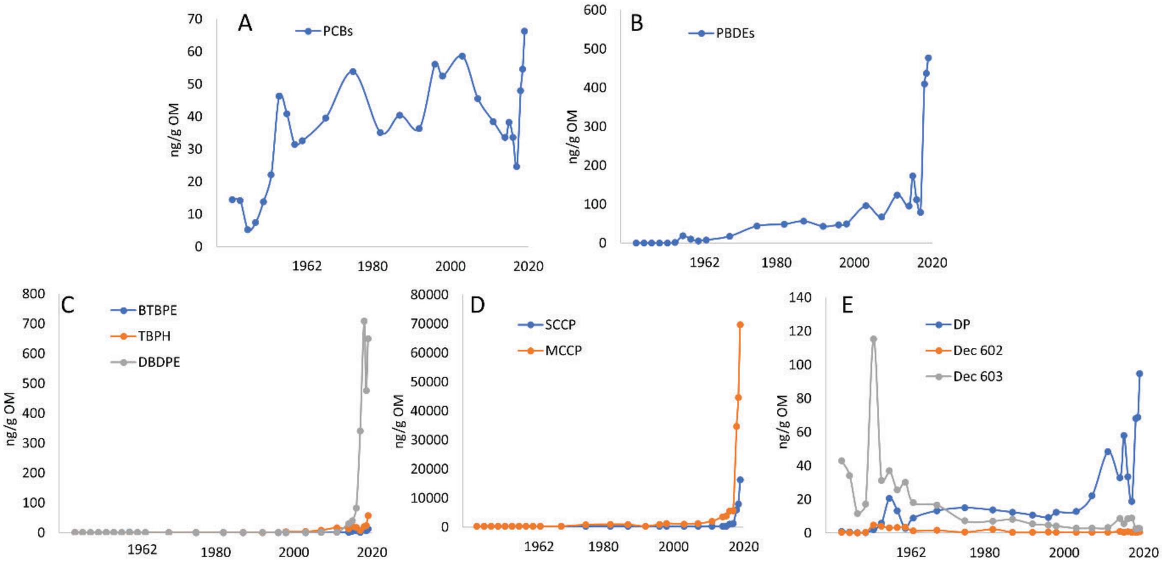

Figure S12: A & B: Organic matter normalized concentration of $\sum_{32}$PCBs and $\sum_{25}$PBDEs, respectively, in sediments layers dated from before 1962 to 2019. C, D, & E: Organic matter normalized concentration of aBFRs, CPs, and dechloranes, respectively, in sediments layers dated from before 1962 to 2019.

5 References

Bogdal, C., Alsberg, T., Diefenbacher, P.S., MacLeod, M., and Berger, U. (2015). Fast quantification of chlorinated paraffins in environmental samples by direct injection high-resolution mass spectrometry with pattern deconvolution. *Analytical chemistry* 87(5)**,** 2852-2860.

Chen, M.-Y., Luo, X.-J., Zhang, X.-L., He, M.-J., Chen, S.-J., and Mai, B.-X. (2011). Chlorinated paraffins in sediments from the Pearl River Delta, South China: spatial and temporal distributions and implication for processes. *Environmental science & technology* 45(23)**,** 9936-9943.

Helsel, D.R. (2011). *Statistics for censored environmental data using Minitab and R.* John Wiley & Sons.

Jorgenson, J.L. (2001). Aldrin and dieldrin: a review of research on their production, environmental deposition and fate, bioaccumulation, toxicology, and epidemiology in the United States. *Environmental health perspectives* 109(suppl 1)**,** 113-139.

Kishimba, M., Henry, L., Mwevura, H., Mmochi, A.J., Mihale, M., and Hellar, H. (2004). The status of pesticide pollution in Tanzania. *Talanta* 64(1)**,** 48-53.

Marvin, C., Painter, S., Tomy, G., Stern, G., Braekevelt, E., and Muir, D. (2003). Spatial and temporal trends in short-chain chlorinated paraffins in Lake Ontario sediments. *Environmental science & technology* 37(20)**,** 4561-4568.

Mwevura, H., Othman, O.C., and Mhehe, G.L. (2002). Organochlorine pesticide residues in sediments and biota from the coastal area of Dar es Salaam city, Tanzania. *Marine Pollution Bulletin* 45(1-12)**,** 262-267.

NBS (2019). "National E-Waste Statistics Report", (ed.) V.S. National Bureau of Statistics and United Nations University. National Bureau Statistics, Dodoma, Tanzania, United Nations University, ViE – SCYCLE, Bonn, Germany).

NIP (2005). "National Implementation Plan (NIP) for the Stocholm Convention on Persistent Organic Pollutants", (http://chm.pops.int/Implementation/NIPs/NIPTransmission/tabid/253/Default.aspx).

Nipen, M., Vogt, R.D., Bohlin-Nizzetto, P., Borgå, K., Mwakalapa, E.B., Borgen, A.R., et al. (2021). Spatial trends of chlorinated paraffins and dechloranes in air and soil in a tropical urban, suburban, and rural environment. *Environmental Pollution***,** 118298.

Tomy, G., Stern, G., Lockhart, W., and Muir, D. (1999). Occurrence of C10− C13 polychlorinated n-alkanes in Canadian midlatitude and arctic lake sediments. *Environmental science & technology* 33(17)**,** 2858-2863.

Zeng, L., Wang, T., Wang, P., Liu, Q., Han, S., Yuan, B., et al. (2011). Distribution and trophic transfer of short-chain chlorinated paraffins in an aquatic ecosystem receiving effluents from a sewage treatment plant. *Environmental science & technology* 45(13)**,** 5529-5535.

Paper III

Mercury in air and soil on an urban-rural transect in East Africa

Maja Nipen[a,b*], Susanne Jøntvedt Jørgensen[a], Pernilla Bohlin-Nizzetto[b], Katrine Borgå[c], Knut Breivik[a,b], Aviti John Mmochi[d], Eliezer Brown Mwakalapa[e], M. Isabel Quant[f], Martin Schlabach[b], Rolf David Vogt[g], Frank Wania[f]

[a]Centre for Biogeochemistry in the Anthropocene, Department of Chemistry, University of Oslo, P.O. Box 1033, 0315 Oslo, Norway, [b]NILU-Norwegian Institute for Air Research, P.O. Box 100, 2027 Kjeller, Norway, [c]Aquatic Biology and toxicology and Centre of Biogeochemistry in the Anthropocene, Department of Biosciences, University of Oslo, P.O. Box 1066, 0316 Oslo, Norway, [d]Institute for Marine Sciences, University of Dar es Salaam, Zanzibar, Tanzania, [e]Department of Natural Sciences, Mbeya University of Science and Technology, Mbeya, Tanzania, [f]Department of Physical and Environmental Sciences, University of Toronto Scarborough, 1265 Military Trail, ON MIC 1A4 Toronto, Canada, [g]Norwegian Institute for Water Research, 0579 Oslo, Norway.

* Corresponding author. Centre for Biogeochemistry in the Anthropocene, Department of Chemistry, University of Oslo, P.O. Box 1033, 0315 Oslo, Norway.

Email address: majanip@kjemi.uio.no; mni@nilu.no

Abstract

There are large knowledge gaps concerning concentrations, sources, emissions, and spatial trends of mercury (Hg) in the atmosphere in developing regions of the Southern Hemisphere, particularly in urban areas. Filling these gaps is prerequisite for assessing the effectiveness of international regulation and for enabling a better understanding of the global transport of Hg in the environment. Here we use a passive sampling technique to study the spatial distribution of gaseous elemental Hg (Hg(0), GEM) and assess emissions sources in and around Dar es Salaam, Tanzania`s largest city. Included in the study were the city’s main municipal waste dumpsite and an e-waste processing facility as potential sources for GEM. To complement the GEM data, and for a better overview of the Hg contamination status of Dar es Salaam, soil samples were collected from the same locations where passive air samplers were deployed and analysed for total Hg. Overall, GEM concentrations ranged between <0.86 and 5.34 ng/m^3, indicating significant local sources within the urban area. The municipal waste dumpsite and e-waste site had GEM concentrations elevated above background, at 2.41 and 1.77 ng/m^3, respectively. Hg concentrations in soil in the region (range 0.0067 to 0,098 mg/kg) were low compared to other urban areas and were not correlated with atmospheric GEM concentrations. This study demonstrates that GEM is a significant environmental issue in the urban region of Dar es Salaam. Further studies from urban areas in the Global South are needed to better identify sources for GEM.

1 Introduction

Harmful effects of mercury (Hg) on human health and ecosystems have been thoroughly documented and have resulted in national, regional, and international regulation e.g., in the form of the Minamata Convention.[1] This has led to declining Hg emissions to the environment in Europe and North America.[2] On the global scale however, these declines are being offset by increased emissions in Asia and Africa.[2] These temporal and spatial trends in Hg emissions are reflected in atmospheric Hg concentrations, where North America and Europe have seen declines.[2, 3] On the other hand, Hg concentrations at Cape Point in South Africa show signs of increasing concentrations during recent years.[4, 5]

Primary sources of Hg to the atmosphere include natural processes (i.e., rock weathering and volcanism), though these emissions are exceeded by anthropogenic emissions.[6] Major anthropogenic sources for primary Hg emissions include fossil fuel combustion, artisanal and small-scale gold mining (ASGM), metal smelting, cement production, waste incineration, processing of e-waste, and burning of biomass.[7-11] Most of these activities are conducted within urban areas, which are thus important source regions for atmospheric Hg. Hg also has secondary sources, in the form of re-emissions of legacy Hg from contaminated surface reservoirs.[12]

Hg in the form of gaseous elemental Hg (Hg(0), GEM) is globally distributed through atmospheric transport.[12, 13] Environmental monitoring of air is thus vital to assess the effectiveness of regulation. Monitoring of GEM has generally been conducted using active sampling techniques providing data on long-term temporal trends at a limited number of sites.[14, 15] Spatial coverage is however also of importance to better identify the sources, and assess emission levels, as well as the biogeochemical mobility and transport processes, governing the GEM concentrations, particularly in urban environments.[16] However, the practical feasibility to concurrently deploy active sampling instruments at multiple locations is limited, due to their high cost, requirements for trained personnel, electricity, and compressed carrier gases. Studies using mobile instruments have been conducted,[17] but it is difficult to attribute concentration variations specifically to spatial or temporal factors. Passive air samplers (PAS) offer a low-cost alternative. PAS are easy to use, and can be deployed simultaneously at multiple locations, thereby allowing for the determination of both spatial and temporal trends, including in remote and developing regions.[18-21] A recent comparison determined the PAS developed and tested on a global scale by McLagan et al.[22, 23] to be the most accurate and precise PAS for GEM at the present time.[24]

Besides the atmosphere, soil is also an important environmental compartment for Hg, as it represents the largest Hg reservoir.[25] On a large scale, the terrestrial environment acts as a sink for Hg in the Southern Hemisphere.[26] Hg is deposited from the atmosphere to soil by oxidation of GEM to Hg(II), followed by wet and dry deposition, or by plant uptake of GEM followed by oxidation to Hg(II) in the leaf interior and deposition through litterfall.[12, 25, 27] The soils' ability to retain Hg is dependent on soil properties and climate.[25, 28] Hg emissions from soil to the atmosphere generally occur in the form of GEM, and are a result of e.g., photoreduction of Hg(II).[29-31]

Most studies on GEM are conducted in the Northern Hemisphere. Data on spatial and temporal trends of GEM in the Southern Hemisphere, including Sub-Saharan Africa, therefore remain limited.[13, 14] The Global Mercury Observation System (GMOS), which was established in 2010 to provide global monitoring data, reflects this. This monitoring network comprises 40 atmospheric monitoring stations,[14] though includes only six stations in the Southern Hemisphere and only one on the African continent (Cape Point, South Africa).[14] Most data on GEM from Sub-Saharan Africa are thus derived from this one location in South Africa, in addition to some studies from ASGM communities in Ghana and Burkina Faso.[11, 32, 33] Consequently, there are large knowledge gaps regarding GEM levels and emissions in sub-Saharan Africa.

Socioeconomic factors are known to affect anthropogenic sources and emissions, leading to potential differences between the industrialised Northern Hemisphere and developing regions in sub-Saharan Africa.[34] In addition, differences in land/ocean ratio, vegetation coverage, and climate may furthermore affect physical- and biogeochemical processes governing mobility, transport, and sinks of Hg compared to the Northern Hemisphere.[26] The gap in GEM data from sub-Saharan Africa is therefore important to fill in order to assess the effectiveness of current and future regulation, and to gain more complete insight into the global cycling of Hg. The greater Dar es Salaam area, Tanzania, has more than six million inhabitants and a tropical climate. As a consequence of its rapidly growing economy, population, and consumption, the region suffers from insufficient systems for handling waste and e-waste.[35-37] In this study, areas in and around Dar es Salaam were therefore chosen as study region.

The main objective of this study is thus to characterize spatial trends of GEM and identify potential emission sources in an urban area in sub-Saharan Africa using the PAS by McLagan et al.[22] Total Hg content in soil is also reported to provide an extended image of urban Hg contamination, and thus complement the understanding of the spatial trends of atmospheric GEM. This study represents the first documentation of spatial trends of GEM in air across an urban area in the Southern Hemisphere.

2 Materials and Methods

2.1 Passive air sampler

The PAS used in this study is described in detail in McLagan et al.[22] The sampler consists of a sulphur impregnated activated carbon sorbent (HGR-AC, Calgon Carbon Corporation) in a Radiello® diffusive barrier that constrains the sampling rate. Sorbent and diffusive barrier are housed in a polyethylene terephthalate housing to protect them from rain and minimize the effect of wind speed on sampling rates.[38] The sampler collects GEM, while other forms of airborne Hg (gaseous oxidised mercury and particle bound mercury) are unable to pass the diffusive barrier to any significant extent.[39] GEM typically comprises >95% of total gaseous mercury (TGM),[12] meaning that GEM levels provide a good estimate of TGM under most conditions.

2.2 Sampling

PAS were deployed at 33 locations in and around the city of Dar es Salaam, Tanzania, for approximately 60 days, between February and April 2019. PAS were deployed in duplicate at two locations and five field blanks were collected along with the PAS. The deployment of the

PAS and treatment of field blanks was done according to standard operating procedures described in McLagan et al.[23] The study had two main components, aimed at (i) determining GEM levels and its spatial distribution within and between urban and rural/suburban areas, in order to assess the significance of urban emission sources, and (ii) to specifically evaluate the role of handling of municipal waste and e-waste as sources for GEM. The first study component was addressed by sampling at 24 locations along an urban-rural transect across the city of Dar es Salaam, as well as 40 and 60 km upwind and downwind, respectively. The sampling locations within Dar es Salaam were selected to cover different urbanized areas, including commercial districts downtown, heavily trafficked areas, areas with heavy industry, and more and less affluent residential areas. Samples were additionally collected in the vicinity of two cement production facilities, one located 30 km to the south and one 20 km to the north of Dar es Salaam. These samplers were collected as close to the facilities as achievable (within ~1000 m) within site access restrictions. For the second study component, eight samples were collected along a transect (12 km) covering the city’s main municipal waste dumpsite and an e-waste recycling facility 20 km west of Dar es Salaam. Soil samples were collected from 28 locations in February 2019, as described in Nipen et al.[40] Table S1 in the supporting information (SI) provides detailed information on sampling locations.

2.3 Sample preparation and analysis

2.3.1 Analysis of PAS for Hg

PAS for GEM were analysed at the University of Toronto Scarborough following US EPA method 7473,[41] thermal combustion, amalgamation, and atomic absorption spectroscopy. Detailed descriptions of the procedures are given in McLagan et al.[42, 23] Briefly, the sorbent was weighed, placed in ceramic sample boats, and covered with sodium carbonate (VWR Chemicals BDH®), to prevent sulphur poisoning of the instrument catalyst tube.[42] The entire mass of sorbent in each PAS was analysed (in two aliquots) to account for possible heterogeneity of Hg distribution within the sorbent. Analysis was performed using a Mercury Analyzer-3000 (Nippon Instruments).

The measured Hg content in the PAS was converted to volumetric GEM air concentrations by dividing the Hg mass by sampling time (days) and a sampling rate (m^3/day). A global calibration study determined the PAS sampling rate to be 0.135 ± 0.016 m^3/day.[23] This sampling rate was adjusted for temperature and wind speed at each site (average for the duration of the sampling period) according to equations given in McLagan et al.[43] Location specific meteorological data were extracted from the ERA5-dataset from ECMWF (European Centre for Medium-Range Weather Forecasts).[44]

2.3.2 Analysis of soil

Soil samples were analysed at the University of Oslo, Norway. Samples were air dried at room temperature (21 ℃) for between two days and one week until stable weight. The dry soils were carefully crushed before being sifted through a 2 mm sieve.[45]

Soil samples (~50 mg) were analysed for total Hg content using a Direct Mercury Analyser (DMA-80) (Milestone, Italy), with a similar method to the PAS analysis.[45] Nickel sample boats were used, and no sodium carbonate addition was necessary given the lower content of sulphur in the analysed soil compared to the PAS sorbent. Soil pH was determined potentiometrically according to ISO10390, and effective cation exchange capacity (CEC) was determined using barium chloride adhering to ISO11260. Soil organic matter (SOM) content was determined gravimetrically by loss on ignition (LOI) at 550 ℃. LOI was subsequently corrected for structural water loss according to Hoogsteen et al.[46] to determine OM content. Clay content was roughly estimated according to Ritchey et al.[47]

2.4 QA/QC

For the analysis of GEM in the PAS, three types of standards were analysed between samples. Liquid standards (N=14) showed 98±1% recovery, NIST standard reference material (Bituminous coal; SRM-2685c) (N=8) showed 93±2% recovery, while an in-house reference material (PAS sorbent loaded with Hg) (N=6) showed 102±5% recovery. Concentration of Hg in field blanks (N=5) represented on average 12% of Hg concentration in samples (Table S3). Samples were blank corrected based on the average of field blanks, after one field blank was omitted as an outlier. Detection and quantification limits (LOD, LOQ) were calculated as three and 10 times the standard deviation of the field blanks, respectively, and correspond to 0.26 ng/m^3 and 0.86 ng/m^3 using the average sampling volume. The LOD and LOQ reported here are comparable to LODs and LOQs reported by Quant et al.,[48] and in the lower range of LODs and LOQs reported by Snow et al.,[11] but higher than those reported by McLagan et al.[22] Two duplicate samples showed 6% and 9% deviation. This is comparable to the precision achieved by Quant et al.,[48] and at the lower end of precision achieved by McLagan et al.[23] using the same type of PAS.

For the analysis of Hg in soils, a light sandy soil JRC reference material (BCR-142), was analysed with 95.7% compliance with the certified concentration. Blank levels for the soils were low, representing <1% of the average Hg content in soil samples (Table S6). Soil Hg concentrations were therefore not blank corrected, and LOD (0.0003 mg/kg) and LOQ (0.0005 mg/kg) were determined as the average plus three and 10 times the standard deviation of blanks (N=10), respectively, divided by the average sample amount. One rural sample (R-1, average concentration 0.012 mg/kg) was analysed in five parallels, yielding a relative standard deviation of 13%.

2.5 Emission estimates for the urban area

GEM emissions from the urban area were estimated using a simple inflow - outflow box model of the urban atmosphere. As the Dar es Salaam region has varying degrees of urbanization, only the most central 37 of the ~90 wards of Dar es Salaam were defined as urban in this study, covering an area of approximately 100 km^2. Assuming an atmospheric boundary layer at 1.2 km, the total volume of the urban atmosphere in the model was 120 km^3. We assumed steady-state conditions and a well-mixed atmosphere. Background GEM concentration (air inflow) was based on Slemr et al.[49] For urban GEM concentrations (air outflow) we used the mean GEM concentrations for urban locations found in this study after removal of outliers. Wind speed used in the model represented the mean for all urban sampling locations in Dar es Salaam.[44] Table S4 provides the parameters and equations used for the urban emission model. Uncertainty in the emissions were estimated using a Monte Carlo approach including likely variability in atmospheric boundary layer height, wind speed, and GEM concentration in inflowing and outflowing air (further described in the SI). Predicted annual emissions from urban Dar es Salaam based on measured concentrations were compared to the gridded AMAP/UNEP global Hg emissions inventory for 2010.[50]

2.6 Statistical analysis

Data treatment was conducted using Microsoft Excel and R studio version 4.0.5. Differences between location categories was tested using the non-parametric Wilcoxon rank sum test. Correlations between GEM, Hg in soil, and soil properties were determined using Spearman rank correlation.

3 Results and discussion

3.1 General overview

The LOQ for GEM obtained in this study (0.86 ng/m^3) lies at the lower end of annual mean background concentrations in air reported for the Southern Hemisphere between 2007 and 2013 (range: 0.85-1.05 ng/m^3).[49] Two rural/suburban locations had GEM concentrations between the LOD and the LOQ. GEM concentrations below the LOQ are reported in italic in the following text. One sample from the municipal waste/e-waste transect had GEM concentration considerably lower than the blanks. This sample has thus likely been subject to some unknown instrumental error and was therefore excluded from the study. An additional PAS from the outer edge of the municipal waste/e-waste transect was lost during transport.

GEM concentrations over the study area as a whole ranged between *0.79* and 5.34 ng/m^3 for the two-month sampling period (Figure 1, Table 1). Concentration data are provided in Table S2.

Figure 1 (double column)

Table 1 (double column)

Concentrations of Hg in soil in the present study ranged from 0.0067 to 0.098 mg/kg (Table 2, Table S5). Globally, background Hg content in soil varies, but reported values lie in the range of 0.01 to 0.1 mg/kg (Beckers and Rinklebe[51] and references therein). As such, the range of Hg concentrations in soil found in the region is comparable to background concentrations. Hg concentrations in soil were poorly correlated with GEM concentrations in air (Spearman’s rho 0.34, p = 0.076).

Table 2 (double column)

3.2 Urban-rural transect

3.2.1 Air

Urban locations in this study showed a median GEM concentration of 1.55 ng/m^3 (mean 2.13 ± 1.57 ng/m^3). Variability in GEM concentrations within the urban area was large, with a range of 1.07 to 5.34 ng/m^3. GEM concentrations at all urban sites exceeded the highest background value (1.05 ng/m^3) of the range reported by Slemr et al.[49] for the Southern Hemisphere. The two highest GEM concentrations in the study (5.13 and 5.34 ng/m^3) were found at urban locations. Both these samples were collected in areas with mainly residential character, but not in vicinity of each other, and with differences in e.g., traffic level, affluence, and proximity to industry.

The mean GEM concentrations found in urban areas in this study were compared to GEM concentrations found in other urban areas of the world in the last decade (Table 1). Only one study from the Southern Hemisphere including urban areas could be found in the peer reviewed literature, illustrating the need for the present study. This is of relevance when comparing concentrations between the Hemispheres, as background concentrations in air in the Northern Hemisphere (1.3 to 1.7 ng/m^3) are higher than in the Southern Hemisphere (0.85 to 1.05 ng/m^3).[12, 15, 49] The mean GEM concentration for urban locations found in our study was higher than GEM concentrations found in Toronto, Canada and in Bronx, Rochester, and Beltsville, USA.[16, 52, 53] The GEM concentrations were comparable to GEM concentrations in Pretoria, South Africa; Basel, Switzerland; Taoyuan, Taiwan, and Chicago, USA,[54-57] and lower compared to Da Nang, Vietnam, Seoul, South Korea, and Shanghai, Beijing, Nanjing, and Guiyang, China.[21, 58-62]

Studies assessing spatial trends of GEM using PAS in urban areas have as far as we are aware only been conducted in Toronto, Canada,[16] and in Basel, Switzerland,[55] Both these studies showed lower spatial variability in Hg concentrations in the urban environment (range Toronto: 0.94 to 2.37 ng/m^3, range Basel: 1.83 to 2.52 ng/m^3) compared to our study (1.07 to 5.34 ng/m^3). However, the Canadian study also contained a component where samples were collected along transects in the vicinity of industrial facilities registered as Hg emission sources. The highest measured GEM concentration amongst these samples was 12.3 ng/m^3, collected within a few metres of a facility handling disposal of Hg containing products. The GEM concentrations along the transects in the Toronto study decreased exponentially, approaching average urban concentrations after 2000 to 3500 m. The two locations in our study with GEM concentrations in excess of 5 ng/m^3 thus suggests the presence of significant local sources of Hg. However, given the unknown nature of these sources and thus unknown distance between sampler and source, no quantitative estimate of the magnitude of GEM emissions from the sources can be made.

Using the mean urban GEM concentrations measured in this study (excluding the two highest concentrations as outliers) we estimated an annual emission of 500 ± 400 kg for the 100 km^2 Dar es Salaam urban area using a simple box model. Estimated annual Hg emissions from the AMAP/UNEP emissions inventory for the grid cell corresponding to Dar es Salaam (covering 3070 km^2) is lower than this, at 20 kg.[50] The AMAP/UNEP emission estimate for Dar es Salaam is also low compared to grid cells corresponding to other urban areas in Africa, e.g., Nairobi, Kenya (170 kg) and Johannesburg, South Africa (1100 kg).[50] Fossil fuel combustion (notably coal combustion) and ASGM are considered the dominating Hg emission sources in Africa.[2, 7, 63] However, to our knowledge, there are no coal fired power plants and no major ASGM activity within or near Dar es Salaam. Despite high associated uncertainty, our emission estimates based on measurements suggests that there are significant Hg sources within urban Dar es Salaam that are not accounted for in UNEP/AMAP emission estimates, which therefore could be biased low.

The median GEM concentration measured at rural and suburban sites of 1.05 ng/m^3 (range *0.79* to 2.16 ng/m^3) is consistent with the Southern Hemisphere background concentrations reported by Slemr et al.[49] Elevated GEM concentrations at three rural and suburban locations (1.99, 2.05, and 2.16 ng/m^3) indicate the presence of local emissions. Two of these sites were at the outer edges of the urban/rural transect, excluding proximity to the urban environment as an explanatory factor for these elevated concentrations. Consequently, no significant difference was seen between urban locations and rural/suburban locations ($p = 0.27$). Belelie et al.[64] reported spatial variability in GEM concentrations in the South African Highveld region by measuring at three monitoring sites in a suburban area with comparatively high industrial activity. Their range of averages from 1.04 to 1.99 ng/m^3 is very similar to the range measured at the rural/suburban locations in the present study.

GEM concentrations in the vicinity of two cement production facilities (1.34 and 1.48 ng/m^3) were slightly elevated above Southern Hemisphere background. This suggests that these facilities may represent Hg sources locally. A larger number of samples, and/or samples collected in closer vicinity to the facilities would be required to determine the extent of local Hg contamination.

3.2.2 Soil

Hg concentrations in urban soils ranged from 0.011 to 0.098 mg/kg, with a median of 0.027 mg/kg. This is low compared to the Hg concentrations found in urban soils elsewhere in the world (Table 2). They were similar to those reported for urban soil in Kumasi, Ghana, and Vanadzor, Armenia[65-67] and lower than those from Beijing and Wuhu, China, Brno, Czech Republic, Athens, Greece, and Arak, Iran.[68-74] Intense solar radiation and high temperature all year round in Dar es Salaam likely contribute to the low levels of Hg in soil, as this favours photoreduction of Hg(II) to GEM and volatilization of GEM, respectively.[29-31] Limited vegetation cover in the region may contribute to the low Hg levels in soil due to more exposure to photoreduction and less deposition via litterfall.[28]

The highest soil Hg concentration was found close to the downtown area, potentially influenced by both traffic, industrial activity, and e-waste processing. SOM content at this location was low. This location does not correspond to either of the two locations with the highest GEM concentrations in air. In combination with the lack of correlation between GEM in air and Hg in soil, this suggests that historically contaminated soil in the urban area is not a dominating source for GEM.

In rural and suburban regions, the Hg concentrations in soil ranged from 0.0067 to 0.092 mg/kg, with a median of 0.012 mg/kg. More remote locations had Hg concentrations below 0.015 mg/kg, while some suburban locations showed elevated concentrations. This was particularly the case at one location where also the SOM content was high. The presence of a few high Hg concentrations in suburban regions, and the presence of some lower Hg concentrations in urban regions ensured no significant difference in Hg concentrations between urban and rural/suburban regions for soil ($p = 0.23$).

Soil physicochemical properties (pH, CEC, SOM and clay content) are known to influence soil capacity to bind Hg and thus its spatial distribution.[51, 75] Of these properties, SOM showed the strongest positive correlation with Hg concentrations in soil (Table S9) (Spearman's rho 0.44, $p = 0.019$), however this correlation was strongly influenced by one location. Soils in the region generally have low SOM content, but with relatively large variability (median 1.7%, range <0.01-9.6%). Overall, it seems likely that soil Hg concentrations are influenced by the physicochemical properties of the soil in form of the SOM content, in combination with proximity to sources, given the presence of some higher concentrations in urban locations.

3.3 Municipal waste and e-waste transect

3.3.1 Air

GEM concentrations at sites along the municipal waste/e-waste transect had a median of 1.32 ng/m^3 and a range of 1.08 to 2.41 ng/m^3 (Figure 1B). The highest GEM concentration within this transect was found at the municipal waste dumpsite, while the two locations furthest downwind in the transect showed only slightly elevated concentrations (1.12 and 1.15 ng/m^3) compared to the range reported by Slemr et al.[49] for the Southern Hemisphere background (0.85 to 1.05 ng/m^3). The e-waste handler (1.77 ng/m^3) and most sites in the immediate vicinity of the e-waste handler and the municipal waste site (1.08, 1.72, and 1.32 ng/m^3) had intermediate GEM concentrations, identifying the municipal waste dumpsite (2.41 ng/m^3) rather than the e-waste handler as the main source for GEM along this transect. On the other hand, three urban locations within the urban-rural transect that were located near identified e-waste handling or recycling sites, all showed somewhat elevated GEM concentrations (1.44, 1.69, and 1.84 ng/m^3). An urban location near a decommissioned municipal waste dumpsite did however not show elevated GEM concentration (1.10 ng/m^3).

PAS have previously been applied to determine GEM concentrations near a landfill known to contain Hg contaminated material in Switzerland,[76] and at an e-waste handling facility in Norway[11] (Table 1). The GEM concentration at the municipal waste dumpsite in our study were within the lower range of GEM measured in the Swiss study. Moreover, GEM concentration at the e-waste site in our study was lower than the range of GEM concentrations in ambient air in the vicinity of the Norwegian facility, and comparable to ambient air some distance from it.[11] Overall, the spatial distribution of GEM concentrations in the present study suggest that both general waste and e-waste are sources for GEM. The relatively low levels of GEM around the e-waste handler and municipal waste dumpsite compared to similar sites in industrialized countries could be explained by an overall lower volume of Hg containing products entering the waste stream in Tanzania.

3.3.2 Soil

Along the municipal waste/e-waste transect, Hg concentrations in soil ranged between 0.0069 and 0.065 mg/kg, with a median of 0.015 mg/kg. The soil at the e-waste site (0.033 mg/kg) had higher Hg concentration compared to the soil collected at the edge of the municipal waste site (0.022 mg/kg). The highest soil Hg concentration was nevertheless found at a site towards the periphery of the transect (0.065 mg/kg). Soil properties at this site differed from the rest of the transect, with e.g., higher content of SOM. In general, the soil along the municipal waste/e-waste transect had lower SOM content and lower CEC compared to the soil in the urban-rural transect (Table S8), indicating lower capacity to retain Hg. Along the urban-rural transect, soil was sampled at two urban locations in the vicinity of e-waste processing, one of which showed the highest Hg soil concentration in the present study, while the other showed low Hg concentration (0.098 and 0.011 mg/kg, respectively). An urban location near a decommissioned municipal waste dumpsite also had low soil Hg concentration (0.018 mg/kg).

The municipal waste dumpsite had a soil Hg concentration in the lower range of concentrations reported from a municipal waste dumpsite in Sierra Leone.[77] Moreover, the Hg concentration in the soil at the e-waste site were lower than concentrations reported from an informal e-waste site in Ghana.[77]

3.4 Concluding remarks

This study shows that urban ambient GEM concentrations in Dar es Salaam are lower than found in some urban areas in Asia. Nevertheless, GEM concentrations exceeded 5 ng/m^3 at two locations, demonstrating the presence of significant local sources. Further investigations using multiple PAS should be conducted in the vicinity of these locations to identify sources, and to facilitate estimation of the magnitude of their emissions. The comparatively high estimated annual GEM emissions in Dar es Salaam further support the presence of significant unidentified sources. This raises questions regarding current emission estimates for Africa, as the sources expected to be most important in Africa, i.e., AGSM and coal power plants, are not known to be relevant for Dar es Salaam. Further studies should also be carried out in other urban regions in Africa to gain further insight into urban emissions and sources for GEM. The PAS applied in this study has been shown to be suitable to carry out such investigations in urban areas in the Global South, given quantification limits in the lower range of GEM background concentrations for the Southern Hemisphere. Longer deployment times could further lower the quantification limits.

In addition to disclosing unidentified sources of GEM in Dar es Salaam, our study shows that handling of municipal waste and e-waste represent sources for GEM at waste sites in the outskirts of the city, and that e-waste also represent a source within Dar es Salaam. Further efforts in waste management at the regional level should be made, but this should also be addressed in regulatory efforts at the international level to reduce trade in products and waste which contain Hg.

Acknowledgements

This study was conducted as part of the AnthroTox project, a convergence environment at the University of Oslo combining social and natural sciences to study anthropogenic toxicants. The AnthroTox project is funded through the University of Oslo and the Norwegian Ministry of Education and Research. We would like to thank Ane Haarr, Franziska Klaas, Samwel Moses Ntapanta, and Signe Mikkelsen for their contributions during fieldwork; local authorities for their cooperation; the residents and businesses of Dar es Salaam and the

Coastal Region who allowed us to collect samples on their properties; Sabine Eckhart for providing meteorological data; Katrine Aspmo Pfaffhuber for valuable advice; and Helene Lunder Halvorsen who helped produce Figure 1 using QGIS.

References

1. UNEP, Minamata Convention on Mercury: Text and Annexes, United Nations Environmental Programme, Geneva, Switzerland, 2013.
2. D. G. Streets, H. M. Horowitz, Z. Lu, L. Levin, C. P. Thackray and E. M. Sunderland, Global and regional trends in mercury emissions and concentrations, 2010–2015, *Atmospheric environment*, 2019, **201**, 417-427.
3. Y. Zhang, D. J. Jacob, H. M. Horowitz, L. Chen, H. M. Amos, D. P. Krabbenhoft, F. Slemr, V. L. S. Louis and E. M. Sunderland, Observed decrease in atmospheric mercury explained by global decline in anthropogenic emissions, *Proceedings of the National Academy of Sciences*, 2016, **113**, 526-531.
4. L. G. Martin, C. Labuschagne, E.-G. Brunke, A. Weigelt, R. Ebinghaus and F. Slemr, Trend of atmospheric mercury concentrations at Cape Point for 1995–2004 and since 2007, *Atmospheric Chemistry and Physics*, 2017, **17**, 2393-2399.
5. F. Slemr, L. Martin, C. Labuschagne, T. Mkololo, H. Angot, O. Magand, A. Dommergue, P. Garat, M. Ramonet and J. Bieser, Atmospheric mercury in the Southern Hemisphere–Part 1: Trend and inter-annual variations in atmospheric mercury at Cape Point, South Africa, in 2007–2017, and on Amsterdam Island in 2012–2017, *Atmospheric Chemistry and Physics*, 2020, **20**, 7683-7692.
6. D. G. Streets, M. K. Devane, Z. Lu, T. C. Bond, E. M. Sunderland and D. J. Jacob, All-time releases of mercury to the atmosphere from human activities, *Environmental science & technology*, 2011, **45**, 10485-10491.
7. E. G. Pacyna, J. Pacyna, K. Sundseth, J. Munthe, K. Kindbom, S. Wilson, F. Steenhuisen and P. Maxson, Global emission of mercury to the atmosphere from anthropogenic sources in 2005 and projections to 2020, *Atmospheric Environment*, 2010, **44**, 2487-2499.
8. N. Pirrone, S. Cinnirella, X. Feng, R. B. Finkelman, H. R. Friedli, J. Leaner, R. Mason, A. B. Mukherjee, G. B. Stracher and D. Streets, Global mercury emissions to the atmosphere from anthropogenic and natural sources, *Atmospheric Chemistry and Physics*, 2010, **10**, 5951-5964.
9. N. E. Selin, Global biogeochemical cycling of mercury: a review, *Annual Review of Environment and Resources*, 2009, **34**, 43-63.
10. X. Huang, M. Li, H. R. Friedli, Y. Song, D. Chang and L. Zhu, Mercury emissions from biomass burning in China, *Environmental science & technology*, 2011, **45**, 9442-9448.
11. M. A. Snow, G. Darko, O. Gyamfi, E. Ansah, K. Breivik, C. Hoang, Y. D. Lei and F. Wania, Characterization of inhalation exposure to gaseous elemental mercury during

artisanal gold mining and e-waste recycling through combined stationary and personal passive sampling, *Environmental Science: Processes & Impacts*, 2021, **23**, 569-579.

12. C. T. Driscoll, R. P. Mason, H. M. Chan, D. J. Jacob and N. Pirrone, Mercury as a global pollutant: sources, pathways, and effects, *Environmental science & technology*, 2013, **47**, 4967-4983.

13. N. Pirrone, W. Aas, S. Cinnirella, R. Ebinghaus, I. M. Hedgecock, J. Pacyna, F. Sprovieri and E. M. Sunderland, Toward the next generation of air quality monitoring: Mercury, *Atmospheric Environment*, 2013, **80**, 599-611.

14. F. Sprovieri, N. Pirrone, M. Bencardino, F. D'Amore, F. Carbone, S. Cinnirella, V. Mannarino, M. Landis, R. Ebinghaus and A. Weigelt, Atmospheric mercury concentrations observed at ground-based monitoring sites globally distributed in the framework of the GMOS network, *Atmospheric chemistry and physics*, 2016, **16**, 11915-11935.

15. F. Sprovieri, N. Pirrone, R. Ebinghaus, H. Kock and A. Dommergue, A review of worldwide atmospheric mercury measurements, *Atmospheric Chemistry and Physics*, 2010, **10**, 8245-8265.

16. D. S. McLagan, B. A. Hussain, H. Huang, Y. D. Lei, F. Wania and C. P. Mitchell, Identifying and evaluating urban mercury emission sources through passive sampler-based mapping of atmospheric concentrations, *Environmental Research Letters*, 2018, **13**, 074008.

17. E. Cairns, K. Tharumakulasingam, M. Athar, M. Yousaf, I. Cheng, Y. Huang, J. Lu and D. Yap, Source, concentration, and distribution of elemental mercury in the atmosphere in Toronto, Canada, *Environmental Pollution*, 2011, **159**, 2003-2008.

18. J. Huang, H.-D. Choi, M. S. Landis and T. M. Holsen, An application of passive samplers to understand atmospheric mercury concentration and dry deposition spatial distributions, *Journal of Environmental Monitoring*, 2012, **14**, 2976-2982.

19. H. Skov, B. T. Sørensen, M. S. Landis, M. S. Johnson, P. Sacco, M. E. Goodsite, C. Lohse and K. S. Christiansen, Performance of a new diffusive sampler for Hg0 determination in the troposphere, *Environmental Chemistry*, 2007, **4**, 75-80.

20. M. S. Gustin, S. N. Lyman, P. Kilner and E. Prestbo, Development of a passive sampler for gaseous mercury, *Atmospheric Environment*, 2011, **45**, 5805-5812.

21. W. Zhang, Y. Tong, D. Hu, L. Ou and X. Wang, Characterization of atmospheric mercury concentrations along an urban–rural gradient using a newly developed passive sampler, *Atmospheric environment*, 2012, **47**, 26-32.

22. D. S. McLagan, C. P. Mitchell, H. Huang, Y. D. Lei, A. S. Cole, A. Steffen, H. Hung and F. Wania, A high-precision passive air sampler for gaseous mercury, *Environmental Science & Technology Letters*, 2015, **3**, 24-29.

23. D. S. McLagan, C. P. Mitchell, A. Steffen, H. Hung, C. Shin, G. W. Stupple, M. L. Olson, W. T. Luke, P. Kelley and D. Howard, Global evaluation and calibration of a passive air sampler for gaseous mercury, *Atmospheric Chemistry and Physics*, 2018, **18**, 5905-5919.

24. A. Naccarato, A. Tassone, M. Martino, S. Moretti, A. Macagnano, E. Zampetti, P. Papa, J. Avossa, N. Pirrone and M. Nerentorp, A field intercomparison of three

passive air samplers for gaseous mercury in ambient air, *Atmospheric Measurement Techniques*, 2021, **14**, 3657-3672.

25. D. Obrist, J. L. Kirk, L. Zhang, E. M. Sunderland, M. Jiskra and N. E. Selin, A review of global environmental mercury processes in response to human and natural perturbations: Changes of emissions, climate, and land use, *Ambio*, 2018, **47**, 116-140.

26. J. Bieser, H. Angot, F. Slemr and L. Martin, Atmospheric mercury in the Southern Hemisphere–Part 2: Source apportionment analysis at Cape Point station, South Africa, *Atmospheric Chemistry and Physics*, 2020, **20**, 10427-10439.

27. A. P. Rutter, J. J. Schauer, M. M. Shafer, J. E. Creswell, M. R. Olson, M. Robinson, R. M. Collins, A. M. Parman, T. L. Katzman and J. L. Mallek, Dry deposition of gaseous elemental mercury to plants and soils using mercury stable isotopes in a controlled environment, *Atmospheric Environment*, 2011, **45**, 848-855.

28. D. Obrist, C. Pearson, J. Webster, T. Kane, C.-J. Lin, G. R. Aiken and C. N. Alpers, A synthesis of terrestrial mercury in the western United States: Spatial distribution defined by land cover and plant productivity, *Science of the Total Environment*, 2016, **568**, 522-535.

29. C. S. Eckley, M. T. Tate, C.-J. Lin, M. Gustin, S. Dent, C. Eagles-Smith, M. A. Lutz, K. P. Wickland, B. Wang and J. E. Gray, Surface-air mercury fluxes across Western North America: A synthesis of spatial trends and controlling variables, *Science of the Total Environment*, 2016, **568**, 651-665.

30. A. Carpi and S. E. Lindberg, Sunlight-mediated emission of elemental mercury from soil amended with municipal sewage sludge, *Environmental Science & Technology*, 1997, **31**, 2085-2091.

31. M. Xin and M. S. Gustin, Gaseous elemental mercury exchange with low mercury containing soils: investigation of controlling factors, *Applied Geochemistry*, 2007, **22**, 1451-1466.

32. E. de Barros Santos, P. Moher, S. Ferlin, A. H. Fostier, I. O. Mazali, K. Telmer and A. G. Brolo, Proof of concept for a passive sampler for monitoring of gaseous elemental mercury in artisanal gold mining, *Scientific reports*, 2017, **7**, 1-11.

33. O. Gyamfi, P. B. Sorenson, G. Darko, E. Ansah and J. L. Bak, Human health risk assessment of exposure to indoor mercury vapour in a Ghanaian artisanal small-scale gold mining community, *Chemosphere*, 2020, **241**, 125014.

34. F. Steenhuisen and S. Wilson, Development and application of an updated geospatial distribution model for gridding 2015 global mercury emissions, *Atmospheric environment*, 2019, **211**, 138-150.

35. R. S. Mahenge, P. Ulanga, M. Malabeja, J. Pilly and W. Massoy, *Performance audit report on electronic waste management*, 2018, Available at ELECTRONIC-WASTE-MANAGEMENT-2018.pdf (nao.go.tz). (Accessed March 2021).

36. M. Yhdego, From a Sanitary Landfill to a Dump Site: Pugu Kinyamwezi Community Curse in Dar es Salaam, 2017, DOI: 10.13140/RG.2.2.27828.04483.

37. WorldBank, The World Bank in Tanzania, http://www.worldbank.org/en/country/tanzania/overview, (accessed January 2021).

38. F. Wania and C. Shunthirasingham, Passive air sampling for semi-volatile organic chemicals, *Environmental Science: Processes & Impacts*, 2020, **22**, 1925-2002.

39. N. Szponar, D. S. McLagan, R. J. Kaplan, C. P. Mitchell, F. Wania, A. Steffen, G. W. Stupple, F. Monaci and B. A. Bergquist, Isotopic characterization of atmospheric gaseous elemental mercury by passive air sampling, *Environmental Science & Technology*, 2020, **54**, 10533-10543.

40. M. Nipen, R. D. Vogt, P. Bohlin-Nizzetto, K. Borgå, E. B. Mwakalapa, A. R. Borgen, S. J. Jørgensen, S. M. Ntapanta, A. J. Mmochi and M. Schlabach, Spatial trends of chlorinated paraffins and dechloranes in air and soil in a tropical urban, suburban, and rural environment, *Environmental Pollution*, 2022, 118298.

41. USEPA, Method 7473: Mercury in solids and solutions by thermal decomposition, amalgamation, and atomic absorption spectrophotometry (Vol. 17), 2007.

42. D. S. McLagan, H. Huang, Y. D. Lei, F. Wania and C. P. Mitchell, Application of sodium carbonate prevents sulphur poisoning of catalysts in automated total mercury analysis, *Spectrochimica Acta Part B: Atomic Spectroscopy*, 2017, **133**, 60-62.

43. D. S. McLagan, C. P. Mitchell, H. Huang, B. Abdul Hussain, Y. D. Lei and F. Wania, The effects of meteorological parameters and diffusive barrier reuse on the sampling rate of a passive air sampler for gaseous mercury, *Atmospheric Measurement Techniques*, 2017, **10**, 3651-3660.

44. ECMWF, European Centre for Medium-Range Weather Forecasts, ERA5 dataset, 2021.

45. S. J. Jørgensen, Studying spatial trends of heavy metals in soil from a tropical region, Master’s thesis, University of Oslo, 2020.

46. M. J. Hoogsteen, E. A. Lantinga, E. J. Bakker, J. C. Groot and P. A. Tittonell, Estimating soil organic carbon through loss on ignition: effects of ignition conditions and structural water loss, *European Journal of Soil Science*, 2015, **66**, 320-328.

47. E. L. Ritchey, J. M. McGrath and D. Gehring, Determining soil texture by feel, *Agriculture and Natural Resources Publications, 2015,* **139**.

48. M. I. Quant, M. Feigis, S. Mistry, Y. D. Lei, C. P. Mitchell, R. Staebler, A. Di Guardo, E. Terzaghi and F. Wania, Using passive air samplers to quantify vertical gaseous elemental mercury concentration gradients within a forest and above soil, *Journal of Geophysical Research: Atmospheres*, 2021, **126**, e2021JD034981.

49. F. Slemr, H. Angot, A. Dommergue, O. Magand, M. Barret, A. Weigelt, R. Ebinghaus, E.-G. Brunke, K. A. Pfaffhuber and G. Edwards, Comparison of mercury concentrations measured at several sites in the Southern Hemisphere, *Atmospheric Chemistry and Physics*, 2015, **15**, 3125-3133.

50. AMAP/UNEP, Technical Background Report for the Global Mercury Assessment 2013. Arctic Monitoringand Assessment Programme, Oslo, Norway/UNEP ChemicalsBranch, Geneva, Switzerland. vi + 263 pp, 2013.

51. F. Beckers and J. Rinklebe, Cycling of mercury in the environment: Sources, fate, and human health implications: A review, *Critical Reviews in Environmental Science and Technology*, 2017, **47**, 693-794.

52. H. Zhou, C. Zhou, P. K. Hopke and T. M. Holsen, Mercury wet deposition and speciated mercury air concentrations at rural and urban sites across New York state:

Temporal patterns, sources and scavenging coefficients, *Science of the Total Environment*, 2018, **637**, 943-953.

53. X. Ren, W. T. Luke, P. Kelley, M. D. Cohen, R. Artz, M. L. Olson, D. Schmeltz, M. Puchalski, D. L. Goldberg and A. Ring, Atmospheric mercury measurements at a suburban site in the Mid-Atlantic United States: Inter-annual, seasonal and diurnal variations and source-receptor relationships, *Atmospheric Environment*, 2016, **146**, 141-152.

54. L. E. Gratz, G. J. Keeler, F. J. Marsik, J. A. Barres and J. T. Dvonch, Atmospheric transport of speciated mercury across southern Lake Michigan: Influence from emission sources in the Chicago/Gary urban area, *Science of the total environment*, 2013, **448**, 84-95.

55. L. Wohlgemuth, D. McLagan, B. Flückiger, D. Vienneau and S. Osterwalder, Concurrently measured concentrations of atmospheric mercury in indoor (household) and outdoor air of basel, Switzerland, *Environmental science & technology letters*, 2020, **7**, 234-239.

56. G.-R. Sheu, L. S. P. Nguyen, M. T. Truong and D.-W. Lin, Characteristics of atmospheric mercury at a suburban site in northern Taiwan and influence of trans-boundary haze events, *Atmospheric Environment*, 2019, **214**, 116827.

57. P. Higueras, R. Oyarzun, J. Kotnik, J. M. Esbrí, A. Martínez-Coronado, M. Horvat, M. A. López-Berdonces, W. Llanos, O. Vaselli and B. Nisi, A compilation of field surveys on gaseous elemental mercury (GEM) from contrasting environmental settings in Europe, South America, South Africa and China: separating fads from facts, *Environmental geochemistry and health*, 2014, **36**, 713-734.

58. G.-R. Sheu, N.-H. Lin, C.-T. Lee, J.-L. Wang, M.-T. Chuang, S.-H. Wang, K. H. Chi and C.-F. Ou-Yang, Distribution of atmospheric mercury in northern Southeast Asia and South China Sea during Dongsha experiment, *Atmospheric Environment*, 2013, **78**, 174-183.

59. Y.-J. Han, J.-E. Kim, P.-R. Kim, W.-J. Kim, S.-M. Yi, Y.-S. Seo and S.-H. Kim, General trends of atmospheric mercury concentrations in urban and rural areas in Korea and characteristics of high-concentration events, *Atmospheric Environment*, 2014, **94**, 754-764.

60. X. Qin, X. Wang, Y. Shi, G. Yu, N. Zhao, Y. Lin, Q. Fu, D. Wang, Z. Xie and C. Deng, Characteristics of atmospheric mercury in a suburban area of east China: sources, formation mechanisms, and regional transport, *Atmospheric Chemistry and Physics*, 2019, **19**, 5923-5940.

61. X. Fu, X. Feng, G. Qiu, L. Shang and H. Zhang, Speciated atmospheric mercury and its potential source in Guiyang, China, *Atmospheric Environment*, 2011, **45**, 4205-4212.

62. J. Zhu, T. Wang, R. Talbot, H. Mao, C. Hall, X. Yang, C. Fu, B. Zhuang, S. Li and Y. Han, Characteristics of atmospheric total gaseous mercury (TGM) observed in urban Nanjing, China, *Atmospheric Chemistry and Physics*, 2012, **12**, 12103-12118.

63. K. E. Masekoameng, J. Leaner and J. Dabrowski, Trends in anthropogenic mercury emissions estimated for South Africa during 2000–2006, *Atmospheric Environment*, 2010, **44**, 3007-3014.

64. M. Belelie, S. Piketh, R. Burger, A. Venter and M. Naidoo, Characterisation of ambient Total Gaseous Mercury concentrations over the South African Highveld, *Atmospheric Pollution Research*, 2019, **10**, 12-23.

65. G. Darko, M. Dodd, M. A. Nkansah, E. Ansah and Y. Aduse-Poku, Distribution and bioaccessibility of metals in urban soils of Kumasi, Ghana, *Environmental Monitoring and Assessment*, 2017, **189**, 260.

66. O. Akoto, N. Bortey-Sam, Y. Ikenaka, S. M. Nakayama, E. Baidoo, Y. B. Yohannes and M. Ishizuka, Contamination levels and sources of heavy metals and a metalloid in surface soils in the Kumasi Metropolis, Ghana, *Journal of Health and Pollution*, 2017, **7**, 28-39.

67. L. Sahakyan, G. Tepanosyan, G. Melkonyan, N. Maghakyan and A. Saghatelyan, Mercury soil contents and associated ecological and health risks in kindergartens and functional areas of the city of Vanadzor (Armenia), *GEOGRAPHY, ENVIRONMENT, SUSTAINABILITY*, 2019, **12**, 252-271.

68. X. Chen, X. Xia, S. Wu, F. Wang and X. Guo, Mercury in urban soils with various types of land use in Beijing, China, *Environmental Pollution*, 2010, **158**, 48-54.

69. Q. Liu, Y. Liu and M. Zhang, Mercury and cadmium contamination in traffic soil of Beijing, China, *Bulletin of environmental contamination and toxicology*, 2012, **88**, 154-157.

70. X.-H. Li, H.-X. Cheng, C.-D. Zhao and X.-B. Xu, Mercury contamination in the topsoil and subsoil of urban areas of Beijing, China, *Bulletin of environmental contamination and toxicology*, 2010, **85**, 224-228.

71. F. Fang, H. Wang and Y. Lin, Spatial distribution, bioavailability, and health risk assessment of soil Hg in Wuhu urban area, China, *Environmental monitoring and assessment*, 2011, **179**, 255-265.

72. P. Pelcová, I. Zouharová, A. Ridošková and V. Smolíková, Evaluation of mercury availability to pea parts (Pisum sativum L.) in urban soils: Comparison between diffusive gradients in thin films technique and plant model, *Chemosphere*, 2019, **234**, 373-378.

73. E. Kelepertzis and A. Argyraki, Mercury in the urban topsoil of Athens, Greece, *Sustainability*, 2015, **7**, 4049-4062.

74. E. Solgi, A. Esmaili-Sari and A. Riyahi-Bakhtiari, Spatial distribution of mercury in the surface soils of the urban areas, Arak, Iran, *Bulletin of environmental contamination and toxicology*, 2014, **93**, 710-715.

75. D. O'Connor, D. Hou, Y. S. Ok, J. Mulder, L. Duan, Q. Wu, S. Wang, F. M. Tack and J. Rinklebe, Mercury speciation, transformation, and transportation in soils, atmospheric flux, and implications for risk management: A critical review, *Environment international*, 2019, **126**, 747-761.

76. D. S. McLagan, S. Osterwalder and H. Biester, Temporal and spatial assessment of gaseous elemental mercury concentrations and emissions at contaminated sites using active and passive measurements, *Environmental Research Communications*, 2021, **3**, 051004.

77. C. Möckel, K. Breivik, T. H. Nøst, A. Sankoh, K. C. Jones and A. Sweetman, Soil pollution at a major West African E-waste recycling site: Contamination pathways

and implications for potential mitigation strategies, *Environment International*, 2020, **137**, 105563.

Figure captions:

Figure 1: A: Spatial variation in the concentrations of GEM in Dar es Salaam and surrounding regions, time-averaged over a two-month period from February to April in 2019. B: Spatial variation in the concentrations of GEM along the municipal waste/e-waste transect, time-averaged over a two-month period from February to April in 2019. Base maps produced in QGIS.

Table 1:

Table 1: GEM concentrations (ng/m^3) in ambient air in this study and recent studies from other regions for comparison. Ranges are given for PAS, reflecting the spatial variation, and not for active measurements, which reflect temporal variation. Values below LOQ given in italic.

Category	**Sampling**	**Location**	**Mean (Median)**	**Range**	**Reference**
Urban-rural, (e-)waste	PAS	Dar es Salaam, Tanzania	1.57 (1.15)	*0.79*-5.34	this study
Urban	PAS	Basel, Switzerland	2.21	1.83-2.52	[55]
Urban	PAS	Toronto, Canada	1.46	0.94-2.37	[16]
Urban	Active	Taoyuan, Taiwan	2.61		[56]
Urban	Active	Da Nang, Vietnam	3.86		[58]
Urban (TGM)	Active	Seoul, Korea	3.72		[59]
Urban	Active	Bronx, NY, USA	1.92 (1.77)		[52]
Urban	Active	Rochester, NY, USA	1.66 (1.50)		[52]
Urban	Active	Beltsville, USA	1.41		[53]
Urban	Active	Shanghai, China	2.77		[60]
Urban (TGM)	Active	Nanjing, China	7.9		[62]
Urban	Active	Guiyang, China	9.72		[61]
Urban	Active	Chicago, USA	2.50		[54]
Urban	Active	Pretoria, South Africa	2.24		[57]
Urban-rural transect	PAS	Beijing, China		1.4-7.0	[21]
Suburban/industrial (TGM)	Active	Highveld, South Africa	1.04, 1.25, 1.99 [a]		[64]
Landfill	PAS	Gamsenried, Switzerland		1.22-10.8	[76]
E-waste	PAS	Norway		0.9-75	[11]
Background, Southern Hemisphere	Active	Multiple remote sites	0.85-1.05[b]		[49]

[a] Means from three locations within the Highveld.

[b] Range of means.

Table 2:

Table 2: Hg concentrations (mg/kg) in soil from this study and recent studies from other regions for comparison.

Category	Location	Mean (Median)	Range	Reference
Urban-rural, (e-)waste	Dar es Salaam, Tanzania	0.024 (0.015)	0.0067-0.098	this study
Urban	Beijing, China	(0.26)	0.022-9.4	[68]
Urban	Beijing, China	1.67 (1.34)	0.16-3.68	[69]
Urban	Beijing, China		0.012-8.49	[70]
Urban	Wuhu, China	0.21	0.024-2.84	[71]
Urban	Brno, Czech Republic		0.084-0.326	[72]
Urban	Athens, Greece	(0.096)	0.010-1.08	[73]
Urban	Vanadzor, Armenia	0.042 (0.039)	0.0015-0.29	[67]
Urban	Arak, Iran	(0.088)	0.066-0.581	[74]
Urban	Kumasi, Ghana	0.051		[66]
Urban	Kumasi, Ghana	0.050		[65]
Waste	Kingtom, Sierra Leone	0.18	0.03-0.33	[77]
E-waste	Agbogbloshie, Ghana	0.47	0.12-0.94	[77]
Global background			0.01-0.1	[51]

Figure 1:

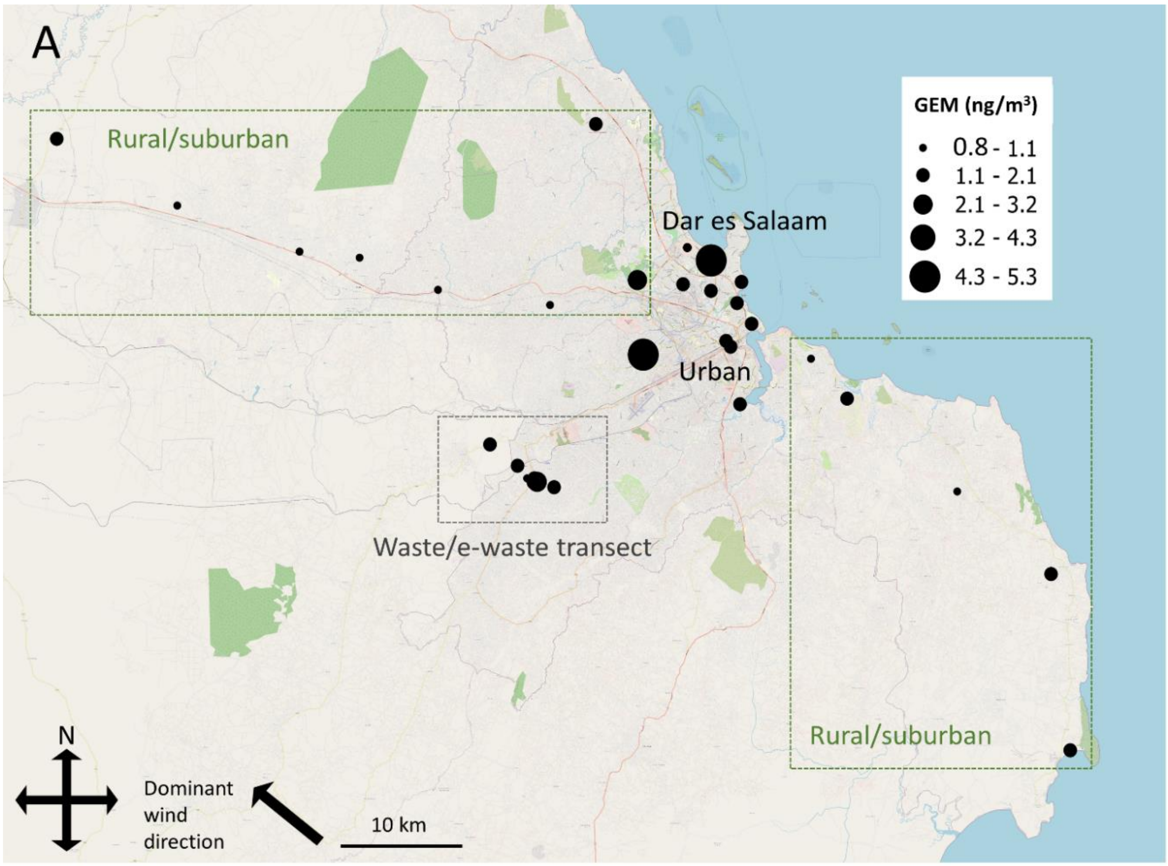
A
Rural/suburban
Dar es Salaam
Urban
Waste/e-waste transect
Rural/suburban
GEM (ng/m³)
0.8 - 1.1
1.1 - 2.1
2.1 - 3.2
3.2 - 4.3
4.3 - 5.3
N
Dominant wind direction
10 km

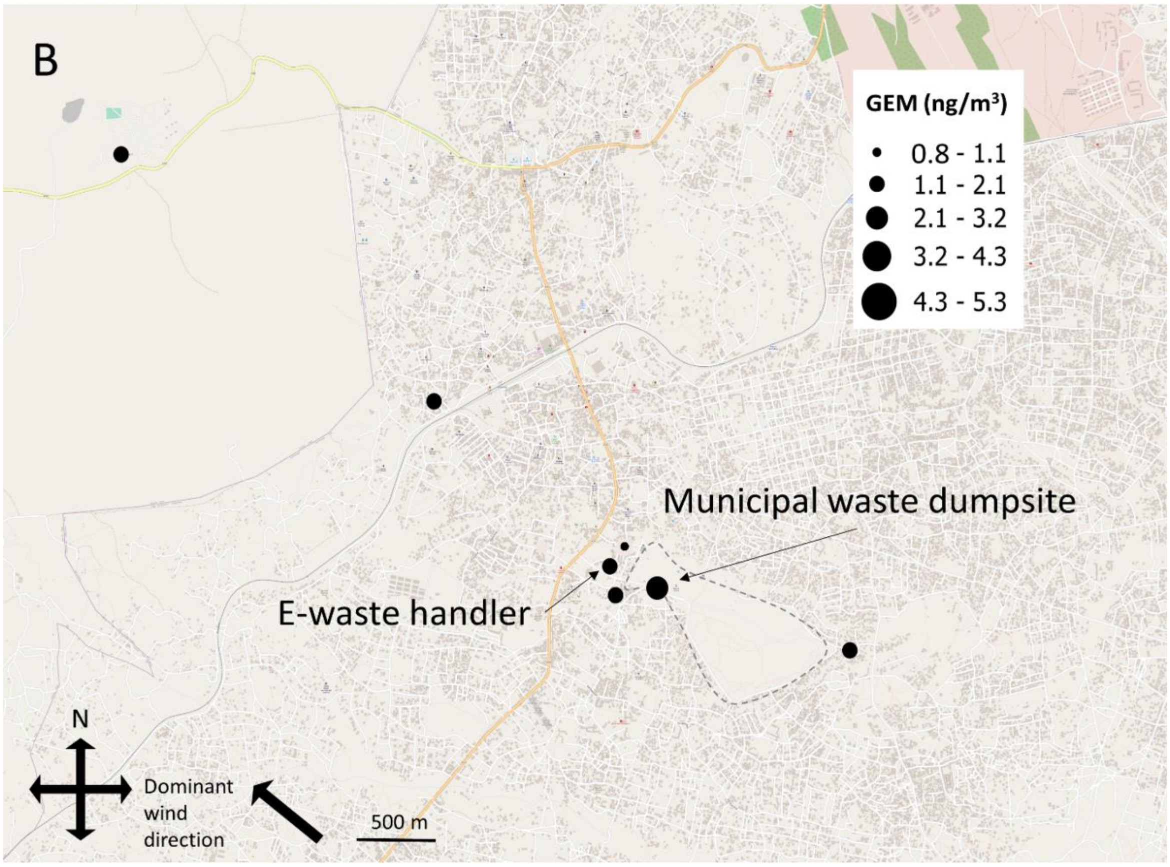
B
GEM (ng/m³)
0.8 - 1.1
1.1 - 2.1
2.1 - 3.2
3.2 - 4.3
4.3 - 5.3
Municipal waste dumpsite
E-waste handler
N
Dominant wind direction
500 m

Supporting information

For

Mercury in air and soil on an urban-rural transect in East Africa

Maja Nipen[a,b*], Susanne Jøntvedt Jørgensen[a], Pernilla Bohlin-Nizzetto[b], Katrine Borgå[c], Knut Breivik[a,b], Aviti John Mmochi[d], Eliezer Brown Mwakalapa[e], M. Isabel Quant[f], Martin Schlabach[b], Rolf David Vogt[g], Frank Wania[f]

[a]Centre for Biogeochemistry in the Anthropocene, Department of Chemistry, University of Oslo, P.O. Box 1033, 0315 Oslo, Norway, [b]NILU-Norwegian Institute for Air Research, P.O. Box 100, 2027 Kjeller, Norway, [c]Aquatic Biology and toxicology and Centre of Biogeochemistry in the Anthropocene, Department of Biosciences, University of Oslo, P.O. Box 1066, 0316 Oslo, Norway, [d]Institute for Marine Sciences, University of Dar es Salaam, Zanzibar, Tanzania, [e]Department of Natural Sciences, Mbeya University of Science and Technology, Mbeya, Tanzania, [f]Department of Physical and Environmental Sciences, University of Toronto Scarborough, 1265 Military Trail, ON MIC 1A4 Toronto, Canada, [g]Norwegian Institute for Water Research, 0579 Oslo, Norway.

* Corresponding author. Centre for Biogeochemistry in the Anthropocene, Department of Chemistry, University of Oslo, P.O. Box 1033, 0315 Oslo, Norway.

Email address: majanip@kjemi.uio.no; mni@nilu.no

Table S1: Location information. PAS from location W-25 and W-28 lost during sampling or analysis. Temperature and wind speed are means for the PAS deployment period.

Location	Category	Matrix	Deployment Date PAS	Retrieval Date PAS	Temp (℃)	Wind speed (m/s)	Location detail
RS-1	Rural/suburban	Air/soil	08.02.2019	11.04.2019	28.20	4.44	Coastal/rural
RS-2	Rural/suburban	Air/soil	09.02.2019	11.04.2019	28.82	3.13	Sparsely residential
RS-3	Rural/suburban	Air/soil	09.02.2019	11.04.2019	28.53	3.46	Sparsely residential
RS-4	Rural/suburban	Air/soil	08.02.2019	11.04.2019	28.52	3.50	Residential
U-5	Urban	Air/soil	12.02.2019	11.04.2019	28.19	2.85	Disused waste dump
U-6	Urban	Air/soil	13.02.2019	10.04.2019	28.21	2.83	Near e-waste handler
U-7	Urban	Air/soil	13.02.2019	10.04.2019	28.21	2.83	Near electronics market
U-8	Urban	Air/soil	12.02.2019	12.04.2019	28.15	2.85	Embassy neighbourhood
U-9	Urban	Air/soil	12.02.2019	12.04.2019	28.15	2.85	Residential (affluent)
U-10	Urban	Air/soil	11.02.2019	12.04.2019	28.15	2.86	Residential
U-11	Urban	Air/soil	12.02.2019	12.04.2019	28.15	2.85	Densely residential
U-12	Urban	Air/soil	12.02.2019	14.04.2019	28.10	2.84	Densely residential
RS-13	Rural/suburban	Air/soil	11.02.2019	12.04.2019	28.15	2.86	University
RS-14	Rural/suburban	Air/soil	10.02.2019	13.04.2019	28.11	2.89	Residential
RS-15	Rural/suburban	Air/soil	10.02.2019	13.04.2019	28.15	2.35	Residential
RS-16	Rural/suburban	Air/soil	10.02.2019	13.04.2019	28.15	2.35	Residential
RS-17	Rural/suburban	Air/soil	10.02.2019	13.04.2019	28.15	2.35	Sparsely residential
RS-18	Rural/suburban	Air/soil	10.02.2019	13.04.2019	28.18	2.24	Farmland
RS-19	Rural/suburban	Air/soil	11.02.2019	13.04.2019	28.48	2.14	School grounds
W-20	Waste	Air/soil	06.02.2019	10.04.2019	28.46	2.70	Near dumpsite
W-21	Waste	Air/soil	06.02.2019	10.04.2019	28.46	2.70	Dumpsite
W-22	Waste	Air/soil	06.02.2019	10.04.2019	28.46	2.70	Near dump/e-waste site
W-23	Waste	Air/soil	06.02.2019	10.04.2019	28.46	2.70	E-waste handler
W-24	Waste	Air/soil	06.02.2019	10.04.2019	28.46	2.70	Near dump/e-waste site
W-25	Waste	(Air)/soil	07.02.2019	10.04.2019	28.46	2.67	Near dump/e-waste site
W-26	Waste	Air/soil	06.02.2019	10.04.2019	28.46	2.70	Downwind dumpsite
W-27	Waste	Air/soil	07.02.2019	10.04.2019	27.96	2.48	Downwind dumpsite
W-28	Waste	(Air)/soil	07.02.2019	10.04.2019	28.46	2.67	School grounds
U-29	Urban	Air	14.02.2019	12.04.2019	28.14	2.83	Small scale e-waste site
RS-30	Rural/suburban	Air	14.02.2019	12.04.2019	28.37	3.16	Cement production
U-31	Urban	Air	14.02.2019	12.04.2019	28.14	2.83	Residential
RS-32	Rural/suburban	Air	08.02.2019	11.04.2019	28.19	4.44	Cement production
U-33	Urban	Air	14.02.2019	12.04.2019	28.14	2.83	School grounds

Table S2: Analytical results for PAS. Highlighted PAS excluded from analysis.

Location	**Mass Carbon (g)**	**Measured Hg (ng)**	**Blank corrected (ng)**	**GEM concentration (ng/m^3)**	**Adjusted sampling rate (m^3/day)**	**LOD**	**LOQ**
RS-1A	0.73	11.76	10.06	1.05	0.1551	0.25	0.84
RS-1B	0.71	12.32	10.67	1.11	0.1551	0.25	0.82
RS-2	0.69	9.57	7.96	0.86	0.1517	0.25	0.83
RS-3	0.69	20.12	18.52	1.99	0.1524	0.25	0.82
RS-4	0.71	10.17	8.52	0.90	0.1525	0.25	0.83
U-5A	0.70	10.79	9.15	1.05	0.1503	0.27	0.90
U-5B	0.70	11.62	10.00	1.15	0.1503	0.27	0.89
U-6	0.69	13.72	12.12	1.44	0.1503	0.27	0.91
U-7	0.72	15.91	14.24	1.69	0.1503	0.29	0.95
U-8	0.68	11.74	10.17	1.15	0.1503	0.25	0.85
U-9	0.74	11.74	10.01	1.13	0.1503	0.28	0.93
U-10	0.69	11.28	9.66	1.07	0.1503	0.26	0.86
U-11	0.72	19.09	17.42	1.97	0.1503	0.27	0.90
U-12	0.70	48.58	46.95	5.13	0.1502	0.26	0.85
RS-13	0.68	21.10	19.51	2.16	0.1503	0.25	0.84
RS-14	0.67	8.88	7.33	*0.79*	0.1503	0.24	0.80
RS-15	0.72	11.31	9.64	1.05	0.1487	0.26	0.87
RS-16	0.72	9.54	7.86	*0.85*	0.1487	0.26	0.87
RS-17	0.69	9.84	8.22	0.89	0.1487	0.25	0.84
RS-18	0.68	11.31	9.71	1.06	0.1485	0.25	0.83
RS-19	0.71	20.22	18.56	2.05	0.1484	0.26	0.87
W-20	0.72	14.21	12.52	1.32	0.1501	0.26	0.85
W-21	0.72	24.45	22.78	2.41	0.1501	0.25	0.84
W-22	0.72	17.96	16.29	1.72	0.1501	0.25	0.84
W-23	0.70	18.40	16.76	1.77	0.1501	0.25	0.82
W-24	0.70	11.87	10.23	1.08	0.1501	0.25	0.83
W-25	0.72	0.00	0.00	0.00	0.1500	0.26	0.86
W-26	0.72	12.51	10.83	1.15	0.1501	0.25	0.85
W-27	0.67	11.88	10.32	1.12	0.1490	0.24	0.81
W-28							
U-29	0.73	17.50	15.79	1.84	0.1502	0.29	0.96
RS-30	0.70	13.18	11.54	1.34	0.1514	0.27	0.90
U-31	0.73	47.43	45.73	5.34	0.1502	0.28	0.95
RS-32	0.72	15.94	14.27	1.48	0.1551	0.25	0.83
U-33	0.71	14.93	13.27	1.55	0.1502	0.28	0.93

Table S3: Field blank results for PAS. Highlighted field blank excluded as outlier.

Location	**Mass Carbon (g)**	**Measured Hg (ng)**
U-5FB	0.70	2.06
U-6FB	0.71	5.63
U-10FB	0.71	2.39
U-7FB	0.70	0.58
RS-32FB	0.72	1.57

Emission estimates and associated uncertainty

The following equation was used to estimate emissions in the urban area:

Emissions (kg/year) = $(L\ x\ B\ x\ R\ x\ 31.6\ x\ 10^6\ s/year\ x\ (O - I))/1x10^{12}$ (eq. S1)

The parameters *L, B, R, O,* and *I* are defined in Table S4. The uncertainty of the emission estimate was studied using a simple Monte Carlo approach using the values and variability given in Table S4 and 1000 runs (Figure S1). The value and variability in GEM concentration outflow is the mean and standard deviation, respectively, of the measured GEM concentrations in the urban area of Dar es Salaam. The two highest concentrations were excluded from this calculation as outliers. Atmospheric boundary layer (ABL) height is based on mean daytime ABL height for the tropics (~1900m)[1], adjusted down to account for diurnal variation. Seasonal variation, and hence variation in mean ABL height, is small in the studied region.[1]

Table S4: Parameters used to estimate urban GEM emissions.

Parameter	**Value**	**Variability (±)**	**Unit**
Length, width urban area (*L*)	10 000		m
Height atmos. boundary layer (*B*)	1200	200	m
Inflow/outflow rate (*R*)[a]	2.84	0.1	m/s
GEM concentration inflow (*I*)[b]	0.95	0.1	ng/m^3
GEM concentration outflow: median (mean) (*O*)[c]	1.44	0.3	ng/m^3

[a] Mean and standard deviation of wind speed at urban locations in Dar es Salaam[2]

[b] From Slemr et al[3]

[c] Mean and standard deviation of GEM concentrations in urban locations in this study.

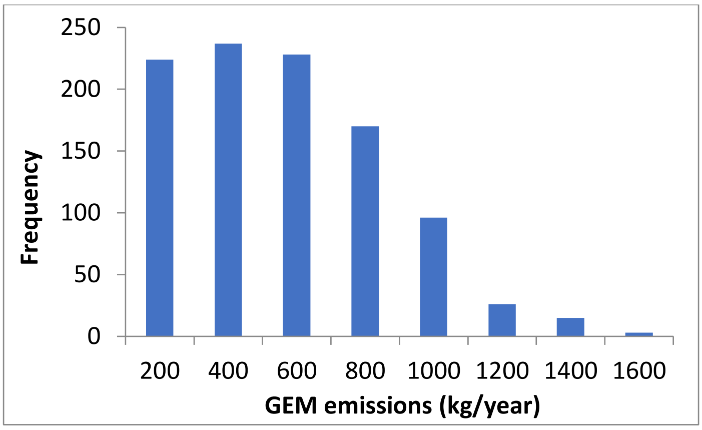

Figure S1: Histogram showing results from Monte Carlo uncertainty estimation

Table S5: Analytical results for soil.

	Measured Hg (ng)	Concentration (mg/kg)	SOM (%)
RS-1	0,60	0,012	8.6
RS-2	0,62	0,012	1.4
RS-3	0,37	0,0074	0.4
RS-4	1,11	0,022	2.2
U-5	0,92	0,018	3.3
U-6	4,89	0,098	2.1
U-7	0,55	0,011	1.9
U-8	1,33	0,027	3.0
U-9	1,54	0,031	7.4
U-10	0,57	0,011	1.7
U-11	2,05	0,041	0.3
U-12	1,40	0,028	1.7
RS-13	4,62	0,092	9.6
RS-14	1,06	0,021	0.2
RS-15	0,54	0,011	1.5
RS-16	0,34	0,0067	0.9
RS-17	0,55	0,011	2.3
RS-18	0,74	0,015	3.6
RS-19	0,57	0,011	1.8
W-20	0,54	0,011	0.8
W-21	1,14	0,023	1.5
W-22	0,34	0,0069	1.0
W-23	1,66	0,033	1.1
W-24	0,39	0,0078	0.9
W-25	0,46	0,0093	<0.01
W-26	0,76	0,015	<0.01
W-27	3,23	0,065	7.4
W-28	1,08	0,022	2.4

Table S6: Blank results soil. Highlighted blank excluded as outlier.

	Measured Hg (ng)
B-1	0,016
B-2	0,014
B-3	0,011
B-4	0,0097
B-5	0,010
B-6	0,011
B-7	0,0098
B-8	0,0092
B-9	0,0096
B-10	0,0096

Table S7: Detection limit (LOD) and quantification limit (LOQ) for soil.

Mean blank (ng)	0,011
Standard deviation blank (ng)	0,0014
Mean sample amount (mg)	50
LOD (mg/kg)	0,00030
LOQ (mg/kg)	0,00049

Table S8: Soil properties in the Dar es Salaam region by location category.

	Category	**Mean**	**Median**	**Min**	**Max**
CEC (cmol$^+$/kg)	Rural/suburban	18.52	16.87	9.18	32.80
	Urban	13.66	10.89	4.53	36.21
	Waste	7.90	7.26	2.50	16.56
pH	Rural/suburban	7.33	7.71	6.73	8.32
	Urban	8.00	8.34	7.39	8.78
	Waste	6.84	7.84	6.10	8.71
OM (%)	Rural/suburban	2.96	1.84	0.20	9.56
	Urban	2.68	2.01	0.29	7.40
	Waste	1.68	0.99	<0.01	7.35
Clay content (%)	Rural/suburban	18.10	17.50	15.00	21.35
	Urban	15.34	17.50	5.00	21.35
	Waste	14.44	17.50	5.00	17.50

Table S9: Spearman rank correlation between soil Hg concentrations and soil properties.

	Hg	p-value
OM	0.44	0.019
c(H)	-0.31	0.11
CEC	0.13	0.52
Clay content	0.00	0.99

References

1. E. L. McGrath-Spangler and A. S. Denning, Global seasonal variations of midday planetary boundary layer depth from CALIPSO space-borne LIDAR, *Journal of Geophysical Research: Atmospheres*, 2013, **118**, 1226-1233.
2. ECMWF, European Centre for Medium-Range Weather Forecasts, ERA5 dataset, 2021.
3. F. Slemr, H. Angot, A. Dommergue, O. Magand, M. Barret, A. Weigelt, R. Ebinghaus, E.-G. Brunke, K. A. Pfaffhuber and G. Edwards, Comparison of mercury concentrations measured at several sites in the Southern Hemisphere, *Atmospheric Chemistry and Physics*, 2015, **15**, 3125-3133.